AN ABSTRACT OF THE THESIS OF

Somsak Chaiyapinunt for the degree of Doctor of Philosophy in Mechanical Engineering presented on December 7, 1983.

Title: Linearized Model for Wind Turbines in Yaw

Redacted for privacy

Abstract approved: ___________

Robert E. Wilson

The analysis of rigid hub, three-bladed horizontal-axis, axisymmetric wind turbines in yaw is made using a linearized, four-degree-of-freedom model. The linearized equations of motion of rotor and nacelle are developed using quasi-steady blade element theory and Lagrange's equations.

The yaw behavior of the system is studied from coefficients of the equations of motion. Analytical results for two wind turbines are presented and studied. The study shows that yaw tracking error is primarily caused by tower shadow. The contribution of the nacelle to the yaw stability is proved to be a destabilizing one. The yaw stability of a wind turbine in a reverse position is investigated and used for verification of the analysis.

The characteristics of yaw static stability are primarily determined by the characteristics of the in-plane force coefficient and the location of the yaw axis relative to the rotor plane. A sensitivity study of the terms in the yaw stiffness coefficient is

made. The yaw static stability is strongly affected by a change in the coning angle.

Two Fortran computer programs are developed to compute the numerical values of coefficients of the equations of motion. Program listings and sample outputs are included.

Linearized Model for Wind Turbines in Yaw

by

Somsak Chaiyapinunt

A THESIS

submitted to

Oregon State University

in partial fulfillment of
the requirements for the
degree of

Doctor of Philosophy

Completed December 7, 1983

Commencement June 1984

APPROVED:

Redacted for privacy

Professor of Mechanical Engineering in charge of major

Redacted for privacy

Head of Department of Mechanical Engineering

Redacted for privacy

Dean of Graduate School

Date thesis is presented December 7, 1983

Typed by Express Typing Service for Somsak Chaiyapinunt

ACKNOWLEGMENTS

I would like to express my sincere gratitude to Dr. Robert E. Wilson, my major professor, for his guidance, encouragement, criticism, and financial support. I am also grateful to Dr. James R. Welty, the department head, for providing me teaching assistantships during the course of my graduate studies. I also wish to thank Dr. Charles E. Smith for his advice and useful discussions about the dynamics of wind turbines, and Rockwell International Corporation, Rocky Flats Plant for its financial support from September 1981 to March 1982.

Finally, I would like to express my deepest gratitude to my parents, Surin and Suwannee Chaiyapinunt, for their love, encouragement, and untiring support.

TABLE OF CONTENTS

LIST OF FIGURES

Figure		Page

LIST OF TABLES

NOMENCLATURE

a	axial induction factor
A	area
B	number of blades
c	blade chord
C_D	drag coefficient
C_L	lift coefficient
C_{F_n}	force coefficient in the direction normal to the rotor
C_{F_t}	force coefficient in the direction tangential to the rotor
C_n	normal force coefficient
C_P	power coefficient
C_Q	torque coefficient
C_t	tangential force coefficient
C_T	thrust coefficient
D	drag force
e	distance from mass center to shear center of the blade cross section
e_1	distance from 1/4 blade chord to shear center of the blade cross section
e_2	distance from 3/4 blade chord to shear center of the blade cross section
e_3	distance from mid-blade chord to shear center of the blade cross section
E	modulus of elasticity

f_1	mode shape of the blade twisting
f_2	mode shape of the blade deflection
f_3	mode shape of the lead-lag deflection
f_4	mode shape of the yaw displacement
F	tip loss factor
F_1	linearized aerodynamic force term
F_2	linearized aerodynamic force term
F_3	linearized aerodynamic force term
F_4	linearized aerodynamic force term
g	gravitational force
G	shear modulus of rigidity
G_1	linearized aerodynamic force term
G_2	linearized aerodynamic force term
G_3	linearized aerodynamic force term
G_4	linearized aerodynamic force term
h	a function defined in gravitational force
I	moment of inertia
I_1	mass moment of inertia in n_1 direction
I_2	mass moment of inertia in n_2 direction
I_3	mass moment of inertia in n_3 direction
j_n	Glauert coefficient
J	polar moment of inertia
J_1	moment of inertia in n_1 direction
J_2	moment of inertia in n_2 direction
J_3	moment of inertia in n_3 direction
k_n	Glauert coefficient
k_{nn}	stiffness coefficient of the system

ℓ	distance from nacelle yaw axis to rotor center
L	lift force
m_{nn}	mass coefficient of the system
M	moment
n_n	unit vector
N_n	linearized normal force
P	power
q_∞	dynamic pressure $\frac{1}{2}\rho_\infty V_\infty^2$
q_1	generalized coordinate of pitch angle
q_2	generalized coordinate of flap deflection
q_3	generalized coordinate of the variation of azimuth angle
q_4	generalized coordinate of yaw angle
q_s	static tip deflection
r	local blade radius
r_N	local blade radius in the rotor plane
r_S	distance of the local blade radius to blade root
R	blade radius
R_H	hub radius
R_S	distance from blade tip to blade root
S	cross-sectional area of nacelle
t	time
H_n	linearized tangential force
u	axial velocity at the rotor
u_n	radial displacement
U	strain energy
v_n	normal displacement

V_∞	wind velocity
V_R	wind velocity at reference point
w	flap deflection
W	relative velocity
W_e	relative velocity excluding the pitching velocity at 3/4 blade chord
W_n	normal relative velocity
W_t	tangential relative velocity
x	local tip speed ratio
X	tip speed ratio
x_1, x_2, x_3	coordinate system on the blade cross section after blade pitching
$x_\theta, y_\theta, z_\theta$	coordinate system on the blade cross section after blade flapping
$x_\beta, y_\beta, z_\beta$	coordinate system on the blade cross section after accounting for the pretwist angle
x_ρ, y_ρ, z_ρ	coordinate system at rotor center accounting for the coning angle
$\underline{x}, \underline{y}, \underline{z}$	coordinate system fixed to the blade at azimuth angle ψ
$\hat{x}, \hat{y}, \hat{z}$	coordinate system with its origin is at the rotor center and the system is fixed to the nacelle
x, y, z	coordinate system fixed to the nacelle and its origin located at nacelle yaw axis
X, Y, Z	coordinate system located on top of the tower

Greek Symbols

θ	blade pitch angle
χ	variation of azimuth angle
ψ	azimuth angle ($\Omega t + \chi$)
γ	yaw angle
ρ	coning angle
ρ_∞	density
η	dummy variable
Ω	rotor angular velocity
β	pretwist angle
ω_1	blade angular velocity in x_1 direction
ω_2	blade angular velocity in x_2 direction
ω_3	blade angular velocity in x_3 direction
α	angle of attack
α_E	angle of attack plus the effect of pitching velocity
Π_i	integral term for the variation of axial induction factor

Linearized Model for Wind Turbines in Yaw

1. INTRODUCTION

Wind-powered machines can be classified into two types according to the orientation of the axis of rotation: horizontal-axis wind turbines and vertical-axis wind turbines. For a horizontal-axis wind turbine, the system can be further distinguished as either a downwind rotor or an upwind rotor system. When the rotor is upwind of the tower, the system usually has a yaw controller to force the wind turbine to track the wind mechanically. There is often no need for a yaw controller in the downwind rotor case. When the rotor is downwind of the tower, the wind turbine will typically track the wind. Most of the downwind turbines are free-yaw systems.

Unfortunately, in many free-yaw systems, a yaw instability can occur: instead of tracking with the wind, the turbine yaws away from the wind.

Little work has been done on wind turbines in yaw. Most of the previous work has been on the structural dynamics and control of wind turbine systems. The cause of the yaw instability has still not been fully understood.

The technology and methodology used to develop present-day wind turbines are adapted from the fixed and rotating wing aircraft technology. Ribner [16] has done an analysis of induction velocity and side force in terms of the shape of the blade when the propeller is yawing. For wind turbines, Miller [13] looked into the static stability characteristics of horizontal-axis wind turbines with a free-yaw system operating only in a low wind condition (i.e., no stall model). Hirschbein [7] analyzed the dynamics and control of large horizontal-axis axisymmetric wind turbines in his Ph.D. thesis. He modeled the blade motion by considering the blades to be composed of an inboard series of massless, rigid links restrained by linear springs and dampers with a much larger, massive blade attached to the outermost link.

In this dissertation, yaw of wind turbines will be studied by using a four-degree-of-freedom system to represent the axisymmetric wind turbine system. The study will focus on the cause of yaw tracking errors and the characteristics of the yaw static stability. This will be done by developing the equations of motion of the system and then studying from the coefficients of the equations. The equations of motion of the rotor are developed using the Lagrange method, and the aerodynamic forces and moments are developed using the quasi-static blade element theory. The aerodynamics of wind turbines in the stall region is also considered.

The analysis is primarily developed for a three-bladed horizontal axis wind turbine, but it also can easily be applied to a turbine with any number of blades greater than three. The contribution of the nacelle to the rotor system is also examined.

2. ANALYSIS

Development of the Equations of Motion

A four-degree-of-freedom system is chosen to model the axisymmetric turbine system. The degrees of freedom are blade pitch deflection, blade flap, nacelle yaw, and rotor speed. These degrees of freedom are defined as follows: Blade pitch is defined as the rotation of the blade cross section around the control axis; Blade flap is defined as the deflection of the blade in the direction perpendicular to the blade chord; Nacelle yaw angle is defined as the angle of the nacelle around the yaw axis with respect to the wind; and Rotor speed variation is defined as the variation of the rotor speed from the nominal value.

The equations of motions are developed using the Lagrange method. Since each of the variables is a function of time and radial distance, the partial derivatives of these variables will be encountered during the development of the equations of motions.

To avoid dealing with partial differential equations, the assumed modes method [11] is used in this study. The purpose of this method is to eliminate the spatial dependence from the dependent variable by discretizing the spatial variable. Thus each of the system's degrees of freedom is expressed as the product of the displacement function (assumed mode shape), which is the function of the spatial coordinate, and the time-dependent generalized coordinate. By this method, the equations of motion of the system will be developed in ordinary rather than partial differential forms.

In order to attack the problem, the kinematics of the rotor are first developed. Then, the kinetic energy is obtained from the expression of the kinematics. The potential energy expression is developed from the strain energy of the rotor system. With quasi-steady blade element theory, the aerodynamic forces and moments are developed. Then, the nonconservative forces in Lagrange's equation are derived from the virtual work of the aerodynamic forces and moments. Finally, when the Lagrangian functions and nonconservative forces are substituted back into Lagrange's equation, a set of nonlinear equations of motion of the rotor system is obtained.

The rotor extracts energy from the wind, converting it into mechanical energy. Since the energy is extracted from the airstream, the velocity of the wake will be decreased. To represent the reduction of the wind velocity at the rotor and in the wake, the axial induction factor "a" [20, 22] is introduced. In this study the nonrotating wake model is used. The local value of the axial induction factor can be calculated by equating the windwise force developed by using momentum theory, and the same force developed by using blade element theory. The Glauert empirical relationship [4] is used instead of the momentum theory when the axial induction factor is greater than 0.38. The tip loss model is used to account for the flow at the tip of the turbine blade. The development of the axial induction factor and the tip loss model is presented in Appendix II.

The above steps lead to a set of nonlinear equations. If the ranges of values of the dependent variables can be retricted, the system may be well-approximated as linear. In this study, the system is analyzed in the linear range.

In the process of equation linearization, the variation of the axial induction factor with yaw, pitch, flap, and rotational speed will be encountered. Linearized aerodynamic forces and moments are developed.

Let us define the variation of the induction factor with the dependent variables as the summation of two terms: 1) the product of a coefficient and the distance along the yaw axis of the rotor, and 2) the product of a coefficient and the distance along the rotor pitch axis.

$$\frac{\partial a}{\partial \eta} = j_\eta \frac{r}{R} \cos\psi + k_\eta \frac{r}{R} \sin\psi$$

Here, ψ is the blade azimuth angle.

The value of the two coefficients, j_η and k_η, can be calculated by equating the derivative of yaw or pitch moment developed by the momentum theorem to the derivative of yaw or pitch moment developed by the blade element theory.

With the known values of the coefficients, j_η and k_η, the variation of the axial induction factor can be determined. The result shows that the variation of the axial induction factor exists only for the yaw and yaw rate variables in the uniform flow case.

The linearization of the aerodynamic forces and the variation of the axial inducation factor are presented in Appendix II.

The linearized rotor equations of motion are expressed in matrix form

$$[M]\{\ddot{q}_i\} + [C]\{\dot{q}_i\} + [K]\{q_i\} = \{G\}$$

where $\{q_i\}$ is a four-dimensional generalized coordinate column vector representing the system's degrees of freedom; $\{G\}$ is a four-dimensional forcing function column vector; $[M]$, $[C]$, and $[K]$ are the four dimensional square mass, damping, and stiffness coefficient matrices, respectively.

For a large wind turbine system, gravity loads are very important to dynamic and structural analyses. To make the analytical model for the turbine system applicable regardless of the size of the system, gravity loads are included in this study. The gravitational force is added to the system by means of a potential function.

For a downwind system, the rotor is located behind the nacelle and tower. The effect of the nacelle and tower shadow on the system was studied.

The nacelle is considered as a slender body. The shape of the nacelle is assumed to be a cylinder with hemispheres on both ends. The equation of motion of the nacelle will be developed by using the Lagrange method. The nacelle will be considered as a rigid body rotating around its yaw axis when the kinetic and potential energy are calculated. The nonconservative force on the nacelle is derived from the virtual work of the nacelle. The forces on the nacelle are calculated by using slender body theory with forces generated only from the forebody part of the nacelle.

The tower shadow is modeled as a velocity deficit from the rotor axial velocity value over a selected region of the rotor disk. The system's equations of motion are developed with the tower shadow.

Throughout this analysis the wind turbine is modeled with a three-bladed rotor. The turbine blades are elastic. The hub, nacelle, and tower are rigid. The nacelle is allowed to yaw freely. The center of mass of the nacelle and rotor is located over the central axis of the tower. This axis will be referred to as the nacelle yaw axis.

The absolute motion of the turbine blade is determined by the motion of blade deflection relative to the hub, the motion due to rotor rotation, and the motion of the nacelle and tower. Since in this analysis no movement of the tower is allowed, the tower is considered as an inertial reference frame. A series of coordinate systems is used to describe a point on the blade. A series of transformation matrices is then used to transform the coordinate systems that describe motion of a point on the blade in its original reference frame into the inertial reference frame.

Two computer codes have been written to handle the numerical computations which yield the coefficients for the equations of motion. One of them has a simplified lift and drag curve in the stall region. The other was developed later and was necessary because of the need for a more accurate model for lift and drag in the stall region. This second computer code only emphasizes the yaw equation, since it was found from the analytical results that there is no coupling between yaw and the other degrees of freedom. The inputs to the computer code are the geometry of the rotor, the wind condition, and the operating conditions. Both computer codes will calculate the axial induction factor along the blade at a particular tip speed ratio. At the same time, they also calculate the integral terms for variation of the axial induction factor with yaw and yaw rate. Finally, the programs will calculate the coefficients in the equations of motion (mass, damping, stiffness, and forcing function). Besides the coefficients of the equations of motion, the codes also calculate the thrust and power coefficients for the rotor.

3. PHYSICAL CHARACTERISTICS OF TEST CASES

Two test cases are chosen to verify the analysis. The test cases are the Grumman WS33 and the Enertech 1500. Both of these machines are three-bladed horizontal axis downwind wind turbines.

Grumman WS33

The Grumman WS33 is a three-bladed, downwind machine designed to interface directly with an electrical utility network. The machine is rated at 15 kw at 24 mph and peak power of 18 kw at 35 mph. Utility compatible electrical power is generated in winds between a cut-in speed of 9 mph (4.0 m/s) and a cut-out speed of 50 mph (22 m/s) by using torque characteristics of the unit's induction generator combined with rotor aerodynamics to maintain essentially constant speed.

The rotor's diameter is 33.3 feet. The blades are extruded aluminum alloy with a modified NACA 64_4-421 airfoil section. The blades are adjusted in pitch by a redundant pitch actuator system controlled by a solid state programmable logic controller, the Microcomputer Control Unit. The overall weight of the nacelle and rotor assembly including the blades is 2,589 pounds. The blades weighed 185 pounds each.

Power is generated by a 240/280 volt, 30,60Hz induction generator with a 20kw capacity. The generator operates between 1800 and 1835 rpm. The gear box with 25.1 to 1 ratio will cut in at about 72 rpm with full power being generated at a little above 74 rpm.

The physical and operating characteristics of the rotor, the blade, and the nacelle are given in tables 3.1, 3.2, and 3.3, respectively. The information describing the Grumman WS33 was obtained from reference 1.

The airfoil lift and drag coefficient of the Grumman WS33 are plotted as functions of Reynolds number and angle of attack in Figure 3.1. These data are obtained from reference 19.

Table 3.1 Physical and operating characteristics of the rotor of the Grumman WS33.

Rotor diameter	33.25 ft
Blade chord	1.5 ft
Root cut-out	1.625 ft
Airfoil type	NACA 64_4-421 (modified)
Rotor speed	74.1 rpm
Rotor coning angle	3.5°
Number of blades	3

Table 3.2 Physical and operating characteristics of the blade of the Grumman WS33.

Blade density	5.2502 slug/ft^3
Mass per unit length	0.38655 slug/ft
Moment of inertia in flapwise direction	14.46 in^4
Moment of inertia in chordwise direction	238.03 in^4
Moment of inertia in radial direction	252.49 in^4
Modulus of elasticity	10x10^6 psi
Shear modulus	3.8x10^6 psi

Table 3.3 Nacelle properties of the Grumman WS33.

Distance of the nacelle yaw axis to blade hub	2.931 ft
Length of the nacelle	9.177 ft
Cross section area of the forebody end	3.713 ft^2
Cross section area of the nacelle	6.674 ft^2
Mass moment of inertia of the nacelle and hub assembly around the yaw axis	556.23 slug-ft^2

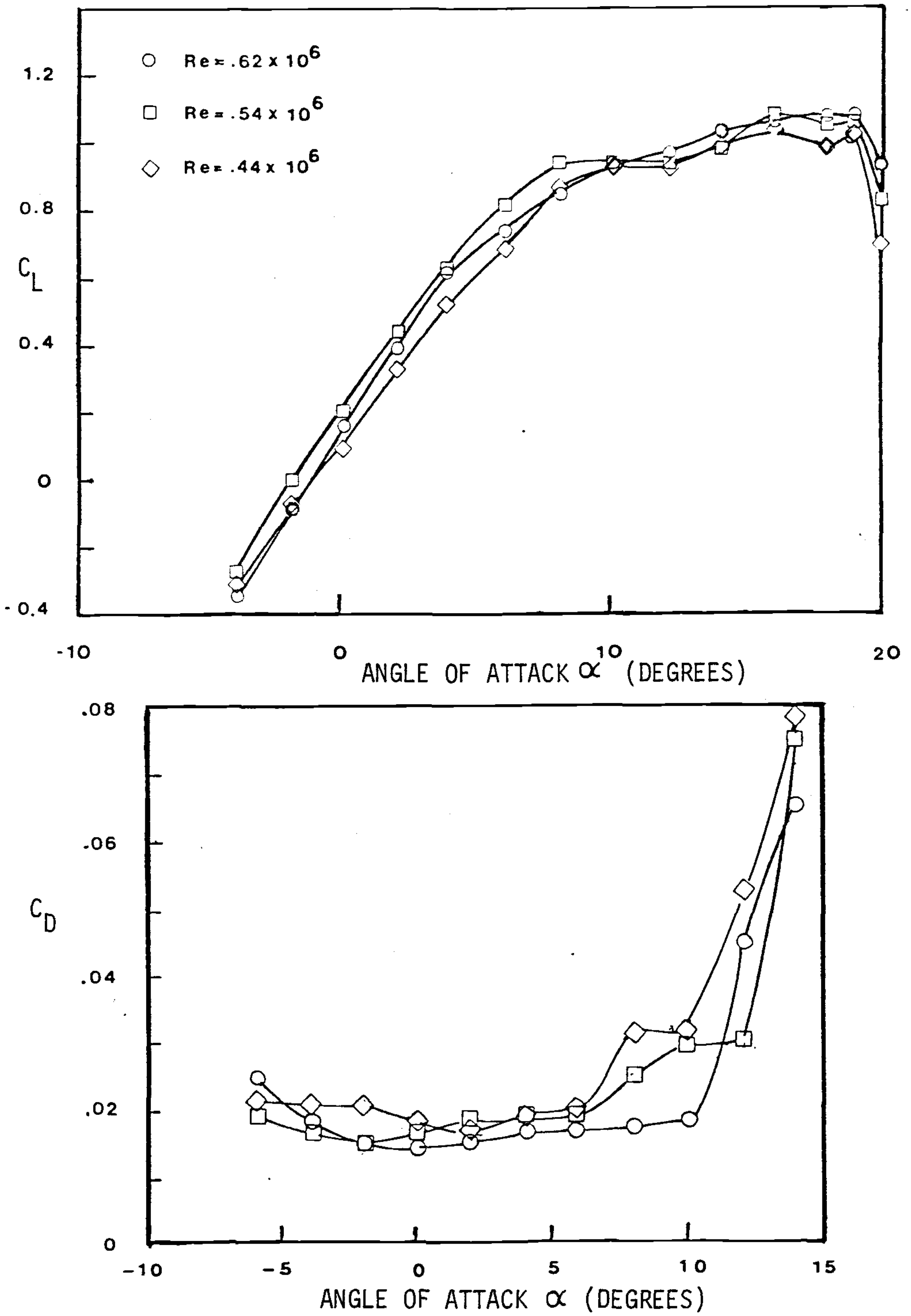

Figure 3.1 Airfoil sectional data for NACA 64_4-421 from reference 19.

Enertech 1500

The Enertech 1500 is a downwind system with a three-bladed rotor. The geometry and material properties of a blade of an Enertech 1500 wind turbine were measured. The blade has linear twist with slight linear taper over the outer 22 percent of the rotor blade and the blade's thickness is varied from root to tip. For the calculation of the aerodynamic forces and moments, the blade profile section was represented by the NACA 4415 airfoil section. The airfoil lift and drag coefficients are plotted as functions of Reynolds number and angle of attack in Figure 3.2. These data are obtained from reference 9. This rotor is designed to operate at tip speed of 117 fps (170 rpm). The physical characteristics of the rotor are presented in Table 3.4.

Table 3.4 Physical and operating characteristics of the rotor of the Enertech 1500.

Rotor diameter	13.12 ft
Blade chord	6.8 in. from root to r/R = 0.6545 linear taper to 6.1 in. at r/R = 1.0
Airfoil type	NACA 4415*
RPM	170
Tip speed	117 fps
Number of blades	3
Root cut-out	0.84 ft
Twist	5° from root linear to 1° at blade tip
Precone	0°

*Used as representative airfoil section.

The profile of the blade cross sections were measured at six stations along the blade. The weight of the blade was measured. By knowing the weight and the profile of each cross section, properties

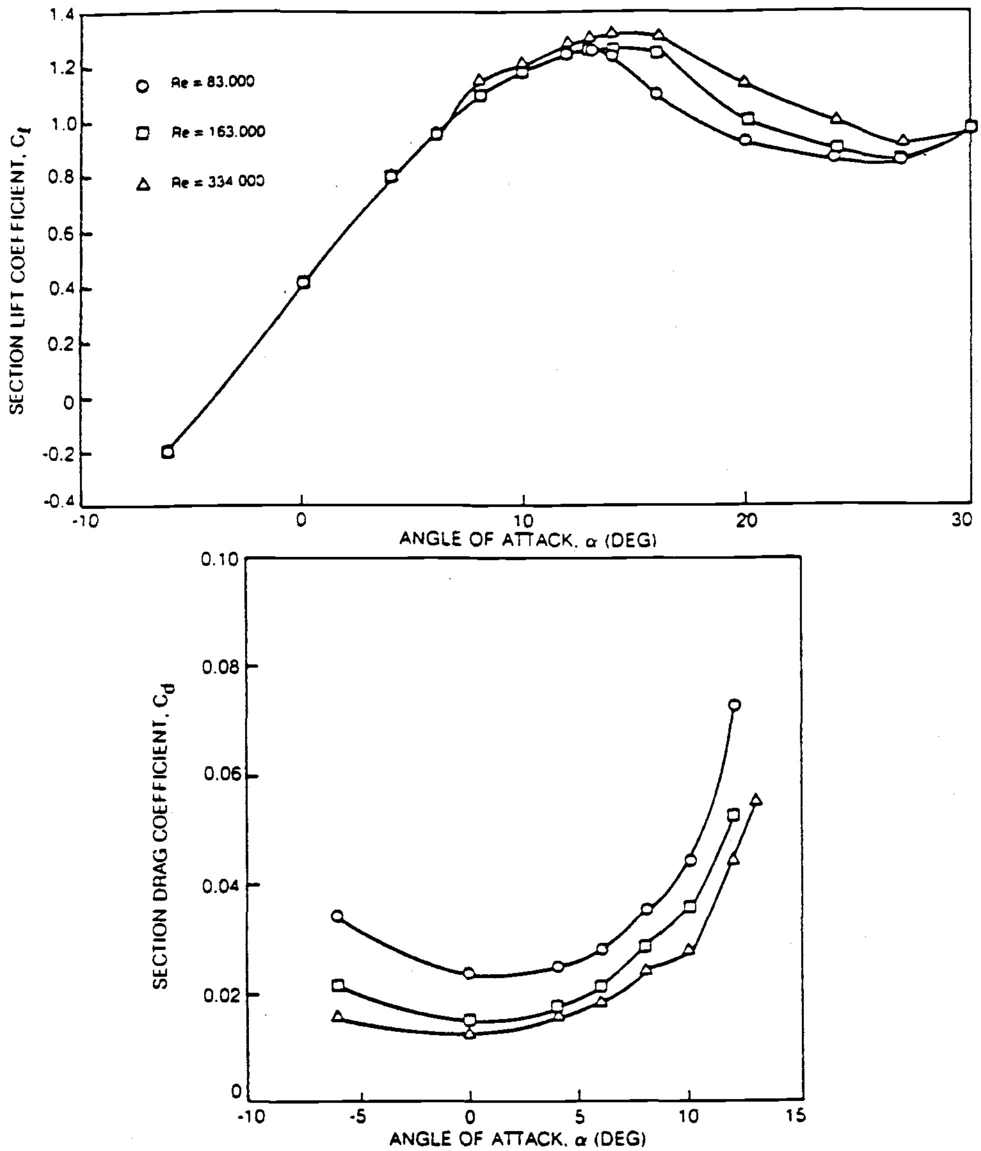

Figure 3.2 Lift and drag coefficient for the NACA 4415 airfoil section (Ref. 9).

of the blade were calculated. The expressions for the moment of inertia and mass distribution per unit length of the blade were written as a function of the distance along the blade. These expressions are given in tables 3.5 and 3.6.

Table 3.5 The moment inertia of the blade cross section of the Enertech 1500.

r/R	J_2 (in 4)	J_3 (in 4)
1 - 0.6545	5.673 exp (-3.313 r/R)	67.3636 exp (-2.0236 r/R)
0.6545 - 0.3648	2.111 exp (-1.802 r/R)	29.44 exp (-0.76 r/R)
0.3648 - 0.2440	2.111 exp (-1.802 r/R)	11.3726 $(r/R)^{-0.6585}$
0.2440 - 0.1393	4.5679 exp (-4.8604 r/R)	11.3726 $(r/R)^{-0.6585}$
0.1393 - 0.1280	2.3210	41.924

Here J_i's are the moment of inertias of the blade cross section at the mass center in x_i direction and $J_1 = J_2 + J_3$.

Table 3.6 Mass distribution of the blade of the Enertech 1500.

r/R	μ (slug/ft)
1 - 0.6545	0.090898 exp (-1.3266 r/R)
0.6545 - 0.3648	0.05847 exp (-0.6447 r/R)
0.3648 - 0.1393	0.081772 $(r/R)^{-0.3695}$
0.1393 - 0.1280	0.06593

Since the blade is made of wood (orthotropic material), its material properties depend on the orientation of wood grain. It is difficult to find the mechanical properties of a nonuniform orthotropic beam by experiment. Thus, it was decided to treat the blade as an isotropic material and use the values obtained from the U.S. Forest Products Laboratory on Sitka Spruce with 10 percent moisture content. The values are

$$E_L = 1.84 \times 10^6 \text{ psi},\ G_{LR} = 1.089 \times 10^5 \text{ psi},\ \nu_{LR} = 0.25$$

For simplicity, the elastic axis was assumed to be a straight line which is parallel to the trailing edge of the blade. The location of the elastic axis on the blade cross section was chosen arbitrarily. The location of the axis then is varied to see the effect on the system.

The nacelle of the Enertech 1500 has a cylindrical shape with a hemisphere on each end. The properties and geometry of the nacelle are given in Table 3.7.

Table 3.7 Nacelle properties of the Enertech 1500.

Distance of the nacelle yaw axis to the blade hub	2.46 ft
Length of the nacelle	5.896 ft
Radius of the nacelle cross section	0.84 ft
Mass moment inertia of the nacelle around the yaw axis	14.41 slug-ft^2

The generator for the Enertech 1500 is a single-phase induction motor connected to a gearbox having a measured 11.28 to 1 ratio.

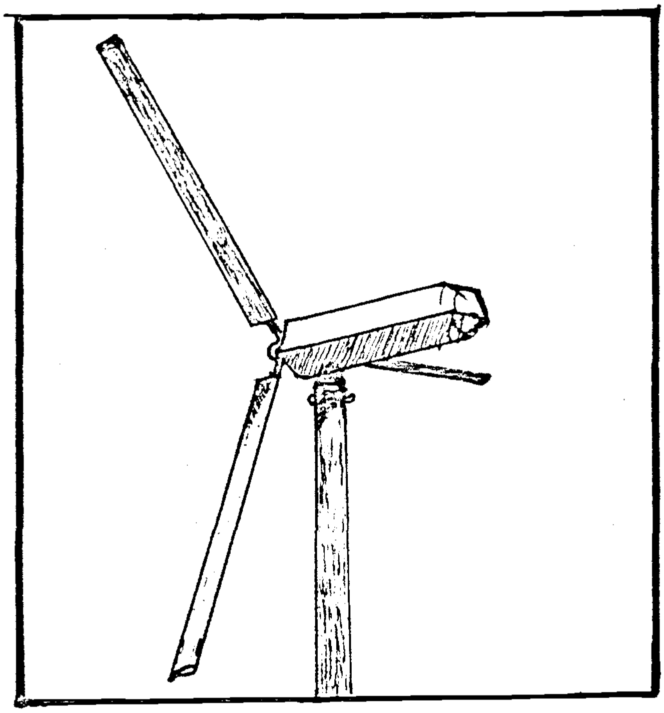

The Grumman Windstream 33

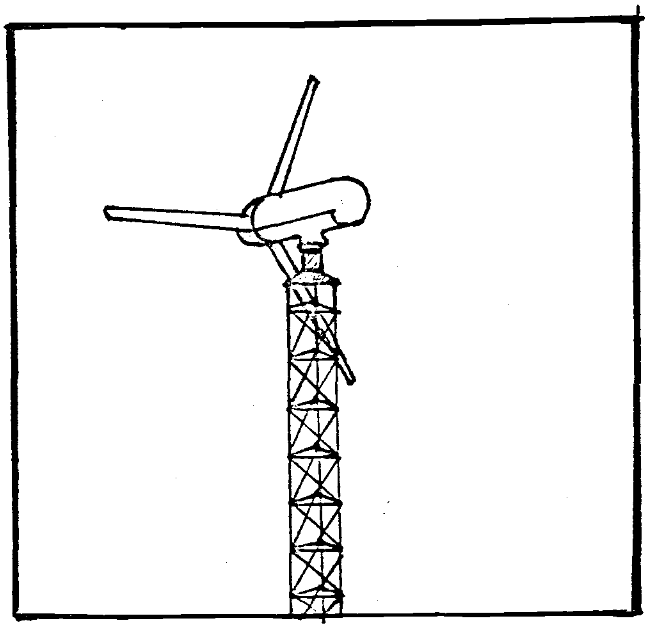

The Enertech 1500

Figure 3.3 The Grumman WS33 and the Enertech 1500.

4. RESULTS AND DISCUSSION

The Enertech 1500 and the Grumman WS33 were used as the test cases. Two computer codes, AERO code and PROP code, were used to generate the numerical values of the analytical results. The AERO code uses a simplified lift and drag curve to calculate the axial induction factor and its variation. The AERO code also generates the coefficients of the equation of motion for a four-degree-of-freedom system. The revised version of PROP code [21] uses the actual lift curve to calculate the axial induction factor and its variation. The PROP code also gives more accurate results for the static tip deflection and the coefficients of the equations of motion in yaw. More detail regarding these two computer codes is shown in Appendix VI. It was found that the PROP code is preferred because of the accuracy of the lift and drag models in the stall region.

The yaw response of wind turbines will be examined from the numerical values of coefficients in the equations of motion generated from the computer codes. The analytical results of the Grumman WS33 is examined first. The cause of yaw tracking error is obtained from studying the coefficients in the yaw equation. The tower shadow effect is included in this analysis. The verification of the analysis is obtained from the calculated yaw stability of the Grumman WS33 in the upwind position.

The analytical results for the Enertech 1500 are presented and discussed in brief.

Analytical Results for the Grumman WS33

With the numerical values of the coefficients in the equations of motion, the static pitch angle and the static flapwise deflection are first examined. Then, the sources of yaw forcing function, which are wind shear, gravity, blade cyclic force, blade flap, and tower shadow, are investigated.

Static Pitch Angle

The equilibrium pitch angle can be obtained from the pitch stiffness coefficient and the pitch forcing function. The equilibrium pitch angles that differed from the assumed zero value for different tip speed ratios are given in Table 4.1. These angles are so small that they have negligible effect on the system.

Table 4.1 Static tip pitch angles at $\beta = 4°$.

X	θst (degree)
2	0.0279
3	0.0176
4	0.0136
5	0.0102
6	0.0073
7	0.0051
8	0.0034

Static Flapwise Deflection

The flapwise deflection (coning due to blade load) is examined. The static tip deflections for the Grumman machine from the AERO code and PROP code are given in Table 4.2.

Table 4.2 Static tip deflections at $\beta = 4°$.

X	AERO ds (ft)	PROP ds (ft)
2	0.02457	0.02543
3	0.00645	0.00807
4	-0.00161	0.00206
5	-0.01009	-0.01039
6	-0.01718	-0.01724
7	-0.02238	-0.02265
8	-0.02617	-0.02673

The difference between the values obtained from the AERO and PROP codes is small except at the tip speed ratio 3 and 4. Those are the conditions under which most of the blade is operating in the stall region, and the AERO code does not have an accurate model in the stall region.

The results in Table 4.2 show that the blades exhibit a negative coning effect under low wind. The blade tips are deflected upwind because the centrifugal deflection overcomes the aerodynamic deflection.

Coefficients of the Equation of Motion in Yaw

For a uniform wind condition, there is no coupling between the yaw angle and the other three variables explicitly on the equations of motion.

For the nacelle, the equation of motion is in the form of undamped second order system in yaw. The stiffness coefficient of the nacelle is not dependent on the tip speed ratio. The development of the nacelle is given in Appendix III.

Because of the linearity of the system, the nacelle's equation of motion can be added directly to the rotor equation of motion in yaw. The nacelle destablized the system in yaw. The coefficients for the equation of motion in yaw from both computer codes are given in tables 4.3, 4.4, 4.5, and 4.6.

Table 4.3 Coefficients of the equation of motion in yaw from AERO code.

X	m_{44}	C_{44}	k_{44}	$m_{44_{n*}}$	k_{44_n}
2	0.0991	0.0415	0.01172	0.02531	-0.0028564
3	0.2224	0.0680	0.00245	0.05694	-0.0028564
4	0.3947	0.1850	0.01957	0.10123	-0.0028564
5	0.6159	0.3397	0.03685	0.15817	-0.0028564
6	0.8858	0.4522	0.04331	0.22776	-0.0028564
7	1.2046	0.5557	0.04654	0.31001	-0.0028564
8	1.5724	0.6646	0.04886	0.40492	-0.0028564

*n refers to the nacelle

Table 4.4 Coefficients of the equation of motion in yaw for the combined rotor and nacelle system from AERO code.

X	m_{44_T}	C_{44_T}	k_{44_T}
2	0.12441	0.0415	0.008864
3	0.27934	0.0680	-0.000406
4	0.49593	0.1850	0.016713
5	0.77407	0.3397	0.033994
6	1.11356	0.4522	0.040475
7	1.51461	0.5557	0.043684
8	1.97732	0.6646	0.046004

Table 4.5 Coefficients of the equation of motion in yaw from PROP code.

X	m_{44}	C_{44}	k_{44}	m_{44_n}	k_{44_n}
2	0.0952	0.0432	0.01548	0.02531	-0.0028564
3	0.2136	0.0728	0.00509	0.05694	-0.0028564
4	0.3791	0.1674	0.01943	0.10123	-0.0028564
5	0.5916	0.2961	0.03230	0.15817	-0.0028564
6	0.8509	0.4197	0.03929	0.22776	-0.0028564
7	1.1573	0.5258	0.04308	0.31001	-0.0028564
8	1.5106	0.6292	0.04554	0.40492	-0.0028564

Table 4.6 Coefficients of the equation of motion in yaw for the combined rotor and nacelle system from PROP code.

X	m_{44_T}	C_{44_T}	k_{44_T}
2	0.12051	0.0432	0.012624
3	0.27054	0.0728	0.002234
4	0.48033	0.1674	0.016574
5	0.74977	0.2961	0.029444
6	1.07866	0.4197	0.036434
7	1.46731	0.5258	0.040224
8	1.91552	0.6292	0.042684

There is some doubt in the accuracy of the stiffness coefficient for the Grumman WS33's nacelle. The analytical model of the nacelle in this analysis is based on slender body theory. Unfortunately, the shape of the Grumman WS33's nacelle and most other wind turbines' nacelles are not slender. There are some correction factors suggested to use with the slender body theory by reference 2 and 8 for a noncircular body and a fineness ratio effect. However, the experimental results for a fineness ratio effect on the aerodynamic characteristics of bodies of revolution in reference 6 does not agree with the correction factors given in references 2 and 8. There is no accurate model for the noncircular body with blunt nose. More work is needed in order to obtain an accurate model.

The values in tables 4.3 and 4.5 are given without the correction factors. These correction factors, given in Appendix III, are always less than one. Therefore, the values in tables 4.3 and 4.5 are the most destablizing condition for the nacelle effect based on the slender body theory. According to the PROP code, the system is stable for all of the tip speeds considered. However, a negative stiffness coefficient is encountered for the AERO code's result at the tip speed ratio equal to 3.

The expression for the stiffness coefficient consists of the derivative of the aerodynamic force and its moment arm. The derivative of the aerodynamic force is dependent on the slope of the lift and drag curve versus the angle of attack. Therefore, an accurate model of the lift and drag curve is needed to obtain an accurate result. Thus, the PROP code is preferred to the AERO code, which uses the simplified lift and drag curve in the stall region.

Yaw Forcing Function

Possible candidates for a yaw forcing function are wind shear, blade pitch, blade flap, and tower shadow. The in-plane yaw force on the rotor is related nonlinearly to the wind speed; therefore, the difference in the axial velocity on the rotor due to wind shear would result in a yaw moment created by the net in-plane yaw force. However, there was no wind shear in the test data obtained from the Rocky Flat Research Energy Center for the Enertech 1500 or the Grumman WS33.

Gravity and blade cyclic pitch.

The gravitational force is added to the system equations of motion by means of a potential function. The analysis shows that there is no effect of gravity appearing in the yaw equation. Therefore, the gravity is not a source for the yaw forcing function.

The gravity effect also appears as a cyclic moment in the pitch equation for a single-bladed rotor. However, this moment cancels out for an axisymmetric three-bladed rotor.

The effect of the blade cyclic force on the cyclic pitch angle is also examined by considering the gravitational force on a single blade. The cyclic moment due to gravity appears in the stiffness coefficient and forcing function in pitch. These cyclic moment terms are given in the following forms:

$$(Cg \cos\psi + Dg \sin\psi)q_i = (Eg \cos\psi + Fg \sin\psi)$$

The coefficients Cg, Dg, Eg, and Fg are given in Table 4.7. The stiffness coefficient and forcing function also are given in Table 4.7.

Table 4.7 Coefficients for harmonic terms (Cg, Dg, Eg, Fg), stiffness coefficient, and forcing function of a single-blade equation of motion in pitch.

X	k_{11}	G_{01}	$Cg\times10^3$	$Dg\times10^2$	$Eg\times10^3$	$Fg\times10^4$
2	80.998	.03957	-.2367	.6308	-.1647	-.6246
3	182.286	.05604	-.5326	1.4193	-.3362	-1.4053
4	323.631	.07679	-.9468	2.5232	-.5705	-2.4984
5	504.815	.08998	-1.4794	3.9425	-.8468	-3.9037
6	726.471	.09291	-2.1303	5.6771	-1.1657	-5.6213
7	988.547	.08795	-2.8996	7.7272	-1.5330	-7.6512
8	1291.04	.07691	-3.7872	10.0927	-1.9513	-9.9933

For the static condition, the cyclic pitch angle is given as the following form:

$$q_{1_s} = \frac{G_{01}/3 + (Eg\cos\psi + Eg\sin\psi)}{k_{11}/3 + (Cg\cos\psi + Dg\sin\psi)}$$

It can be seen from the magnitude of the coefficients given in Table 4.7 that the blade cyclic force has a negligible effect on the static pitch angle.

Blade flap.

The flapwise displacement appears implicitly and explicitly in most of the coefficient terms. The flapwise deflection definitely affects the yaw behavior, but it is not a source of the yaw forcing function. The effect of blade flap will be discussed in a later section.

Tower shadow.

The tower shadow is modeled as a velocity deficit from the axial velocity over a sector of the rotor disk, centered about the tower centerline. The development for the equations of motion with the tower shadow is given in Appendix III.

Because of the difference of the axial velocity on the rotor inside and outside of the tower shadow region (i.e., when the blade is in the 6 o'clock position and the 12 o'clock position), there will be different values of aerodynamic forces. The difference of the in-plane force (force that is tangential to the rotor plane) in the tower shadow produces a net yaw moment around yaw axis, creating a static yaw angle. This yaw moment turns out to be the yaw forcing function that is needed.

Consider the yaw moment inside the tower shadow. The expression of this yaw moment can be simplified as follows:

$$M_y = \left\{ \int_{R_H}^{R} F_t \left(\frac{\ell}{R} + \frac{r}{R}\sin\rho\right)\frac{dr}{R} - \int_{R_H}^{R} N_0 \frac{e_1}{R}\frac{dr}{R} + \int_{R_H}^{R} H_0 \frac{w_0}{R}\frac{dr}{R}\right\}\frac{B}{2\pi} \quad 2\sin\frac{\lambda}{2} \tag{1}$$

Here F_t is the in-plane force, ℓ is the distance from the rotor to the yaw axis, ρ is the coning angle, N_0 and H_0 are the forces normal and tangent to the blade chord, e_1 is the distance from the shear center to the blade 1/4 chord, and w_0 is the static flapwise deflection. The full expression of this yaw moment is given in Appendix IV.

The first term in the equation (1) primarily depends on the in-plane force. This in-plane force is directly related to the power output. Therefore, the power output response would be similar to the in-plane force.

The third term is the yaw moment due to the tangential force and flapwise deflection acting in the same direction as the moment in the first term.

The second term is the yaw moment due to the normal force and the offset distance of the shear center (e_1). This yaw moment acts in the opposite direction of the other two terms in the equation (1).

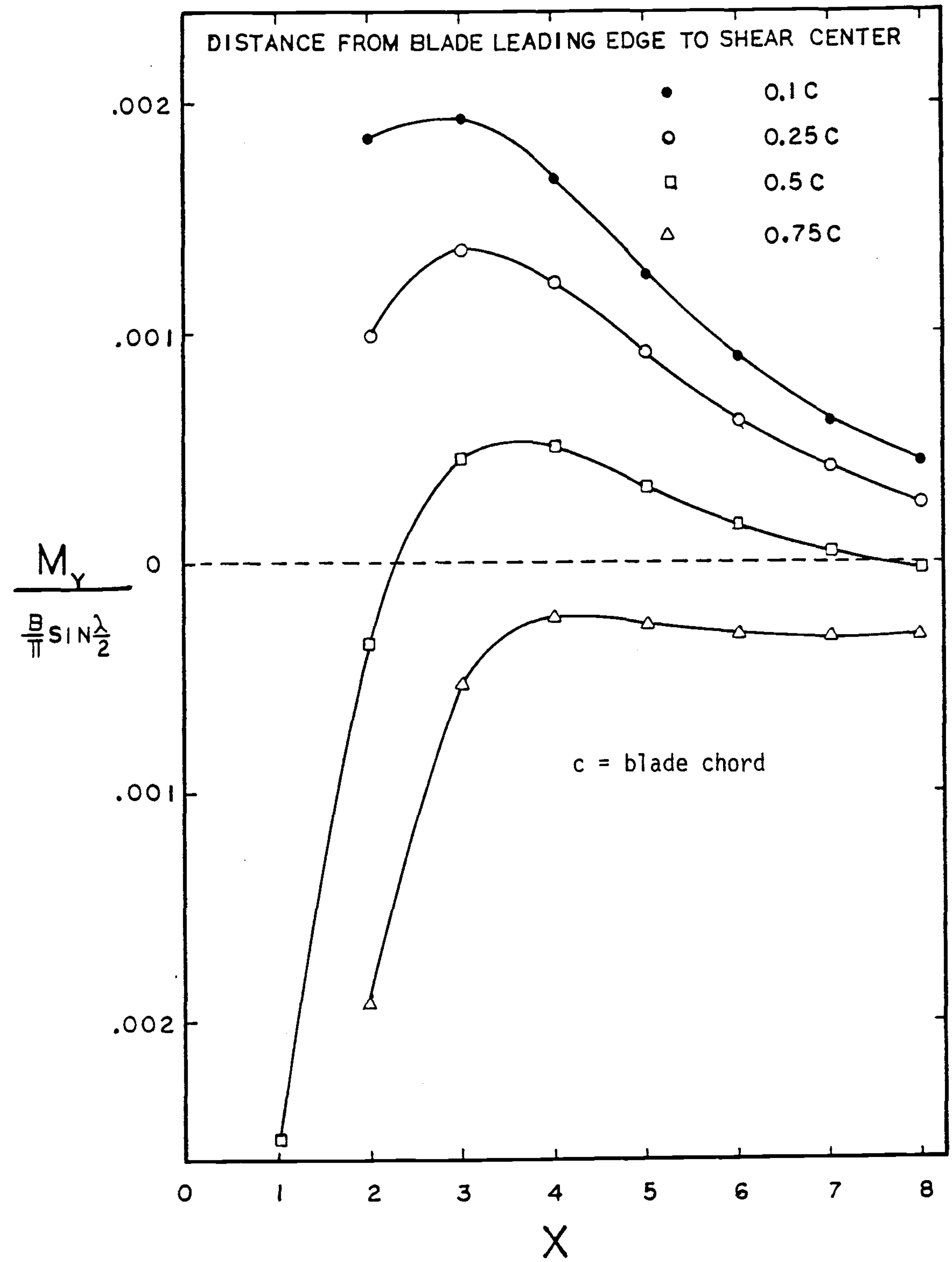

Figure 4.1 Variations of yaw moment per shadow width for selected locations of blade shear center, the Grumman WS33.

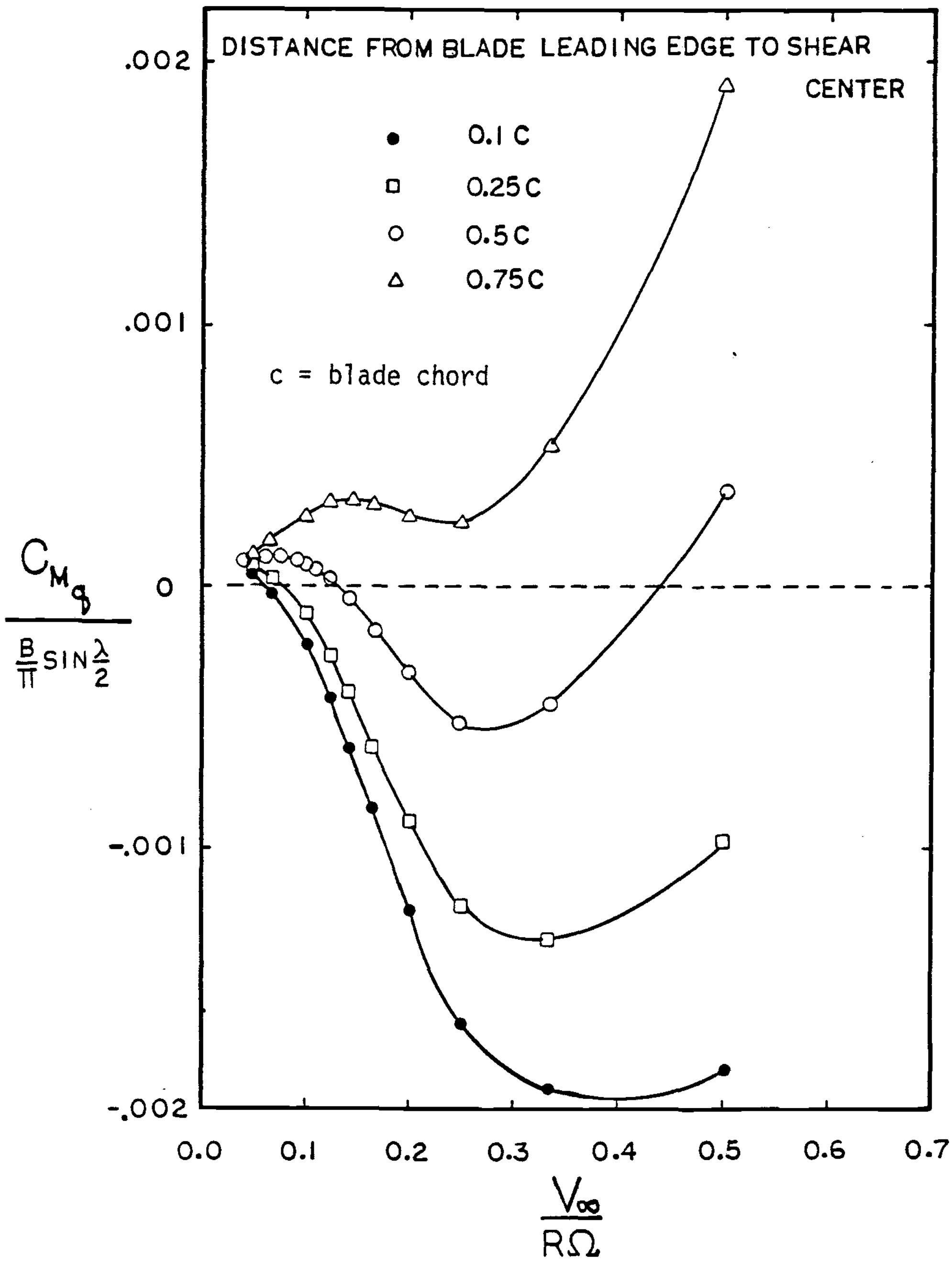

Figure 4.2 Variations of yaw moment per shadow width based on RPM for selected locations of blade shear center, the Grumman WS33.

The yaw forcing function due to tower shadow is obtained by subtracting the yaw moment created inside the tower shadow from the one created outside the tower shadow (i.e., 6 o'clock position and 12 o'clock position).

The yaw moment created by forces inside the tower shadow is shown in Figure 4.1. The effect of the shear center position on the yaw moment is that if the shear center is behind the 1/4 blade chord position, the yaw moment is decreased by the effect of this positive offset distance. Vice versa, the yaw moment will be increased if the shear center is ahead of the 1/4 blade chord.

For the purpose of illustration, the yaw moment normalized by RPM is considered. The yaw forcing function is given by

$$G_{04} = C_{Mq_1} - C_{Mq_2} \tag{2}$$

Here, $C_{Mq_1} = -M_{y_1}/X_1{}^2$

$$C_{Mq_2} = +M_{y_2}/X_2{}^2$$

Subscript 1 refers to the condition at the rotor outside the tower shadow in the opposite direction of the tower shadow region. Subscript 2 refers to the condition inside the tower shadow.

The plot of C_{Mq} versus the advance ratio ($V_\infty/R\Omega$) for different shear center positions are shown in Figure 4.2.

The yaw forcing is dependent upon: 1) the width of the tower shadow; 2) the velocity deficit in the tower shadow; 3) the shear center position; and 4) the power output of the rotor.

For zero offset distance, if the power increases continuously with wind speed, the in-plane force also is expected to increase continuously with wind speed. For such a situation the net yaw force produced by the tower shadow would always have the same sign since the wind speed in the tower shadow is less than in the free stream, then the in-place force in the tower shadow would be less than the in-plane force in the free stream. If the power peaked and then decreased with the wind speed, then the yaw force would change sign as the velocity increased. This effect has been observed on the Enertech 1500 and the Grumman WS33. As the peak power is achieved, the rotor yaw changes sign.

The yaw forcing function due to tower shadow with 40° shadow width, 50% velocity deficit, and 80% velocity deficit is shown in Figure 4.3.

Yaw Tracking Error

A yaw tracking error is defined as an angle which the rotor yaws away from the wind in a static condition. The static yaw angle of a downwind turbine is obtained by dividing the yaw forcing function with the stiffness coefficient of the rotor and nacelle. The yaw angles for the Grumman WS33 with a 40° shadow width and a 50% velocity deficit are given in Table 4.8. The predicted static yaw angle must be small according to the linear analysis. Therefore, any large predicted static yaw angle would indicate that the result is not accurate. This is shown in Table 4.8 at tip speed ratio equal to 3 and 4.

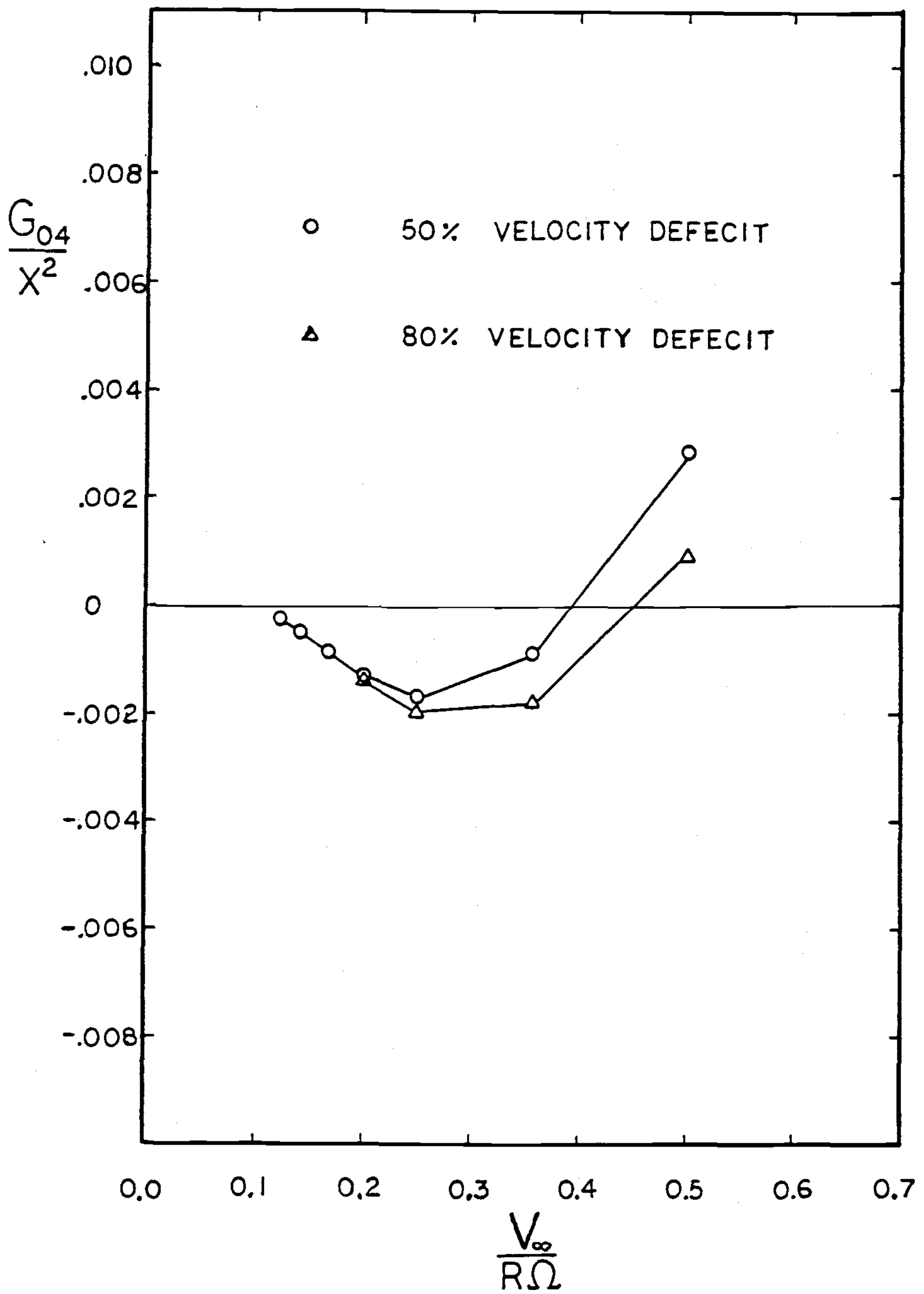

Figure 4.3 Variations of yaw forcing function based on RPM for selected values of velocity deficit, the Grumman WS33.

Table 4.8 Yaw tracking error for the Grumman WS33 with $\beta = 4°$, $e_1/C = 0.25$, $40°$ shadow width, and 50% velocity deficit.

X	γ (degree)
1	1.72
2	5.13
3	-21.76
4	-9.57
5	-6.47
6	-4.79
7	-3.42
8	-2.23

It can be seen that for this analysis the yaw angles depend on many variables. These variables are tower shadow width, velocity deficit, nacelle stiffness coefficient, the position of the shear center, and the power output of the rotor. With many uncertainties in these variables, especially the stiffness coefficient of the nacelle, there is no exact solution for the yaw tracking error. Thus, the values given in Table 4.8 are for the preliminary study of the yaw behavior of the system rather than the prediction of the magnitude of yaw tracking error.

Verification of the Analysis With the Test Data

The test data from the Rocky Flats Research Energy Center indicates that the Grumman WS33 has a yaw instability near start-up. The machine will rotate about the yaw axis from a downwind position to an upwind position. Although the analysis indicated that the Grumman WS33 in a downwind position is stable in yaw, it is possible that with a more accurate model of the nacelle, the system could be unstable in yaw near start-up. Thus, the focus of the analysis is directed to the yaw stability of a reverse turbine (a downwind turbine rotating to an upwind position). If the analytical result indicates that there is a region of stability for the reverse turbine, this result would verify the analysis.

Reverse turbine.

When a downwind turbine is rotating to the upwind position, the upper surface of the blade cross section will be facing the wind instead of the lower surface of the blade cross section. This reflection of the blade cross section will result in a negative angle of attack and pitch angle. The geometry of a reverse turbine blade and a conventional one are shown in Figure 4.4.

The shape of the hub (nose cone) of the Grumman WS33 is a hemisphere of 4.875 in. radius. The hub is considered as the forebody part of the nacelle for the turbine in an upwind condition.

The coefficients of the equation of motion in yaw for the reverse turbine including the hub effect are given in Table 4.9.

Table 4.9 Coefficients of the equation of motion in yaw for the reverse turbine, static tip deflection, and power coefficient.

X	m_{44_T}	C_{44}	k_{44_T}	ds (ft)	C_p
2	0.11853	0.04297	-0.007142	0.1092	-0.02089
3	0.26739	0.06995	-0.007207	0.08747	-0.04108
4	0.47577	0.10257	-0.000208	0.08034	-0.00645
5	0.74379	0.15582	0.002958	0.07593	0.08966
6	1.07157	0.24023	-0.008378	0.07193	0.1734
7	1.45922	0.33522	-0.019993	0.06809	0.18492
8	1.90672	0.44306	-0.025429	0.06458	0.12155

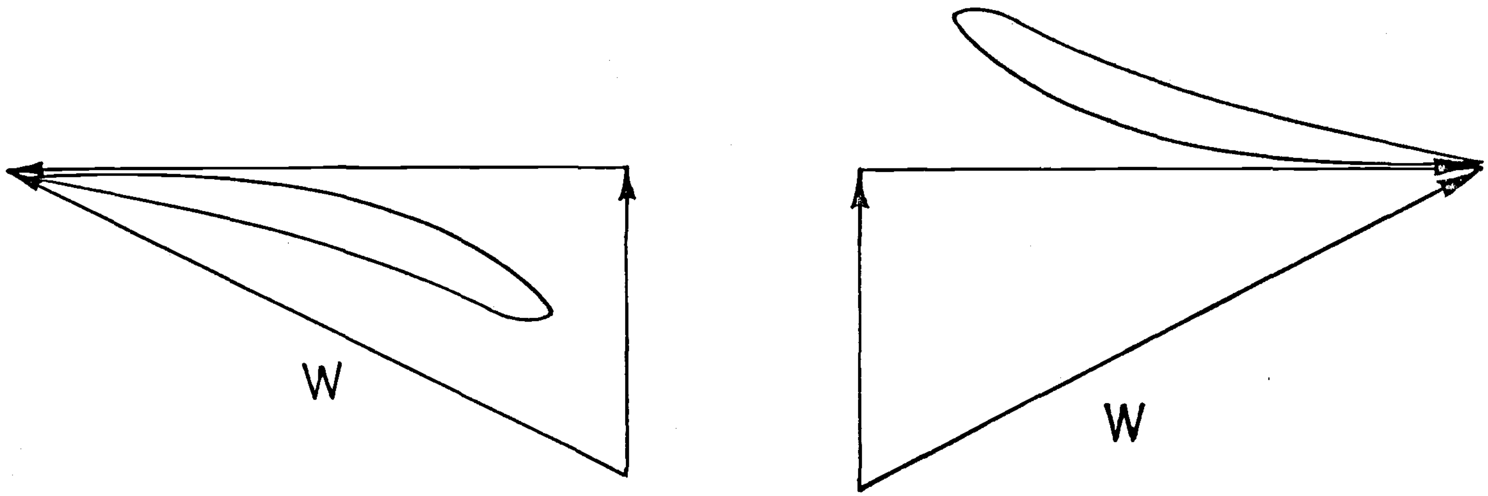

(a) conventional position

(b) reverse position

Figure 4.4 Velocity diagrams for a turbine blade section in a conventional position and in a reverse position.

As shown in Table 4.9, the system is unstable in yaw because of the negative yaw stiffness coefficient, except at the tip speed ratio equal to 5. This result indicates that for a certain operating condition if the Grumman WS33 rotates to an upwind position, it could operate as a stable upwind turbine. This yaw stability verifies the analysis.

The static flapwise tip deflections for the reverse turbine also are given in Table 4.9. When a downwind turbine with a coning angle (coning away from the wind) rotates to an upwind position, the blade will be coning to the wind. This negative coning yields a positive flapwise deflection (deflect in the wind direction) because the bending moments created by the aerodynamic force and the centrifugal force are in the same direction.

Yaw Stiffness Coefficient

The numerical value of the yaw stiffness coefficient for a small blade element is obtained and its distribution along the blade is examined to see what causes the destablizing effect. The yaw stiffness coefficient is the linearized variation of the yaw moment from its nominal value with respect to the yaw angle. This linearized variation of the yaw moment can be expressed as the product of the derivative of the aerodynamic force and its moment arm around the nacelle's yaw axis. Therefore, the stiffness coefficient is primarily dependent on the derivative of the aerodynamic force instead of the force itself.

The behavior of the aerodynamic force in the coordinates of the airfoil, normal and tangential to the blade chord, is observed. Let C_n and C_t be the force coefficients expressed in the normal and the tangential directions to the blade chord. Figures 4.5 and 4.6 show the plots of C_n and C_t versus the angle of attack α for the Grumman blade section in a conventional position (downwind turbine) and in a reverse position (reverse turbine). Note should be made that for the reverse turbine, although the blade is operating with a negative angle of attack, the sign convention of the analysis makes the aerodynamic forces on the blade result in a positive value.

Figures 4.7 and 4.8 show the distribution of the yaw stiffness coefficient along the blade at different tip speed ratios for the Grumman turbine in a downwind position. The destablizing effect (a negative value) of the yaw stiffness coefficient appears in figures 4.7 and 4.8 as a reverse hump curve starting at the blade tip at the tip speed ratio equal to 2 and moving in board as the tip speed ratio is increased. The further the reverse hump curve moves in board, the smaller the magnitude of the hump curve becomes. This hump curve starts at the portion of the blade which is experiencing a 14° angle of attack and stops at the portion of the blade which is experiencing an angle of attack greater than 21°. These two angles are the angles which the slope of the tangential force for a Grumman rotor blade changes sign.

For the Grumman turbine with a reverse position (staying upwind), the distribution of the yaw stiffness coefficient is shown in figures 4.9 and 4.10. It can be seen that the shape of the distribution of the yaw stiffness for a reverse turbine has the overall shape similar to the shape of the distribution of the yaw stiffness coefficient for a downwind turbine except it is upside down. The destabilizing effect becomes the stabilizing effect. Now the hump curves in figures 4.9

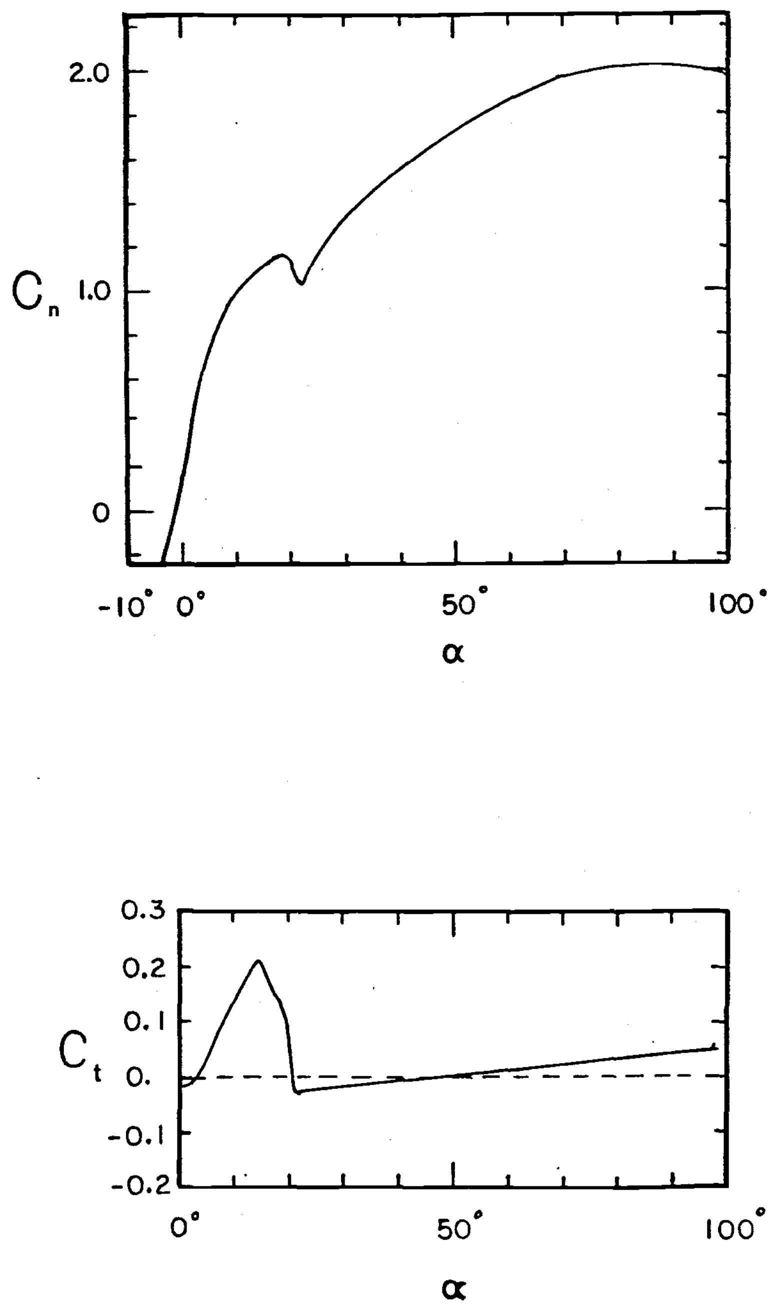

Figure 4.5 Force coefficients for the NACA 64_4-421 airfoil section in the airfoil's coordinates.

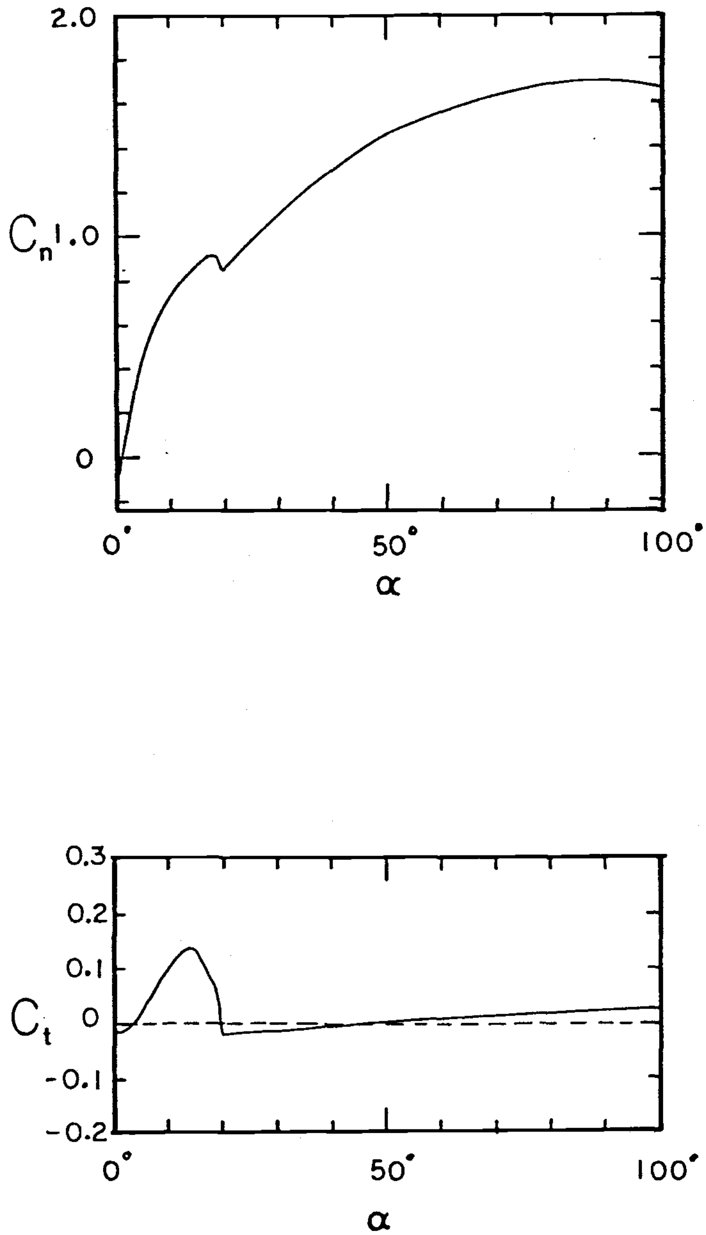

Figure 4.6 Force coefficients for the reverse NACA 64_4-421 airfoil section in the airfoil's coordinates.

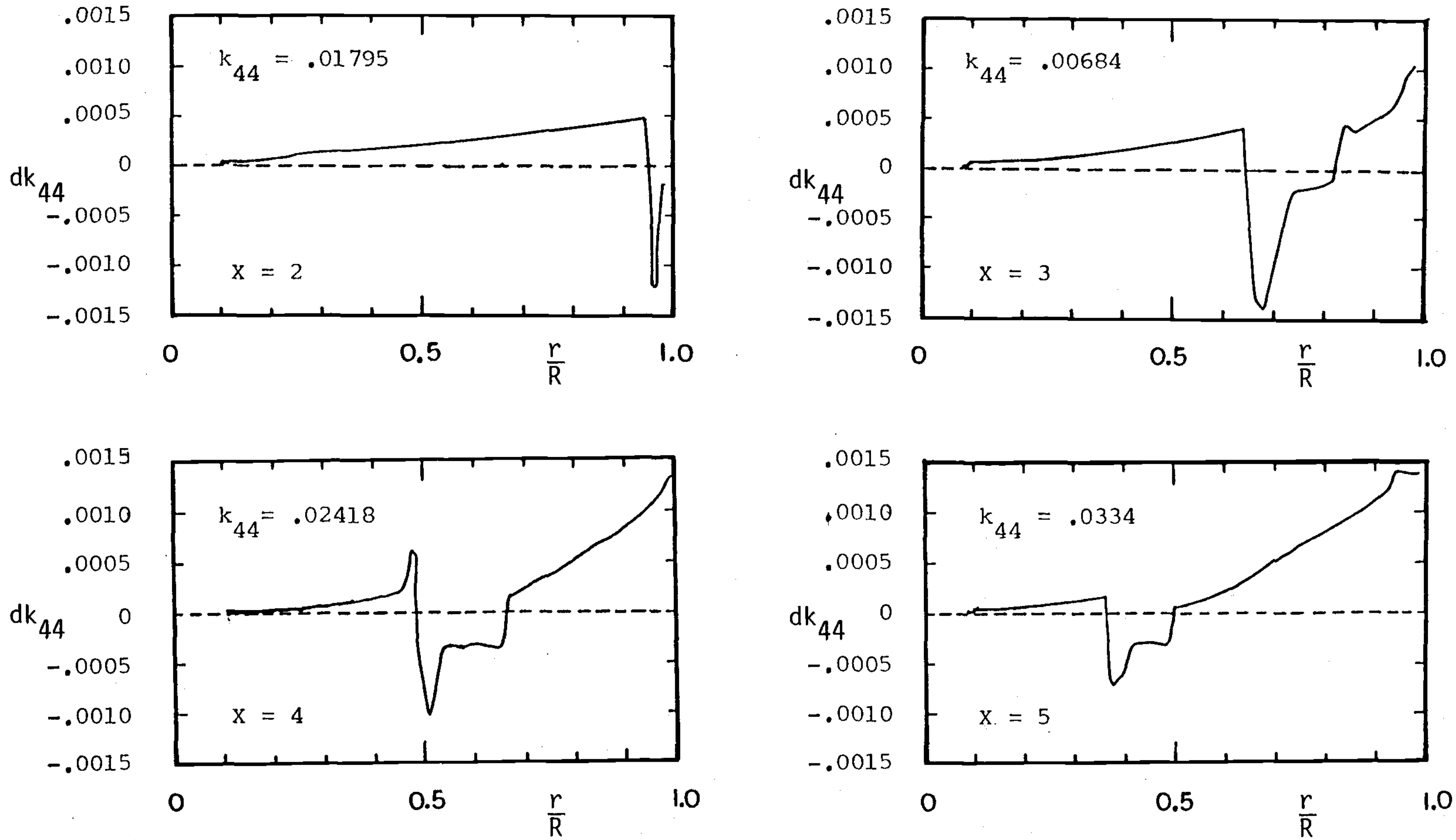

Figure 4.7 Spanwise distribution of yaw stiffness coefficient for the Grumman WS33.

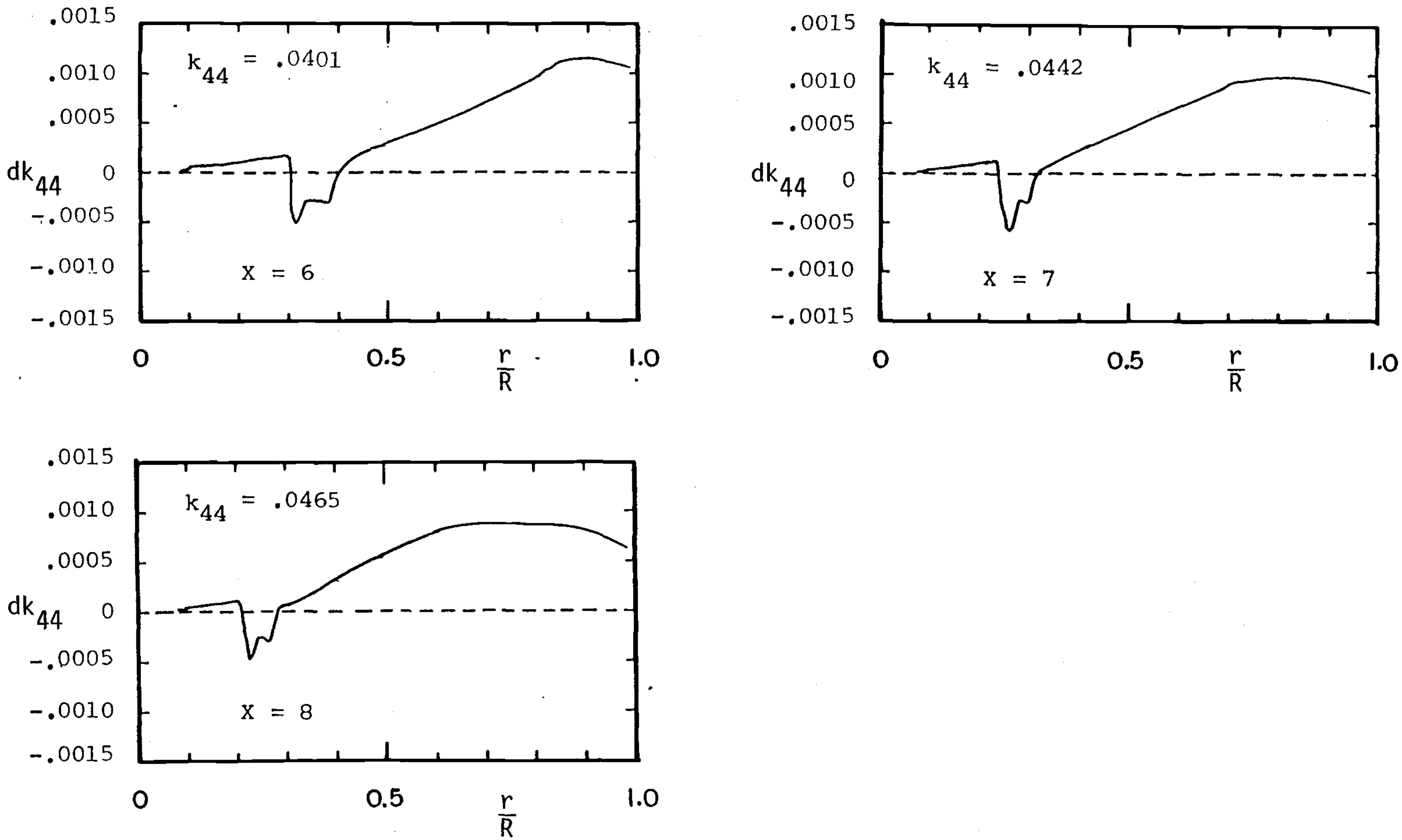

Figure 4.8 Spanwise distribution of yaw stiffness coefficient for the Grumman WS33.

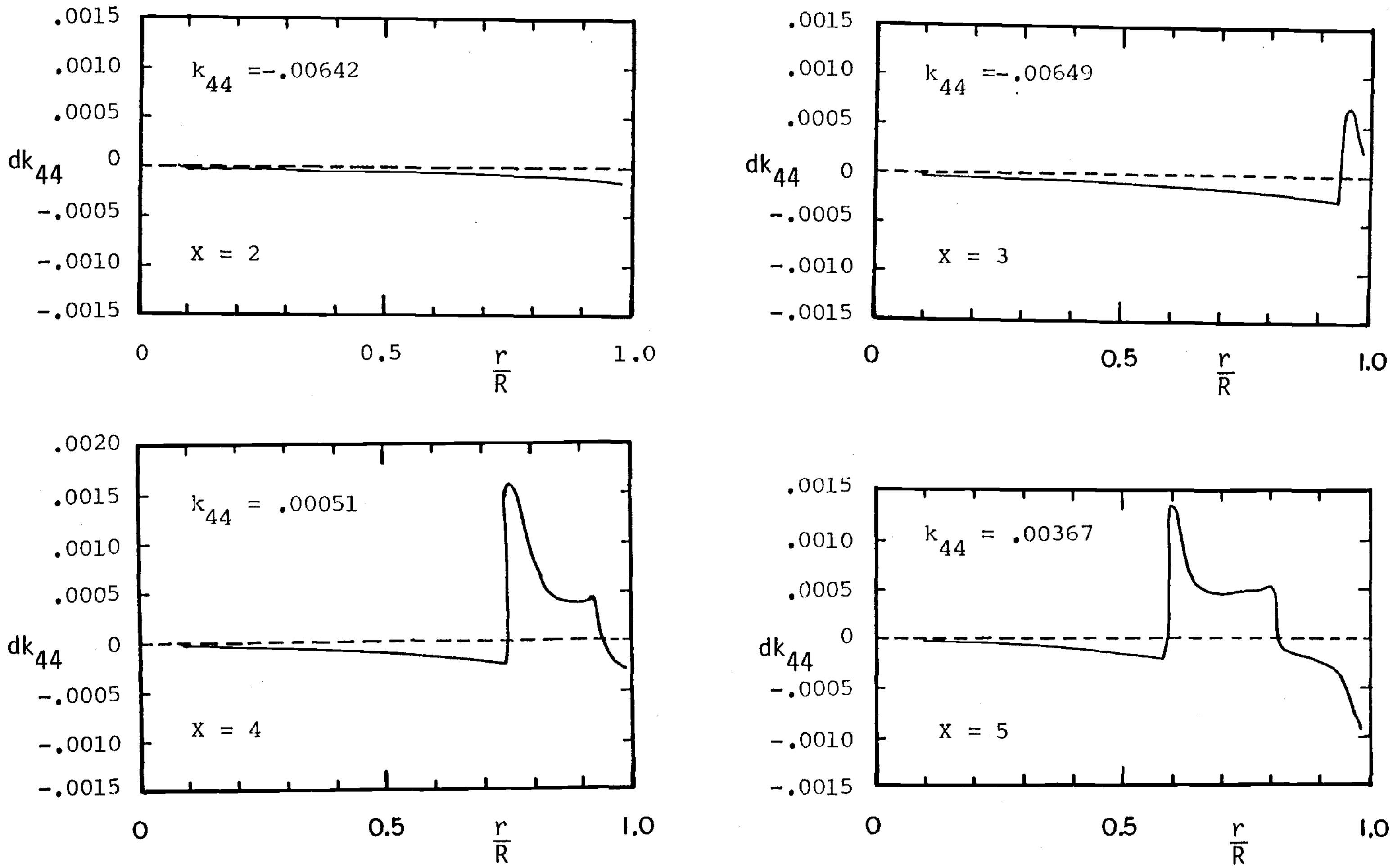

Figure 4.9 Spanwise distribution of yaw stiffness coefficient for the Grumman WS33 in a reverse position.

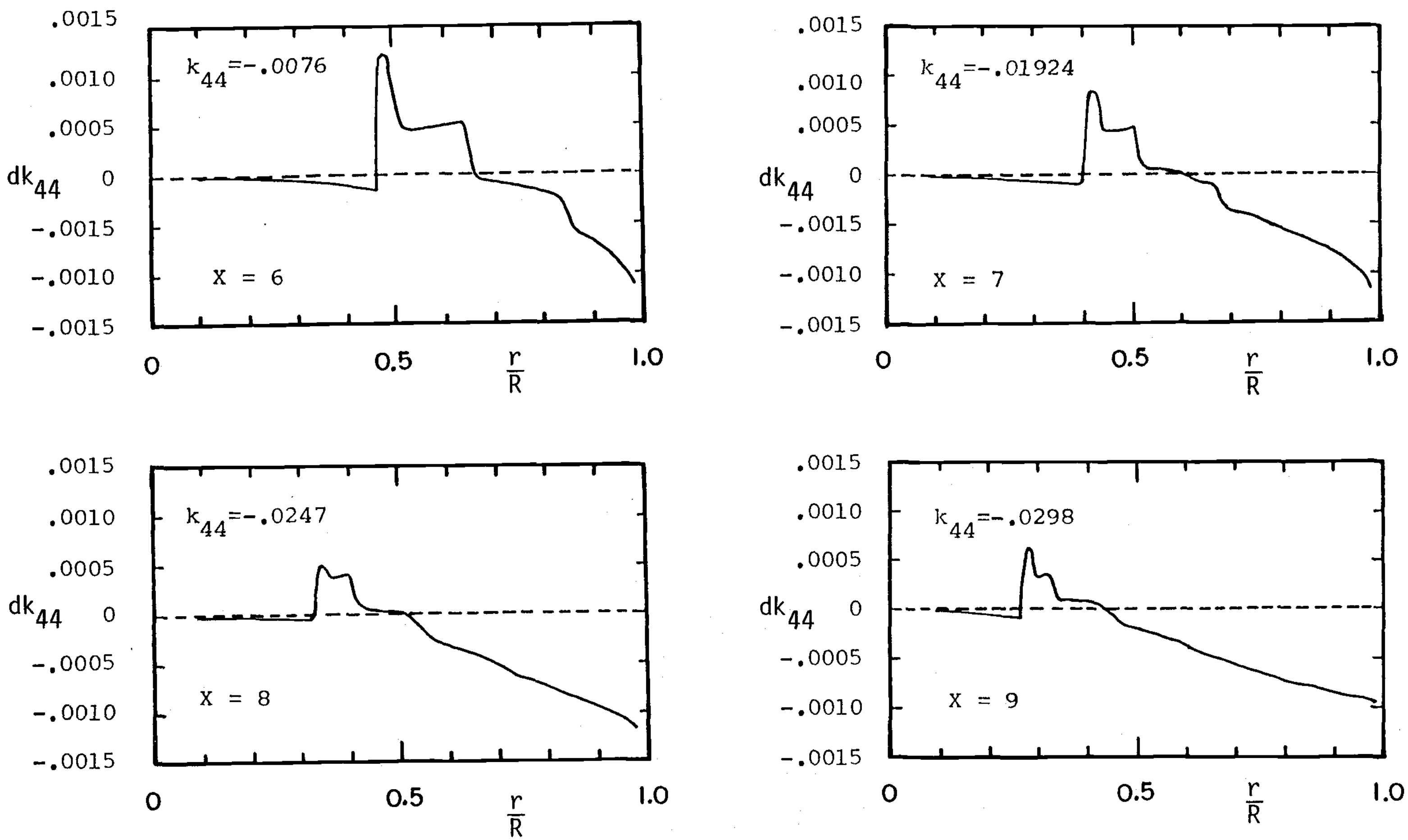

Figure 4.10 Spanwise distribution of yaw stiffness coefficient for the Grumman WS33 in a reverse position.

and 4.10 represent the stabilizing effect and this curve also is governed by the slope of the tangential force in Figure 4.6.

It would be difficult to analyze the yaw stiffness coefficient explicitly from its lengthy expression (see expression of k_{44} in Appendix IV). The purpose of this section is to analyze the yaw stiffness coefficient in more detail. To accomplish this task, a simple model of the rotor geometry is chosen and studied. The expression of the yaw stiffness coefficient can be expressed into three terms according to the sine of the coning angle: 1) terms with zero order of the sine of the coning angle; 2) terms with first order of the sine of the coning angle; and 3) terms with second order of the sine of the coning angle. They are

$$k_{44} = k_{44_0} + k_{44_1} \sin\rho + k_{44_2} \sin^2\rho \tag{3}$$

The expression of k_{44_0}, k_{44_1}, and k_{44_2} are given in Appendix V.

The expression of the stiffness coefficient is then simplified by assuming 1) the coning angle is zero; 2) the variation of the axial induction factor with yaw and yaw rate is zero; and 3) the shear center is at the 1/4 blade chord position (i.e., $e_1 = 0$). From this simple model, the stiffness coefficient can be expressed into two components: the component of the linear equation of the yaw moment due to an in-plane force (force in the rotor plane) and the one due to an out-of-plane force (force normal to the rotor plane). These two terms can be expressed as

$$k_{44} = \frac{3}{2} \int_{R_H}^{R} G_T \frac{\ell}{R} f_4^2 \frac{dr}{R} + \frac{3}{2} \int_{R_H}^{R} F_A \frac{r}{R} f_4^2 \frac{dr}{R} \tag{4}$$

where G_T is the derivative of the in-plane force and F_A is the derivative of the out-of-plane force. The expressions for the G_T and F_A are given in Appendix V.

From equation (4), it can be seen that the stiffness coefficient is dependent on the derivative of the in-plane and the derivative of the out-of-plane force with respect to the angle of attack. Furthermore, the sign of the distance from the yaw axis to the rotor, $\frac{\ell}{R}$, is a factor which controls the in-plane force term to be either the stablizing term or destabilizing term.

Figures 4.11 and 4.12 show the plots of the in-plane and the out-of-plane force coefficient versus the angle of attack for the Grumman turbine blade in a downwind position and in an upwind position.

The distribution of the first term and second term in equation (4) along the blade is superimposed on each other for a reverse turbine in Figure 4.13.

The effect of the flapwise deflection on the stiffness coefficient is investigated from Figure 4.13. Since this expression of the derivative of the out-of-plane force F_A consists of the sine of the local slope of flapwise deflection, the flapwise deflection is therefore essential for the out-of-plane force contribution to the stiffness coefficient. According to Figure 4.13, it can be seen that

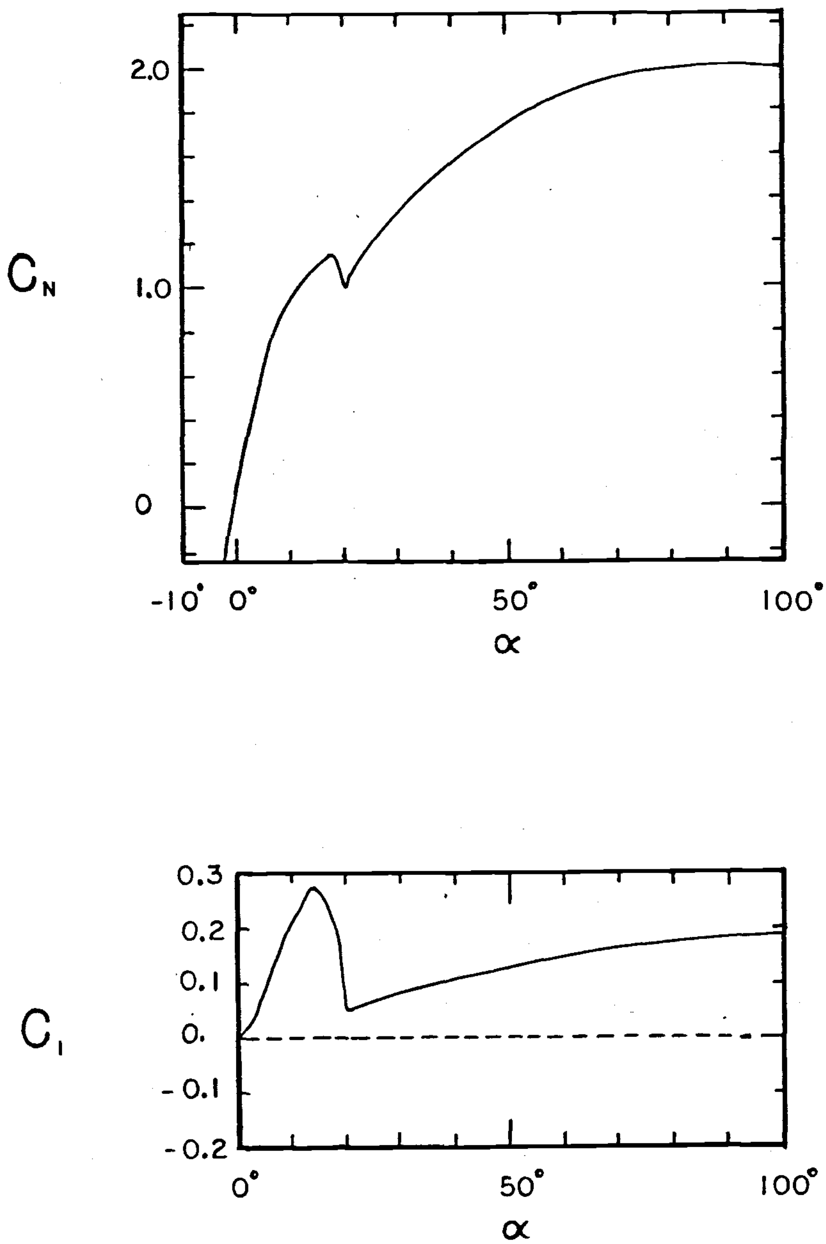

Figure 4.11 Force coefficients for the Grumman WS33's blade section in the rotor's coordinates versus angle of attack.

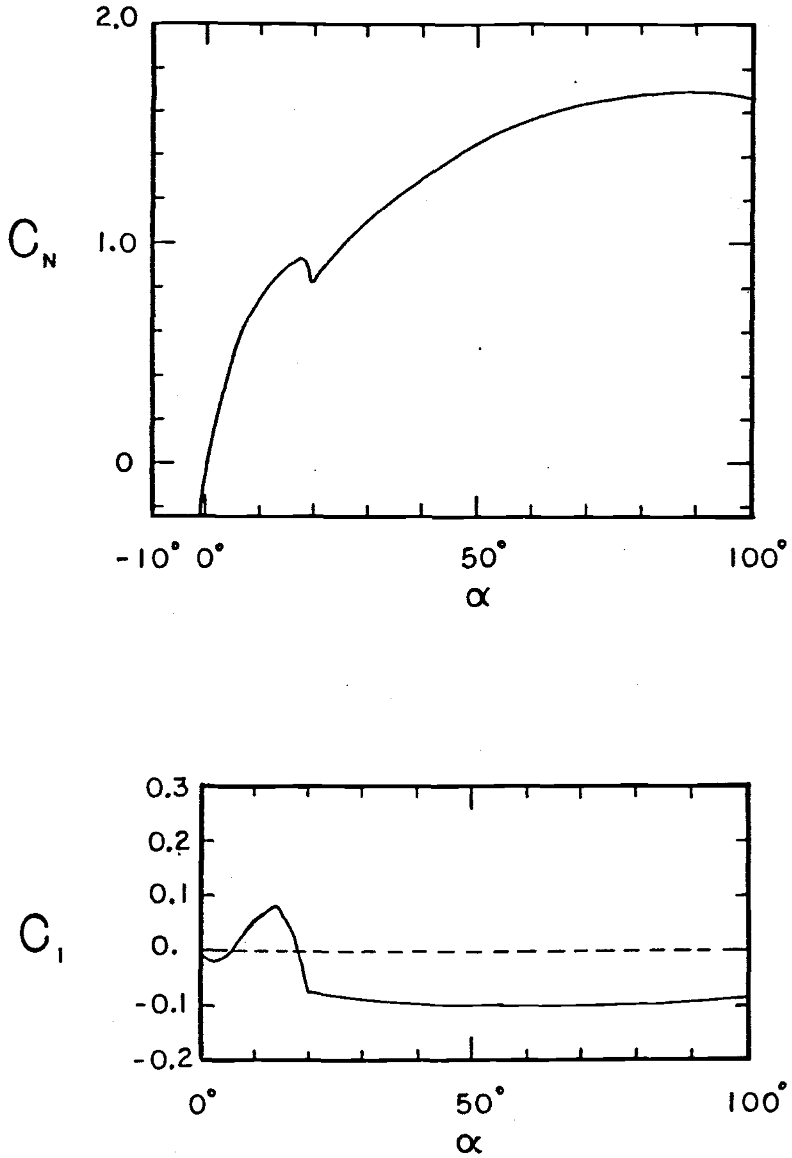

Figure 4.12 Force coefficients for the Grumman WS33's blade section, *in a reverse position, in the rotor's coordinates* versus angle of attack.

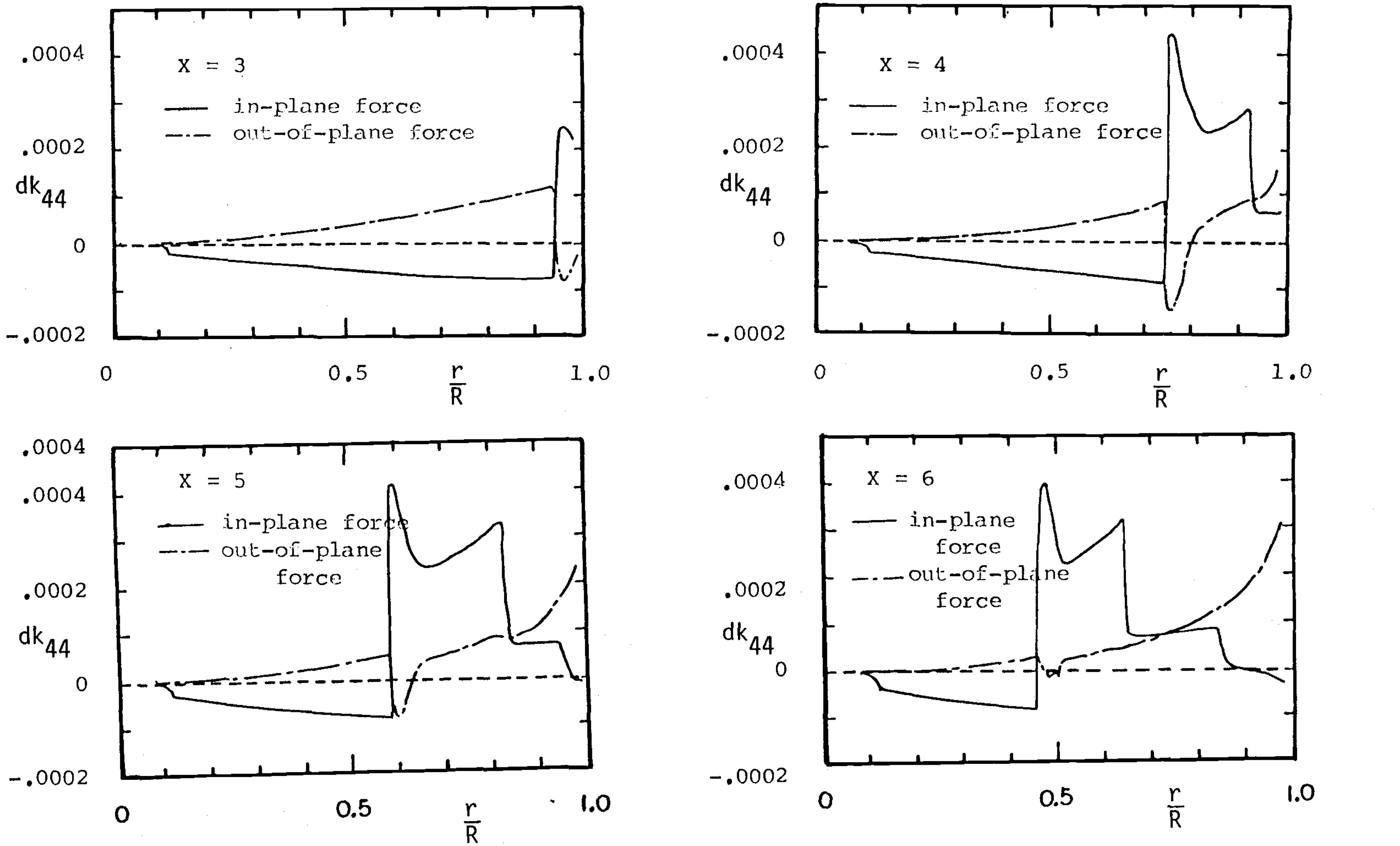

Figure 4.13 Spanwise distribution of components of yaw stiffness coefficient for the Grumman WS33 due to in-plane force and out-of-plane force.

though the magnitude of the flapwise deflection is small, the magnitude of the out-of-plane force term is almost the same order of the in-plane force term. Thus, the effect of the flapwise deflection on the stiffness coefficient is that it adds the contribution of the out-of-plane force to the stiffness coefficient.

The effect of the coning angle on the yaw stability can be investigated from the expression of the stiffness coefficient in equation (3). For small coning angle, the numerical value of the third term (term involved with square of sine of the coning angle) in equation (3) is negligible and k_{44_1} turns out to be a positive definite number. Therefore, the sign of the coning angle is the indication whether $k_{44_1} \sin \rho$ will act as a stabilizing term or a destabilizing term.

In conclusion, the yaw stability of the system can be improved by adding a positive coning angle to the system. The numerical values of the yaw stiffness coefficient for different values of tip speed ratio are given in the sensitivity study section.

Sensitivity Study

The yaw stability of the wind turbine system in this analysis is primarily determined by the sign and magnitude of the yaw stiffness coefficient of the rotor and the nacelle. Thus, the sensitivity of the yaw stiffness coefficient to the selected input parameters is studied.

In the previous sections, the coefficients for the equation of motion are given by

$$k_{\eta\eta} = \frac{\text{stiffness coefficient}}{1/2\,\rho_\infty\,V_\infty^{\,2}R^3}$$

However, the turbine is operating at a constant rotor speed in the test condition. Therefore, for the purpose of comparison, the coefficents normalized by RPM and the advance ratio are used.

The coefficient based on RPM is related to the coefficient normalized by the dynamic pressure by

$$K_{\eta\eta} = \frac{\text{stiffness coefficient}}{1/2\,\rho_\infty(R\,\Omega)^2R^3} = \frac{k_{\eta\eta}}{X^2}$$

The advance ratio is seen to be the reciprocal of the tip speed ratio.

$$J = \frac{V_\infty}{\Omega R} = \frac{1}{X}$$

Because of the linearized system, the stiffness coefficient of the rotor and the nacelle can be separately studied.

Rotor stiffness coefficient.

The sensitivity of the rotor stiffness coefficient in yaw normalized by RPM to the selected input parameters for the Grumman WS33 is examined.

Torsional stiffness. The effect of the blade's torsional stiffness (blade's shear modulus G) on the yaw stiffness coefficient is examined. The only effect of the blade's torsional stiffness appears in the pitch equation (of the four-degree-of-freedom system).

Unless the static pitch deflection is significantly different from the zero value, there will not be any effect on the yaw equation.

Pitch angle. Figure 4.14 shows the plots of the yaw stiffness coefficient versus the advance ratio for different values of pitch angle. First, let us consider the curve of the yaw stiffness coefficient for pitch angle equal to 4 as the typical case. The stiffness coefficient increases as the wind velocity is increasing to a certain value. Then the stiffness coefficient starts to decrease when the wind velocity is further increased because the destabilizing effect due to the negative slope of in-place force is starting to dominate (i.e., the blade is experiencing the angle of attack from 14° to 20° near the tip). When the wind velocity is further increased, the stiffness coefficient then starts to increase again because the stabilizing effect due to the stall region (a positive slope of in-plane force versus angle of attack) dominates the destablizing effect. Finally, when the whole blade is stalled, the stiffness coefficient is controlled by the stabilizing term due to a positive slope of the forces (in-plane force and out-of-plane force) versus angle of attack. This results in a large magnitude of the stiffness coefficient in high wind.

With the understanding of the nature of the stiffness coefficient related to the wind velocity, the effect of the pitch angle on the stiffness coefficient is investigated. Increasing pitch angle lowers the angle of attack. Thus, increasing the pitch angle delays the destabilizing effect in the stiffness coefficient at the same wind condition. For $\beta = 6°$ and $10°$, the stiffness coefficient is increased

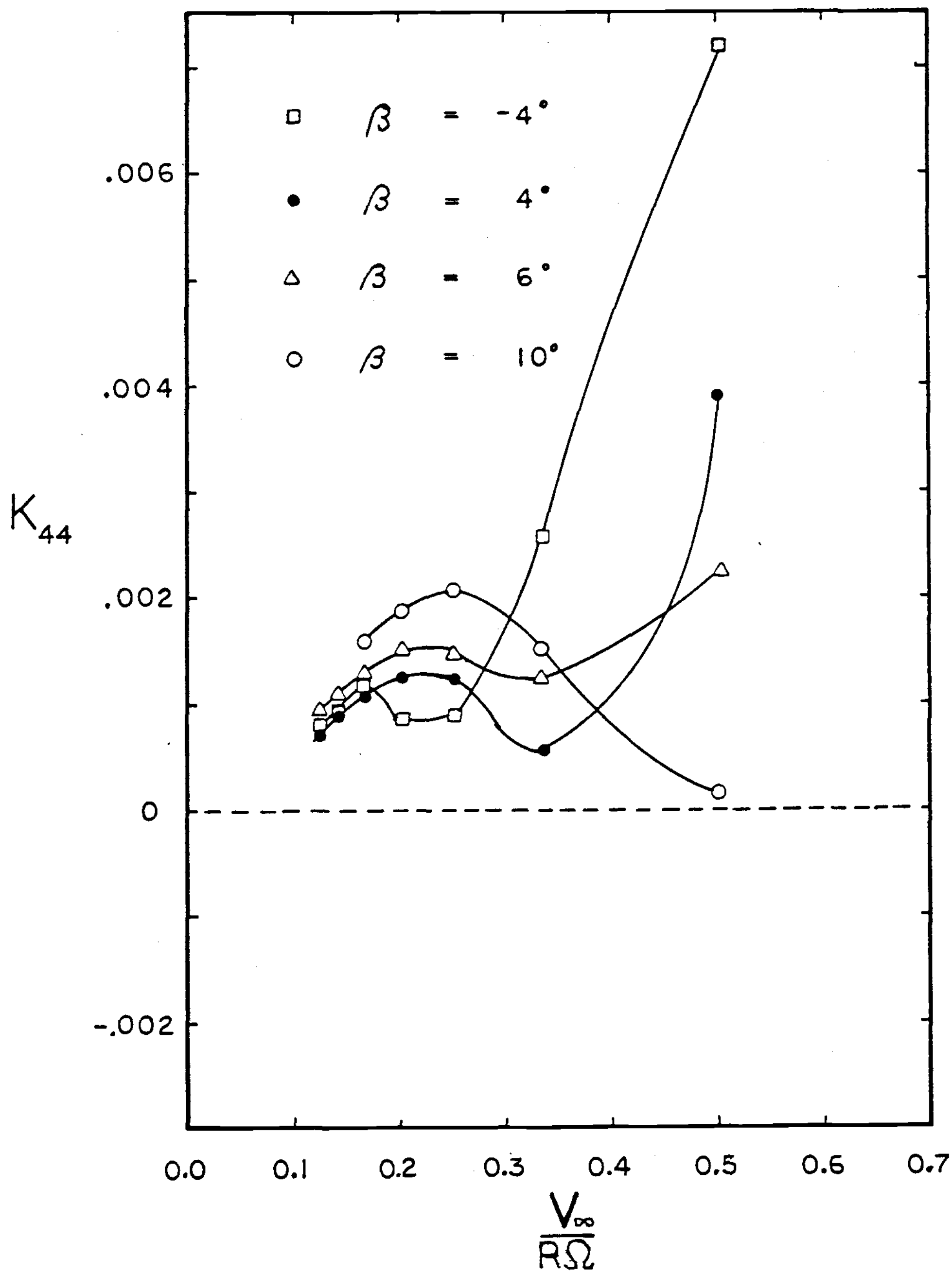

Figure 4.14 Effect of pitch angle on yaw stiffness coefficient for the Grumman WS33.

at a low wind condition and decreased at a high wind condition. For the negative pitch angle, the opposite is true. That is, the curve is shifted to the left-hand side. The stiffness coefficient is decreased at the advance ratio 0.175 to 0.25 and then increased again. The blade experiences the destabilizing effect at lower wind than the one with a positive pitch angle.

Modulus of elasticity and flapwise deflection. The flapwise deflection depends on the blade stiffness (modulus of elasticity E), the centrifugal force, and the aerodynamic load. The static tip flapwise deflections for the Grumman machine with $E = 10 \times 10^6$ psi and $E = 20 \times 10^6$ psi are given in Figure 4.15. The stiffer blade has a smaller deflection.

According to Figure 4.16, the stiffer blade causes the stiffness coefficient in yaw to increase except at the advance ratio equal to 0.5. However, under the values of blade stiffness considered, the increasing of this stiffness coefficient in yaw is negligibly small.

Although the stiffness coefficient in yaw is less sensitive to the changes of flapwise deflection, the flapwise deflection itself is an essential part of the stiffness coefficient for the contribution of the out-of-plane force.

Speed. The effect of a change in rotor speed on the yaw stiffness coefficient is considered. Figure 4.17 shows the curves of the yaw stiffness coefficient for rotor speeds of 60, 74, and 90 rpm. Increasing the rotor speed slightly increases the nondimensional yaw stiffness coefficient at a high wind condition but slightly decreases the nondimensional yaw stiffness coefficient at a low wind condition.

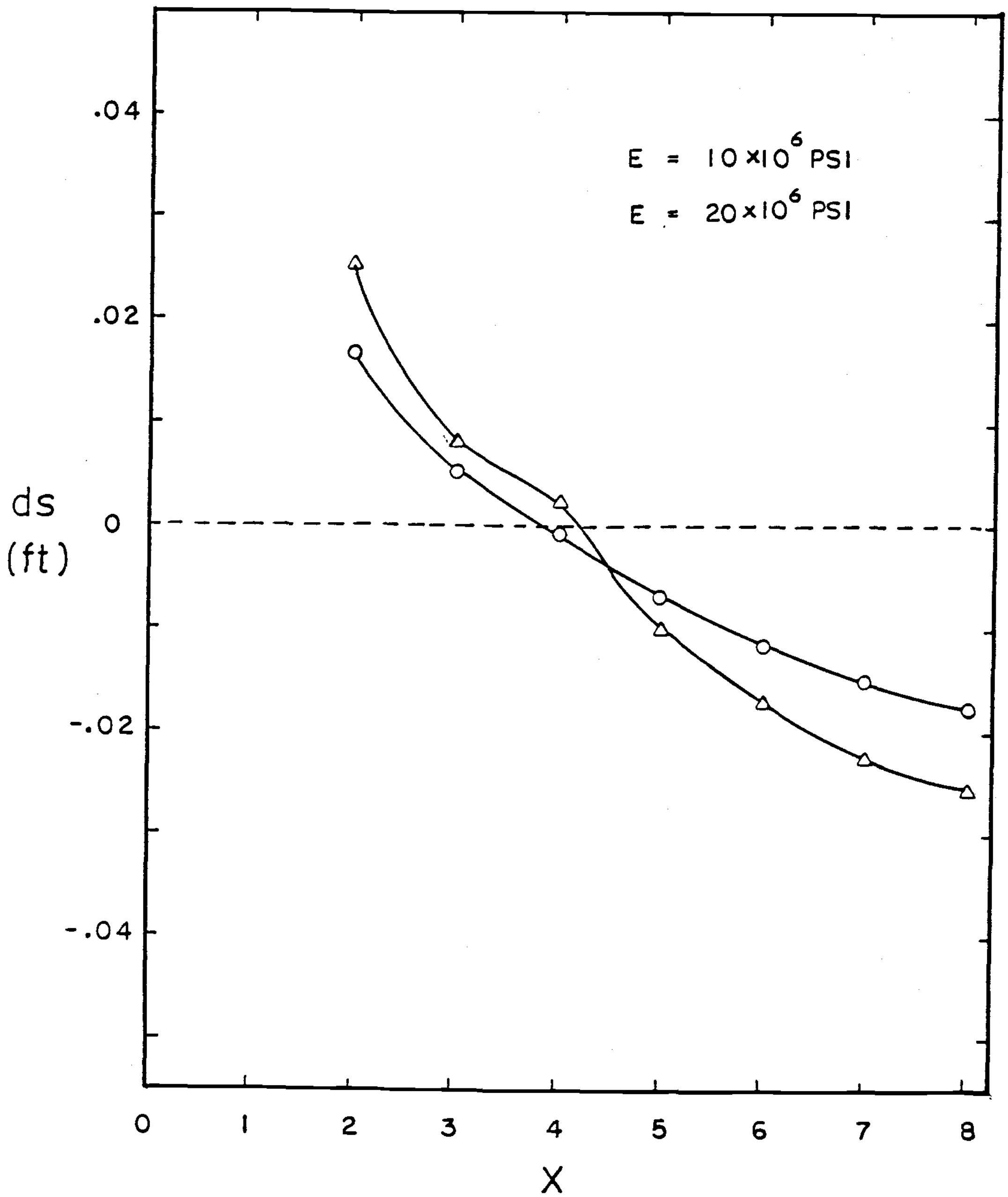

Figure 4.15 Effect of modulus of elasticity on static flapwise tip deflection for the Grumman WS33.

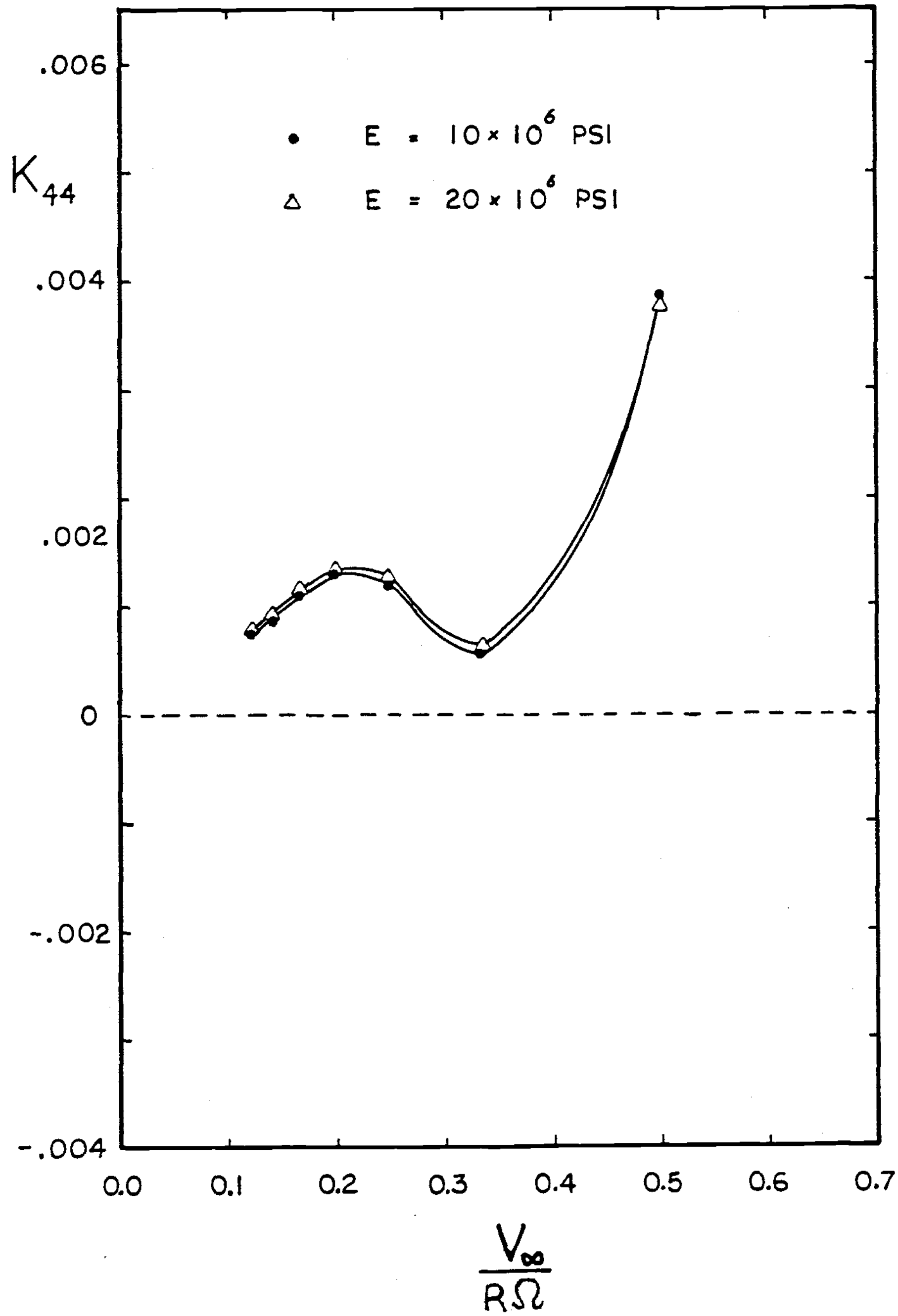

Figure 4.16 Effect of modulus of elasticity on yaw stiffness coefficient for the Grumman WS33.

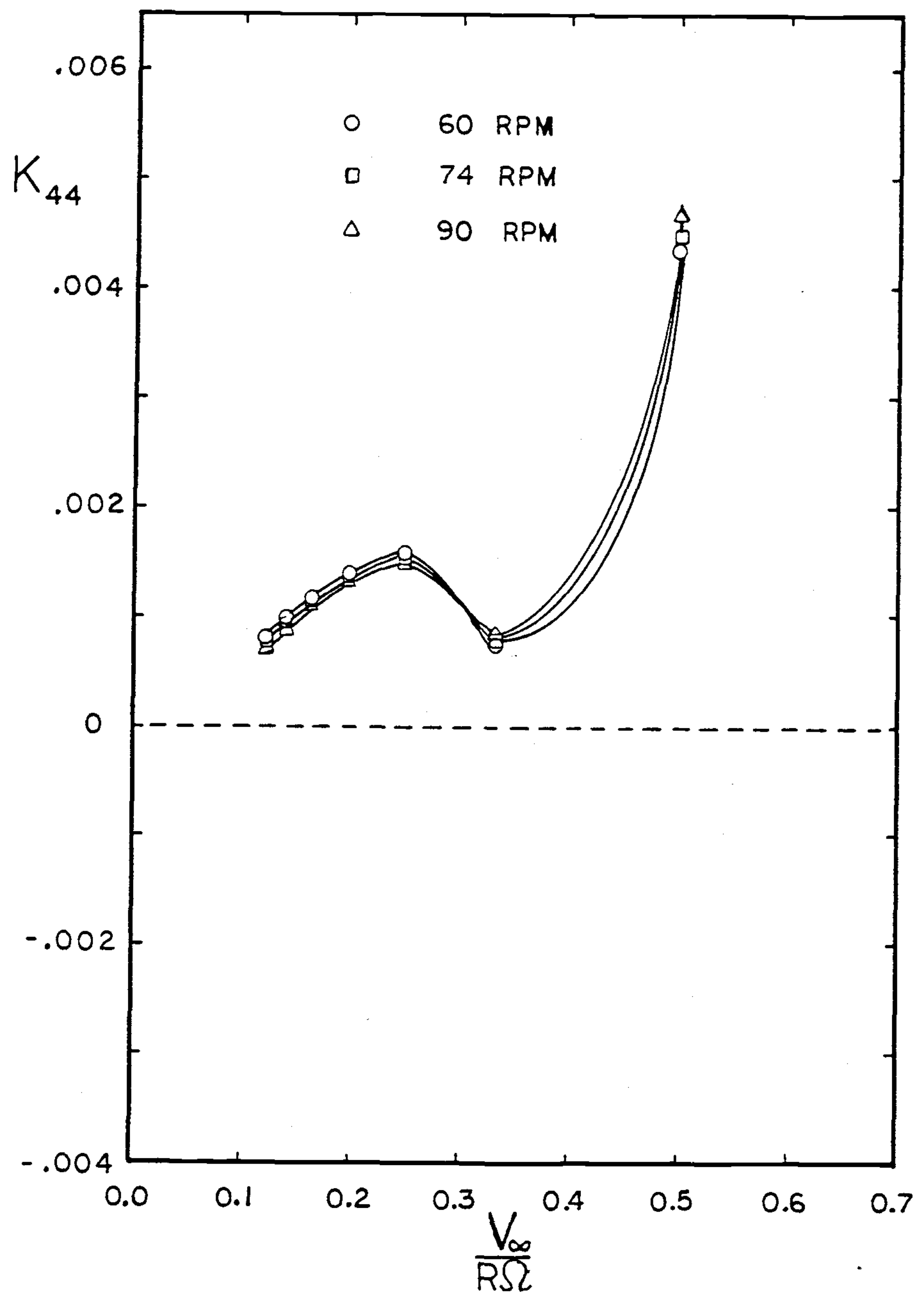

Figure 4.17 Effect of rotor speed on yaw stiffness coefficient for the Grumman WS33.

Note should be made that the different curves of the nondimensionalized yaw stiffness coefficient are based on the different rotor speeds. In order to compare the net difference in the yaw stiffness coefficient due to change in rotor speed, the nondimensional yaw stiffness coefficients in Figure 4.17 are corrected so that they are based on the same rotor speed, 74 rpm. These conditions are shown in Figure 4.18. The relative values of these yaw stiffness coefficients are large.

Shear center position. The stiffness coefficient in yaw with shear center positions at 10%, 25%, 50%, and 75% of the blade chord, measured from the leading edge of the turbine blade, are shown in Figure 4.19. The stiffness coefficient is increased by moving the shear center closer to the trailing edge. This effect is significant at a higher wind condition.

Distance from the rotor to the nacelle yaw axis. The distance from the rotor to the nacelle yaw axis is varied to see its effect on the stiffness coefficient in yaw. Figure 4.20 shows the curves of the stiffness coefficient versus the advance ratio for $\ell/R = 0.1, 0.176, 0.25$, and 0.5. The effect of this parameter is small at a low wind condition and rather significant at a high wind condition. For the advance ratio less than 0.16, the stiffness coefficient is increased when ℓ/R is increased. For the advance ratio greater than 0.16, the effect is reversed: increasing ℓ/R decreases the stiffness coefficient.

Coning angle. From the previous section, it was found that the coning angle is one of the important parameters in determining the

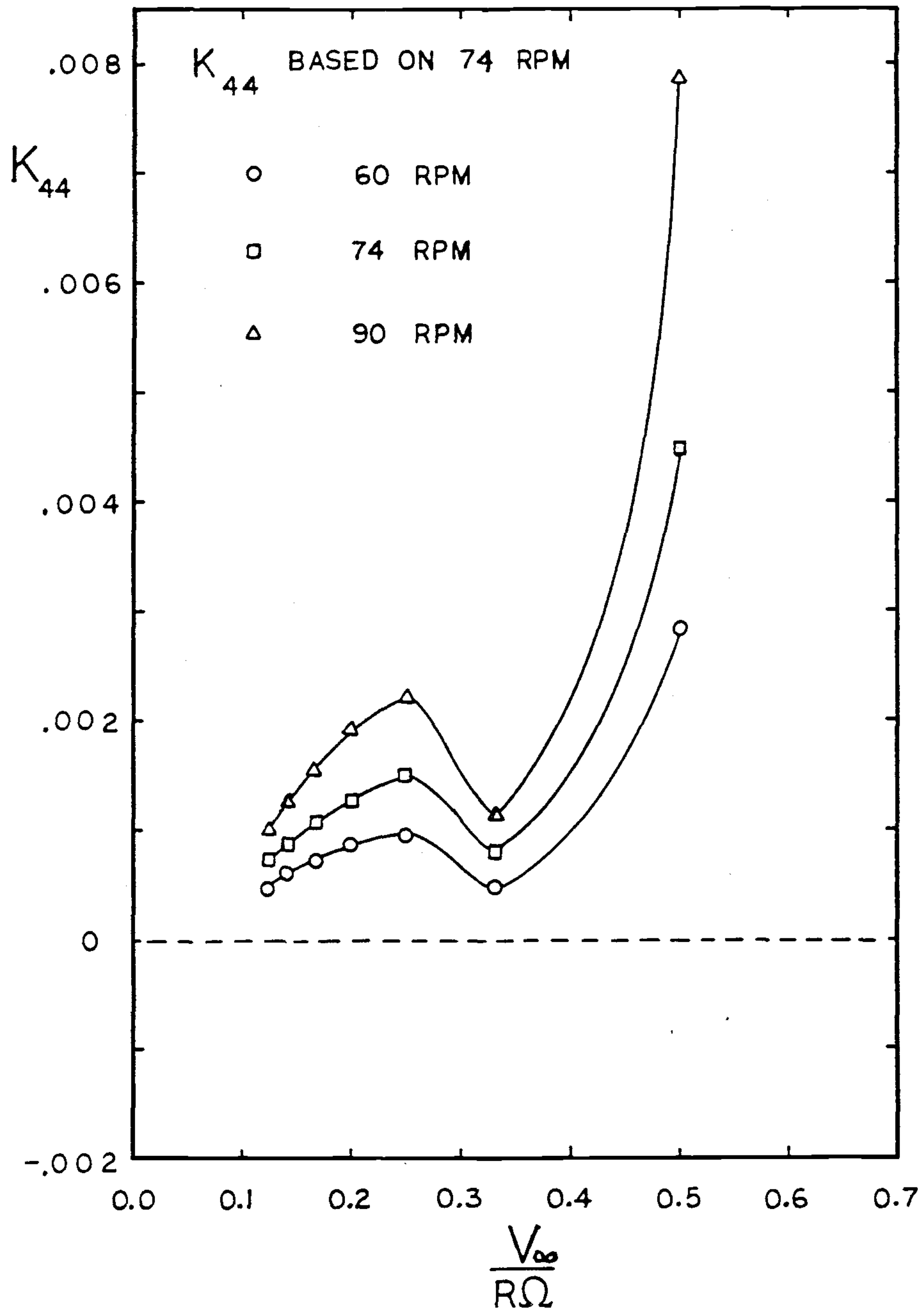

Figure 4.18 Effect of rotor speed on yaw stiffness coefficient based on the same RPM for the Grumman WS33.

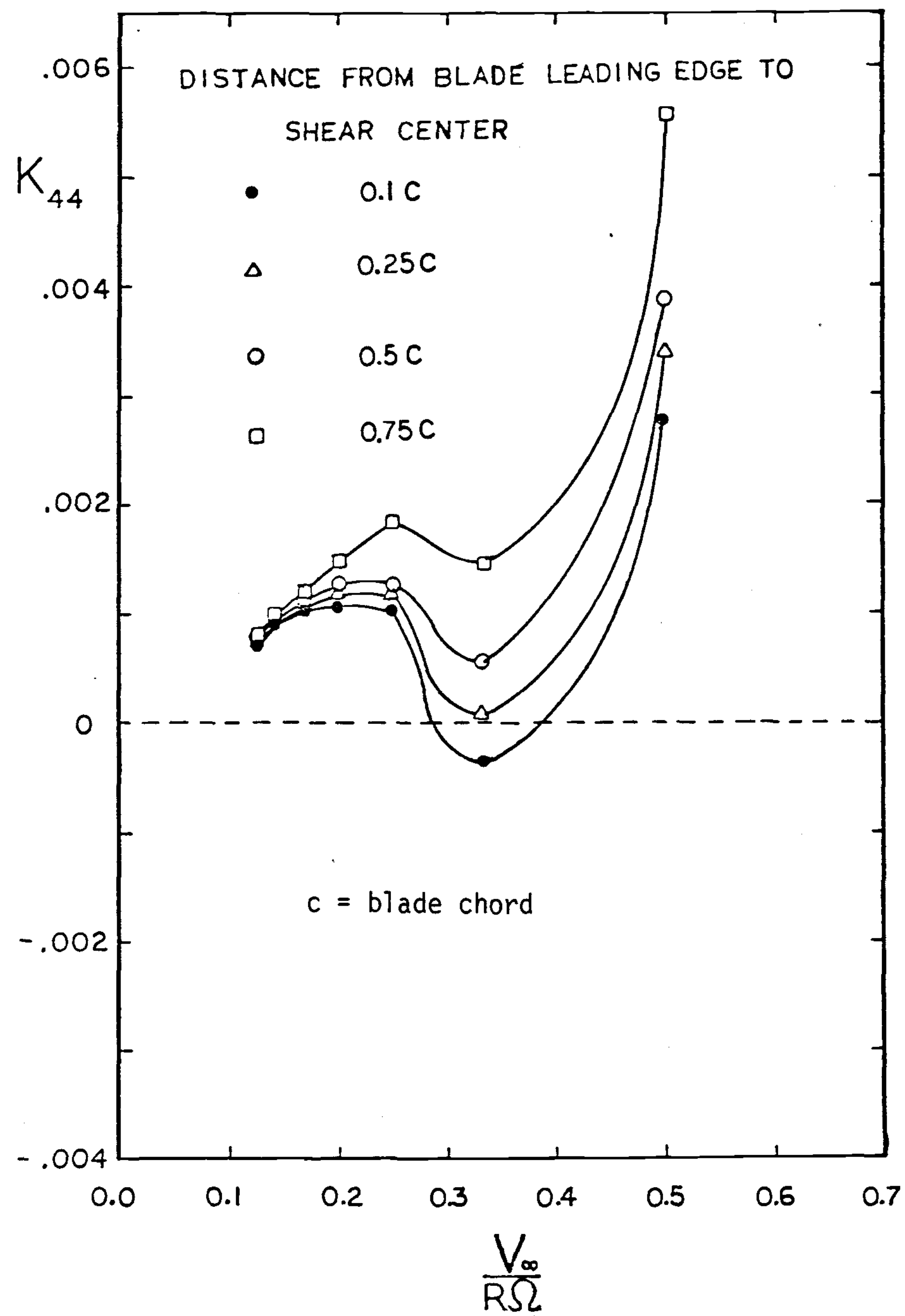

Figure 4.19 Effect of the location of the blade cross section's shear center on yaw stiffness coefficient for the Grumman WS33.

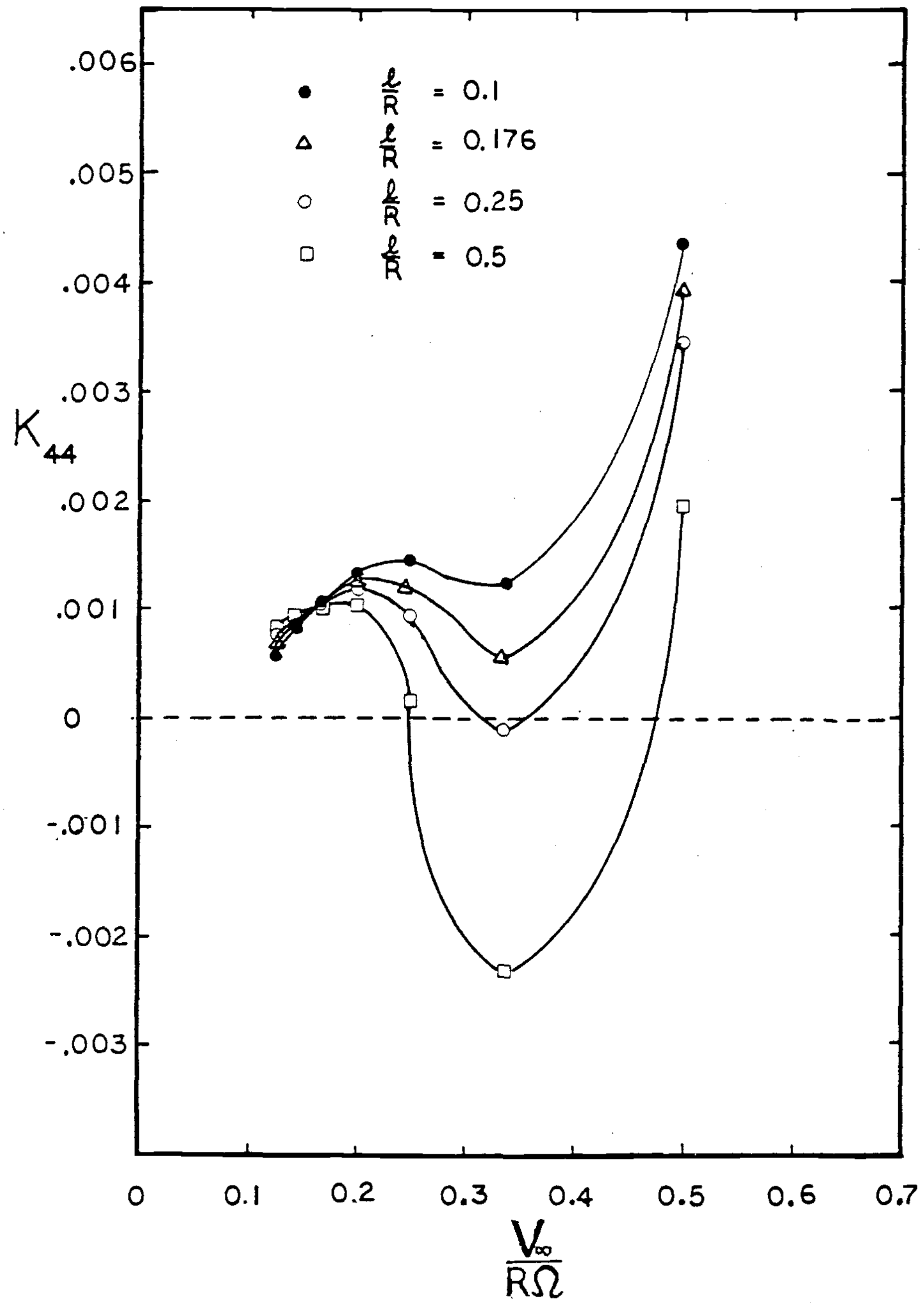

Figure 4.20 Effect of the location of the yaw axis relative to the rotor plane on yaw stiffness coefficient for the Grumman WS33.

yaw behavior. The positive coning angle adds the stablizing effect to the stiffness coefficient in yaw. The vice versa is true: the negative coning angle causes the destabilizing effect to the system. This coning angle effect is illustrated in Figure 4.21.

Figure 4.21 shows the system is unstable for a negative coning angle (ρ = -3.5°), partially stable for a zero coning angle, and stable for a positive coning angle (ρ = 3.5°, 10°).

Stiffness coefficient of the nacelle.

The nacelle plays an important role in the yaw stability of the system because of its largest negative value in the stiffness coefficient. So, reducing the negative value of its stiffness coefficient would mean improving the yaw stability.

The effect of the distance from the rotor to the nacelle yaw axis on the stiffness coefficient of the nacelle is examined.

The stiffness coefficients of the nacelle with different values of the distance from the rotor to the nacelle yaw axis are given in Figure 4.22. Increasing ℓ/R decreases the yaw stiffness coefficient of the nacelle. So, the yaw stability can be improved by increasing the distance from the rotor to nacelle yaw axis. However, for a given nacelle, the distance from the yaw axis to the rotor is limited by the space necessary to install the generator unit. In addition, the effect of the ℓ/R on the nacelle will be dominated by the rotor for the combined system (rotor and nacelle), especially for a high wind condition (low tip speed ratio). These effects are shown in Figure 4.23 for the stiffness coefficient for the rotor and nacelle.

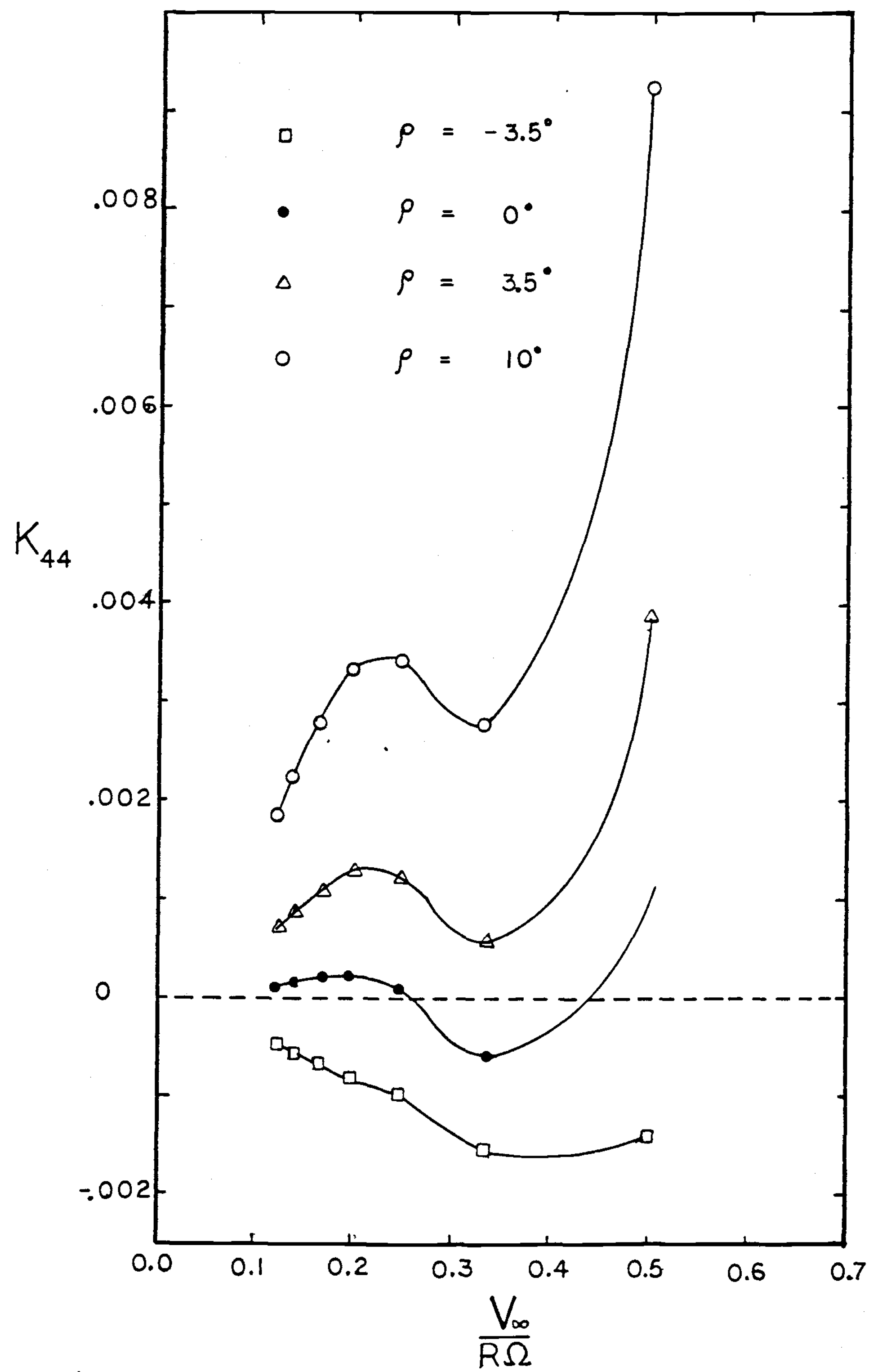

Figure 4.21 Effect of coning angle on yaw stiffness coefficient for the Grumman WS33.

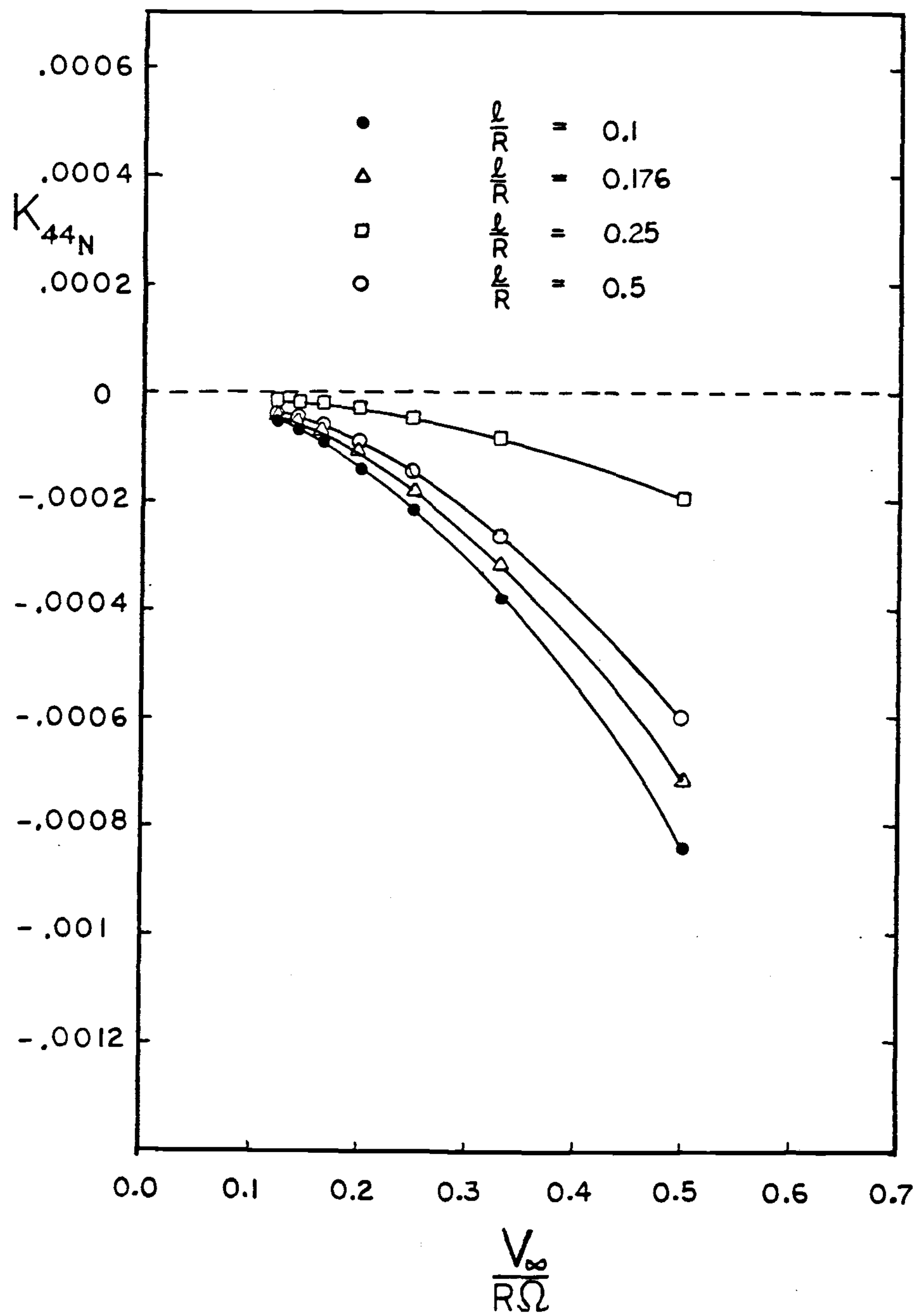

Figure 4.22 Effect of the location of the yaw axis relative to the rotor plane on yaw stiffness coefficient of the Grumman WS33's nacelle.

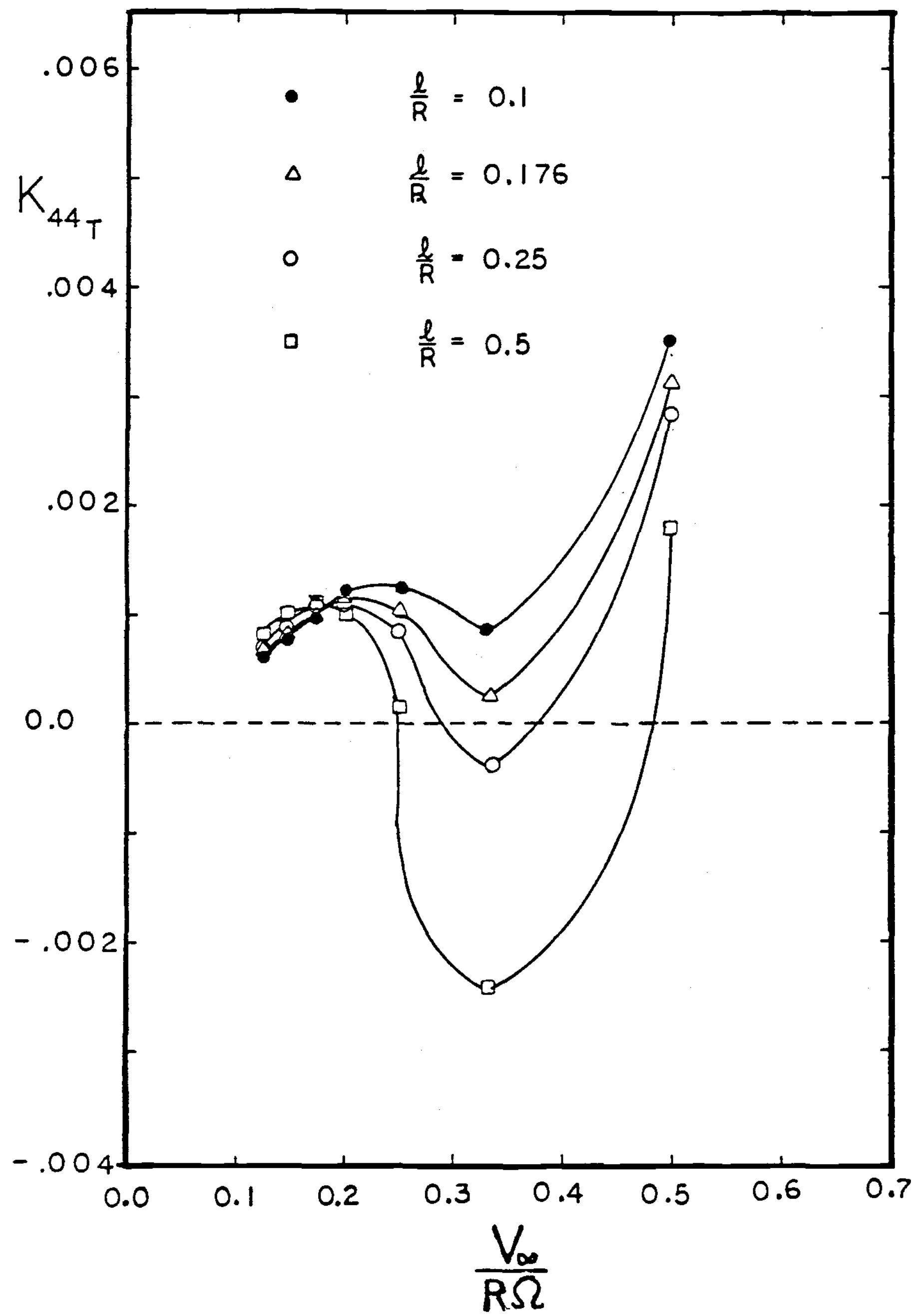

Figure 4.23 Effect of the location of the yaw axis relative to the rotor plane on yaw stiffness coefficient of the nacelle and rotor for the Grumman WS33.

Analytical Results for the Enertech 1500

The Enertech 1500 was used as a test case in this section. The Enertech 1500 and the Grumman WS33 are basically the same, according to the type of wind turbine: both of them are three-bladed horizontal axis downwind wind turbines. The differences between these two turbines are the geometry and physical properties of the rotor and the nacelle. Therefore, the general trend of the Enertech 1500's yaw behavior would be similar to the Grumman WS33's. The discussion of the yaw behavior of the Enertech 1500 would be qualitatively the same as the previous section (i.e., the discussion of the Grumman WS33). Thus, the purpose of this section is to show the analytical results of another wind turbine rather than to discuss or verify the results in detail.

The tower shadow is also the source of the yaw forcing function for the Enertech 1500. The static pitch angle, static flapwise deflection, and coefficients in the equation of motion in yaw are given in tables 4.10, 4.11, 4.12, 4.13, 4.14, and 4.15.

Table 4.10 Static pitch angle under normal operating condition.

X	θ st (degree)
2	0.0430
3	0.0323
4	0.0312
5	0.0305
6	0.0218
7	0.0177
8	0.0147

Table 4.11 Static flapwise tip deflection under normal operating condition from both computer codes.

X	AERO $\overline{ds\ (ft)}$	PROP $\overline{ds\ (ft)}$
2	0.01644	0.01807
3	0.01279	0.01597
4	0.01269	0.01366
5	0.01057	0.01108
6	0.00839	0.00893
7	0.00676	0.00727
8	0.00558	0.00603

Table 4.12 Coefficients of the equation of motion in yaw from AERO code.

X	m_{44}	C_{44}	k_{44_n}	$m_{44_{n*}}$	k_{44_n}
2	0.01605	0.01486	-0.00226	0.01315	-0.03647
3	0.03605	0.02666	-0.01716	0.02958	-0.03647
4	0.06409	0.06306	-0.00909	0.05259	-0.03647
5	0.10007	0.11496	0.00803	0.08217	-0.03647
6	0.14398	0.13952	0.01457	0.11833	-0.03647
7	0.19585	0.17117	0.01554	0.16106	-0.03647
8	0.25569	0.20538	0.01592	0.21036	-0.03647

*n refers to the nacelle

Table 4.13 Coefficients of the equation of motion in yaw for the combined rotor and nacelle system from AERO code.

X	m_{44_T}	C_{44_T}	k_{44_T}
2	0.02920	0.01486	-0.03874
3	0.06563	0.02666	-0.05364
4	0.11668	0.06306	-0.04557
5	0.18224	0.11496	-0.02845
6	0.26231	0.13952	-0.02191
7	0.35691	0.17117	-0.02094
8	0.46605	0.20538	-0.02056

Table 4.14 Coefficients of the equation of motion in yaw from PROP code.

X	m_{44}	C_{44}	k_{44_n}	m_{44_n}	k_{44_n}
2	0.01517	0.01376	0.00016	0.01315	-0.03647
3	0.03411	0.01380	-0.03102	0.02958	-0.03647
4	0.06059	0.06278	-0.01082	0.05259	-0.03647
5	0.09461	0.10991	0.00589	0.08217	-0.03647
6	0.13614	0.14596	0.01138	0.11833	-0.03647
7	0.18519	0.17419	0.01335	0.16106	-0.03647
8	0.24179	0.20753	0.01521	0.21036	-0.03647

Table 4.15 Coefficients of the equation of motion in yaw for the combined rotor and nacelle system from PROP code.

X	m_{44_T}	C_{44_T}	k_{44_T}
2	0.02832	0.01376	-0.03631
3	0.06369	0.01380	-0.06750
4	0.11318	0.06278	-0.04729
5	0.17678	0.10991	-0.03059
6	0.25447	0.14596	-0.02510
7	0.34625	0.17419	-0.02312
8	0.45215	0.20753	-0.02127

It can be seen from Table 4.10 that the magnitudes of the static pitch angle are so small that they have negligible effect on the system. As shown in Table 4.11, the blade exhibits a positive flapwise deflection for all the tip speed ratios considered. The difference in the static tip deflections between the ones obtained from the AERO code and the PROP code is significant at the tip speed ratio equal to 3 and 4. The cause of this difference is primarily due to the simplified lift and drag curve in the AERO.

The coefficients in tables 4.13 and 4.15 show that the system is unstable in yaw due to the negative stiffness coefficient. The primary causes of this yaw instability are proved to be the nacelle and lack of blade coning.

The yaw forcing function due to tower shadow with 20° shadow width and velocity deficit equal to 50% is given in Table 4.16.

Table 4.16 Yaw forcing function with 20° shadow width and velocity deficit = 50%.

X	G_{04}
2	0.00106
3	-0.00025
4	-0.00330
5	-0.00455
6	-0.00449
7	-0.00391
8	-0.00321

One of the reasons that the Enertech 1500 was chosen as a test case is the availability of the data for yaw tracking error to verify the analysis. These test results were obtained from the Rocky Flats Wind Energy Research Center. The test procedure is explained in reference 23. This yaw tracking error is shown in Figure 4.24.

Since the analysis used the linear approximation method, the analytical results are valid only in a small region around zero yaw angle. Therefore, the analytical results for the Enertech 1500 should represent the linear part around the tip speed ratio equal to 3 and 4 or the linear part around the tip speed ratio equal to 9. A sign change of yaw angle in the analytical results would confirm the analysis.

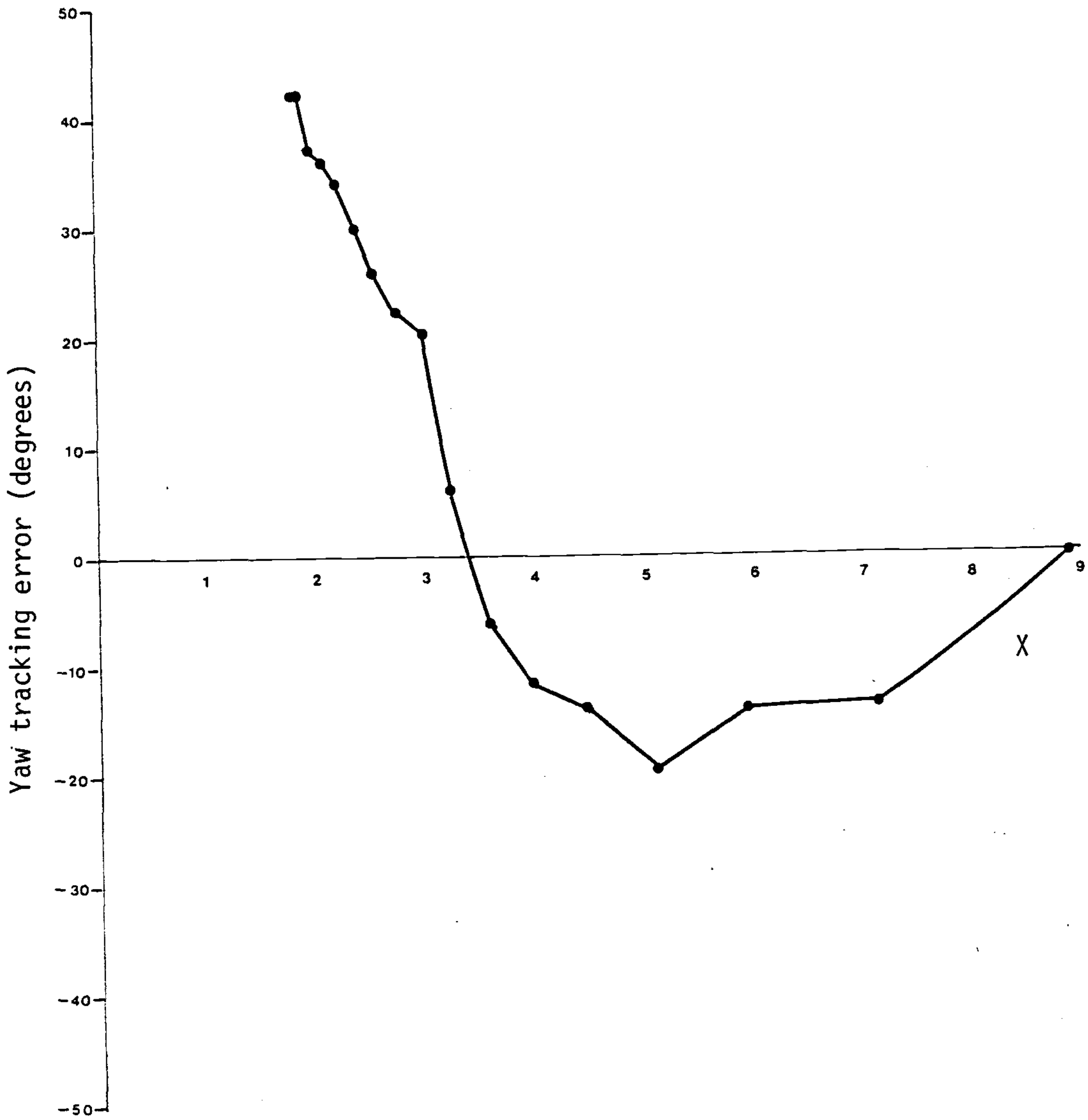

Figure 4.24 Yaw tracking errors versus tip speed ratio for the Enertech 1500.

Unfortunately, according to the analysis the system is unstable in yaw. This contradicts the test data that the system is stable and operating with the static yaw angle.

The explanation for this contradiction may be the use of single-section data (e.g., 3/4 radius) to represent the aerodynamics for the entire variable thickness blade. The analysis used airfoil NACA 4415 to represent the variable thickness blade of the Enertech 1500 for calculating the aerodynamic forces and moments.

One positive thing about the analytical results of the Enertech 1500 is the nacelle. The Enertech 1500's nacelle has a cylindrical shape with a hemisphere on each end. And the forces and moments calculated from the nacelle in this analysis are based on the slender body theory. Thus, with the Enertech 1500's nacelle shape, the model agrees well with the theory. The predicted forces and moments on a cylindrical body with a hemisphere at the end, which yaws at a small angle to the wind, agrees quite well to the experimental result. This can be seen by comparing the theoretical result to the experimental result in reference 14.

Finally, the yaw stiffness coefficient normalized by RPM for the Enertech 1500 with different wind condition is shown in Figure 4.25.

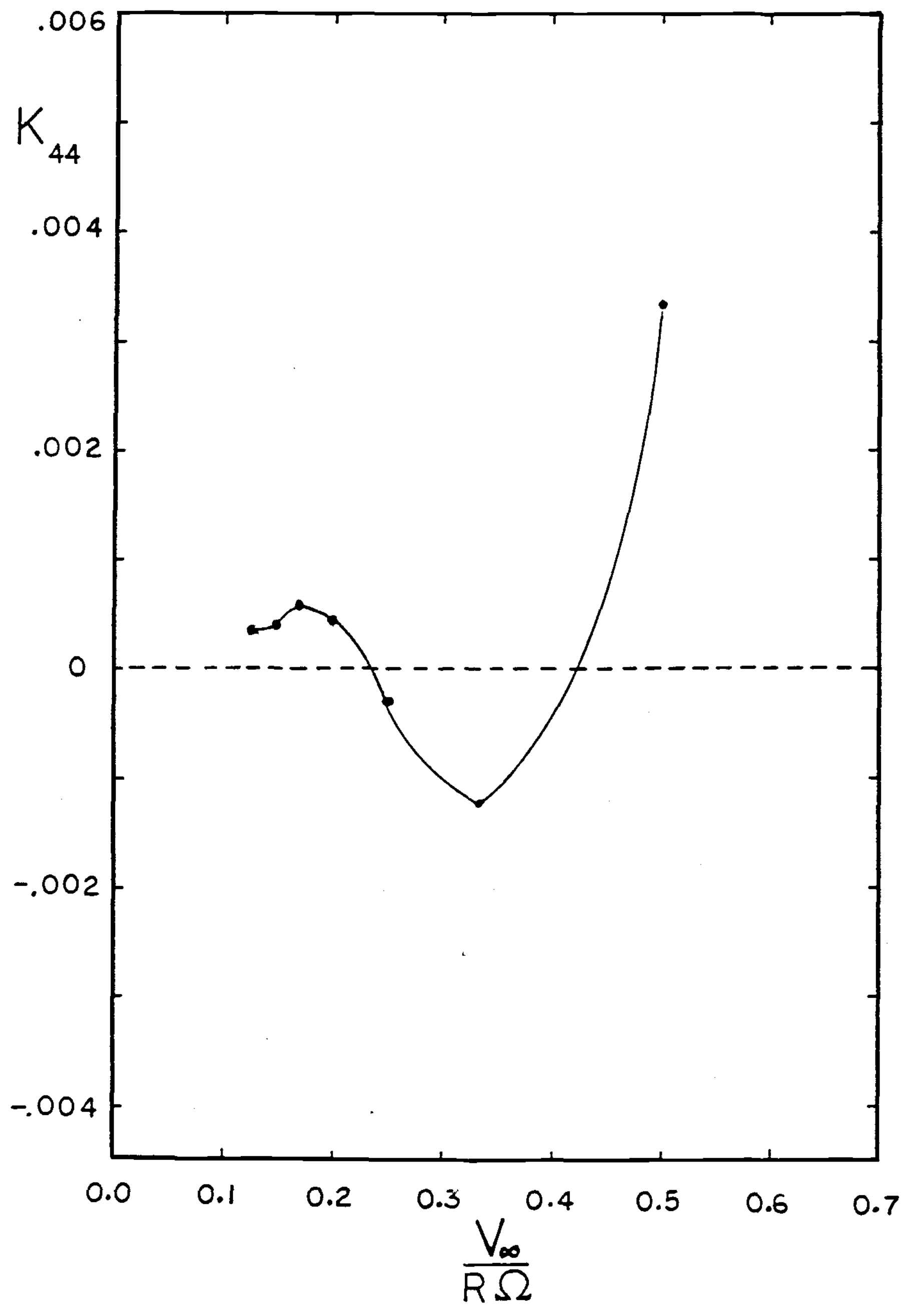

Figure 4.25 Yaw stiffness coefficient versus velocity ratio for the Enertech 1500.

5. CONCLUSION

The yaw behavior of horizontal-axis wind turbines was examined in this dissertation. The study of the yaw behavior undertook to find the cause of poor yaw tracking, investigate the parameters that control yaw behavior, and perform the sensitivity study of those parameters.

The yaw behavior of wind turbines was analyzed by studying the linearized equations of motion around the zero yaw angle. Two computer codes, AERO and PROP, were developed to handle the numerical values of coefficients of the equations of motion. The PROP code was perferred because of its accuracy in the stall region.

Results were obtained for the Grumman WS33 and the Enertech 1500: three-bladed horizontal-axis wind turbines with free yawed system. Between these two test cases,the Grumman WS33 was preferred to the Enertech 1500 because of the geometry and material properities of its blade. The Grumman WS33's blade is made of aluminum (isotopic material) and has a uniform cross section. The Enertech 1500's blade is made of wood (orthotropic material) and has a variable thickness and chord.

The study showed that the yaw tracking error of a downwind wind turbine without wind shear was primarily caused by tower shadow. The effect of the tower shadow appears as the yaw forcing function in the yaw equation. This yaw forcing function is dependent on 1) the width of the tower shadow, 2) the velocity deficit in the tower shadow,

3) the position of the blade's shear center, and 4) the power output of the rotor.

The yaw forcing function for zero offset distance (the blade's shear center is at 1/4 chord) will always have the same sign if the power output of the rotor increases with the wind speed. If the power peaked and then decreased with wind speed, then the yaw forcing function would change sign as the velocity increased. This is exactly the case with the Grumman WS33 and the Enertech 1500. As the peak power is achieved, the rotor yaw changes sign.

The presence of the nacelle in a downwind wind turbine destablizes the system in yaw in the form of a negative stiffness coefficient. The analytical model of the nacelle was developed using the slender body theory. However, the nacelle of the Grumman WS33 is not a slender body; therefore, the predicted yaw behavior from its nacelle contains some uncertainty. Thus, the predicted yaw tracking error of the turbine system (rotor and nacelle) for the Grumman WS33 should be viewed as the qualitative behavior rather than the exact magnitude. In order to obtain accurate predictions of yaw behavior, an accurate nacelle model must be available.

The yaw stability of the Grumman WS33 in an upwind position was used to verify the analysis. The analytical results indicated that the Grumman WS33 in the upwind position is stable in yaw at tip speed ratio equal to 5.

The sign and the magnitude of the yaw stiffness coefficient were found to be the indicators of yaw stability for the Grumman WS33.

Therefore, the characteristic of the yaw stiffness was studied to gain more understanding about the yaw behavior.

The yaw stiffness coefficient is the linear variation of the yaw moment around the zero yaw angle. This yaw moment consists of the moment due to the in-plane force and the moment due to the out-of-plane force. The yaw moment due to the out-of-plane forces exists only when the static flapwise deflection exists.

Because the derivative of force was encountered in calculating the yaw stiffness coefficient rather than the force itself, the negative derivative of the in-plane force (negative slope of the in-plane force versus the angle of attack) and its position on the blade length were therefore the important factors in calculating the yaw stiffness coefficient. If this negative derivative force appears near the blade tip, its contribution would be large. The further the negative derivative force moves in-board, the smaller its contribution becomes. This contribution will act as a stabilizing or destabilizing term depending on the sign of the distance from the rotor to the yaw axis (i.e., downwind or upwind turbine). It will act to destabilize for a downwind turbine and act to stabilize for an upwind turbine.

The sensitivity of the yaw stiffness coefficient to the selected input parameters was studied. The coning angle was found to be the most sensitive parameter. Increasing the coning angle increases the rotor yaw stiffness coefficient. Decreasing the coning angle (i.e., negative coning angle) decreases the rotor yaw stiffness coefficient.

The next parameters to which yaw stiffness coefficient is sensitive are the position of the blade's shear center and the distance from the rotor to the yaw axis. The effect of these parameters on the yaw stiffness coefficient is small at low wind conditions and is increased as the wind speed increases. Moving the shear center closer to the blade trailing edge increases the yaw stiffness coefficient. Increasing the distance from the rotor to the yaw axis increases the yaw stiffness coefficient at a low wind condition. But as the wind increases, the effect is reverse: increasing the distance from the rotor to the yaw axis decreases the yaw stiffness coefficient.

The effect of this distance on the nacelle is reverse to the effect on the rotor. That is, increasing the distance from the rotor to the yaw axis increases the stiffness coefficient to the nacelle. However, for a given nacelle, this distance can be varied only slightly because of the space necessary to install a generator unit. For the Grumman WS33, the effect of this distance on the rotor yaw stiffness coefficient is dominant over the effect of this distance on the nacelle yaw stiffness coefficient.

Increasing blade pitch angle increases the yaw stiffness coefficient at a low wind condition and decreases the yaw stiffness coefficient at a high wind condition. The yaw stiffness coefficient is slightly increased by decreasing blade stiffness. Increasing the rotor speed increases the yaw stiffness coefficient but the nondimensional yaw stiffness is hardly affected by the changes in rotor speed.

Finally, the analytical results for the Enertech 1500 were studied. It was found that the theory developed for the Grumman WS33 can be applied to the Enertech 1500 since they are the same type of wind turbine: three-bladed horizontal-axis wind turbine.

The study indicated that the Enertech 1500 was unstable in yaw. The nacelle and lack of blade coning are the primary causes of the system instability.

The yaw prediction for the Enertech 1500 is in contradiction with test data. This contradiction could have resulted from 1) using single airfoil-section data (e.g., 3/4 radius), NACA 4415, to represent a variable thickness blade and 2) using the analysis for isotropic material to predict the yaw behavior of a rotor made of orthotropic material.

In order to obtain more accurate results, more accurate models of the rotor and the nacelle are needed.

BIBLIOGRAPHY

1. Adler, F. M., P. Henton, and P. W. King. "Grumman WS33 Wind System, Prototype Construction and Testing, Phase II Technical Report," Report under Subcontract No. PF71787-F, prepared for Rockwell International Corporation, November 1, 1980.

2. Munk, Max. M. "Aerodynamics of Airships," in W. F. Durand (Ed.), Aerodynamic Theory, Vol. 6, Division Q, Julius Springer, Berlin, 1935.

3. Fung, Y. C. An Introduction to the Theory of Aeroelasticity, John Wiley, 1955.

4. Glauert, H. "The Analysis of Experimental Results in the Windmill Brake and Vortex Ring States of an Airscrew," Reports and Memoranda, No. AE.222, February 1926.

5. Goldstein, S. "On the Vortex Theory of Screw Propellers," Proc. Royal Soc., A123, 440, 1929.

6. Hayes, William C., and William P. Henderson. "Some Effects of Nose Bluntness and Fineness Ratio of the Static Longitudinal Aerodynamic Characteristics of Bodies of Revolution at Subsonic Speeds," NASA Technical Note D-650.

7. Hirschbein, M. S. "Dynamics and Control of Large Horizontal-Axis Axisymmetric Wind Turbines," Ph.D. thesis, University of Delaware, 1979.

8. Hoerner, Sighard F., and Henry V. Borst. Fluid-Dynamic Lift, published by Mrs. Hoerner, New Jersey, 1975, Chapter 19.

9. Jacobs, E. N., and A. Sherman. "Airfoil Section Characteristics as Affected by Variations of Reynolds Number," NACA TR586, 1936.

10. Kane, Thomas R. Dynamics, Stanford University, 3rd edition, 1978.

11. Meirovitch, L. Analytical Methods in Vibrations, Macmillan and Co., 1967.

12. Miley, S. J. "A Catalog of Low Reynolds Number Airfoil Data for Wind Turbine Applications," Report under Subcontract No. PFY12781-W, prepared for Rockwell International Corporation, February 1982.

13. Miller, R. H. "On the Weatherizing of Wind Turbines," AIAA Journal of Energy, Vol. 3, No. 5, September-October 1979.

14. Polhamus, Edward C. "Effect of Nose Shape on Subsonic Aerodynamic Characteristics of a Body of Revolution Having a Fineness Ratio of 10.94," NACA Research Memorandum RM L57 F25, August 1957.

15. Prandtl, L. Gottinger Nachr., p. 193, Appendix, 1919.

16. Ribner, H. S. "Propellers in Yaw," NACA Technical Report No. 820.

17. Satrou, D., and M. H. Snyder. "Two-Dimensional Test of GA(W)-1 and GA(W)-2 Airfoils at Angles-of-Attack from 0 to 360 Degrees," WER-1, Wind Energy Laboratory, Wichita State University, Wichita, Kansas, 1977.

18. Sheldahl, Robert E., and Paul C. Klimas. "Aerodynamic Characteristics of Seven Symmetrical Airfoil Sections Through 180-Degree Angle of Attack for Use in Aerodynamic Analysis of Vertical Axis Wind Turbines," SAND 80-2114, Sandia National Laboratory, Albuquerque, New Mexico, 1981.

19. Sweeney, T. E., and W. B. Nixon. "Two Dimensional Lift and Drag Characteristics of Grumman Windmill Blade Section," Department of Aerospace and Mechanical Sciences, Princeton University, February 1978.

20. Wilson, R. E., and P. B. S. Lissaman. Applied Aerodynamics of Wind Power Machines, Oregon State University, May 1974.

21. Wilson, R. E., and S. N. Walker. "A Fortran Program for the Determination of Performance, Loads, and Stability Derivatives of Wind Turbines," Oregon State University, 25 October 1974.

22. Wilson, R. E., P. B. S. Lissaman, and S. N. Walker. Aerodynamic Performance of Wind Turbines, Oregon State University, June 1976.

23. Wilson, R. E., and E. M. Patton. "Performance Prediction and Comparison with Test Results for Horizontal Axis Wind Turbines," Report under Subcontract No. PFN-13318W, prepared for Rockwell International Corporation, February 1982.

APPENDICES

APPENDIX I

KINEMATICS

A four-degree-of-freedom wind turbine system is illustrated in Figure I.1. The degrees of freedom of the axisymmetric rotor system are blade pitch deflection, blade flap, speed variation, and yaw angle.

In developing the mathematical model for the turbine system, we use assumed mode shapes and generalized coordinates to represent the dependent variables. By this method we can derive the governing equations in ordinary differential form rather than partial differential form. Each degree of freedom is expressed as the product of the displacement function (assumed mode shape) and the generalized coordinate.

These relations are given as:

$$\theta(r,t) = f_1(\tfrac{r}{R})q_1(t) \qquad \text{(blade pitch)} \qquad (1)$$

$$w(r,t) = R_S f_2(\tfrac{r}{R})(q_2(t) + q_s) \qquad \text{(blade flap)} \qquad (2)$$

$$\dot{x}(r,t) = f_3(\tfrac{r}{R})\dot{q}_3(t) \qquad \text{(speed variation)} \qquad (3)$$

$$\gamma(r,t) = f_4(\tfrac{r}{R})q_4(t) \qquad \text{(yaw angle)} \qquad (4)$$

where R_S is the distance from the tip of the blade to the hub of the rotor. The $q_i(t)$ terms are the generalized coordinates of the rotor system and the $f_i(\frac{r}{R})$ terms are the assumed mode shapes. The mode shapes are expressed as:

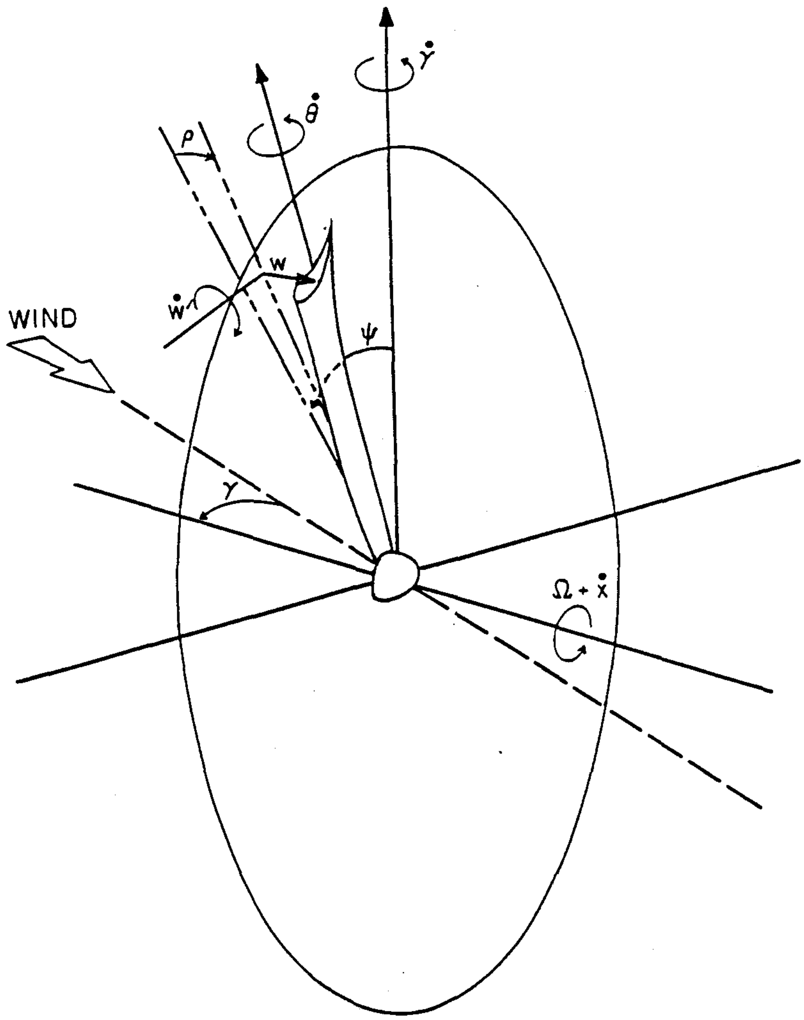

Figure I.1 Rotor system.

$$f_1(\frac{r}{R}) = \frac{2r_S}{R_S} - (\frac{r_S}{R_S})^2 \tag{5}$$

$$f_2(\frac{r}{R}) = 6(\frac{r_S}{R_S})^2 - 4(\frac{r_S}{R_S})^3 + (\frac{r_S}{R_S})^4 \tag{6}$$

$$f_3(\frac{r}{R}) = 1 \tag{7}$$

$$f_4(\frac{r}{R}) = 1 \tag{8}$$

Here r_S is the radial distance from the local point on the blade to the blade root.

The mode shape in Eq. (5) is for a uniform cantilever beam in static equilibrium with applied torque at the open end. The mode shape in Eq. (6) is for a uniform cantilever beam in static equilibrium with uniform forces applied on the beam. The mode shapes in Eqs. (7) and (8) are those of a rigid body.

For a turbine blade with blade stub, the mode shapes of blade pitch and blade flap differ from the ones in Eqs. (5) and (6). They are expressed as follows:

for $r > R_H$

$$f_1(\frac{r}{R}) = 2(\frac{R_H}{R_S})\frac{(GJ)}{(GJ)_H} + 2\frac{r_S}{R_S} - (\frac{r_S}{R_S})^2$$

$$f_2(\frac{r}{R}) = K_o + K_1(\frac{r_S}{R_S}) + 6(\frac{r_S}{R_S})^2 - 4(\frac{r_S}{R_S})^3 + (\frac{r_S}{R_S})^4$$

for $0 < r < R_H$

$$f_1(\frac{r}{R}) = 2\frac{EI}{(EI)_H}(\frac{R_H}{R_S} + \frac{r_S}{R_S})\ (\ 3 + 4(\frac{R_H}{R_S}) - 2(\frac{r_S}{R_S}))$$

$$f_2(\frac{r}{R}) = 2(\frac{R_H}{R_S})\frac{GJ}{(GJ)_H}(\ 1 + (\frac{R_S}{R_H})(\frac{r_S}{R_S}))$$

where $\quad r_S = r - R_H$

$$K_o = 2(\frac{R_H}{R_S})^2\frac{EI}{(EI)_H}(\ 3 + 4(\frac{R_H}{R_S}))$$

$$K_1 = 12(\frac{R_H}{R_S})\frac{EI}{(EI)_H}(\ 1 + (\frac{R_H}{R_S}))$$

Here R_H is the length of blade stub, measured from the blade section to the rotor center. $(EI)_H$ and $(GJ)_H$ are flapwise stiffness and torsional stiffness of the blade stub.

Having defined the degrees of freedom in terms of generalized coordinates, we are now ready to develop the kinematics of the rotor system.

The absolute motion of the turbine blade is determined by the motion of blade deflection relative to the hub, the motion due to rotor rotation, plus the motion of the nacelle and tower. Since in this analysis no movement of the tower is allowed, we consider the reference frame fixed to the tower as the inertial reference frame. Consider the motion of a point on the blade whose absolute position is represented by a series of relative position vectors. A series of coordinate systems is used to describe these vectors. Let the coordinate system X,Y,Z be located on the top of the tower. The coordinate system x,y,z is fixed on the nacelle and its origin is at the same point as the coordinate system X,Y,Z. The coordinate system $\hat{x},\hat{y},\hat{z}$ is the same as the coordinate system x,y,z except its origin is moved to the center of the rotor. The coordinate system $\underline{x},\underline{y},\underline{z}$ is obtained by rotating the coordinate system $\hat{x},\hat{y},\hat{z}$ by the magnitude of angle ψ (where $\psi = \Omega t + \chi$). The coordinate system x_ρ, y_ρ, z_ρ is obtained by rotating the coordinate system $\underline{x},\underline{y},\underline{z}$ around the $\underline{y}$ axis by the angle ρ. Then, at position r on the blade, the coordinate system $x_\beta, y_\beta, z_\beta$ represents the effect of the pretwist angle, β. The coordinate system $x_\theta, y_\theta, z_\theta$ is obtained by moving the origin of the coordinate system $x_\beta, y_\beta, z_\beta$ in the z_β direction over the distance "w" and rotating it around the y_β axis by the angle w' ($\partial w/\partial r$). Finally, the coordinate system x_1, x_2, x_3 is located on the shear center of the blade cross section and differs from the coordinates $x_\theta, y_\theta, z_\theta$ by the amount of the pitch angle θ.

These coordinate systems are shown in order from the inertial reference frame to the final reference frame that is fixed on a point on the blade in Figures I.2, I.3, and I.4.

A series of transformation matrices is used to transform from one coordinate system to the others. These transformation matrices are shown in Figure I.5.

Another variable that we will deal with is the radial displacement of the blade. This displacement occurs during the blade deflection when the assumption of an inextensible blade is made. This radial displacement is defined as

$$u_c(r) = -\frac{1}{2}\int_{R_H}^{R} \left(\frac{dv_c}{dr}\right)^2 dr \qquad (9)$$

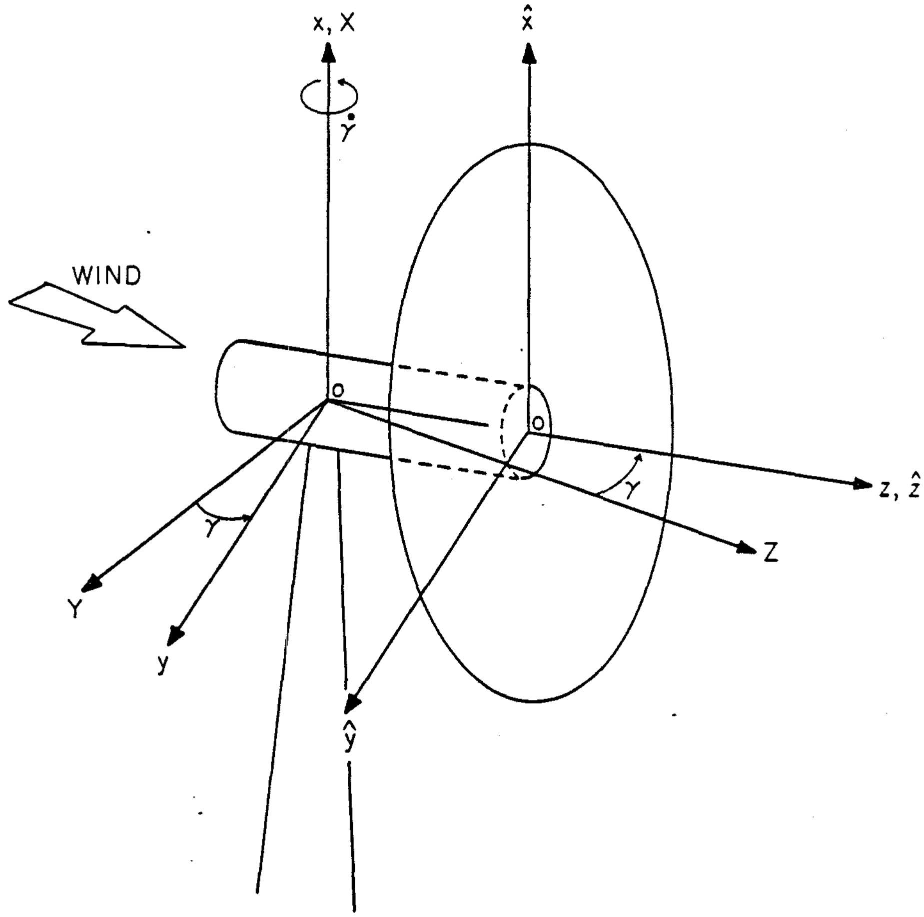

Figure I.2 Coordinate systems XYZ, xyz, and $\hat{x}\hat{y}\hat{z}$.

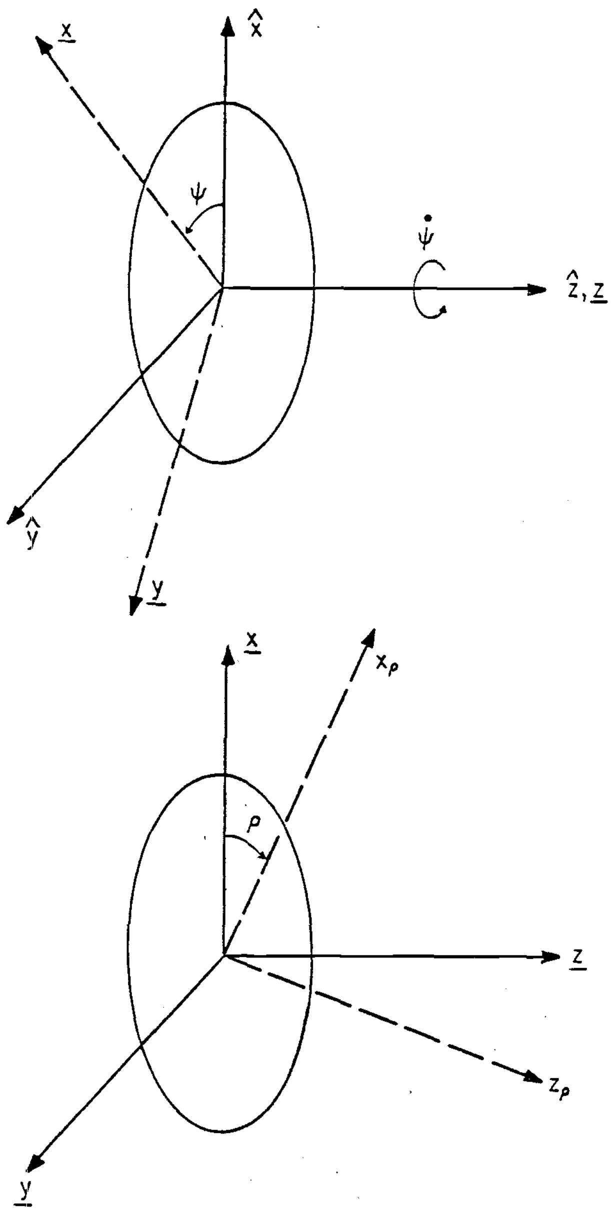

Figure I.3 Coordinate systems $\hat{x}\hat{y}\hat{z}$, $\underline{x}$ $\underline{y}$ $\underline{z}$, $x_\rho y_\rho z_\rho$.

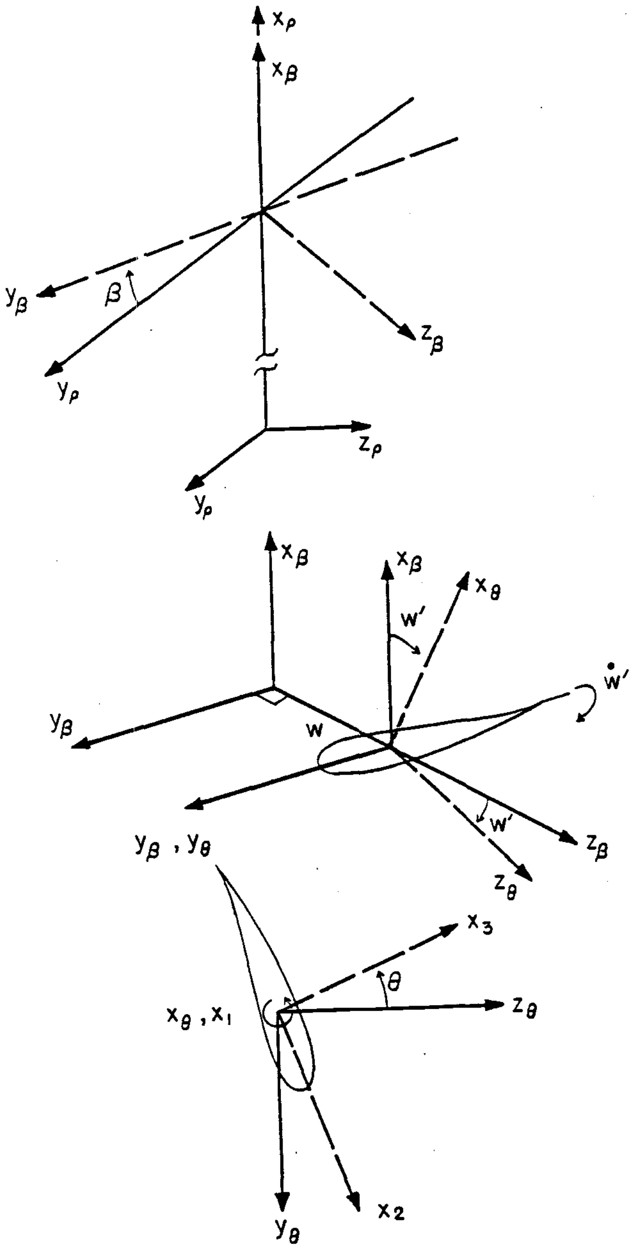

Figure I.4 Coordinate systems $x_\beta y_\beta z_\beta$, $x_\theta y_\theta z_\theta$, and $x_1 x_2 x_3$.

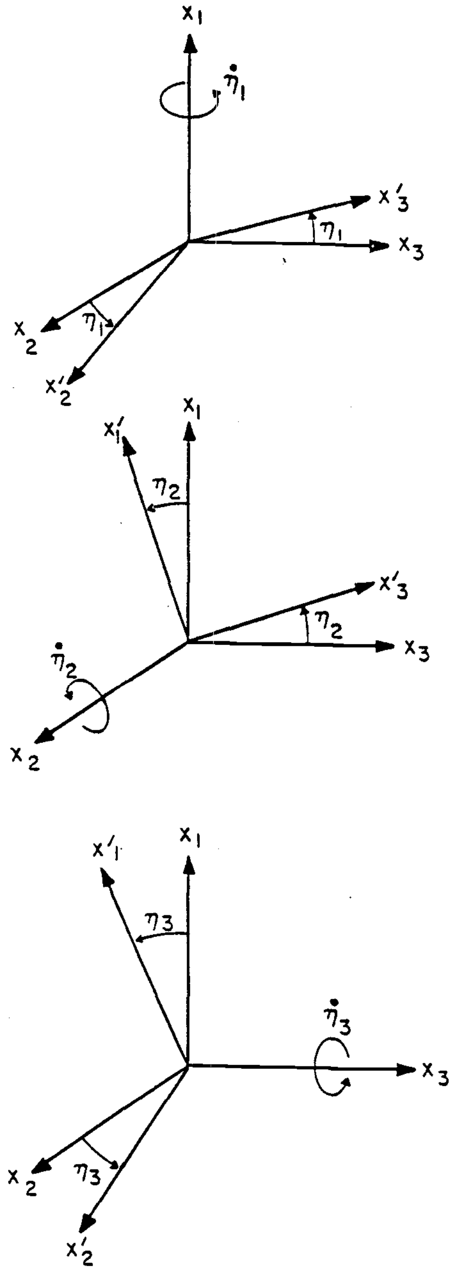

$$(x) = [T]\,(x')$$

$$[T] = \begin{pmatrix} 1 & 0 & 0 \\ 0 & \cos\eta_1 & -\sin\eta_1 \\ 0 & \sin\eta_1 & \cos\eta_1 \end{pmatrix}$$

$$(x) = [T]\,(x')$$

$$[T] = \begin{pmatrix} \cos\eta_2 & 0 & \sin\eta_2 \\ 0 & 1 & 0 \\ -\sin\eta_2 & 0 & \cos\eta_2 \end{pmatrix}$$

$$(x) = [T]\,(x')$$

$$[T] = \begin{pmatrix} \cos\eta_3 & -\sin\eta_3 & 0 \\ \sin\eta_3 & \cos\eta_3 & 0 \\ 0 & 0 & 1 \end{pmatrix}$$

Figure I.5 Transformation matrices.

where v_c is the deflection of the blade in the direction that is perpendicular to the axial line (flapwise direction).

The velocity of a point on the blade is found by using the kinematic relation [10]

$$_R\vec{V}_c = {}_\alpha\vec{V}_c + {}_R\vec{\omega}_\alpha \times \vec{r} \tag{10}$$

where $_R\vec{V}_c$ is the velocity of point c in a reference frame R.

$_\alpha\vec{V}_c$ is the velocity of point c in a reference frame α.

$_R\vec{\omega}_\alpha$ is the angular velocity of the body that the reference frame α is fixed to, observed from the reference frame R.

$\vec{r}$ is the position vector of point c.

For the angular velocity, we have

$$_R\vec{\omega}_\alpha = {}_R\vec{\omega}_B + {}_B\vec{\omega}_\alpha \tag{11}$$

where $_\eta\vec{\omega}_\xi$ is the angular velocity of the body that a reference frame ξ is fixed to, observed from a reference frame η.

The absolute motion of a point on the blade can be found by using the transformation matrices and Eqs. (10) and (11).

The blade velocity and blade angular velocity measured at the center of mass of the blade cross section are:

$$\vec{V}_c = V_{x\rho}\vec{n}_{x\rho} + V_{y\rho}\vec{n}_{y\rho} + V_{z\rho}\vec{n}_{z\rho} \tag{12}$$

where

$$V_{\eta\rho} = V_{\eta\ell} + V_{\eta r} + V_{\eta w} + V_{\eta e} \qquad \eta = x,y,z$$

and

$$V_{x\ell} = -\ell\dot{\gamma}\cos\rho\sin\psi$$

$$V_{xr} = \dot{u}_c$$

$$V_{xw} = -w\dot{\psi}\sin\beta\cos\rho + w\dot{\gamma}(\sin\rho\sin\beta\cos\psi - \cos\beta\sin\psi)$$

$$V_{xe} = \left\{\begin{array}{l} -e\dot{\theta}\sin w'\cos\theta - e\dot{\psi}\cos\rho(\cos\beta\cos\theta + \cos w'\sin\theta\sin\beta) \\ + e\dot{\gamma}(\sin\beta\cos\theta - \cos\beta\cos w'\sin\theta)\sin\psi \\ + e\dot{\gamma}\sin\rho(\cos\beta\cos\theta + \cos w'\sin\theta\sin\beta)\cos\psi \end{array}\right.$$

$$V_{y\ell} = -\ell\dot{\gamma}\cos\psi$$

$$V_{yr} = (r + u_c)\dot{\psi}\cos\rho - (r + u_c)\dot{\gamma}\cos\psi\sin\rho$$

$$V_{yw} = \dot{w}\sin\beta - w\dot{\psi}\sin\rho\cos\beta - w\dot{\gamma}\cos\rho\cos\beta\cos\psi$$

$$V_{ye} = \left\{\begin{array}{l} e\dot{\theta}\cos\theta\cos w'\sin\beta - e\dot{w}'\sin\theta\sin w'\sin\beta \\ + e\dot{\psi}\lfloor\sin\rho(\sin\beta\cos\theta - \cos\beta\cos w'\sin\theta) - \cos\rho\sin w'\sin\theta\rbrack \\ + e\dot{\gamma}\cos\psi\lbrack\cos\rho(\sin\beta\cos\theta - \cos\beta\cos w'\sin\theta) + \sin\rho\sin w'\sin\theta\rfloor \end{array}\right.$$

$$V_{z\ell} = \ell\dot{\gamma}\sin\rho\sin\psi$$

$$V_{zr} = (r + u_c)\dot{\gamma}\sin\psi$$

$$V_{zw} = \dot{w}\cos\beta + w\dot{\psi}\sin\beta\sin\rho + w\dot{\gamma}\cos\rho\sin\beta\cos\psi$$

$$V_{ze} = \left\{\begin{array}{l} + e\dot{\theta}\cos\theta\cos w'\sin\beta - e\dot{w}'\sin\theta\sin w'\cos\beta \\ + e\dot{\psi}\sin\rho(\cos\beta\cos\theta + \cos w'\sin\theta\sin\beta) \\ + e\dot{\gamma}\cos\rho(\cos\beta\cos\theta + \cos w'\sin\theta\sin\beta)\cos\psi \\ - e\dot{\gamma}\cos\rho\sin w'\sin\theta\sin\psi \end{array}\right.$$

where

e = distance from mass center to the shear center of the blade cross section.

ℓ = distance from the rotor plane to the nacelle's yaw axis.

$$w' = \frac{\partial w}{\partial r}$$

$$\dot{w} = \frac{\partial w}{\partial t}$$

$$\dot{w}' = \frac{\partial}{\partial t}\left(\frac{\partial w}{\partial r}\right)$$

$$\dot{\psi} = (\Omega + \dot{\chi})$$

$$\vec{\omega} = \omega_1\vec{n}_1 + \omega_2\vec{n}_2 + \omega_3\vec{n}_3 \tag{13}$$

where

$$\omega_i = \omega_{\theta i} + \omega_{wi} + \omega_{\psi i} + \omega_{\gamma i} \qquad i = 1,2,3$$

and

$$\omega_{\theta 1} = \dot{\theta}$$

$$\omega_{w1} = 0$$

$$\omega_{\psi 1} = \dot{\psi}(\sin\rho\cos w' + \cos\rho\sin w'\cos\beta)$$

$$\omega_{\gamma 1} = \dot{\gamma}\lfloor(\cos\rho\cos w' - \sin\rho\sin w'\cos\beta)\cos\psi - \sin w'\sin\beta\sin\psi\rfloor$$

$$\omega_{\theta 2} = 0$$

$$\omega_{w2} = -\dot{w}'\cos\theta$$

$$\omega_{\psi 2} = -\dot{\psi}(\sin\rho\sin w'\sin\theta + \cos\rho\sin\beta\cos\theta - \cos\rho\cos w'\sin\theta\cos\beta)$$

$$\omega_{\gamma 2} = -\dot{\gamma}(\cos\rho\sin w'\sin\theta - \sin\rho\sin\beta\cos\theta + \sin\rho\cos w'\sin\theta\cos\beta)\cos\psi$$

$$- \dot{\gamma}[(\cos\beta\cos\theta + \cos w'\sin\theta\sin\beta)\sin\psi]$$

$$\omega_{\theta 3} = 0$$

$$\omega_{w3} = \dot{w}'\sin\theta$$

$$\omega_{\psi 3} = -\dot{\psi}(\sin\rho\sin w'\cos\theta - \cos\rho\sin\beta\sin\theta - \cos\rho\cos w'\cos\theta\cos\beta)$$

$$\omega_{\gamma 3} = -\dot{\gamma}(\cos\rho\sin w'\cos\theta + \sin\rho\sin\beta\sin\theta + \sin\rho\cos w'\cos\theta\cos\beta)\cos\psi$$

$$+ \dot{\gamma}(\cos\beta\sin\theta - \cos w'\cos\theta\sin\beta)\sin\psi$$

APPENDIX II

ROTOR AERODYNAMICS

II.1 Relative Velocity

The relative velocity that the blade element experiences at the rotor is defined as the vector sum of the blade element velocity at mid-chord and the wind velocity at the rotor.

$$\vec{W} = \vec{V}_w - \vec{V}_B \tag{1}$$

Here $\vec{V}_w$ is the wind velocity at the rotor and $\vec{V}_B$ is the blade element velocity at mid-chord, it does not include pitch velocity ($\dot{\theta}$). The wind velocity at the rotor is given by

$$\vec{V}_w = V_w\vec{n}_z - aV_w\vec{n}_{\hat{z}} \tag{2}$$

where "a" is the axial induction factor. The development of the axial induction factor will be explained in a later section.

In the strip theory method (2-D assumption), the relative velocity in the spanwise direction does not produce lift force or drag force. The velocity to be considered in evaluation of the aerodynamic forces and moments is the relative velocity in the plane of the blade cross section. Thus the relative velocity is expressed as

$$\vec{W}_e = \{(\vec{V}_w - \vec{V}_B)\cdot\vec{n}_{y\theta}\}\vec{n}_{y\theta} + \{(\vec{V}_w - \vec{V}_B)\cdot\vec{n}_{z\theta}\}\vec{n}_{z\theta} \tag{3}$$

By using the unit vectors $\vec{e}_n$ and $\vec{e}_t$, we obtain

$$\vec{W}_e = W_n \vec{e}_n - W_t \vec{e}_t \tag{4}$$

where

$$W_n = (\vec{V}_w - \vec{V}_B) \cdot \vec{n}_{z\theta} \tag{5}$$

$$W_t = - (\vec{V}_w - \vec{V}_B) \cdot \vec{n}_{y\theta} \tag{6}$$

$$\vec{e}_n = \vec{n}_{z\theta}$$

$$\vec{e}_t = \vec{n}_{y\theta}$$

The expression for $\vec{V}_B$ can be obtained by following the same procedure used in Appendix I.

Substituting the value of $\vec{V}_B$ and $\vec{V}_w$ into Eqs. (5) and (6) we obtain the normal and tangential relative velocities as

$$W_n = V_{wn} + V_{Bn}$$

$$W_t = V_{wt} + V_{Bt}$$

$$V_{wn} = \begin{cases} - V_\infty(\cos\gamma - a)(\sin\rho\sin w' - \cos\rho\cos w'\cos\beta) \\ - V_\infty\sin\gamma[(\cos\rho\sin w' + \sin\rho\cos w'\cos\beta)\sin\psi - \cos w'\sin\beta\cos\psi] \end{cases}$$

$$V_{Bn} = \begin{cases} - \ell\dot{\gamma}[(\sin\rho\cos\beta\cos w' + \sin w'\cos\rho)\sin\psi - \sin\beta\cos w'\cos\psi] \\ + \dot{u}_d\sin w' - (r + u_d)\dot{\psi}\cos w'\cos\rho\sin\beta \\ - (r + u_d)\dot{\gamma}(\cos\beta\cos w'\sin\psi - \sin\rho\sin\beta\cos w'\cos\psi) \\ - \dot{w}\cos w' - w\dot{\psi}\sin w'\cos\rho\sin\beta \\ - w\dot{\gamma}(\sin w'\sin\rho\sin\beta\cos\psi - \sin w'\cos\beta\sin\psi) \\ + e_3\dot{\psi}\cos\theta(\sin\rho\cos w' + \cos\rho\sin w'\cos\beta) \\ + e_3\dot{\gamma}\cos\theta[(\cos\rho\cos w' - \sin\rho\sin w'\cos\beta)\cos\psi - \sin w'\sin\beta\sin\psi] \end{cases}$$

$$V_{wt} = \{- V_\infty(\cos\gamma - a)\cos\rho\sin\beta - V_\infty\sin\gamma(\sin\rho\sin\beta\sin\psi + \cos\beta\cos\psi)\}$$

$$V_{Bt} = \begin{cases} - \ell\dot{\gamma}(\cos\beta\cos\psi + \sin\rho\sin\beta\sin\psi) \\ + (r + u_d)\dot{\psi}\cos\rho\cos\beta - (r + u_d)\dot{\gamma}(\sin\beta\sin\psi + \sin\rho\cos\beta\cos\psi) \\ - w\dot{\psi}\sin\rho - w\dot{\gamma}\cos\rho\cos\psi \\ + e_3\dot{\psi}\sin\theta(\sin\rho\cos w' + \cos\rho\sin w'\cos\beta) \\ + e_3\dot{\gamma}\sin\theta[(\cos\rho\cos w' - \sin\rho\sin w'\cos\beta)\cos\psi - \sin w'\sin\beta\sin\psi] \end{cases}$$

where e_3 is the distance from the mid-chord to the shear center of the blade cross section.

The velocity diagram of the relative velocity at the blade cross section is shown in Figure II.1.1.

II.2 Aerodynamic Forces and Moments

Figure II.1.1 shows a blade profile section at radius r with the relevant velocities and forces. The air flow gives rise to a lift force L and a drag force D whose resultant can be resolved into components of normal force dF_n and tangential force dF_t.

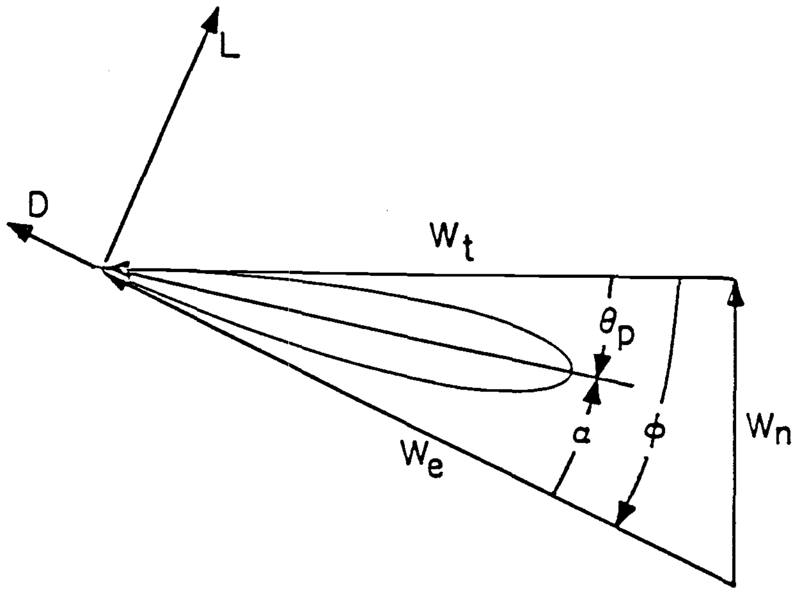

$\vec{\dot{\theta}}_p = -\vec{\dot{\theta}}$

Figure II.1.1 Velocity diagram at blade cross section .

From the geometry we have

$$dF_n = dL \cos\phi + dD \sin\phi \tag{7}$$

$$dF_t = dL \sin\phi - dD \cos\phi \tag{8}$$

The expression for the normal force and tangential force can also be expressed as

$$dF_n = \frac{1}{2} \rho_\infty w_e^2 c C_n dr \tag{9}$$

$$dF_t = \frac{1}{2} \rho_\infty w_e^2 c C_t dr \tag{10}$$

where

$$C_n = C_L \cos\phi + C_D \sin\phi$$

$$C_t = C_L \sin\phi - C_D \cos\phi$$

The aerodynamic moment at 1/4 chord can be expressed as

$$dM_{c/4} \vec{n}_1 = \frac{1}{2} \rho_\infty w_e^2 c^2 C_{M_{c/4}} dr \vec{n}_1 \tag{11}$$

and according to Fung [3]

$$C_{M_{c/4}} = -\frac{\pi c}{8} \cos\alpha \dot{\theta} \tag{12}$$

Substituting the expression of $C_{M_{c/4}}$ back into Eq. (11), we obtain

$$dM_{c/4} = -\rho_\infty W_e \cos\alpha \frac{\pi c^3}{16} \dot{\theta}\, dr \tag{13}$$

II.3 Linearized Aerodynamic Forces

In this study the linearized aerodynamic forces will be developed. These functions will consist of the nominal terms plus the linear variations of the aerodynamic forces with the dependent variables.

Let us first consider the aerodynamic forces. Figure II.3.1 shows the blade profile section at radius r with the relevant velocities and forces. The components of the aerodynamic forces are expressed as

$$dF_n = \frac{1}{2}\rho_\infty W_e^2 c C_n dr \tag{14}$$

$$dF_t = \frac{1}{2}\rho_\infty W_e^2 c C_t dr \tag{15}$$

where

$$C_n = C_L(\alpha_E)\cos\phi + C_D(\alpha_E)\sin\phi$$

$$C_t = C_L(\alpha_E)\sin\phi - C_D(\alpha_E)\cos\phi$$

$$W_e = W_n + W_t$$

α_E is the effective angle of attack measured at 3/4 chord when including the effect of the pitching velocity at that point.

Normalizing Eqs. (14) and (15) by dividing through with $\frac{1}{2}\rho_\infty V_\infty^2 R^2$ yields

$$C_{F_n} = \left(\frac{W_e}{V_\infty}\right)^2 \frac{c}{R} C_n \frac{dr}{R} \tag{16}$$

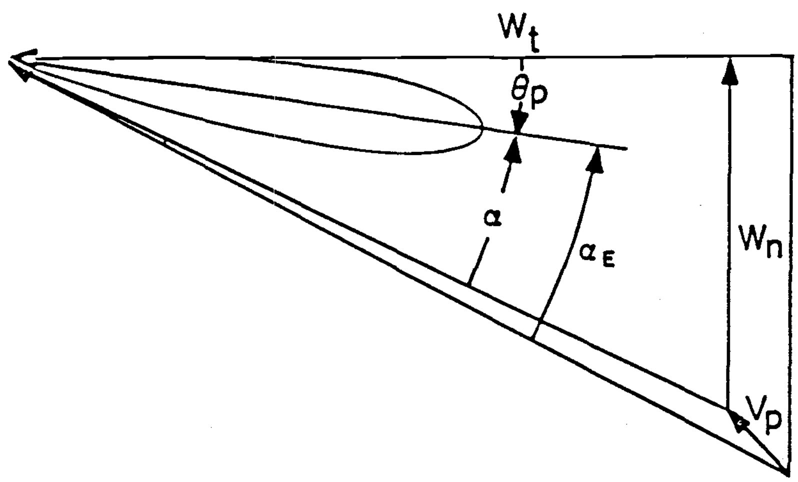

$$\vec{\dot{\theta}}_p = -\vec{\dot{\theta}}$$

Figure II.3.1 Velocity diagram at blade cross section.

$$C_{F_t} = \left(\frac{W_e}{V_\infty}\right)^2 \frac{c}{R} C_t \frac{dr}{R} \tag{17}$$

The derivative of the normal force with respect to the dependent variables is defined as

$$N_\eta \frac{dr}{R} = \frac{\partial C_{F_n}}{\partial \eta}$$

$$N_\eta = \frac{c}{R} C_n \left[2 \frac{W_n}{V_\infty} \frac{\partial}{\partial \eta} \left(\frac{W_n}{V_\infty}\right) + \frac{2W_t}{V_\infty} \frac{\partial}{\partial \eta} \left(\frac{W_t}{V_\infty}\right)\right] + \frac{c}{R} \left(\frac{W_e}{V_\infty}\right)^2 \frac{\partial}{\partial \eta} C_n \tag{18}$$

The derivative of C_n with respect to η becomes

$$\frac{\partial C_n}{\partial \eta} = \frac{\partial C_n}{\partial \alpha_E} \frac{\partial \alpha_E}{\partial \eta} + \frac{\partial C_n}{\partial \phi} \frac{\partial \phi}{\partial \eta} \tag{19}$$

The velocity of the fluid that accounts for the pitching velocity at 3/4 chord is expressed as

$$V_p = e_2 \dot{\theta} \cos\theta \vec{e}_n - e_2 \dot{\theta} \sin\theta \vec{e}_t \tag{20}$$

and

$$W^2 = (W_n + e_2 \dot{\theta} \cos\theta)^2 + (W_t + e_2 \dot{\theta} \sin\theta)^2$$

From the velocity diagram in Figure II.3.1, the tangent and cosine of the effective angle are expressed as

$$\tan\phi_E = \frac{W_n + e_2 \dot{\theta} \cos\theta}{W_t + e_2 \dot{\theta} \sin\theta} \tag{21}$$

$$\cos\phi_E = \frac{W_t + e_2\dot{\theta}\sin\theta}{W} \tag{22}$$

where

$$\phi_E = \alpha_E - \theta$$

From trigonometric relations we obtain

$$\frac{\partial}{\partial\eta}\left(\tan\phi_E\right) = \sec^2\phi_E \frac{\partial\phi_E}{\partial\eta}$$

$$\frac{\partial\alpha_E}{\partial\eta} = \cos^2\phi_E \frac{\partial}{\partial\eta}\left(\tan\phi_E\right) + \frac{\partial\theta}{\partial\eta} \tag{23}$$

By substituting Eqs. (21) and (22) into Eq. (23), we obtain the expression of $\frac{\partial\alpha_E}{\partial\eta}$ as

$$\frac{\partial\alpha_E}{\partial\eta} = \frac{1}{W^2}\Big[\Big(W_{n_\eta} + e_2\frac{\partial}{\partial\eta}(\dot{\theta}\cos\theta)\Big)(W_t + e_2\dot{\theta}\sin\theta)$$

$$- (W_n + e_2\dot{\theta}\cos\theta)\Big(W_{t_\eta} + e_2\frac{\partial}{\partial\eta}(\dot{\theta}\sin\theta)\Big)\Big] + \frac{\partial\theta}{\partial\eta} \tag{24}$$

where

$$W_{n_\eta} = \frac{\partial W_n}{\partial\eta}$$

$$W_{t_\eta} = \frac{\partial W_t}{\partial\eta}$$

In the same way, the expression of $\frac{\partial\phi}{\partial\eta}$ can be expressed as

$$\frac{\partial\phi}{\partial\eta} = \frac{1}{W_e^2}\left[Wn\eta W_t - WnWt\eta\right] \tag{25}$$

Substituting Eqs. (19), (24), and (25) back into Eq. (18) we then evaluate all the dependent variables at nominal values. The derivative of the normal force can be expressed as

$$
\begin{aligned}
N_\eta &= F_1 \frac{W_{n_\eta}}{V_\infty} + F_2 \frac{W_{t_\eta}}{V_\infty} \qquad \text{for } \eta \neq q_1, \dot{q}_1 \\
N_{q_1} &= F_1 \frac{W_{n_{q_1}}}{V_\infty} + F_2 \frac{W_{t_{q_1}}}{V_\infty} + F_4 \\
N_{\dot{q}_1} &= F_1 \frac{W_{n_{\dot{q}_1}}}{V_\infty} + F_2 \frac{W_{t_{\dot{q}_1}}}{V_\infty} + F_3
\end{aligned} \tag{26}
$$

where

$$F_1 = \frac{c}{R}\left\{2\frac{W_n}{V_\infty} C_n + C_{n_\nu}\frac{W_t}{V_\infty}\right\}$$

$$F_2 = \frac{c}{R}\left\{2\frac{W_t}{V_\infty} C_n - C_{n_\nu}\frac{W_n}{V_\infty}\right\}$$

$$F_3 = \frac{c}{R} C_{n_\alpha} \frac{e_2}{V_\infty}\frac{W_t}{V_\infty} f_1$$

$$F_4 = \frac{c}{R}\left(\frac{W_e}{V_\infty}\right)^2 C_{n_\alpha} f_1$$

Figure II.3.2 shows the velocity diagram of the blade evaluated at the nominal value. The relation of lift and drag at the nominal value can be expressed as

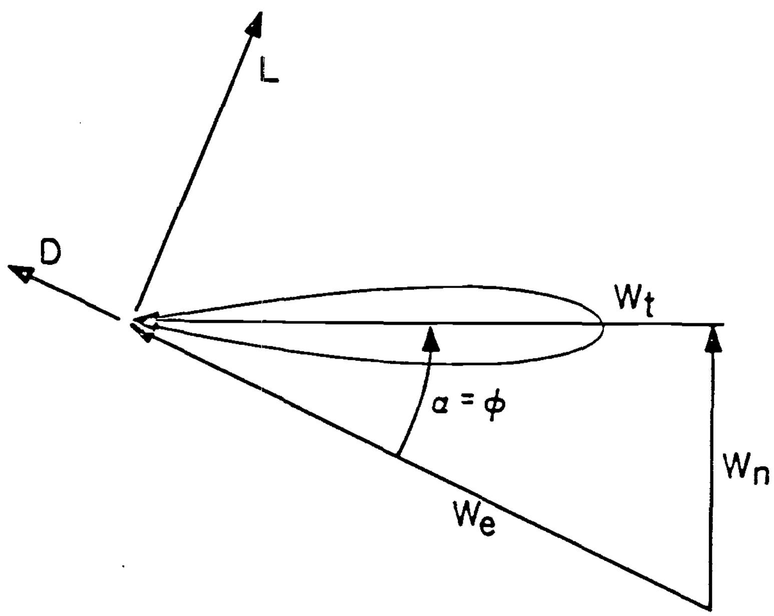

Figure II.3.2 Velocity diagram at blade cross section evaluated at nominal value.

$$C_n = C_L \cos\alpha + C_D \sin\alpha$$

$$C_{n_\nu} = C_{L_{\alpha_E}} \cos\alpha + C_{D_{\alpha_E}} \sin\alpha - C_t$$

$$C_t = C_L \sin\alpha - C_D \cos\alpha$$

$$C_{t_\nu} = C_{L_{\alpha_E}} \sin\alpha - C_{D_{\alpha_E}} \cos\alpha + C_n$$

$$C_{n_\alpha} = C_{L_{\alpha_E}} \cos\alpha + C_{D_{\alpha_E}} \sin\alpha$$

$$C_{t_\alpha} + C_{L_{\alpha_E}} \sin\alpha - C_{D_{\alpha_E}} \cos\alpha$$

The variation of the tangential force with the dependent variables can be found in the same way. The derivative of the tangential force is defined as

$$H_\eta \frac{dr}{R} = \frac{\partial C_{F_t}}{\partial \eta}$$

and

$$H_\eta = G_1 \frac{W_{n_\eta}}{V_\infty} + G_2 \frac{W_{t_\eta}}{V_\infty} \qquad \text{for } \eta \neq q_1, \dot{q}_1$$

$$H_{q_1} = G_1 \frac{W_{n_{q_1}}}{V_\infty} + G_2 \frac{W_{t_{q_1}}}{V_\infty} + G_4 \tag{27}$$

$$H_{\dot{q}_1} = G_1 \frac{W_{n_{\dot{q}_1}}}{V_\infty} + G_2 \frac{W_{t_{\dot{q}_1}}}{V_\infty} + G_3$$

where

$$G_1 = \frac{c}{R}\left\{\frac{2W_n}{V_\infty} C_t + C_{t_\nu} \frac{W_t}{V_\infty}\right\}$$

$$G_2 = \frac{c}{R}\left\{\frac{2W_t}{V_\infty} C_t - C_{t_\nu} \frac{W_n}{V_\infty}\right\}$$

$$G_3 = \frac{c}{R} C_{t_\alpha} \frac{e_2}{V_\infty} \frac{W_t}{V_\infty} f_1$$

$$G_4 = \frac{c}{R}\left(\frac{W_e}{V_\infty}\right)^2 C_{t_\alpha}$$

II.4 Axial Induction Factor "a"

In this analysis, the nonrotating wake model is used. We can calculate the local value of the axial induction factor by equating the windwise force developed on the blade to the momentum flux in an annular ring of radius r.

Applying the momentum theorem to the flow in the annulus "dr" one obtains an expression for the windwise force as

$$\begin{aligned} dT &= \rho_\infty(2\pi r dr)u(V_\infty - V_2) \\ &= \rho_\infty V_\infty^2 (1 - a)2a2\pi r dr \end{aligned} \qquad (28)$$

Defining a local thrust coefficient by

$$(C_T)_L = \frac{dT}{\frac{1}{2}\rho_\infty V_\infty^2 dA}$$

Equation (28) becomes

$$(C_T)_L = 4a(1 - a) \qquad (29)$$

The local thrust coefficient based on the blade force in the windwise direction is developed using the blade element theory

$$dT = \frac{1}{2} \rho_\infty W_e^2 Bc\ C_n dr \tag{30}$$

Using the definition of $(C_T)_L$, we obtain

$$(C_T)_L = \left(\frac{Bc}{r}\right)\left(\frac{W_e}{V_\infty}\right)^2 \frac{C_n}{2\pi} \tag{31}$$

With a given value of C_L, the local axial induction factor can be found by equating Eqs. (29) and (31).

The simple momentum theory approach leads to the result that the induction factor "a" cannot be greater than 0.5 as this would yield zero downstream velocity. However, increasing thrust coefficient values are obtained for $a > 0.5$.

When the axial induction factor "a" is greater than $a_{critical}$, the Glauert relationship [4] has been used instead of the simple momentum theorem. The Glauert relationship is shown in Figure II.4.1. This empirical relationship can be approximated by a straight line with good accuracy using wind tunnel test data. The straight line approximation used in this analysis for $a > a_c$ is

$$(C_T)_L = 4a_c(1 - a_c) + 4(1 - 2a)(a - a_c) \tag{32}$$

where $a_c = 0.38$.

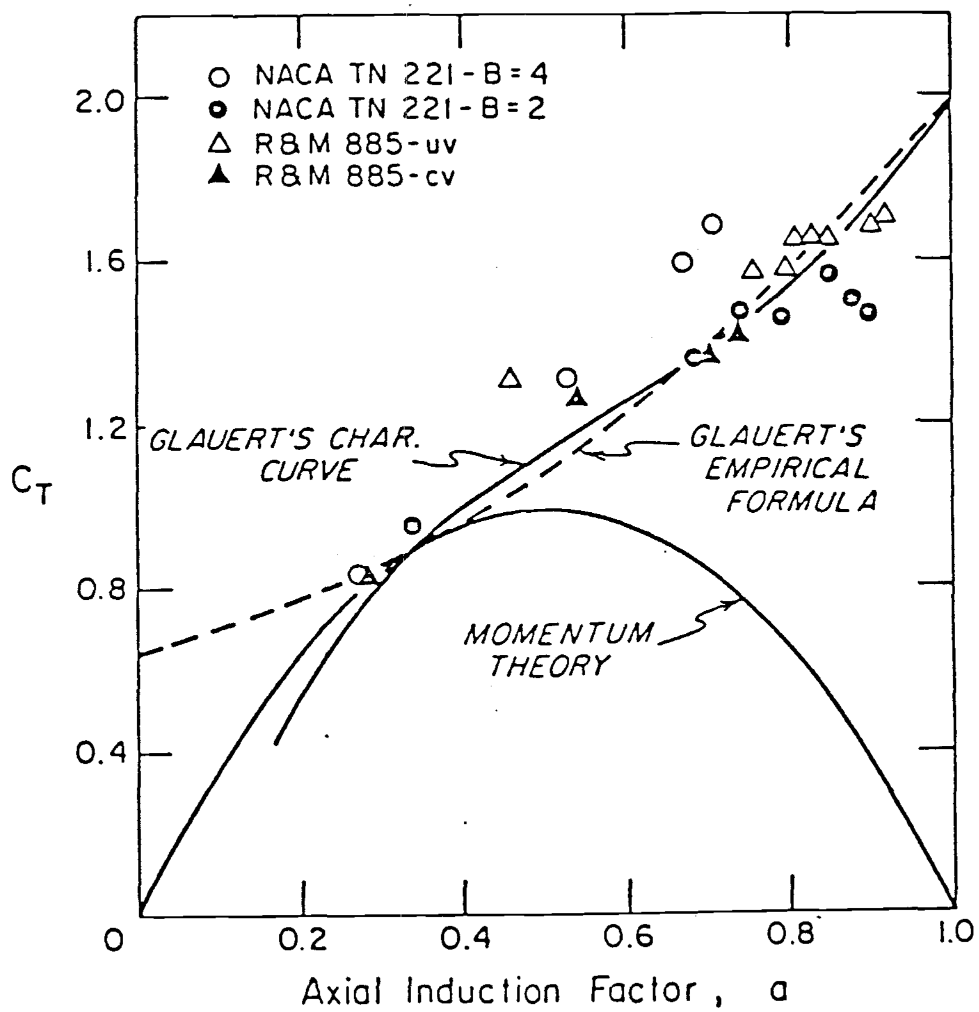

Figure II.4.1 Windmill brake state performance.

II.5 Variation of Axial Induction Factor with Generalized Coordinates

In the process of linearizing the aeroforces, the variation of the axial induction factor with the dependent variables is encountered. We can calculate the local variation of the axial induction factor by equating the derivative of the moments developed by the blade force to the derivative of the moments developed by the momentum flux.

Defining the variation of the axial induction factor as

$$\frac{\partial a}{\partial \eta} = k_\eta \frac{r}{R} \sin\psi + j_\eta \frac{r}{R} \cos\psi \tag{33}$$

Substituting the expression for the variation of the axial induction factor back into the linearized aerodynamic forces terms, we now have two new coefficients to solve for, k_η and j_η.

The coefficient k_η can be calculated by equating the derivative of the yaw moment developed by the momentum theorem to the yaw moment derivative developed by the blade element theory. In the same way, the coefficient j_η can be calculated by equating the derivative of the pitching moment developed by the momentum theorem to the pitching moment derivative obtained from the blade element theory.

Considering the segment "$r_N dr_N d\psi$" of the annulus "dr", we obtain the expression of the moment as the cross product of the r_N vector and the windwise force of that segment.

$$d\vec{M} = \vec{r}_N \times d\vec{T} \tag{34}$$

where

$$r_N = (r + u_m)\cos\rho - w\sin\rho \tag{35}$$

$$dT = \rho_\infty V_\infty^2 (\cos\gamma - a)2a\ r_N dr_N d\psi \tag{36}$$

A local moment coefficient is defined as

$$dC_M = \frac{dM}{\frac{1}{2}\rho_\infty V_\infty^2 \pi R^3} \tag{37}$$

Substituting Eqs. (35) and (36) into Eq. (37), we obtain the expression of the yaw moment as the component of the vector "dC_M" in the n_x direction and the pitching moment in the n_y direction.

The expression for the yaw moment is

$$dC_{M_x} = \frac{1}{\pi} 4a(\cos\gamma - a) \frac{r_N^2}{R} \sin\psi \frac{dr_N}{R} d\psi \tag{38}$$

The expression for the pitching moment is

$$dC_{M_y} = \frac{1}{\pi} 4a(\cos\gamma - a) \frac{r_N^2}{R} \cos\psi \frac{dr_N}{R} d\psi \tag{39}$$

By taking the derivative of the yaw moment and the pitching moment with respect to the dependent variables then integrating over the whole rotor, we obtain the expression

$$\frac{\partial C_{M_x}}{\partial \eta} = + \frac{1}{\pi} \int_0^R \int_0^{2\pi} \frac{\partial C_{T_L}}{\partial a} \frac{\partial a}{\partial \eta} \frac{r_N^2}{R^2} \sin\psi d\psi \frac{dr_N}{R} \tag{40}$$

$$\frac{\partial C_{M_y}}{\partial \eta} = - \frac{1}{\pi} \int_0^R \int_0^{2\pi} \frac{\partial C_{T_L}}{\partial a} \frac{\partial a}{\partial \eta} \frac{r_N^2}{R^2} \cos\psi d\psi \frac{dr_N}{R} \tag{41}$$

where

$$C_{T_L} = 4a(1 - a)$$

Substituting the expression of $\frac{\partial a}{\partial \eta}$ from Eq. (33) into Eqs. (40) and (41), we obtain

$$\frac{\partial C_{M_x}}{\partial \eta} = k_\eta \Pi_1 \tag{42}$$

$$\frac{\partial C_{M_y}}{\partial \eta} = - j_\eta \Pi_1 \tag{43}$$

where

$$\Pi_1 = \int_0^R \frac{\partial C_{T_L}}{\partial a} \frac{r_N^3}{R^3} \frac{dr_N}{R} \tag{44}$$

Now we will look into the same yaw moment and the same pitching moment but they will be developed by blade force instead of momentum flux.

Considering the small element of blade "dr", the moment created by the aeroforces and aeromoments are expressed as

$$d\vec{M} = \vec{r}_M \times d\vec{F} + d\vec{M}_{\frac{c}{4}} \tag{45}$$

where

$$\vec{r}_M = (r + u_m)\vec{n}_{x\rho} + w_{z\beta} + e_1\vec{n}_2$$

$$d\vec{F} = dF_n\vec{n}_{z\theta} + dF_t\vec{n}_{y\theta}$$

$$d\vec{M}_{\frac{c}{4}} = dM_{\frac{c}{4}} \, \vec{n}_1$$

the expression for the yaw moment is obtained from the component of $d\vec{C}_M$ in the n_x direction

$$dC_{M_x} = \frac{N}{\pi} \, (TL1) \, \frac{dr}{R} \, d\psi + \frac{H}{\pi} \, (TL2) \, \frac{dr}{R} \, d\psi \tag{46}$$

where

$$N = \left(\frac{W_e}{V_\infty}\right)^2 C_n \, \frac{c}{R}$$

$$H = \left(\frac{W_e}{V_\infty}\right)^2 C_t \, \frac{c}{R}$$

$$TL1 = \left\{ \begin{array}{l} \frac{e_1}{R} \cos\theta[(\cos\rho\cos w' - \sin\rho\sin w'\cos\beta)\cos\psi - \sin w'\sin\beta\sin\psi] \\ \\ -[\frac{(r+u_m)}{R} \cos w' - \frac{w}{R} \sin w'](\sin\rho\sin\beta\cos\psi - \cos\beta\sin\psi) \end{array} \right.$$

$$TL2 = \left\{ \begin{array}{l} -[\frac{(r+u_m)}{R} \sin w' - \frac{w}{R} \cos w' - \frac{e_1}{R} \sin\theta][(\sin w'\sin\beta\sin\psi) \\ \\ \qquad + (\cos\rho\cos w' - \sin\rho\sin w'\cos\beta)\cos\psi] \\ \\ -[\frac{(r+u_m)}{R} \cos w' + \frac{w}{R} \sin w'][(\cos\rho\sin w' + \sin\rho\cos w'\cos\beta)\cos\psi \\ \\ \qquad + \cos w'\sin\beta\sin\psi] \end{array} \right.$$

Now we take the derivative of this moment with respect to the dependent variables. Then we add the effect which accounts for the "B" turbine blades in the system. The expression of the average yaw moment derivative is given as

$$\frac{\partial C_{M_x}}{\partial \eta} = \frac{B}{2\pi^2} \int_{R_H}^{R} \int_{0}^{2\pi} N_\eta (TL1) \frac{dr}{R} d\psi + \frac{B}{2\pi^2} \int_{R_H}^{R} \int_{0}^{2\pi} H_\eta (TL2) \frac{dr}{R} d\psi \tag{47}$$

where

$$N_\eta = \frac{\partial N}{\partial \eta}$$

$$H_\eta = \frac{\partial H}{\partial \eta}$$

By substituting the expression of $\frac{\partial a}{\partial \eta}$ from Eq. (33) into N_η and H_η terms, the derivative of the yaw moment is expressed in terms of k_η and j_η.

The expression of the pitching moment developed by the blade force is expressed as the component of $d\vec{C}_M$ in Eq. (45) in the n_y direction. Then the derivative of the pitching moment $\frac{\partial C_{M_y}}{\partial \eta}$ is obtained in the same way as it is done in $\frac{\partial C_{M_x}}{\partial \eta}$.

Now we can equate the derivative of the yaw moment developed by momentum flux to the one developed by blade force and the derivative of pitching moment developed by momentum flux to the one developed by blade force. The analysis results in two equations and two unknowns (k_η and j_η).

The result of this linearized analysis shows that the variation of the axial induction factor exists only for the yaw and yaw rate variables

$$\frac{\partial a}{\partial \eta} = 0 \qquad \eta \neq q_4 \text{ and } \dot{q}_4 \tag{48}$$

The coefficients k_η and j_η for yaw and yaw rate are given by

$$k_{q_4} = \frac{(\Pi_4 + \Pi_5 + \Pi_6 + \Pi_7)(\Pi_1 - \Pi_3) - \Pi_2(\Pi_{12} + \Pi_{13} + \Pi_{14} + \Pi_{15})}{(\Pi_1 - \Pi_3)^2 + \Pi_2^2} \quad (49)$$

$$j_{q_4} = - \frac{\{(\Pi_4 + \Pi_5 + \Pi_6 + \Pi_7)\Pi_2 + (\Pi_1 - \Pi_3)(\Pi_{12} + \Pi_{13} + \Pi_{14} + \Pi_{15})\}}{(\Pi_1 - \Pi_3)^2 + \Pi_2^2} \quad (50)$$

$$k_{\dot{q}_4} = \frac{(\Pi_8 + \Pi_9 + \Pi_{10} + \Pi_{11})(\Pi_1 - \Pi_3) - \Pi_2(\Pi_{16} + \Pi_{17} + \Pi_{18} + \Pi_{19})}{(\Pi_1 - \Pi_3)^2 + \Pi_2^2} \quad (51)$$

$$j_{\dot{q}_4} = \frac{-\{(\Pi_8 + \Pi_9 + \Pi_{10} + \Pi_{11})\Pi_2 + (\Pi_1 - \Pi_3)(\Pi_{16} + \Pi_{17} + \Pi_{18} + \Pi_{19})\}}{(\Pi_1 - \Pi_3)^2 + \Pi_2^2} \quad (52)$$

where Π_i's are the integral terms.

These integral terms are given as follows:

$$\Pi_1 = \int_{R_H}^{R} \frac{\partial C_{T_L}}{\partial a} \left(\frac{r_N}{R}\right)^3 \frac{dr_N}{R}$$

$$\Pi_2 = \left| \begin{aligned} & \frac{3}{2\pi} \int_{R_H}^{R} (N1) \frac{e_1}{R} (\cos\rho\cos w_o' - \sin\rho\sin w_o'\cos\beta) \frac{r_N}{R}\frac{dr}{R} \\ & - \frac{3}{2\pi} \int_{R_H}^{R} (N1) \left(\frac{(r+u_m)}{R} \cos w_o' + \frac{w_o}{R} \sin w_o'\right) \sin\rho\sin\beta \frac{r_N}{R}\frac{dr}{R} \\ & + \frac{3}{2\pi} \int_{R_H}^{R} (H1)\left(\frac{(r+u_m)}{R} \sin w_o' - \frac{w_o}{R} \cos w_o'\right)(\cos\rho\cos w_o' \\ & \quad - \sin\rho\sin w_o'\cos\beta) \frac{r_N}{R}\frac{dr}{R} \\ & - \frac{3}{2\pi} \int_{R_H}^{R} (H1)\left(\frac{(r+u_m)}{R} \cos w_o' + \frac{w_o}{R} \sin w_o'\right)(\cos\rho\sin w_o' \\ & \quad + \sin\rho\cos w_o'\cos\beta) \frac{r_N}{R}\frac{dr}{R} \end{aligned} \right.$$

$$\Pi_3 = \left\{ \begin{array}{l} -\frac{3}{2\pi}\int_{R_H}^{R} (N1)\ \frac{e_1}{R}\sin w_0' \sin\beta\ \frac{r_N}{R}\frac{dr}{R} \\ \frac{3}{2\pi}\int_{R_H}^{R} (N1)\ \left(\frac{(r+u_m)}{R}\cos w_0' + \frac{w_0}{R}\sin w_0'\right)\cos\beta\ \frac{r_N}{R}\frac{dr}{R} \\ -\frac{3}{2\pi}\int_{R_H}^{R} (H1)\left(\frac{(r+u_m)}{R}\sin w_0' - \frac{w_0}{R}\cos w_0'\right)\sin w_0' \sin\beta\ \frac{r_N}{R}\frac{dr}{R} \\ -\frac{3}{2\pi}\int_{R_H}^{R} (H1)\left(\frac{(r+u_m)}{R}\cos w_0' + \frac{w_0}{R}\sin w_0'\right)\cos w_0' \sin\beta\ \frac{r_N}{R}\frac{dr}{R} \end{array} \right.$$

$$\Pi_4 = \frac{3}{2\pi}\int_{R_H}^{R} (N2)\Big[\frac{e_1}{R}(\cos\rho\cos w_0' - \sin\rho\sin w_0'\cos\beta) - \Big(\frac{(r+u_m)}{R}\cos w_0' + \frac{w_0}{R}\sin w_0'\Big)\ \sin\rho\sin\beta\Big] f_4\ \frac{dr}{R}$$

$$\Pi_5 = \frac{3}{2\pi}\int_{R_H}^{R} (N3)\Big(\frac{e_1}{R}\sin w_0'\sin\beta - \Big(\frac{(r+u_m)}{R}\cos w_0' + \frac{w_0}{R}\sin w_0'\Big)\cos\beta\Big) f_4\ \frac{dr}{R}$$

$$\Pi_6 = \left\{ \begin{array}{l} \frac{3}{2\pi}\int_{R_H}^{R} (H2)\left(\frac{(r+u_m)}{R}\sin w_0' - \frac{w_0}{R}\cos w_0'\right)(\cos\rho\cos w_0' \\ \qquad - \sin\rho\sin w_0'\cos\beta) f_4\ \frac{dr}{R} \\ -\frac{3}{2\pi}\int_{R_H}^{R} (H2)\left(\frac{(r+u_m)}{R}\cos w_0' + \frac{w_0}{R}\sin w_0'\right)(\cos\rho\sin w_0' \\ \qquad + \sin\rho\cos w_0'\cos\beta) f_4\ \frac{dr}{R} \end{array} \right.$$

$$\Pi_7 = \frac{3}{2\pi}\int_{R_H}^{R} (H3)\left[\left(\frac{(r+u_m)}{R}\cos w_o' + \frac{w_o}{R}\sin w_o'\right)\cos w_o'\sin\beta + \left(\frac{(r+u_m)}{R}\sin w_o' - \frac{w_o}{R}\cos w_o'\right)\sin w_o'\sin\beta\right] f_4 \frac{dr}{R}$$

$$\Pi_8 = \frac{3}{2\pi}\int_{R_H}^{R} (N4)\left[\frac{e_1}{R}\left(\cos\rho\cos w_o' - \sin\rho\sin w_o'\cos\beta\right) - \left(\frac{(r+u_m)}{R}\cos w_o' + \frac{w_o}{R}\sin w_o'\right)\sin\rho\sin\beta\right] f_4 \frac{dr}{R}$$

$$\Pi_9 = \frac{3}{2\pi}\int_{R_H}^{R} (N5)\left[\frac{e_1}{R}\sin w_o'\sin\beta - \left(\frac{(r+u_m)}{R}\cos w_o' + \frac{w_o}{R}\sin w_o'\right)\cos\beta\right] f_4 \frac{dr}{R}$$

$$\Pi_{10} = \left\{\begin{array}{l} \frac{3}{2\pi}\int_{R_H}^{R} (H4)\left(\frac{(r+u_m)}{R}\sin w_o' - \frac{w_o}{R}\cos w_o'\right)(\cos\rho\cos w_o' - \\ \quad - \sin\rho\sin w_o'\cos\beta) f_4 \frac{dr}{R} \\ - \frac{3}{2\pi}\int_{R_H}^{R} (H4)\left(\frac{(r+u_m)}{R}\cos w_o' + \frac{w_o}{R}\sin w_o'\right)(\cos\rho\sin w_o' \\ \quad + \sin\rho\cos w_o'\cos\beta) f_4 \frac{dr}{R} \end{array}\right.$$

$$\Pi_{11} = \frac{3}{2\pi}\int_{R_H}^{R} (H5)\left[\left(\frac{(r+u_m)}{R}\cos w_o' + \frac{w_o}{R}\sin w_o'\right)\cos w_o'\sin\beta + \left(\frac{(r+u_m)}{R}\sin w_o' - \frac{w_o}{R}\cos w_o'\right)\sin w_o'\sin\beta\right] f_4 \frac{dr}{R}$$

$$\Pi_{12} = \frac{3}{2\pi}\int_{R_H}^{R} (N2)\left(\frac{e_1}{R}\sin w_o'\sin\beta - \left(\frac{(r+u_m)}{R}\cos w_o' + \frac{w_o}{R}\sin w_o'\right)\cos\beta\right) f_4 \frac{dr}{R}$$

$$\Pi_{13} = \frac{3}{2\pi}\int_{R_H}^{R} (N3)\left(\frac{e_1}{R}\left(\sin\rho\sin w_o'\cos\beta - \cos\rho\cos w_o'\right) + \left(\frac{(r+u_m)}{R}\cos w_o' + \frac{w_o}{R}\sin w_o'\right)\sin\rho\sin\beta\right) f_4 \frac{dr}{R}$$

$$\Pi_{14} = \frac{3}{2\pi}\int_{R_H}^{R} (H2)[(\frac{(r+u_m)}{R}\sin w_o' - \frac{w_o}{R}\cos w_o')\sin w_o'\sin\beta$$

$$+ (\frac{(r+u_m)}{R}\cos w_o' + \frac{w_o}{R}\sin w_o')\cos w_o'\sin\beta]f_4\frac{dr}{R}$$

$$\Pi_{15} = \left| \begin{array}{l} - \frac{3}{2\pi}\int_{R_H}^{R} (H3)(\frac{(r+u_m)}{R}\sin w_o' - \frac{w_o}{R}\cos w_o')(\cos\rho\cos w'_o \\ - \sin\rho\sin w_o'\cos\beta)f_4\frac{dr}{R} \\ + \frac{3}{2\pi}\int_{R_H}^{R} (H3)(\frac{(r+u_m)}{R}\cos w_o' + \frac{w_o}{R}\sin w_o')(\cos\rho\sin w_o' \\ + \sin\rho\cos w_o'\cos\beta)f_4\frac{dr}{R} \end{array} \right.$$

$$\Pi_{16} = \frac{3}{2\pi}\int_{R_H}^{R} (N4)[\frac{e_1}{R}\sin w_o'\sin\beta - (\frac{(r+u_m)}{R}\cos w_o' + \frac{w_o}{R}\sin w_o')\cos\beta]f_4\frac{dr}{R}$$

$$\Pi_{17} = -\frac{3}{2\pi}\int_{R_H}^{R} (N5)[\frac{e_1}{R}(\cos\rho\cos w_o' - \sin\rho\sin w_o'\cos\beta)$$

$$- (\frac{(r+u_m)}{R}\cos w_o' + \frac{w_o}{R}\sin w_o')\sin\rho\sin\beta]f_4\frac{dr}{R}$$

$$\Pi_{18} = \frac{3}{2\pi}\int_{R_H}^{R} (H4)[(\frac{(r+u_m)}{R}\sin w_o' - \frac{w_o}{R}\cos w_o')\sin w_o'\sin\beta$$

$$+ (\frac{(r+\dot{u}_m)}{R}\cos w_o' + \frac{w_o}{R}\sin w_o')\cos w_o'\sin\beta]f_4\frac{dr}{R}$$

$$\Pi_{19} = \left\{ \begin{array}{l} -\frac{3}{2\pi} \int_{R_H}^{R} (H5)\left(\frac{(r+u_m)}{R} \sin w_o' - \frac{w_o}{R} \cos w_o'\right)(\cos\rho \cos w_o' \\ \qquad - \sin\rho \sin w_o' \cos\beta) f_4 \frac{dr}{R} \\ + \frac{3}{2\pi} \int_{R_H}^{R} (H5)\left(\frac{(r+u_m)}{R} \cos w_o' + \frac{w_o}{R} \sin w_o'\right)(\cos\rho \sin w_o' \\ \qquad + \sin\rho \cos w_o' \cos\beta) f_4 \frac{dr}{R} \end{array} \right.$$

where

$$N1 = (\sin\rho \sin w_o' - \cos\rho \cos w_o' \cos\beta) F_1 - \cos\rho \sin\beta F_2$$

$$N2 = \cos w_o' \sin\beta F_1 - \cos\beta F_2$$

$$N3 = (\cos\rho \sin w_o' + \sin\rho \cos w_o' \cos\beta) F_1 + \sin\rho \sin\beta F_2$$

$$N4 = \left\{ \begin{array}{l} \left(\frac{\ell}{V_\infty} \sin\beta \cos w_o' + \frac{(r+u_d)}{V_\infty} \sin\rho \sin\beta \cos w_o' + \frac{w_o}{V_\infty} \sin w_o' \sin\rho \sin\beta\right) F_1 \\ + \frac{e_3}{V_\infty} (\cos\rho \cos w_o' - \sin\rho \sin w_o' \cos\beta) F_1 \\ -\left(\frac{\ell}{V_\infty} \cos\beta + \frac{(r+u_d)}{V_\infty} \sin\rho \cos\beta + \frac{w_o}{V_\infty} \cos\rho\right) F_2 \end{array} \right.$$

$$N5 = \left\{ \begin{array}{l} \left(\frac{\ell}{V_\infty} (\sin\rho \cos\beta \cos w_o' + \sin w_o' \cos\rho) + \frac{(r+u_d)}{V_\infty} \cos\beta \cos w_o' \right. \\ \qquad \left. + \frac{w_o}{V_\infty} \sin w_o' \cos\beta + \frac{e_3}{V_\infty} \sin w_o' \sin\beta\right) F_1 \\ +\left(\frac{\ell}{V_\infty} \sin\rho \sin\beta + \frac{(r+u_d)}{V_\infty} \sin\beta\right) F_2 \end{array} \right.$$

The expressions for H1, H2, H3, H4, and H5 are the same as N1, N2, N3, N4, and N5, respectively, except F_1 and F_2 in Ni terms are replaced by G_1 and G_2 in Hi terms.

II.6 Tip Loss Model

In order to account for nonuniform flow in the wake of a wind turbine, flow models have been adapted from the propeller theory. Physically, the tip correction accounts for the fact that the maximum change in axial velocity, $2aV_\infty$, in the wake occurs only at the vortex sheets and the average velocity change in the wake is $2aV_\infty F$, where F is the tip loss factor.

"Tip losses" have been treated in a variety of different manners in the propeller and helicopter industries. The simplest method is to reduce the maximum rotor radius by some fraction of the actual radius, which in helicopter studies is of the order of 0.03R. A more detailed analysis was done by Prandtl [15] as a method for estimation of lightly loaded propeller tip losses. Later Goldstein [5] developed a more rigorous analysis.

But due to the ease of use and the fact that the available experimental data are not sufficiently accurate to resolve the differences predicted by various approaches, only the Prandtl method will be considered.

Prandtl's factor is defined as

$$F = \frac{2}{\pi} \text{arc cos } e^{-f}$$

where

$$f = \frac{B}{2} \frac{R-r}{R\sin\phi_T} = \frac{B}{2} \frac{R/r-1}{\sin\phi}$$

The expression for f can be suitably approximated by writing $r\sin\phi$ in place of $R\sin\phi_T$. Here B represents the number of blades; ϕ_T is the angle of the helical surface with the slipstream boundary.

II.7 Power and Thrust Coefficient

From the blade elementary theory, the windwise force and torque at the nominal value are given as

$$dT = \frac{1}{2}\rho_\infty BW_e^2 cC_N \frac{dr}{R} \tag{53}$$

$$dQ = \frac{1}{2}\rho_\infty BW_e^2 cC_t r \frac{dr}{R} \tag{54}$$

Power is defined as the product of torque and angular speed

$$dP = \Omega dQ \tag{55}$$

Normalizing Eqs. (53) and (55) with $\frac{1}{2}\rho_\infty V_\infty^2 \pi R^2$ and $\frac{1}{2}\rho_\infty V_\infty^3 \pi R^2$, respectively and making use of the relationship of the relative velocities and angles at the blade cross section, one obtains

$$C_P = \frac{\cos^3\rho}{\pi X} \int_{x_{hub}}^{x_{tip}} \frac{Bc}{R}\sqrt{1 + \left(\frac{1-a}{x}\right)^2}\,\left[(1-a)C_L - xC_D\right]x^2 dx \tag{56}$$

$$C_T = \frac{\cos^3\rho}{\pi X} \int_{x_{hub}}^{x_{tip}} \frac{Bc}{R}\sqrt{1 + \left(\frac{1-a}{x}\right)^2}\,\left[xC_L + (1-a)C_D\right]x dx \tag{57}$$

APPENDIX III

DERIVATION OF GOVERNING EQUATIONS

In order to develop the equations of motion, the Lagrange method is used. The expression of kinetic and potential energy of the system will be developed. Then, by using the virtual work concept an expression for the nonconservative forces can be obtained.

Lagrange's equation is used to develop the equations of motion. The Lagrange equation is given as

$$\frac{d}{dt}\left(\frac{\partial L}{\partial \dot{q}_i}\right) - \frac{\partial L}{\partial q_i} = Q_i$$

where

L = Lagrangian function = KE-PE

Q_i = nonconservative force

q_i = generalized coordinate

With the expression of KE, PE and Q_i substituted back into Lagrange's equations, we obtain the equations of motion.

III.1 Kinetic and Potential Energy

In order to obtain the expression for kinetic energy of the rotor system, the velocity and angular velocity of the blade element are first developed. With known values of mass and mass moment of inertia of the blade element, the kinetic energy is expressed as

$$d(KE) = V_c^2 dm + \omega_1^2 dI_1 + \omega_2^2 dI_2 + \omega_3^2 dI_3 \tag{1}$$

Here V_c is the velocity of the blade element of length dr, ω_i's are angular velocities of the blade element in the direction normal and tangent to the blade, dm is the mass of the blade element, and dI_i's are the mass moment of inertias of the blade element at mass center in the same direction as the ω_i's.

The total kinetic energy of the blade system is obtained by integrating over the blade length and adding the contributions of each blade

$$KE = \sum_{i=1}^{B} \int_{R_H}^{R} V_c^2 dm + \sum_{i=1}^{B} \int_{R_H}^{R} \omega_1^2 \, dI_1 + \sum_{i=1}^{B} \int_{R_h}^{R} \omega_2^2 dI_2 + \sum_{i=1}^{B} \int_{R_h}^{R} \omega_3^2 dI_3 \tag{2}$$

where B is the number of blades.

The additional kinetic energy due to the hub mass and generator are considered. The additional kinetic energy terms are expressed as

$$KE = \frac{1}{2} I_H \dot{\psi}^2 + \frac{1}{2} I_G (N_G \dot{\psi})^2 \tag{3}$$

Here I_H is the mass moment of inertia of the hub around the rotor shaft, I_G is the mass moment of inertia of generator around the rotor shaft, and N_G is the step-up gearing ratio between the turbine and the generator.

An expression for the potential energy of the rotor system can be derived from the strain energy due to the blade deflection and blade twisting. The expression for the strain energy of an element of a blade is first developed, then integrating along the blade span and adding the contribution of each blade to get the total potential energy. Thus, we obtain

$$U = \sum_{i=1}^{B} \frac{1}{2} \int_{R_H}^{R} EI(r)\left(\frac{\partial^2 W}{\partial r^2}\right)^2 dr + \sum_{i=1}^{B} \frac{1}{2} \int_{R_H}^{R} GJ(r)\left(\frac{\partial \theta}{\partial r}\right)^2 dr \qquad (4)$$

III.2 Virtual Work

The virtual work principle can be stated as, "If a system of forces is in equilibrium, the work done by the externally applied forces through virtual displacements compatible with the constraint of the system is zero," [11]

$$\delta W = \sum_{i=1}^{n} \vec{F}_i \cdot \delta\vec{r}_i = 0$$

where

$\vec{F}_i$ = external force

$\delta\vec{r}_i$ = virtual displacement

Virtual displacement is defined as infinitesimal arbitrary changes in the coordinates of a system. These are small variations from the true position of the system and must be compatible with the constraints of the system.

The total virtual work of the system can be expressed as the summation of the virtual work of conservative forces and the virtual work of nonconservative forces. The conservative forces are the forces that do depend on position and can be derived from a potential function. Conservative forces are the inertia forces, the contact forces, and body forces. The nonconservative forces are energy-dissipating forces, such as friction forces and forces imparting energy to the system, such as external forces. Nonconservative forces are forces that do not depend on position alone and cannot be derived from a potential function.

In this analysis we will consider the virtual work of the nonconservative forces alone. The nonconservative forces in our case are the aerodynamic forces and moments.

III.3 Nonconservative Forces

First, let us redefine the virtual displacement and virtual angular displacement (virtual rotation) of the system. In this analysis, we assume that the aeroforces and moments act at 1/4 chord position of the blade cross section. The virtual displacement and virtual angular displacement are defined as [10]

$$\delta\vec{P} = \frac{\partial \vec{V}_d}{\partial \dot{q}_i}\,\delta q_i \tag{5}$$

$$\delta\vec{\alpha} = \frac{\partial \vec{\omega}}{\partial \dot{q}_i}\,\delta q_i \tag{6}$$

where

$\frac{\partial \vec{V}_d}{\partial \dot{q}_i}$ = the partial rate of change of position with respect to q_i at the 1/4 blade chord in the inertial reference frame.

$\frac{\partial \vec{\omega}}{\partial \dot{q}_i}$ = is the partial rate of change with respect to q_i of orientation of the blade in the inertial reference frame.

The virtual work is defined as the summation of the inner product of the aerodynamic force and the virtual displacement and the inner product of the aerodynamic torque or couple and the virtual angular displacement

$$\delta W = \vec{F} \cdot \delta \vec{P} + \vec{M} \cdot \delta \vec{\alpha} \tag{7}$$

The aerodynamic force and couple at 1/4 chord are defined as

$$\vec{F} = F_n \vec{e}_n + F_t \vec{e}_t \tag{8}$$

$$\vec{M} = M \vec{n}_1$$

Substituting Eqs. (7) and (8) into Eqs. (6) the expression for the virtual work becomes

$$\delta W = Q_1 \delta q_1 + Q_2 \delta q_2 + Q_3 \delta q_3 + Q_4 \delta q_4$$

where Q_i represents the nonconservative force relevant for the right hand side of the Lagrange's equation

$$Q_1 = \vec{F} \cdot \left(\frac{\partial \vec{V}_d}{\partial \dot{q}_1}\right) + \vec{M} \cdot \left(\frac{\partial \vec{\omega}}{\partial \dot{q}_1}\right) \tag{9}$$

$$Q_2 = \vec{F} \cdot \left(\frac{\partial \vec{V}_d}{\partial \dot{q}_2}\right) + \vec{M} \cdot \left(\frac{\partial \vec{\omega}}{\partial \dot{q}_2}\right) \tag{10}$$

$$Q_3 = \vec{F} \cdot \left(\frac{\partial \vec{V}_d}{\partial \dot{q}_3}\right) + \vec{M} \cdot \left(\frac{\partial \vec{\omega}}{\partial \dot{q}_3}\right) \tag{11}$$

$$Q_4 = \vec{F} \cdot \left(\frac{\partial \vec{V}_d}{\partial \dot{q}_4}\right) + \vec{M} \cdot \left(\frac{\partial \vec{\omega}}{\partial \dot{q}_4}\right) \tag{12}$$

Now we have the expression for the Lagrangian function and the non-conservative forces. Substituting these expressions back into Lagrange's equation, we obtain four equations of motion. These equations can be written in matrix form as

$$[M]\,\{\ddot{q}_i\} + [C]\,\{\dot{q}_i\} = \{G(q_1,\ldots q_4,\ \dot{q}_1,\ldots\dot{q}_4,t)\} \tag{13}$$

where

$[M]$ = nonlinear mass coefficient matrix

$[C]$ = nonlinear damping coefficient matrix from $\frac{d}{dt}\left(\frac{\partial L}{\partial \dot{q}_i}\right)$

$\{G\}$ = a vector consisting of nonlinear terms from $\frac{\partial L}{\partial q_i} + Q_i$

III.4 Nacelle, Gravity

Nacelle

In this analysis we will consider the nacelle as a slender body. The shape of the nacelle is assumed to be a cylinder with a hemisphere on the forebody and afterbody. Figure III.4.1 shows a picture of the nacelle.

Since we assume that the nacelle acts like a rigid body and the only movement it is allowed is rotation around the yaw axis, the kinetic energy and potential energy can be expressed as

$$KE = \frac{1}{2} I_n \dot{\gamma}^2$$

$$PE = 0$$

where I_n is the nacelle's mass moment of inertia around the yaw axis

$$KE = \frac{1}{2} I_n f_4^2 \dot{q}_4^2 \tag{14}$$

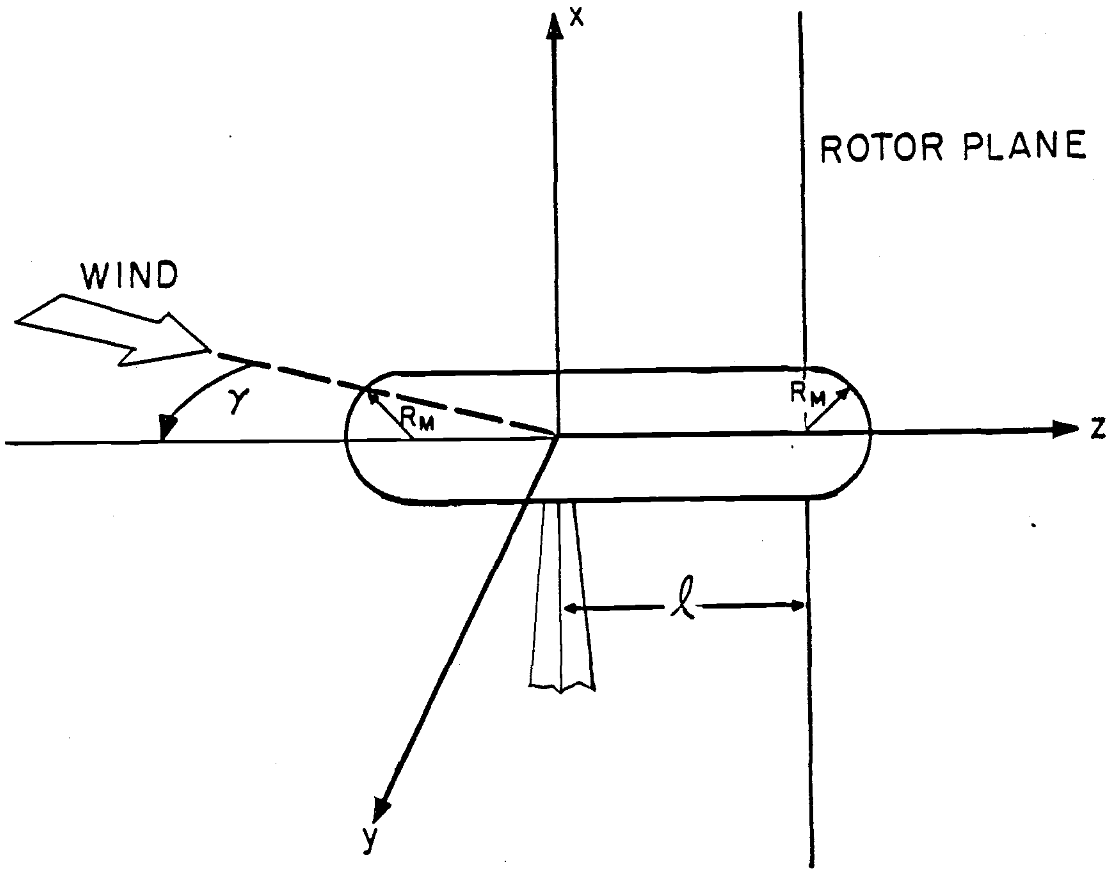

Figure III.4.1 Nacelle geometry.

For the nonconservative force, the forces on the nacelle are calculated by using the slender body theorem. The forces on the body can be expressed as

$$dF_y = 2q_\infty \frac{ds}{dz}\, dz \tag{15}$$

$$dF_z = \{P_\infty - q_\infty(\gamma^2 + \frac{u_{z1}}{V_\infty}(R,z) + (\frac{dR(z)}{dz})^2\} \frac{ds}{dz}\, dz \tag{16}$$

where

s = the cross section area of the body

R(z) = the radius of the body cross section

The virtual displacement of the nacelle is expressed as

$$\delta\vec{P} = zf_4 \delta q_4\, \vec{n}_y \tag{17}$$

The virtual work of the nacelle system is given by

$$d(\delta W) = dF_y\ \delta P$$

$$= (2q_\infty z \frac{ds}{dz}\, dz\ f_4^2 q_4)\delta q_4 \tag{18}$$

The nonconservative force for the nacelle is expressed as

$$dQ_N = 2q_\infty z \frac{ds}{dz}\, dz\ f_4^2\, q_4 \tag{19}$$

The force on the nacelle exists only at the hemispheres at both ends of the nacelle $\left(\frac{ds}{dz} \neq 0\right)$.

The afterbody of the nacelle is in the hub area. In real flow, the flow would separate before it reaches the afterbody. Only the forebody part of the nacelle is considered.

The equation of motion of the nacelle is developed by substituting the expression for kinetic energy and the nonconservative force in Lagrange's equation. The nondimensionalized equation of motion is given by

$$m_{44_n} \ddot{q}_4 + k_{44_n} q_4 = 0 \tag{20}$$

where

$$m_{44_n} = \frac{I_n}{q_\infty R^3} f_4^2$$

$$k_{44_n} = - \frac{2}{R^3} \int_{-(n-R_M)}^{n} z \frac{ds}{dz} f_4^2 \, dz$$

n = distance from the nacelle's yaw axis to the forebody end of the nacelle

R_M = radius of the hemisphere on forebody and afterbody of the nacelle.

The correction factor for the nacelle with a non-circular cross section is obtained from reference 2. From the analysis of airships, Munk[2] defined the inertia factor for the cross section effect on the lateral forces developed by the slender theory as

for common circular cross section

$$\zeta \doteq 1$$

for other cross section

$$\zeta = \frac{b^2}{4S}$$

where S denotes the area of the cross section and b is its largest width or height at right angles to the motion considered.

Hoerner [8] also suggested the correction factor for the effect of fineness ratio on the slender body as

$$p = (1 - d/l)$$

where l is the length of the body and d is the diameter of the body.

With these correction factors, the stiffness coefficient of the nacelle becomes

$$k_{44_n} = -\frac{2}{R^3} \int_{-(\eta - z_1)}^{\eta} z \frac{ds}{dz} f_4^2 \, dz \, (\zeta p)$$

where z_1 is the distance from the forebody end of the nacelle to the point where $\frac{ds}{dz} = 0$.

Gravity Effect

For a larger wind turbine system, the effect of gravity is very important in dynamic and structural analysis. Although the Enertech

1500 is a small wind turbine system, the gravity effect will be included in the analysis to make the analysis applicable to any size turbine system.

The gravity effect will be added to the system by means of a potential function. The gravitational force of the blade element dr is defined as

$$d\vec{G} = -gdm\ \vec{n}_x \tag{21}$$

The potential function for the gravitational force is given by

$$dP = ghdm \tag{22}$$

where h is a function of q_1, ... q_4, and t, whose absolute value is equal to the distance between the mass center of the blade element cross section and any fixed horizontal plane H.

We are dealing with the expression for the derivative of the potential function $\frac{\partial P}{\partial q_i}$ instead of the potential function itself when we develop the equations of motion by using Lagrange's equation. Therefore we take the derivative of the potential function in Eq. (22) with respect to the generalized coordinate

$$\frac{\partial(dP)}{\partial q_i} = gdm\,\frac{\partial h}{\partial q_i} \tag{23}$$

The velocity of the blade element "dr" measured at the mass center can be expressed as

$$\vec{V}_c = -\frac{dh}{dt}\vec{n}_x + \ldots\ldots\ldots\ldots$$

$$= -\left(\sum_{i=1}^{4} \frac{\partial h}{\partial q_i}\dot{q}_i + \frac{\partial h}{\partial t}\right)\vec{n}_x + \ldots\ldots\ldots \tag{24}$$

The expression $\frac{\partial h}{\partial q_i}$ be found by dotting Eq. (24) with the unit vector $\vec{n}_x$ and assuming that $\frac{\partial h}{\partial t}$ equals zero.

$$\frac{\partial h}{\partial q_i} = -\frac{\partial \vec{V}_c}{\partial \dot{q}_i}\cdot\vec{n}_x \tag{25}$$

Substituting the expression $\frac{\partial h}{\partial q_i}$ in Eq. (25) back into Eq. (23), we have the expression $\frac{\partial (dP)}{\partial q_i}$ accounting for the gravity effect to be put into Lagrange's equation

$$\frac{\partial (dP)}{\partial q_i} = gdm\left(-\frac{\partial \vec{V}_c}{\partial \dot{q}_i}\cdot\vec{n}_x\right) \tag{26}$$

III.5 Tower Shadow

When a rotor is downwind of the tower, the blades pass through the wind shadow cast by the tower. The performance of the wind turbine will be affected by this tower shadow.

In this study, the tower shadow is modeled as the velocity deficit from the rotor axial velocity value over a selected region of the rotor disk, centered about the tower center line. For the simplicity of analysis, the width of the tower shadow is assumed as a segment of the rotor area. The width and the velocity deficit of the tower shadow are dependent on the geometry of the tower. This tower shadow model is shown in Figure III.5.1.

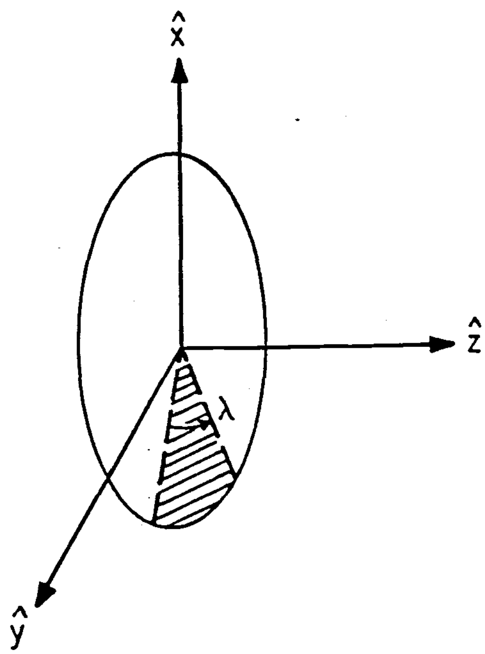

Figure III.5.1 Tower shadow.

To account for the tower shadow effect on the equations of motion of the system, the width and the velocity deficit are arbitrarily chosen. Then for this linear system, the superposition method is used. The average forces on the rotor with the tower shadow will be the average forces on the rotor without the tower shadow, plus the difference of average forces in the shadow region between the one with and the one without the velocity deficit due to the tower shadow.

The coefficients of equations of motion will be recalculated for the shadow region. Many terms in the expression for forces and moments that depend on the azimuth angle, which are usually balanced out in the 3-bladed rotor case, will remain in the tower shadow case.

The average forces and moments in the shadow region are given by

$$F_{shadow} = \frac{B}{2\pi} \int_{\pi - \frac{\lambda}{2}}^{\pi + \frac{\lambda}{2}} \int_{R_H}^{R} (dF)d\psi \tag{27}$$

$$\vec{M}_{shadow} = \frac{B}{2\pi} \int_{\pi - \frac{\lambda}{2}}^{\pi + \frac{\lambda}{2}} \int_{R_H}^{R} (\vec{r} \times d\vec{F})d\psi \tag{28}$$

where

dF = the force on the blade element

λ = the shadow width.

The flow conditions in the tower shadow are developed from a uniform flow model. Thus flow conditions in the tower shadow vary only with velocity deficit and tip speed ratio.

Table III.5.1 gives the values of the integrations from the lower limit of $\pi - \frac{\lambda}{2}$ to $\pi + \frac{\lambda}{2}$.

Table III.5.1. Some integration values.

$$\int_{\pi - \frac{\lambda}{2}}^{\pi + \frac{\lambda}{2}} \sin^2\psi d\psi = \frac{\lambda - \sin\lambda}{2}$$

$$\int_{\pi - \frac{\lambda}{2}}^{\pi + \frac{\lambda}{2}} \cos^2\psi d\psi = - \frac{(\lambda - \sin\lambda)}{2}$$

$$\int_{\pi - \frac{\lambda}{2}}^{\pi + \frac{\lambda}{2}} \sin\psi\cos\psi d\psi = 0$$

$$\int_{\pi - \frac{\lambda}{2}}^{\pi + \frac{\lambda}{2}} \cos\psi d\psi = -2 \sin \frac{\lambda}{2}$$

$$\int_{\pi - \frac{\lambda}{2}}^{\pi + \frac{\lambda}{2}} \sin\psi d\psi = 0$$

APPENDIX IV

LINEARIZED EQUATIONS OF MOTION

IV.1 Linearization

Real systems contain some nonlinearity. If the ranges of values of the dependent variables are sufficiently restricted, the system may be well approximated as linear. In this study we will treat the system in the linear range.

The first thing we need in linearization is the equilibrium value of each dependent variable. Because of the complexity of this rotor system's mathematical model, the equilibrium values have been chosen as

$$\theta_0 = 0 \tag{1}$$

$$w_0 = R_s f_2\left(\frac{r}{R}\right) q_s \tag{2}$$

$$\dot{\chi}_0 = 0 \tag{3}$$

$$\gamma_0 = 0 \tag{4}$$

where q_s is the static tip deflection and the subscript 0 indicates that the values are evaluated at nominal values.

We now define the dependent variable as the nominal (equilibrium) term plus a small variation term.

$$q_i(t) = q_{io} + \delta q_i(t) \tag{5}$$

Substituting the value of the generalized coordinate shown in Eq. (5) into the equations of motion and developing a Taylor's Series for the nonlinear function of the generalized coordinates and their derivatives yields the relation given below

$$f(q_i,\dot{q}_i,\ddot{q}_i) = f(q_{i_o},\dot{q}_{i_o},\ddot{q}_{i_o}) + \frac{\partial f(q_{i_o},\dot{q}_{i_o},\ddot{q}_{i_o})}{\partial q_i}\delta q_i + \frac{\partial f(q_{i_o},\dot{q}_{i_o},\ddot{q}_{i_o})}{\partial \dot{q}_i}\delta \dot{q}_i + \frac{\partial f(q_{i_o},\dot{q}_{i_o},\ddot{q}_{i_o})}{\partial \ddot{q}_i}\delta \ddot{q}_i + \ldots\ldots \quad (6)$$

Neglecting higher order terms, we obtain the linearized equation of motion as

$$f(q_i,\dot{q}_i,\ddot{q}_i) = f(q_{i_o},\dot{q}_{i_o},\ddot{q}_{i_o}) + \frac{\partial f(q_{i_o},\dot{q}_{i_o},\ddot{q}_{i_o})}{\partial q_i}\delta q_i + \frac{\partial f(q_{i_o},\dot{q}_{i_o},\ddot{q}_{i_o})}{\partial \dot{q}_i}\delta \dot{q}_i + \frac{\partial f(q_{i_o},\dot{q}_{i_o},\ddot{q}_{i_o})}{\partial \ddot{q}_i}\delta \ddot{q}_i = 0 \quad (7)$$

Linearized Equation of Motion

With the known values of k_η and j_η, the expression for $\frac{\partial a}{\partial \eta}$ in the linearized aeroforce is defined. Then, the linearized equations of motion of the system are expressed in the matrix form as

$$[M^*]\{\delta\ddot{q}_i\} + [C^*]\{\delta\dot{q}_i\} + [K^*]\{\delta q_i\} = \{G\}$$

where

M^* = linearized mass coefficient matrix

C^* = linearized damping coefficient matrix

K* = linearized stiffness coefficient matrix

G = linearized forcing function vector

The components of the matrices M*, C*, K* and the vector G are:

Mass matrix of the rotor

$$m_{11} = \begin{cases} \frac{3}{q_\infty}\int_{R_H}^{R} \mu\left(\frac{\dot{u}_{c1}}{R}\right)^2 \frac{dr}{R} + \frac{3}{q_\infty}\int_{R_H}^{R} \mu\left(\frac{e}{R}\right)^2 f_1^2 \frac{dr}{R} - \frac{6}{q_\infty}\int_{R_H}^{R} \mu \frac{\dot{u}_{c1}}{R}\frac{e}{R}\sin w_o f_1 \frac{dr}{R} \\ + \frac{3}{q_\infty}\int_{R_H}^{R} \frac{I_1}{R^2} f_1^2 \frac{dr}{R} \end{cases}$$

$$m_{12} = m_{21} = \frac{3}{q_\infty}\int_{R_H}^{R} \mu \frac{\dot{u}_{c1}}{R}\frac{\dot{u}_{c2}}{R}\frac{dr}{R} - \frac{3}{q_\infty}\int_{R_H}^{R} \mu \frac{\dot{u}_{c2}}{R}\frac{e}{R}\sin w_o' f_1 \frac{dr}{R}$$

$$+ \frac{3}{q_\infty}\int_{R_H}^{R} \mu \frac{e}{R}\frac{R_s}{R}\cos w_o' f_1 f_2 \frac{dr}{R}$$

$$m_{13} = m_{31} = \begin{cases} - \frac{3}{q_\infty}\int_{R_H}^{R} \mu \frac{\dot{u}_{c1}}{R}\left(\frac{w_o}{R}\sin\beta\cos\rho + \frac{e}{R}\cos\rho\cos\beta\right) f_3 \frac{dr}{R} \\ \quad + \frac{3}{q_\infty}\int_{R_H}^{R} \mu\left(\frac{e}{R}\right)^2 \sin w_o' \cos\rho\cos\beta f_1 f_3 \frac{dr}{R} \\ + \frac{3}{q_\infty}\int_{R_H}^{R} \mu\left[\frac{e}{R}\frac{(r+u_c)}{R}\cos w_o' \sin\beta\cos\rho + \left(\frac{e}{R}\right)^2 \cos w_o' \sin\rho\right] f_1 f_3 \frac{dr}{R} \\ + \frac{3}{q_\infty}\int_{R_H}^{R} \mu \frac{e}{R}\frac{w_o}{R}\sin w_o' \sin\beta\cos\rho f_1 f_3 \frac{dr}{R} \\ + \frac{3}{q_\infty}\int_{R_H}^{R} \frac{I_1}{R^2}\left(\sin\rho\cos w_o' + \cos\rho\cos\beta\sin w_o'\right) f_1 f_3 \frac{dr}{R} \end{cases}$$

$$m_{14} = m_{41} = 0$$

$$m_{22} = \frac{3}{q_\infty}\int_{R_H}^{R} \mu\left(\frac{\dot{u}_{c2}}{R}\right)^2 \frac{dr}{R} + \frac{3}{q_\infty}\left(\frac{R_s}{R}\right)^2 \int_{R_H}^{R} \mu f_2^2 \frac{dr}{R} + \frac{3}{q_\infty}\int_{R_H}^{R} \frac{I_2}{R^2} f_2^2 \frac{dr}{R}$$

$$m_{23} = m_{32} = \left\{ \begin{aligned} & -\frac{3}{q_\infty} \int_{R_H}^{R} \mu \frac{\dot{u}_{c2}}{R} \left(\frac{w_o}{R} \sin\beta\cos\rho + \frac{e}{R}\cos\rho\cos\beta\right) f_3 \frac{dr}{R} \\ & + \frac{3}{q_\infty} \int_{R_H}^{R} \mu\left(\frac{(r+u_c)}{R} \sin\beta\cos\rho + \frac{e}{R}\sin\rho\right) \frac{R_s}{R} f_2 f_3 \frac{dr}{R} \\ & \qquad + \frac{3}{q_\infty} \int_{R_H}^{R} \frac{I_2}{R^2} \cos\rho\cos\beta f_2' f_3 \frac{dr}{R} \end{aligned} \right.$$

$$m_{24} = m_{42} = 0$$

$$m_{33} = \left\{ \begin{aligned} & \frac{3}{q_\infty} \int_{R_H}^{R} \mu\Big(\frac{w_o^2}{R^2}(\sin^2\beta + \sin^2\rho\cos^2\beta) + \frac{e^2}{R^2}(\cos^2\beta + \sin^2\rho\sin^2\beta) \\ & \qquad + \frac{(r+u_c)^2}{R^2}\cos^2\rho\Big) f_3^2 \frac{dr}{R} \\ & + \frac{6}{q_\infty} \int_{R_H}^{R} \mu\Big(\frac{(r+u_c)}{R} \frac{e}{R} \sin\rho\cos\rho\sin\beta - \frac{(r+u_c)}{R}\frac{w_o}{R}\sin\rho\cos\rho\cos\beta \\ & \qquad + \frac{w_o}{R}\frac{e}{R}\sin\beta\cos\beta\cos^2\rho\Big) f_3^2 \frac{dr}{R} \\ & + \frac{3}{q_\infty} \int_{R_H}^{R} \frac{I_1}{R^2}(\sin\rho\cos w_o' + \cos\rho\cos\beta\sin w_o')^2 f_3^2 \frac{dr}{R} \\ & \qquad + \frac{3}{q_\infty} \int_{R_H}^{R} \frac{I_2}{R^2} \cos^2\rho\sin^2\beta \; f_3^2 \frac{dr}{R} \\ & + \frac{3}{q_\infty} \int_{R_H}^{R} \frac{I_3}{R^2}(\sin\rho\sin w_o' - \cos\rho\cos w_o'\cos\beta)^2 \; f_3^2 \frac{dr}{R} \\ & + \frac{1}{q_\infty R^3}(I_H + n_G^2 \, I_G) f_3^2 \end{aligned} \right.$$

$$m_{34} = m_{43} = 0$$

$$m_{44} = \begin{cases} \frac{3}{2q_\infty} \int_{R_H}^{R} \mu[(\frac{w_o}{R})^2(1 + \cos^2\rho\cos^2\beta) + (\frac{e}{R})^2(1 + \sin^2\beta\cos^2\rho) \\ \quad + \frac{(r+u_c)^2}{R^2}(1 + \sin^2\rho)]f_4^2\,\frac{dr}{R} \\ + \frac{3}{q_\infty} \int_{R_H}^{R} \mu[(\frac{\ell}{R})^2 + \frac{2\ell}{R}\frac{w_o}{R}\cos\rho\cos\beta + \frac{2\ell}{R}\frac{(r+u_c)}{R}\sin\rho \\ \quad - \frac{2\ell}{R}\frac{e}{R}\cos\rho\sin\beta]f_4^2\,\frac{dr}{R} \\ + \frac{3}{q_\infty} \int_{R_H}^{R} \mu(\frac{(r+u_c)}{R}\frac{w_o}{R}\sin\rho\cos\rho\cos\beta - \frac{e}{R}\frac{(r+u_c)}{R}\sin\rho\cos\rho\sin\beta \\ \quad - \frac{e}{R}\frac{w_o}{R}\sin\beta\cos\beta(1 - \sin^2\rho)]f_4^2\,\frac{dr}{R} \\ + \frac{3}{2q_\infty} \int_{R_H}^{R} \frac{I_1}{R^2}(\cos^2\rho\cos^2 w_o' + \sin^2\rho\sin^2 w_o'\cos^2\beta + \sin^2 w_o'\sin^2\beta \\ \quad - 2\sin\rho\cos\rho\sin w_o'\cos w_o'\cos\beta)f_4^2\,\frac{dr}{R} \\ + \frac{3}{2q_\infty} \int_{R_H}^{R} \frac{I_2}{R^2}(\sin^2\rho\sin^2\beta + \cos^2\beta)f_4^2\,\frac{dr}{R} \\ + \frac{3}{2q_\infty} \int_{R_H}^{R} \frac{I_3}{R^2}(\cos^2\rho\sin^2 w_o' + \sin^2\rho\cos^2 w_o'\cos^2\beta + \cos^2 w_o'\sin^2\beta \\ \quad + 2\sin w_o'\cos w_o'\sin\rho\cos\rho\cos\beta)f_4^2\,\frac{dr}{R} \end{cases}$$

where

μ = blade's mass per unit length

$\dot{u}_{c1} = \dfrac{\partial \dot{u}_c}{\partial \dot{q}_1}$ evaluated at nominal value

$$\dot{u}_{c2} = \frac{\partial \dot{u}_c}{\partial \dot{q}_2} \text{ evaluated at nominal value}$$

I_H = mass moment of inertia of the hub

I_G = mass moment of inertia of the generator unit and gear box

<u>Damping coefficient matrix of the rotor</u>

$$C_{11} = \left\{ \begin{aligned} & \frac{3}{q_\infty} \int_{R_H}^{R} \mu\Omega \frac{\partial \dot{u}_{c1}}{R\partial q_1} \left(\frac{w_o}{R} \sin\beta\cos\rho + \frac{e}{R}\cos\rho\cos\beta\right) \frac{dr}{R} \\ & \qquad + \frac{3}{q_\infty} \int_{R_H}^{R} \mu\Omega \frac{\dot{u}_{c1}}{R} \frac{e}{R} \cos\rho\cos w_o' \sin\beta f_1 \frac{dr}{R} \\ & - \frac{3}{q_\infty} \int_{R_H}^{R} \mu\Omega \frac{e}{R} \frac{\partial u_c}{R\partial q_1} \cos w_o' \sin\beta\cos\rho f_1 \frac{dr}{R} - \frac{3}{q_\infty} \int_{R_H}^{R} \mu\Omega \frac{e}{R} \frac{w_o}{R} \sin\rho f_1^2 \frac{dr}{R} \\ & + \frac{3}{q_\infty} \int_{R_H}^{R} \mu\Omega \frac{e}{R} \frac{(r+u_c)}{R} \cos\beta\cos\rho f_1^2 \frac{dr}{R} + \frac{3\pi}{8} \int_{R_H}^{R} \frac{W_t}{V_\infty} \left(\frac{c}{R}\right)^2 \frac{c}{V_\infty} f_1 \frac{dr}{R} \\ & + 3 \int_{R_H}^{R} \frac{W_t}{V_\infty} \frac{c}{R} C_{n_\alpha} \frac{e_2}{V_\infty} \left(\frac{e_1}{R} f_1 - \frac{\dot{u}_{m1}}{R} \sin w_o'\right) f_1 \frac{dr}{R} \end{aligned} \right.$$

$$
C_{12} = \left\{
\begin{aligned}
&\frac{3}{q_\infty}\int_{R_H}^{R} \mu\Omega \frac{\partial \dot{u}_{c2}}{R\partial q_1}\left(\frac{w_o}{R}\sin\eta\beta\cos\rho + \frac{e}{R}\cos\rho\cos\beta\right)\frac{dr}{R} \\
&\quad + \frac{3}{q_\infty}\int_{R_H}^{R} \mu\Omega \frac{\dot{u}_{c2}}{R}\frac{e}{R}\cos\rho\cos w_o'\sin\eta\beta f_1 \frac{dr}{R} \\
&+ \frac{3}{q_\infty}\int_{R_H}^{R} \mu\Omega \frac{e}{R}\frac{R_s}{R}\sin\eta\beta\sin\eta w_o'\cos\rho f_1 f_2 \frac{dr}{R} \\
&\quad + \frac{3}{q_\infty}\int_{R_H}^{R} \mu\Omega \frac{e}{R}\frac{(r+u_c)}{R}\sin\eta w_o'\sin\eta\beta\cos\rho f_1 f_2' \frac{dr}{R} \\
&+ \frac{3}{q_\infty}\int_{R_H}^{R} \mu\Omega\left(\frac{e}{R}\right)^2 \sin\eta\rho\sin\eta w_o' f_1 f_2' \frac{dr}{R} \\
&\quad - \frac{3}{q_\infty}\int_{R_H}^{R} \mu\Omega \frac{e}{R}\cos w_o'\left(\frac{w_o}{R}\sin\eta\beta\cos\rho + \frac{e}{R}\cos\rho\cos\beta\right) f_1 f_2' \frac{dr}{R} \\
&- \frac{3}{q_\infty}\int_{R_H}^{R} \frac{(I_2-I_3)}{R^2}\Omega\left(\sin\eta\rho\sin\eta w_o' - \cos\rho\cos w_o'\cos\beta\right) f_1 f_2' \frac{dr}{R} \\
&+ 3\int_{R_H}^{R} \frac{F_1}{V_\infty}\left(R_s\cos w_o' f_2 - R\left(\frac{\dot{u}_{d2}}{R}\right)\sin\eta w_o'\right)\left(\frac{e_1}{R} f_1 - \frac{\dot{u}_{m1}}{R}\sin\eta w_o'\right)\frac{dr}{R}
\end{aligned}
\right.
$$

$$C_{13} = \begin{cases} \frac{6}{q_\infty} \int_{R_H}^{R} \mu\Omega\left(\frac{e}{R}\right)^2 (\sin\rho\cos\rho\sin\beta\sin w_o' - \sin\beta\cos\beta\cos w_o'(1-\sin^2\rho)) f_1 f_3 \frac{dr}{R} \\ - \frac{6}{q_\infty} \int_{R_H}^{R} \mu\Omega \frac{e}{R} \frac{w_o}{R} (\cos w_o'(\sin^2\beta + \sin^2\rho\cos^2\beta) \\ \qquad + \sin\rho\cos\rho\cos\beta\sin w_o') f_1 f_3 \frac{dr}{R} \\ + \frac{6}{q_\infty} \int_{R_H}^{R} \mu\Omega \frac{e}{R} \frac{(r+u_c)}{R} (\cos^2\rho\sin w_o' + \sin\rho\cos\beta\cos\rho\cos w_o') f_1 f_3 \frac{dr}{R} \\ + \frac{6}{q_\infty} \int_{R_H}^{R} \mu\Omega \frac{\partial u_c}{R\partial q_1} (\frac{(r+u_c)}{R} \cos^2\rho \\ \qquad - (\frac{w_o}{R}\cos\beta - \frac{e}{R}\sin\beta) \sin\rho\cos\rho) f_3 \frac{dr}{R} \\ - \frac{6}{q_\infty} \int_{R_H}^{R} \frac{(I_2 - I_3)}{R^2} \Omega\cos\rho\sin\beta(\sin\rho\sin w_o' - \cos\rho\cos w_o'\cos\beta) f_1 f_3 \frac{dr}{R} \\ + 3 \int_{R_H}^{R} ((\frac{(r+u_d)}{V_\infty}\cos w_o' + \frac{w_o}{V_\infty}\sin w_o')\cos\rho\sin\beta) F_1 (\frac{e_1}{R} f_1 - \frac{\dot{u}_{m1}}{R}\sin w_o') f_3 \frac{dr}{R} \\ -3 \int_{R_H}^{R} \frac{e_3}{V_\infty} (\sin\rho\sin w_o' + \cos\rho\sin w_o'\cos\beta) F_1 (\frac{e_1}{R} f_1 - \frac{\dot{u}_{m1}}{R}\sin w_o') f_3 \frac{dr}{R} \\ + 3 \int_{R_H}^{R} (\frac{w_o}{V_\infty}\sin\rho - \frac{(r+u_d)}{V_\infty}\cos\rho\cos\beta) F_2 (\frac{e_1}{R} f_1 - \frac{\dot{u}_{m1}}{R}\sin w_o') f_3 \frac{dr}{R} \end{cases}$$

$$C_{14} = 0$$

$$C_{21} = \begin{cases} \frac{3}{q_\infty} \int_{R_H}^{R} \mu\Omega \frac{\partial \dot{u}_{c1}}{R\partial q_2} (\frac{w_o}{R} \sin\beta\cos\rho + \frac{e}{R}\cos\rho\cos\beta) \frac{dr}{R} \\ + \frac{3}{q_\infty} \int_{R_H}^{R} \mu\Omega \frac{\dot{u}_{c1}}{R} \frac{R_s}{R} \sin\beta\cos\rho f_2 \frac{dr}{R} + \frac{3}{q_\infty} \int_{R_H}^{R} \mu\Omega \, (\frac{e}{R})^2 \sin\rho\sin w_o' f_1 f_2' \frac{dr}{R} \\ + \frac{3}{q_\infty} \int_{R_H}^{R} \mu\Omega \frac{e}{R} \frac{(r+u_c)}{R} \sin\beta\sin w_o' f_1 f_2' \frac{dr}{R} \\ + \frac{3}{q_\infty} \int_{R_H}^{R} \mu\Omega \frac{e}{R} \frac{R_s}{R} \sin\beta\cos\beta\sin\rho\cos w_o' f_1 f_2 \frac{dr}{R} \\ - \frac{3}{q_\infty} \int_{R_H}^{R} \mu\Omega \frac{\partial u_c}{R\partial q_2} \frac{e}{R} \cos w_o' \sin\beta\cos\rho f_1 \frac{dr}{R} \\ - \frac{3}{q_\infty} \int_{R_H}^{R} \mu\Omega \frac{e}{R} \cos w' (\frac{w_o}{R} \sin\beta\cos\rho + \frac{e}{R} \cos\rho\cos\beta) f_1 f_2' \frac{dr}{R} \\ - \frac{3}{q_\infty} \int_{R_H}^{R} \mu\Omega \frac{R_s}{R} \frac{e}{R} \sin w_o' \sin\beta\cos\rho f_1 f_2 \frac{dr}{R} \\ + \frac{3}{q_\infty} \int_{R_H}^{R} \frac{I_1}{R^2} \Omega (\sin\rho\sin w_o' - \cos\rho\cos w_o' \cos\beta) f_1 f_2' \frac{dr}{R} \\ + 3 \int_{R_H}^{R} \frac{W_t}{V_\infty} \frac{e}{R} C_{n_\alpha} \frac{e_2}{V_\infty} (\frac{R_s}{R} f_2 \cos w_o' - \frac{\dot{u}_{m2}}{R} \sin w_o') f_1 \frac{dr}{R} \end{cases}$$

$$C_{22} = \begin{cases} \frac{3}{q_\infty} \int_{R_H}^{R} \mu\Omega \frac{\partial \dot{u}_{c2}}{R\partial q_2} (\frac{w_o}{R} \sin\beta\cos\rho + \frac{e}{R} \cos\rho\cos\beta) \frac{dr}{R} \\ + \frac{3}{q_\infty} \int_{R_H}^{R} \mu\Omega \frac{\dot{u}_{c2}}{R} \frac{R_s}{R} \sin\beta\cos\rho f_2 \frac{dr}{R} \\ + 3 \int_{R_H}^{R} \frac{F_1}{V_\infty} (R_s \cos w_o' f_2 - R(\frac{\dot{u}_{d2}}{R}) \sin w_o')(\frac{R_s}{R} f_2 \cos w_o' - \frac{\dot{u}_{m2}}{R} \sin w_o') \frac{dr}{R} \end{cases}$$

$$C_{23} = \begin{cases} -\dfrac{6}{q_\infty}\displaystyle\int_{R_H}^{R} \mu\Omega \frac{w_o}{R}\frac{R_s}{R}(\sin^2\beta+\sin^2\rho\cos^2\beta)f_2 f_3\frac{dr}{R} \\ \qquad -\dfrac{6}{q_\infty}\displaystyle\int_{R_H}^{R} \mu\Omega \frac{e}{R}\frac{R_s}{R}\sin\beta\cos\beta(1-\sin^2\rho)f_2 f_3\frac{dr}{R} \\ -\dfrac{6}{q_\infty}\displaystyle\int_{R_H}^{R} \mu\Omega\frac{\partial u_c}{R\partial q_1}\left(\frac{(r+u_c)}{R}\cos^2\rho - \left(\frac{w_o}{R}\cos\beta - \frac{e}{R}\sin\beta\right)\sin\rho\cos\rho\right)f_3\frac{dr}{R} \\ +\dfrac{6}{q_\infty}\displaystyle\int_{R_H}^{R} \mu\Omega\frac{(r+u_c)}{R}\frac{R_s}{R}\sin\rho\cos\beta f_2 f_3\frac{dr}{R} \\ -\dfrac{6}{q_\infty}\displaystyle\int_{R_H}^{R}\frac{(I_2-I_3)}{R^2}\Omega[\sin\rho\cos\rho\cos\beta\cos 2w_o' \\ \qquad + \sin w_o'\cos w_o'(\cos^2\rho\cos^2\beta - \sin^2\rho)]f_2' f_3\frac{dr}{R} \\ +3\displaystyle\int_{R_H}^{R}\left[\frac{(r+u_d)}{V_\infty}\cos w_o'\cos\rho\sin\beta + \frac{w_o}{V_\infty}\sin w_o'\cos\rho\cos\beta\right]F_1\left(\frac{R_s}{R}f_2\cos w_o' \right. \\ \qquad\qquad \left. - \dfrac{\dot{u}_{m2}}{R}\sin w_o'\right)f_3\dfrac{dr}{R} \\ -3\displaystyle\int_{R_H}^{R}\left[\frac{e_3}{V_\infty}(\sin\rho\sin w_o'+\cos\rho\sin w_o'\cos\beta)F_1-\left(\frac{w_o}{V_\infty}\sin\rho\right.\right. \\ \qquad \left.\left. -\dfrac{(r+u_d)}{V_\infty}\cos\rho\cos\beta\right)F_2\right]\left(\dfrac{R_s}{R}f_2\cos w_o' - \dfrac{\dot{u}_{m2}}{R}\sin w_o'\right)f_3\dfrac{dr}{R} \end{cases}$$

$$C_{24} = 0$$

$$C_{31} = \begin{cases} 3 \int_{R_H}^{R} \frac{W_t}{V_\infty} \frac{c}{R} C_{n_\alpha} \frac{e_2}{V_\infty} [\frac{(r+u_m)}{R} \cos w_o' \cos\rho \sin\beta \\ \quad + \frac{w_o}{R} \sin w_o' \cos\rho \sin\beta] f_1 f_3 \frac{dr}{R} \\ 3 \int_{R_H}^{R} \frac{W_t}{V_\infty} \frac{c}{R} C_{n_\alpha} \frac{e_2}{V_\infty} \frac{e_1}{R} (\sin\rho \cos w_o' + \cos\rho \sin w_o' \cos\beta) f_1 f_3 \frac{dr}{R} \\ 3 \int_{R_H}^{R} \frac{W_t}{V_\infty} \frac{c}{R} C_{t_\alpha} \frac{e_2}{V_\infty} (\frac{(r+u_m)}{R} \cos\rho \sin\beta - \frac{w_o}{R} \sin\rho) f_1 f_3 \frac{dr}{R} \\ \frac{3\pi}{8} \int_{R_H}^{R} \frac{W_T}{V_\infty} (\frac{c}{R})^2 \frac{c}{V_\infty} (\sin\rho \cos w_o' + \cos\rho \sin w_o' \cos\beta) f_1 f_3 \frac{dr}{R} \end{cases}$$

$$C_{32} = \begin{cases} 3 \int_{R_H}^{R} \frac{F_1}{V_\infty} (R_s \cos w_o' f_2 - \dot{u}_{d2} \sin w_o') (\frac{(r+u_m)}{R} \cos w_o' \cos\rho \sin\beta \\ \quad + \frac{w_o}{R} \sin w_o' \cos\rho \sin\beta) f_3 \frac{dr}{R} \\ 3 \int_{R_H}^{R} \frac{F_1}{V_\infty} (R_s \cos w_o' f_2 - \dot{u}_{d2} \sin w_o') \frac{e_1}{R} (\sin\rho \cos w_o' + \cos\rho \sin w_o' \cos\beta) f_3 \frac{dr}{R} \\ 3 \int_{R_H}^{R} \frac{G_1}{V_\infty} (R_s \cos w_o' f_2 - \dot{u}_{d2} \sin w_o') (\frac{(r+u_m)}{R} \cos\rho \sin\beta - \frac{w_o}{R} \sin\rho) f_3 \frac{dr}{R} \end{cases}$$

$$C_{33} = \begin{cases} 3 \int_{R_H}^{R} N6 (\frac{(r+u_m)}{R} \cos w_o' \cos\rho \sin\beta + \frac{w_o}{R} \sin w_o' \cos\rho \sin\beta \\ \quad + \frac{e_1}{R} (\sin\rho \cos w_o' + \cos\rho \sin w_o' \cos\beta)) f_3^2 \frac{dr}{R} \\ 3 \int_{R_H}^{R} H6 (\frac{(r+u_m)}{R} \cos\rho \sin\beta - \frac{w_o}{R} \sin\rho) f_3^2 \frac{dr}{R} \quad + C_G \end{cases}$$

$$C_{34} = 0$$

$$C_{41} = C_{42} = C_{43} = 0$$

where

$$N6 = \left\{ \begin{array}{l} \{\frac{(r+u_d)}{V_\infty} \cos w_0' \cos\rho \sin\beta + \frac{w_0}{V_\infty} \sin w_0' \cos\rho \sin\beta\} F_1 \\ - \frac{e_3}{V_\infty}(\sin\rho \sin w_0' + \cos\rho \sin w_0' \cos\beta) F_1 + (\frac{w_0}{V_\infty} \sin\rho - \frac{(r+u_d)}{V_\infty} \cos\rho \cos\beta) F_2 \end{array} \right.$$

$$H6 = \left\{ \begin{array}{l} (\frac{(r+u_d)}{V_\infty} \cos w_0' \cos\rho \sin\beta + \frac{w_0}{V_\infty} \sin w_0' \cos\rho \sin\beta) G_1 \\ - \frac{e_3}{V_\infty}(\sin\rho \sin w_0' + \cos\rho \sin w_0' \cos\beta) G_1 + (\frac{w_0}{V_\infty} \sin\rho - \frac{(r+u_d)}{V_\infty} \cos\rho \cos\beta) G_2 \end{array} \right.$$

C_G = Slip rate

$$
C_{44} = \left\{
\begin{aligned}
&\frac{3}{2}\int_{R_H}^{R} (N4)\Big(\frac{\ell}{R}\sin\beta\cos w_o' + \frac{(r+u_m)}{R}\sin\rho\sin\beta\cos w_o' \\
&\qquad\qquad + \frac{w_o}{R}\sin w_o'\sin\rho\sin\beta\Big) f_4^2\,\frac{dr}{R} \\
&\frac{3}{2}\int_{R_H}^{R} (N4)\,\frac{e_1}{R}\,(\sin\rho\sin w_o'\cos\beta - \cos\rho\cos w_o') f_4^2\,\frac{dr}{R} \\
&\frac{3}{2}\int_{R_H}^{R} (N5)\Big(\frac{\ell}{R}\,(\sin\rho\cos\beta\cos w_o' + \sin w_o'\cos\rho) + \frac{(r+u_m)}{R}\cos\beta\cos w' \\
&\qquad\qquad + \frac{w_o}{R}\sin w_o'\cos\beta\Big) f_4^2\,\frac{dr}{R} \\
&- \frac{3}{2}\int_{R_H}^{R} (N5)\,\frac{e_1}{R}\sin w_o'\sin\beta\, f_4^2\,\frac{dr}{R} \\
&+ \frac{3}{2}\int_{R_H}^{R} (H4)\,\Big(\frac{\ell}{R}\cos\beta + \frac{(r+u_m)}{R}\sin\rho\cos\beta + \frac{w_o}{R}\cos\rho\Big) f_4^2\,\frac{dr}{R} \\
&- \frac{3}{2}\int_{R_H}^{R} (H5)\Big(\frac{\ell}{R}\sin\rho\sin\beta + \frac{(r+u_m)}{R}\sin\beta\Big) f_4^2\,\frac{dr}{R} \\
&+ \frac{3}{2}\, j_{\dot q_4} \int_{R_H}^{R} (N1)\Big(\frac{\ell}{R}\sin\beta\cos w_o' + \frac{(r+u_m)}{R}\sin\rho\sin\beta\cos w_o' \\
&\qquad\qquad + \frac{w_o}{R}\sin w_o'\sin\rho\sin\beta\Big)\,\frac{r_N}{R}\, f_4\,\frac{dr}{R} \\
&+ \frac{3}{2}\, j_{\dot q_4} \int_{R_H}^{R} (N1)\,\frac{e_1}{R}\,(\sin\rho\sin w_o'\cos\beta - \cos\rho\cos w_o')\frac{r_N}{R}\, f_4\,\frac{dr}{R} \\
&+ \frac{3}{2}\, j_{\dot q_4} \int_{R_H}^{R} (H1)\Big(\frac{\ell}{R}\cos\beta + \frac{(r+u_m)}{R}\sin\rho\cos\beta + \frac{w_o}{R}\cos\rho\Big)\frac{r_N}{R}\, f_4\,\frac{dr}{R} \\
&- \frac{3}{2}\, k_{\dot q_4} \int_{R_H}^{R} (N1)\Big(\frac{\ell}{R}\,(\sin\rho\cos\beta\cos w_o' + \sin w_o'\cos\rho) + \frac{(r+u_m)}{R}\cos\beta\cos w_o' \\
&\qquad\qquad + \frac{w_o}{R}\sin w_o'\cos\beta\Big)\frac{r_N}{R}\, f_4\,\frac{dr}{R}
\end{aligned}
\right.
$$

$$+\frac{3}{2}k_{\dot{q}_4}\int_{R_H}^{R}(N1)\,\frac{e_1}{R}\sin w_o'\sin\beta\,\frac{r_N}{R}\,f_4\,\frac{dr}{R}$$

$$+\frac{3}{2}k_{\dot{q}_4}\int_{R_H}^{R}(H1)\,\left(\frac{\ell}{R}\sin\rho\sin\beta+\frac{(r+u_m)}{R}\sin\beta\right)\frac{r_N}{R}\,f_4\,\frac{dr}{R}$$

Stiffness coefficient matrix of the rotor

$$k_{11}=\begin{cases}-\dfrac{3}{q_\infty}\displaystyle\int_{R_H}^{R}\mu\Omega^2\frac{e^2}{R^2}\cos w_o'^2(\sin^2\beta+\sin^2\rho\cos^2\beta)f_1^2\frac{dr}{R}\\[2ex]
\quad+\dfrac{3}{q_\infty}\displaystyle\int_{R_H}^{R}\mu\Omega^2\left(\frac{e}{R}\right)^2(\cos^2\beta+\sin^2\rho\sin^2\beta)f_1^2\frac{dr}{R}\\[2ex]
-\dfrac{6}{q_\infty}\displaystyle\int_{R_H}^{R}\mu\Omega^2\left(\frac{e}{R}\right)^2\sin\rho\cos^2\rho\cos\beta\sin w_o'\cos w_o'f_1^2\frac{dr}{R}\\[2ex]
\quad-\dfrac{3}{q_\infty}\displaystyle\int_{R_H}^{R}\mu\Omega^2\left(\frac{e}{R}\right)^2\cos^2\rho\sin^2 w_o'f_1^2\frac{dr}{R}\\[2ex]
+\dfrac{3}{q_\infty}\displaystyle\int_{R_H}^{R}\mu\Omega^2\frac{e}{R}\frac{w_o}{R}\sin\beta\cos\beta(1-\sin^2\rho)f_1^2\frac{dr}{R}\\[2ex]
\quad+\dfrac{3}{q_\infty}\displaystyle\int_{R_H}^{R}\mu\Omega^2\frac{e}{R}\frac{(r+u_c)}{R}\sin\rho\cos\rho\sin\beta f_1^2\frac{dr}{R}\\[2ex]
-\dfrac{3}{q_\infty}\displaystyle\int_{R_H}^{R}\mu\Omega^2\cos^2\rho\left(\frac{\partial u_c}{R\partial q_1}\right)^2\frac{dr}{R}\\[2ex]
-\dfrac{3}{q_\infty}\displaystyle\int_{R_H}^{R}\mu\Omega^2\left(\frac{(r+u_c)}{R}\cos^2\rho-\frac{w_o}{R}\sin\rho\cos\rho\cos\beta+\frac{e}{R}\sin\rho\cos\rho\sin\beta\right)\frac{\partial^2 u_c}{R\partial q_1^2}\frac{dr}{R}\\[2ex]
-\dfrac{3}{q_\infty}\displaystyle\int_{R_H}^{R}\frac{(I_2-I_3)}{R^2}\Omega^2(\sin\rho\sin w_o'-\cos\rho\cos w_o'\cos\beta)^2f_1^2\frac{dr}{R}\\[2ex]
-\dfrac{3}{q_\infty}\displaystyle\int_{R_H}^{R}\frac{(I_2-I_3)}{R^2}\Omega^2\cos^2\rho\sin^2\beta f_1^2\frac{dr}{R}+\dfrac{3}{q_\infty}\displaystyle\int_{R_H}^{R}\frac{GJ}{R^4}f_1'^2\frac{dr}{R}\\[2ex]
-3\displaystyle\int_{R_H}^{R}\frac{\Omega e_3}{V_\infty}F_2(\sin\rho\cos w_o'+\cos\rho\sin w_o'\cos\beta)\left(\frac{e_1}{R}f_1-\frac{\dot{u}_{m1}}{R}\sin w_o'\right)f_1\frac{dr}{R}\end{cases}$$

$$
\left| \begin{aligned}
&- 3 \int_{R_H}^{R} \frac{\Omega R}{V_\infty} \left(\frac{\partial u_d}{R\partial q_1}\right)\left(-\cos w_o' \cos\rho \sin\beta \; F_1 + \cos\rho\cos\beta \; F_2\right)\left(\frac{e_1}{R} f_1 \right. \\
&\qquad \left. - \frac{\dot{u}_{m1}}{R} \sin w_o'\right) \frac{dr}{R} - 3 \int_{R_H}^{R} F_4 \left(\frac{e_1}{R} f_1 - \frac{\dot{u}_{m1}}{R} \sin w_o'\right) \frac{dr}{R} \\
&+ 3 \int_{R_H}^{R} N_o \frac{\partial \dot{u}_{m1}}{R\partial q_1} \sin w_o' \frac{dr}{R} + 3 \int_{R_H}^{R} H_o \frac{e_1}{R} f_1^2 \frac{dr}{R}
\end{aligned} \right.
$$

$$k_{12} = k_{12a} + k_{12b}$$

$$
k_{12a} = \left\{ \begin{aligned}
&\frac{3}{q_\infty} \int_{R_H}^{R} \mu\Omega^2 \left(\frac{e}{R}\right)^2 \left(\sin\beta\cos\beta\sin w_o'(1-\sin^2\rho) - \sin\rho\cos\rho\sin\beta\cos w_o'\right) f_1 f_2' \frac{dr}{R} \\
&- \frac{3}{q_\infty} \int_{R_H}^{R} \mu\Omega^2 \frac{e}{R} \frac{R_s}{R} \left(\cos w_o'(\sin^2\beta + \sin^2\rho\cos^2\beta)\right. \\
&\qquad \left. + \sin\rho\cos\rho\cos\beta\sin w_o'\right) f_1 f_2 \frac{dr}{R} \\
&+ \frac{3}{q_\infty} \int_{R_H}^{R} \mu\Omega^2 \frac{e}{R} \frac{w_o}{R} \left(\sin w_o'(\sin^2\beta + \sin^2\rho\cos^2\beta)\right. \\
&\qquad \left. - \sin\rho\cos\rho\cos\beta\cos w_o'\right) f_1 f_2' \frac{dr}{R} \\
&- \frac{3}{q_\infty} \int_{R_H}^{R} \mu\Omega^2 \frac{e}{R} \frac{(r+u_c)}{R} \left(\sin\rho\cos\rho\cos\beta\sin w_o' - \cos^2\rho\cos w_o'\right) f_1 f_2' \frac{dr}{R} \\
&- \frac{3}{q_\infty} \int_{R_H}^{R} \mu\Omega^2 \frac{\partial^2 u_c}{R\partial q_1 \partial q_2} \left(\frac{(r+u_c)}{R}\cos^2\rho - \left(\frac{w_o}{R}\cos\beta - \frac{e}{R}\sin\beta\right)\sin\rho\cos\beta\right) \frac{dr}{R} \\
&- \frac{3}{q_\infty} \int_{R_H}^{R} \mu\Omega^2 \frac{\partial u_c}{R\partial q_1} \frac{\partial u_c}{R\partial q_2} \cos^2\rho \frac{dr}{R} \\
&- \frac{3}{q_\infty} \int_{R_H}^{R} \frac{(I_2 - I_3)}{R^2} \Omega^2 \cos\rho\sin\beta\left(\sin\rho\cos w_o' + \cos\rho\sin w_o'\cos\beta\right) f_1 f_2' \frac{dr}{R}
\end{aligned} \right.
$$

$$k_{12b} = \begin{cases} + 3 \int_{R_H}^{R} (N7) \left(\frac{e_1}{R} f_1 - \frac{\dot{u}_{m1}}{R} \sin w_o'\right) \frac{dr}{R} \\ + 3 \int_{R_H}^{R} N_o \frac{\partial \dot{u}_{m1}}{R \partial q_2} \sin w_o' \frac{dr}{R} + 3 \int_{R_H}^{R} N_o \frac{\dot{u}_{m1}}{R} \cos w_o' f_2' \frac{dr}{R} \end{cases}$$

where

$$N7 = \begin{cases} \Big((\sin\rho \cos w_o' + \cos\rho \sin w_o' \cos\beta)(1-a) f_2' - \Omega \frac{(r+u_d)}{V_\infty} \sin w_o' \cos\rho \sin\beta f_2' \\ \qquad + \frac{\Omega R}{V_\infty} \cos w_o' \cos\rho \sin\beta \frac{\partial u_d}{R \partial q_2} \Big) F_1 \\ \Big(\frac{\Omega R}{V_\infty} \frac{R_s}{R} \sin w_o' \cos\rho \sin\beta f_2 + \frac{\Omega w_o}{V_\infty} \cos w_o' \cos\rho \sin\beta f_2' \\ \qquad + \frac{\Omega e_3}{V_\infty} (\sin\rho \sin w_o' - \cos\rho \cos w_o' \cos\beta) f_2' \Big) F_1 \\ \qquad + \left(\frac{\Omega R}{V_\infty} \frac{R_s}{R} \sin\rho f_2 - \frac{\Omega R}{V_\infty} \frac{\partial u_d}{R \partial q_2} \cos\rho \cos\beta \right) F_2 \end{cases}$$

$N_o = [(\frac{W_e}{V_\infty})^2 \frac{c}{R} C_n]$ evaluated at nominal value

$H_o = [(\frac{W_e}{V_\infty}) \frac{c}{R} C_t]$ evaluated at nominal value

$$k_{13} = k_{14} = 0$$

$$k_{21} = k_{12a} + k_{21b}$$

$$k_{21b} = \begin{cases} - 3 \int_{R_H}^{R} \frac{\Omega e_3}{V_\infty} (\sin\rho\cos w_o' + \cos\rho\sin w_o'\cos\beta)F_2(\frac{R_s}{R}\cos w_o' f_2 \\ \qquad - \frac{\dot{u}_{m2}}{R}\sin w_o')f_1 \frac{dr}{R} \\ + 3 \int_{R_H}^{R} \frac{R\Omega}{V_\infty} (\frac{\partial u_d}{R\partial q_1})(\cos w_o'\sin\beta F_1 - \cos\beta F_2)\cos\rho\ (\frac{R_s}{R}\cos w_o' f_2 \\ \qquad - \frac{\dot{u}_{m2}}{R}\sin w_o')\frac{dr}{R} \\ + 3 \int_{R_H}^{R} N_o \frac{\partial \dot{u}_{m2}}{R\partial q_1}\sin w_o' \frac{dr}{R} - 3 \int_{R_H}^{R} F_4(\frac{R_s}{R}\cos w_o' f_2 - \frac{\dot{u}_{m2}}{R}\sin w_o')\frac{dr}{R} \end{cases}$$

$$k_{22} = \begin{cases} - \frac{3}{q_\infty} \int_{R_H}^{R} \mu\Omega^2(\frac{R_s}{R})^2(\sin^2\beta + \cos^2\beta\sin^2\rho)f_2^2 \frac{dr}{R} \\ \qquad - \frac{3}{q_\infty} \int_{R_H}^{R} \mu\Omega^2\cos^2\rho(\frac{\partial u_c}{R\partial q_2})^2 \frac{dr}{R} \\ - \frac{3}{q_\infty} \int_{R_H}^{R} \mu\Omega^2 \frac{\partial^2 u_c}{R\partial q_2^2}\left[\frac{(r+u_c)}{R}\cos^2\rho - (\frac{w_o}{R}\cos\beta - \frac{e}{R}\sin\beta)\sin\rho\cos\rho\right]\frac{dr}{R} \\ + \frac{3}{q_\infty} \int_{R_H}^{R} \frac{(I_1 - I_3)}{R^2}\Omega^2\cos 2w_o'(\sin^2\rho - \cos^2\rho\cos^2\beta)f_2'^2 \frac{dr}{R} \\ + \frac{12}{q_\infty} \int_{R_H}^{R} \frac{(I_1 - I_3)}{R^2}\Omega^2\sin\rho\cos\rho\sin w_o'\cos w_o'\cos\beta f_2'^2 \frac{dr}{R} \\ \qquad + \frac{3}{q_\infty} \int_{R_H}^{R} \frac{EI}{R^4} f_2''^2 \frac{dr}{R} \\ + 3 \int_{R_H}^{R} (N7)\ (\frac{R_s}{R} f_2\cos w_o' - \frac{\dot{u}_{m2}}{R}\sin w_o')\frac{dr}{R} \\ + 3 \int_{R_H}^{R} N_o \frac{R_s}{R}\sin w_o' f_2' f_2 \frac{dr}{R} + 3 \int_{R_H}^{R} N_o \frac{\partial \dot{u}_{m2}}{R\partial q_2}\sin w_o' \frac{dr}{R} \\ + 3 \int_{R_H}^{R} N_o \frac{\partial \dot{u}_{m2}}{R}\cos w_o' f_2' \frac{dr}{R} \end{cases}$$

$$k_{23} = k_{24} = 0$$

$$k_{31} = \left\{ \begin{aligned}
& - 3 \int_{R_H}^{R} \frac{\Omega e_3}{V_\infty} (\sin\rho\cos w_o' + \cos\rho\sin w_o'\cos\beta) F_2 \Big(\frac{(r+u_m)}{R} \cos w_o'\cos\rho\sin\beta \\
& \quad + \frac{w_o}{R}\sin w_o'\cos\rho\sin\beta + \frac{e_1}{R}(\sin\rho\cos w_o' + \cos\rho\sin w_o'\cos\beta)\Big) f_1 f_3 \frac{dr}{R} \\
& - 3 \int_{R_H}^{R} \frac{\Omega e_3}{V_\infty} (\sin\rho\cos w_o' + \cos\rho\sin w_o'\cos\beta) G_2 \Big(\frac{(r+u_m)}{R} \cos\rho\sin\beta \\
& \qquad - \frac{w_o}{R}\sin\rho\Big) f_1 f_3 \frac{dr}{R} \\
& - 3 \int_{R_H}^{R} \Big[\frac{\Omega R}{V_\infty} \Big(\frac{\partial u_d}{R\partial q_1}\Big)(-\cos w_o'\sin\beta F_1 + \cos\beta F_2)\cos\rho + F_4\Big]\Big(\frac{w_o}{R}\sin w_o'\cos\rho\sin\beta \\
& \quad + \Big(\frac{r+u_m}{R}\Big)\cos w_o'\cos\rho\sin\beta + \frac{e_1}{R}(\sin\rho\cos w_o' + \cos\rho\sin w_o'\cos\beta)\Big) f_3 \frac{dr}{R} \\
& - 3 \int_{R_H}^{R} \Big[\frac{\Omega R}{V_\infty}\Big(\frac{\partial u_d}{R\partial q_1}\Big)(-\cos w_o'\sin\beta G_1 + \cos\beta G_2)\cos\rho \\
& \quad + G_4\Big]\Big(\frac{(r+u_m)}{R} \cos\rho\sin\beta - \frac{w_o}{R}\sin\rho\Big) f_3 \frac{dr}{R} \\
& - 3 \int_{R_H}^{R} N_o \frac{\partial u_m}{R\partial q_1}\cos w_o'\cos\rho\sin\beta f_3 \frac{dr}{R} - 3 \int_{R_H}^{R} H_o \frac{\partial u_m}{R\partial q_1}\cos\rho\cos\beta f_3 \frac{dr}{R} \\
& + 3 \int_{R_H}^{R} H_o \frac{e_1}{R} (\sin\rho\cos w_o' + \cos\rho\sin w_o'\cos\beta) f_1 f_3 \frac{dr}{R}
\end{aligned} \right.$$

$$k_{32} = \begin{cases} 3 \int_{R_H}^{R} (N7) \left(\frac{(r+u_m)}{R} \cos w_o' \cos\rho \sin\beta + \frac{w_o}{R} \sin w_o' \cos\rho \sin\beta\right) f_3 \frac{dr}{R} \\ + 3 \int_{R_H}^{R} (N7) \frac{e_1}{R} (\sin\rho \cos w_o' + \cos\rho \sin w_o' \cos\beta) f_3 \frac{dr}{R} \\ + 3 \int_{R_H}^{R} (H7)\left(\frac{(r+u_m)}{R} \cos\rho \sin\beta - \frac{w_o}{R} \sin\rho\right) f_3 \frac{dr}{R} \\ \quad - 3 \int_{R_H}^{R} N_o \frac{\partial u_m}{R \partial q_2} \cos w_o' \cos\rho \sin\beta f_3 \frac{dr}{R} \\ + 3 \int_{R_H}^{R} N_o\left(\frac{(r+u_m)}{R} f_2' - \frac{R_s}{R} f_2\right) \sin w_o' \cos\rho \sin\beta f_3 \frac{dr}{R} \\ \quad - 3 \int_{R_H}^{R} N_o \frac{w_o}{R} \cos w_o' \cos\rho \sin\beta f_2' f_3 \frac{dr}{R} \\ 3 \int_{R_H}^{R} N_o \frac{e_1}{R} (\sin\rho \sin w_o' - \cos\rho \cos w_o' \cos\beta) f_2' f_3 \frac{dr}{R} \\ - 3 \int_{R_H}^{R} H_o \frac{\partial u_m}{R \partial q_2} \cos\rho \cos\beta f_3 \frac{dr}{R} + 3 \int_{R_H}^{R} H_o \frac{R_s}{R} \sin\rho f_2 f_3 \frac{dr}{R} \end{cases}$$

$$k_{33} = k_{34} = 0$$

$$k_{41} = k_{42} = k_{43} = 0$$

$$
k_{44} = \left\{
\begin{aligned}
& \frac{3}{2} \int_{R_H}^{R} (N2)\Big(\frac{\ell}{R}\sin\beta\cos w_o' + \frac{(r+u_m)}{R}\sin\rho\sin\beta\cos w_o' \\
& \qquad + \frac{w_o}{R}\sin w_o'\sin\rho\sin\beta\Big) f_4^2 \frac{dr}{R} \\
& \frac{3}{2} \int_{R_H}^{R} (N2)\, \frac{e_1}{R}\left(\sin\rho\sin w_o'\cos\beta - \cos\rho\cos w_o'\right) f_4^2 \frac{dr}{R} \\
& \frac{3}{2} \int_{R_H}^{R} (N3)\Big(\frac{\ell}{R}(\sin\rho\cos\beta\cos w_o' + \sin w_o'\cos\rho) + \frac{(r+u_m)}{R}\cos\beta\cos w_o' \\
& \qquad + \frac{w_o}{R}\sin w_o'\cos\beta\Big) f_4^2 \frac{dr}{R} - \frac{3}{2}\int_{R_H}^{R} (N3)\, \frac{e_1}{R}\sin w_o'\sin\beta f_4^2 \frac{dr}{R} \\
& - \frac{3}{2} \int_{R_H}^{R} (H3)\Big(\frac{\ell}{R}\sin\rho\sin\beta + \frac{(r+u_m)}{R}\sin\beta\Big) f_4^2 \frac{dr}{R} \\
& + \frac{3}{2} \int_{R_H}^{R} (H2)\Big(\frac{\ell}{R}\cos\beta + \frac{(r+u_m)}{R}\sin\rho\cos\beta + \frac{w_o}{R}\cos\rho\Big) f_4^2 \frac{dr}{R} \\
& + \frac{3}{2} j_{q_4} \int_{R_H}^{R} (N1)\Big(\frac{\ell}{R}\sin\beta\cos w_o' + \frac{(r+u_m)}{R}\sin\rho\sin\beta\cos w_o' \\
& \qquad + \frac{w_o}{R}\sin w_o'\sin\rho\sin\beta\Big)\frac{r_N}{R} f_4 \frac{dr}{R} \\
& + \frac{3}{2} j_{q_4} \int_{R_H}^{R} (N1)\, \frac{e_1}{R}\left(\sin\rho\sin w_o'\cos\beta - \cos\rho\cos w_o'\right)\frac{r_N}{R} f_4 \frac{dr}{R} \\
& + \frac{3}{2} j_{q_4} \int_{R_H}^{R} (H1)\Big(\frac{\ell}{R}\cos\beta + \frac{(r+u_m)}{R}\sin\rho\cos\beta + \frac{w_o}{R}\cos\rho\Big)\frac{r_N}{R} f_4 \frac{dr}{R} \\
& - \frac{3}{2} k_{q_4} \int_{R_H}^{R} (N1)\Big(\frac{\ell}{R}\left(\sin\rho\cos\beta\cos w_o' + \sin w_o'\cos\rho\right) + \frac{(r+u_m)}{R}\cos\beta\cos w_o' \\
& \qquad + \frac{w_o}{R}\sin w_o'\cos\beta - \frac{e_1}{R}\sin w_o'\sin\beta\Big)\frac{r_N}{R} f_4 \frac{dr}{R} \\
& + \frac{3}{2} k_{q_4} \int_{R_H}^{R} (H1)\Big(\frac{\ell}{R}\sin\rho\sin\beta + \frac{(r+u_m)}{R}\sin\beta\Big)\frac{r_N}{R} f_4 \frac{dr}{R}
\end{aligned}
\right.
$$

Forcing function vector

$$G_{01} = \left\{ \begin{aligned} & \frac{3}{q_\infty} \int_{R_H}^{R} \mu\Omega^2 \left(\frac{e}{R}\right)^2 (\sin\beta\cos\beta\cos w_o'(1-\sin^2\rho) - \sin\rho\cos\rho\sin\beta\sin w_o') f_1 \frac{dr}{R} \\ & + \frac{3}{q_\infty} \int_{R_H}^{R} \mu\Omega^2 \frac{e}{R} \frac{w_o}{R} (\cos w_o'(\sin^2\beta + \sin^2\rho\cos^2\beta) \\ & \qquad + \sin\rho\cos\rho\cos\beta\sin w_o') f_1 \frac{dr}{R} \\ & - \frac{3}{q_\infty} \int_{R_H}^{R} \mu\Omega^2 \frac{e}{R} \frac{(r+u_c)}{R} (\cos^2\rho\sin w_o' + \sin\rho\cos\rho\cos\beta\cos w_o') f_1 \frac{dr}{R} \\ & + \frac{3}{q_\infty} \int_{R_H}^{R} \mu\Omega^2 \frac{\partial u_c}{R\partial q_1} \left(\frac{(r+u_c)}{R} \cos^2\rho - \frac{w_o}{R} \sin\rho\cos\rho\cos\beta \right. \\ & \qquad \left. + \frac{e}{R} \sin\rho\cos\rho\sin\beta\right) \frac{dr}{R} \\ & + \frac{3}{q_\infty} \int_{R_H}^{R} \frac{(I_2 - I_3)}{R^2} \Omega^2 \cos\rho\sin\beta(\sin\rho\sin w_o' - \cos\rho\cos w_o'\cos\beta) f_1 \frac{dr}{R} \\ & + 3 \int_{R_H}^{R} N_o\left(\frac{e_1}{R} f_1 - \frac{\dot{u}_{m1}}{R} \sin w_o'\right) \frac{dr}{R} \end{aligned} \right.$$

$$G_{02} = \left\{ \begin{aligned} & \frac{3}{q_\infty} \int_{R_H}^{R} \mu\Omega^2 \frac{R_s}{R} \left(\frac{w_o}{R}(\sin^2\beta + \sin^2\rho\cos^2\beta) + \frac{e}{R}\frac{R_s}{R}\sin\beta\cos\beta\cos 2\rho\right) f_2 \frac{dr}{R} \\ & \qquad - \frac{3}{q_\infty} \int_{R_H}^{R} \mu\Omega^2 \frac{(r+u_c)}{R} \frac{R_s}{R} \sin\rho\cos\beta f_2 \frac{dr}{R} \\ & + \frac{3}{q_\infty} \int_{R_H}^{R} \mu\Omega^2 \frac{\partial u_c}{R\partial q_2} \left(\frac{(r+u_c)}{R} \cos^2\rho - \frac{w_o}{R}\sin\rho\cos\rho\cos\beta + \frac{e}{R}\sin\rho\cos\rho\sin\beta\right) \frac{dr}{R} \\ & + \frac{3}{q_\infty} \int_{R_H}^{R} \frac{(I_2 - I_3)}{R^2} \Omega^2 (\sin\rho\cos\rho\cos\beta\cos 2w_o' \\ & \qquad + \sin w_o'\cos w_o'(\cos^2\rho\cos^2\beta - \sin^2\rho)) f_2' \frac{dr}{R} \\ & - \frac{3}{q_\infty} \int_{R_H}^{R} \frac{EI}{R^4} f_2''^2 \frac{dr}{R} q_s + 3 \int_{R_H}^{R} N_o\left(\frac{R_s}{R} f_2\cos w_o' - \frac{\dot{u}_{m2}}{R} \sin w_o'\right) \frac{dr}{R} \end{aligned} \right.$$

$$G_{03} = \left\{ \begin{array}{l} 3 \int_{R_H}^{R} N_o \{\frac{(r+u_m)}{R} \cos w_o' \cos\rho \sin\beta + \frac{w_o}{R} \sin w_o' \cos\rho \sin\beta \\ \qquad\qquad + \frac{e_1}{R} (\sin\rho \cos w_o' + \cos\rho \sin w_o' \cos\beta)\} f_3 \frac{dr}{R} \\ + 3 \int_{R_H}^{R} H_o \left(\frac{(r+u_m)}{R} \cos\rho \sin\beta - \frac{w_o}{R} \sin\rho \right) f_3 \frac{dr}{R} - n_G T_{G_o} \end{array} \right.$$

where T_{G_o} = generator torque at nominal speed

n_G = gear box ratio

$$G_{04} = 0$$

Yaw moment due to tower shadow

$$M_y = \left\{ \begin{array}{l} \frac{3}{2\pi} \int_{R_H}^{R} (N_o)\{(\frac{\ell}{R} + \frac{(r+u_m)}{R} \sin\rho) \sin\beta \cos w_o' + \frac{w_o}{R} \sin w_o' \sin\rho \sin\beta \\ \qquad\qquad - \frac{e_1}{R} (\cos\rho \cos w_o' - \sin\rho \sin w_o' \cos\beta)\} (2\sin\frac{\lambda}{2})\ f_4 \frac{dr}{R} \\ \frac{3}{2\pi} \int_{R_H}^{R} (H_o)\{ \frac{\ell}{R} \cos\beta + \frac{(r+u_m)}{R} \sin\rho \cos\beta + \frac{w_o}{R} \cos\rho\} (2\sin\frac{\lambda}{2})\ f_4 \frac{dr}{R} \end{array} \right.$$

where M_y is the yaw moment in the tower shadow sector normalized by dynamic pressure.

Note: the computer codes in this dissertation will calculate CQ0 instead of M_y, where $CQ0 = -M_y/\{\frac{3}{2\pi}(2\sin\frac{\lambda}{2})\}$.

Summary of symbols used in this section

u_c = blade's radial displacement at center of mass

u_d = blade's radial displacement at mid-chord

u_m = blade's radial displacement at 1/4 blade chord

$\dot{u}_\eta = \frac{\partial u_\eta}{\partial t}$

$\dot{u}_{\eta i} = \frac{\partial \dot{u}_\eta}{\partial \dot{q}_i}$ evaluated at nominal value

where

$\eta = c,d,n$

$i = 1,2,3,4$

e = distance from mass center to shear center of blade cross section

e_1 = distance from 1/4 blade chord to shear center of blade cross section

e_2 = distance from 3/4 blade chord to shear center of blade cross section

e_3 = distance from mid blade chord to shear center of blade cross section

μ = blade's mass per unit length

$N_o = \left(\frac{W_e}{V_\infty}\right)^2 C_n \frac{c}{R}$ evaluated at nominal values

$H_o = \left(\frac{W_e}{V_\infty}\right)^2 C_t \frac{c}{R}$ evaluated at nominal values

$N1 = \left(\sin\rho \sin w_o' - \cos\rho \cos w_o' \cos\beta\right) F_1 - \cos\rho \sin\beta F_2$

$N2 = \cos w_o' \sin\beta F_1 - \cos\beta F_2$

$N3 = \left(\cos\rho \sin w_o' + \sin\rho \cos w_o' \cos\beta\right) F_1 + \sin\rho \sin\beta F_2$

$$N4 = \begin{cases} \left(\frac{\ell}{V_\infty} \sin\beta\cos w_o' + \frac{(r+u_d)}{V_\infty} \sin\rho\sin\beta\cos w_o' + \frac{w_o}{V_\infty}\sin w_o'\sin\rho\sin\beta\right)F_1 \\ + \frac{e_3}{V_\infty}\left(\cos\rho\cos w_o' - \sin\rho\sin w_o'\cos\beta\right)F_1 \\ - \left(\frac{\ell}{V_\infty}\cos\beta + \frac{(r+u_d)}{V_\infty}\sin\rho\cos\beta + \frac{w_o}{V_\infty}\cos\rho\right)F_2 \end{cases}$$

$$N5 = \begin{cases} \left(\frac{\ell}{V_\infty}\left(\sin\rho\cos\beta\cos w_o' + \sin w_o'\cos\rho\right) + \frac{(r+u_d)}{V_\infty}\cos\beta\cos w_o' + \frac{w_o}{V_\infty}\sin w_o'\cos\beta \right. \\ \left. + \frac{e_3}{V_\infty}\sin w_o'\sin\beta\right)F_1 \\ + \left(\frac{\ell}{V_\infty}\sin\rho\sin\beta + \frac{(r+u_d)}{V_\infty}\sin\beta\right)F_2 \end{cases}$$

$$N6 = \begin{cases} \left(\frac{(r+u_d)}{V_\infty}\cos w_o'\cos\rho\sin\beta + \frac{w_o}{V_\infty}\sin w_o'\cos\rho\sin\beta\right)F_1 \\ - \frac{e_3}{V_\infty}\left(\sin\rho\sin w_o' + \cos\rho\sin w_o'\cos\beta\right)F_1 + \left(\frac{w_o}{V_\infty}\sin\rho - \frac{(r+u_d)}{V_\infty}\cos\rho\cos\beta\right)F_2 \end{cases}$$

$$N7 = \begin{cases} \left(\sin\rho\cos w_o' + \cos\rho\sin w_o'\cos\beta\right)(1-a)f_2' - \Omega\frac{(r+u_d)}{V_\infty}\sin w_o'\cos\rho\sin\beta f_2' \\ \qquad + \frac{\Omega R}{V_\infty}\frac{\partial u_d}{R\partial q_2}\cos w_o'\cos\rho\sin\beta\Big)F_1 \\ + \left(\frac{\Omega R}{V_\infty}\frac{R_s}{R}\sin w_o'\cos\rho\sin\beta f_2 + \frac{\Omega w_o}{V_\infty}\cos w_o'\cos\rho\sin\beta f_2' \right. \\ \qquad \left. + \frac{\Omega e_3}{V_\infty}\left(\sin\rho\sin w_o' - \cos\rho\cos w_o'\cos\beta\right)f_2'\right)F_1 \\ + \left(\frac{\Omega R}{V_\infty}\frac{R_s}{R}\sin\rho f_2 - \frac{\Omega R}{V_\infty}\frac{\partial u_d}{R\partial q_2}\cos\rho\cos\beta\right)F_2 \end{cases}$$

The expressions for H1, H2, H3, H4, H5, H6, and H7 are the same as N1, N2, N3, N4, N5, N6, and N7, respectively, except F_1 and F_2 in Ni terms are replaced by G_1 and G_2 in Hi terms.

APPENDIX V

YAW STIFFNEST COEFFICIENT

V.1 Yaw Stiffness Coefficient

The expression for the yaw stiffness coefficient can be expressed into three terms according to the sine of the coning angle. They are

$$k_{44} = k_{44_o} + k_{44_1}\sin\rho + k_{44_2}\sin^2\rho \qquad (1)$$

where

$$k_{44_o} = \left\{ \begin{array}{l} \frac{3}{2}\int_{R_H}^{R}(N2)(LL1)f_4^2\,\frac{dr}{R} + \frac{3}{2}\int_{R_H}^{R}\cos\rho\sin w_o' F_1(LL2)f_4^2\,\frac{dr}{R} \\ \frac{3}{2}\int_{R_H}^{R}(H2)\left(\frac{\ell}{R}\cos\beta + \frac{w_o}{R}\cos\rho\right)f_4^2\,\frac{dr}{R} \\ -\frac{3}{2}\int_{R_H}^{R}\cos\rho\sin w_o' G_1\frac{(r+u_m)}{R}\sin\beta f_4^2\,\frac{dr}{R} \\ -\frac{3}{2}\,j_{q_4}\int_{R_H}^{R}(N8)\cos\rho(LL1)\frac{r_N}{R}\,f_4\,\frac{dr}{R} \\ -\frac{3}{2}\,j_{q_4}\int_{R_H}^{R}(H8)\cos\rho\left(\frac{\ell}{R}\cos\beta + \frac{w_o}{R}\cos\rho\right)\frac{r_N}{R}\,f_4\,\frac{dr}{R} \\ \frac{3}{2}\,k_{q_4}\int_{R_H}^{R}(N8)\cos\rho(LL2)\frac{r_N}{R}\,f_4\,\frac{dr}{R} \\ -\frac{3}{2}\,k_{q_4}\int_{R_H}^{R}(H8)\cos\rho\frac{(r+u_m)}{R}\sin\beta\,\frac{r_N}{R}\,f_4\,\frac{dr}{R} \end{array} \right.$$

$$
k_{44_1} = \left\{
\begin{array}{l}
\frac{3}{2} \int_{R_H}^{R} (N2)(LL3) f_4^2 \frac{dr}{R} + \frac{3}{2} \int_{R_H}^{R} (H2) \frac{(r+u_m)}{R} \cos\beta f_4^2 \frac{dr}{R} \\
\frac{3}{2} \int_{R_H}^{R} \{F_1 \cos\beta \cos w_o' - G_1 \sin\beta\} \frac{\ell}{R} \cos\rho \sin w_o' \; f_4^2 \frac{dr}{R} \\
\frac{3}{2} \int_{R_H}^{R} (N8)(LL2) f_4^2 \frac{dr}{R} - \frac{3}{2} \int_{R_H}^{R} (H8) \frac{(r+u_m)}{R} \sin\beta \; f_4^2 \frac{dr}{R} \\
- \frac{3}{2} j_{q_4} \int_{R_H}^{R} \{(N8)(LL3) + (H8) \frac{(r+u_m)}{R} \cos\beta\} \cos\rho \; \frac{r_N}{R} f_4 \frac{dr}{R} \\
\frac{3}{2} j_{q_4} \int_{R_H}^{R} \sin w_o' \{F_1 (LL1) + G_1 (\frac{\ell}{R} \cos\beta + \frac{w_o}{R} \cos\rho)\} \frac{r_N}{R} f_4 \frac{dr}{R} \\
\frac{3}{2} k_{q_4} \int_{R_H}^{R} \{(N8) \cos\beta \cos w_o' - (H8) \sin\beta\} \frac{\ell}{R} \cos\rho \; \frac{r_N}{R} f_4 \frac{dr}{R} \\
\frac{3}{2} k_{q_4} \int_{R_H}^{R} \sin w_o' \{F_1 (LL2) - G_1 \frac{(r+u_m)}{R} \sin\beta\} \frac{r_N}{R} f_4 \frac{dr}{R}
\end{array}
\right.
$$

$$
k_{44_2} = \left\{
\begin{array}{l}
\frac{3}{2} \int_{R_H}^{R} \{(N8) \cos\beta \cos w_o' - (H8) \sin\beta\} \frac{\ell}{R} f_4^2 \frac{dr}{R} \\
\frac{3}{2} j_{q_4} \int_{R_H}^{R} \sin w_o' \{F_1 (LL3) + G_1 \frac{(r+u_m)}{R} \cos\beta\} \frac{r_N}{R} f_4 \frac{dr}{R} \\
- \frac{3}{2} k_{q_4} \int_{R_H}^{R} \sin w_o' \{F_1 \cos\beta \cos w_o' - G_1 \sin\beta\} \frac{\ell}{R} \frac{r_N}{R} f_4 \frac{dr}{R}
\end{array}
\right.
$$

and

$$N2 = \cos w_o' \sin\beta F_1 - \cos\beta F_2$$

$$N8 = \cos w_o' \cos\beta F_1 + \sin\beta F_2$$

$$H2 = \cos w_o' \sin\beta G_1 - \cos\beta G_2$$

$$H8 = \cos w_o' \cos\beta G_1 + \sin\beta G_2$$

$$LL1 = \frac{\ell}{R} \sin\beta \cos w_o' - \frac{e_1}{R} \cos w_o' \cos\rho$$

$$LL2 = \frac{\ell}{R} \cos\rho \sin w_o' + \frac{(r+u_m)}{R} \cos\beta \cos w_o' + \frac{w_o}{R} \sin w_o' \cos\beta - \frac{e_1}{R} \sin w_o' \sin\beta$$

$$LL3 = \frac{(r+u_m)}{R} \sin\beta \cos w_o' + \frac{w_o}{R} \sin\beta \sin w_o' + \frac{e_1}{R} \cos\beta \sin w_o'$$

V.2 In-Plane Force and Out-of-Plane Force

The in-plane force is referred to the force tangential to the rotor plane and the out-of-plane force is referred to the force normal to the rotor plane. The yaw stiffness coefficient developed in this dissertation is based on the forces and moments in the airfoil's coordinates. However, the components of the force in the airfoil's coordinates can be related to the components of the force in the rotor's coordinates by

$$\vec{G}_D = G_A \vec{n}_{\underline{x}} + G_B \vec{n}_{\underline{y}} \qquad (2)$$

$$F_D = F_D \vec{n}_{\underline{z}} \qquad (3)$$

where

$$G_A = N \cos w' \sin\beta + H \cos\beta$$

$$G_B = -N(\cos\rho \sin w' + \sin\rho \cos w' \cos\beta) + H \sin\rho \sin\beta$$

$$F_D = N(-\sin\rho\sin w' + \cos\rho\cos w'\cos\beta) - H\cos\rho\sin\beta$$

Here N and H are the forces expressed in the airfoil's coordinates: normal to and tangential to the chord line. G_D and F_D are the in-plane force and the out-of-plane force, respectively. $\vec{n}_{\underline{x}}$, $\vec{n}_{\underline{y}}$, and $\vec{n}_{\underline{z}}$ are the unit vectors in the coordinate system $\underline{x},\underline{y},\underline{z}$ defined in Appendix I.

The expression for the yaw stiffness coefficient can be rewritten in terms of the in-plane force and the out-of-plane force using Eqs. (2) and (3). Let us consider a simple case: a rotor with no conning angle, no variation of the axial induction factor with yaw, no offset distance from the shear center (e_1=0), and no explicit contribution from the flapwise deflection. The expression for the yaw stiffness coefficient becomes

$$k_{44} = \frac{3}{2}\int_{R_H}^{R} G_T \frac{\ell}{R} f_4^2 \frac{dr}{R} + \frac{3}{2}\int_{R_H}^{R} F_A \frac{r}{R} f_4^2 \frac{dr}{R} \qquad (4)$$

where

$$G_T = \{(\cos w_0'\sin\beta F_1 - \cos\beta F_2)\cos w_0'\sin\beta + (\cos w_0'\sin\beta G_1 - \cos\beta G_2)\cos\beta\} + \{(\sin w_0' F_1)\sin w_0'\}$$

$$F_A = \{(\sin w_0' F_1)\cos w_0'\cos\beta - (\sin w_0' G_2)\sin\beta\}$$

Here G_T is a component of the in-plane force coefficient and F_A is a component of the out-of-plane force coefficient.

APPENDIX VI

COMPUTER CODES

Two FORTRAN computer programs, PROP code and AERO code, are developed to handle the numerical values of the coefficients of the equations of motion. The AERO code uses a simplified lift and drag curve for a four-degree-of-freedom system while the PROP code uses an actual lift curve and only emphasizes on the yaw equation. Both codes will calculate the axial induction factor along the blade at a particular tip speed ratio. At the same time, they also calculate the integral terms for the variations of the axial induction factor with yaw and yaw rate. Finally, the codes calculate the coefficients in the equations of motion (mass, damping, stiffness coefficients, and forcing function).

VI.1 PROP Code

The PROP code in this dissertation is a modified version of the original PROP code developed by Wilson [21]. The original PROP code uses the modified strip theory solving for the axial induction factor, thrust coefficient, and power coefficient. Besides these features from the original code, the new PROP code also has the following features:

1) it is written in the FORTRAN V computer program language.
2) it uses the Glauert relationship [4] instead of the momentum theory to calculate the axial induction factor when its value exceeds the critical value.
3) it calculates the variations of the axial induction factor with yaw and yaw rate.
4) it uses the iteration method to calculate the static flapwise

deflection.

5) it calculates the coefficients of the equation of motion in yaw.

Input Data

The input data for the program consists of two parts. The first part of the data is stored in a computer data file (Tape 60). The second part of the data is inputed to the program through the terminal.

The parameters to be inputed in a data file are

R	radius of blade, ft
HB	hub radius, ft
DR	incremental percentage (percent of radius for integration incremental)
THETP	pitch angle, degrees
B	number of blades
H	altitude of hub above sea level, ft
HH	altitude of hub above ground level, ft
GO	tip loss model controller 0 Prandtl 1 Goldstein 2 no tip loss model 3 Mostab tip loss model
HL	hub loss model controller 0 none 1 Prandtl
APP	angular interference model code 0 angular interference factor calculated 1 angular interference factor set equal to 0
XETA	velocity power law exponent

TH	blade maximum thickness/chord
ALO	angle of attack for zero lift, degrees
AMOD	axial interference model code 0 standard 1 Wilson
NF	number of input stations for blade geometry
NFS	number of data points on lift and drag curve
NPROF	NACA profile or profile subroutine 4415 NACA 4415 0012 NACA 0012 8888 data inserted in tabular form 9999 NACA 64_4-421
RR(I)	percent radius for stations
CI(I)	chord for stations, ft
THIT(I)	twist angle for stations, degrees
AAT(I)	angle of attack, degrees
CLT(I)	coefficient of lift data
CDT(I)	coefficient of drag data

The parameters to be inputed through the terminal are pitch angle (degrees), tip speed ratio: minimum, maximum, and increment, rotor speed (rad/sec), conning angle (degrees), blade shear center position given as the ratio of the distance from the blade leading edge to the shear center and blade chord (esc), position of center of mass for the blade cross section given as the ratio of the blade leading edge to center of mass and blade chord (xcg), location of the yaw axis (YL, ft), modulus of elasticity (AE, psi), and modulus of shear (AG, psi).

Output

The output for the program is on a tape file entitled TAPE 61. On this file are written both the program operating conditions and program output. The following are the output quantities:

PCCR	local distance on the blade, r/R
A	axial induction factor
CL	lift coefficient
CD	drag coefficient
PHI	summation of angle of attack and twist angle, $\alpha + \beta$
ALPHA	angle of attack, degrees
F	tip loss factor
RE NO	Reynolds number
CT	thrust coefficient for a rigid rotor
CP	power coefficient for a rigid rotor
QS	non-dimensional static tip deflection (final value after the iterations)

The coefficients of the equation of motion in yaw are

ZMDD	mass coefficient
ZCDD	damping coefficient
ZKDD	stiffness coefficient
CQO	yaw moment coefficient due to the tower shadow per unit shadow width
SKDEL	coefficient accounting for the variation of the axial induction factor with yaw, k_γ
SJDEL	coefficient accounting for the variation of the axial induction factor with yaw, j_γ

SKRDEL coefficient accounting for the variation of the axial induction factor with yaw rate, $k_{\dot{\gamma}}$

SJRDEL coefficient accounting for the variation of the axial induction factor with yaw rate, $j_{\dot{\gamma}}$

CPAA power coefficient for a rotor with flexible blades (accounting for the flapwise deflection effect)

Given the values of the shadow width and the velocity deficit, the yaw forcing function can be obtained from the relation

$$G_{04} = \frac{B}{2\pi} \{CQO|_{x_1} - (SF)^2\ CQO|_{x_2}\}\ 2\sin\frac{\lambda}{2}$$

where

λ = width of the shadow sector (degrees)

B = number of blades

SF = correction factor due to non-dimensionalized value at different tip speed values { =1-(%velocity deficit)/100}

x_1 = tip speed ratio considered

x_2 = tip speed ratio of the shadow sector : $x_2 = (SF)x_1$

VI.2 AERO Code

The AERO code uses a simplified lift and drag curves to calculate the aerodynamic loads. The lift curve is approximated and can be described in a simple yet fairly accurate form by six parameters. The curve consists of four straight line segments as follows:

$$C_L = 2\pi m \sin(\alpha+\alpha_o) \qquad \alpha < \alpha_{C_{L_{max}}}$$

$$C_L = C_{L_{max}} \qquad \alpha_{C_{L_{max}}} < \alpha < \alpha_{BR}$$

$$C_L = C_{L_{flat}} \qquad \alpha_{BR} < \alpha < \alpha_{stall}$$

$$C_L = C_{L_{flat}} \frac{\sin(\frac{\pi}{2} - \alpha)}{\sin(\frac{\pi}{2} - \alpha_{stall})} \qquad \alpha > \alpha_{stall}$$

The six parameters are

m - lift curve slope divided by 2π

α_o - zero lift angle of attack

$\alpha_{C_{L_{max}}}$ - maximum lift coefficient

α_{BR} - angle at which C_L drops to $C_{L_{flat}}$

$C_{L_{flat}}$ - an approximate to the average C_L on the far side of the C_L curve, this can be adjusted up and down depending upon the characteristics of the airfoil

α_{stall} - angle at which C_L begin to decrease

The drag coefficient curve is also in multiple sections. Below $\alpha_{C_{L_{max}}}$, the drag is given by the following:

$$C_D = C_{D_o}(1 + C_\alpha (\frac{\alpha}{\alpha_{C_{L_{max}}}})^n)$$

where C_α, n, and C_{D_o} are constants determined by the airfoil characteristics. If $\alpha > \alpha_{C_{L_{max}}}$ the drag coefficient can be represented by a single curve fit or a series of curve fits.

The axial induction factor "a" is calculated by equating momentum flux to blade force. There are six possible intersections of blade force and momentum relations due to two regions on momentum relations and three regions on blade force. Two regions on momentum relations are the region of parabolic curve when "a" < "$a_{critical}$" and the straight line when "a" > "$a_{critical}$". Three regions on blade force are the linear slope curve where the angle of attack is less than the angle at the maximum lift force, the flat part of lift curve ($C_{L_{max}}$ and $C_{L_{flat}}$), and the lift curve in the stall region. Once the particular region is identified, the solution is a straightforward procedure of finding where the momentum and blade element curves intersect. These intersections of blade force and momentum relations are shown in Figure V.1.

A subroutine and two functions are developed to handle the inner integral term of the double integration. The inner integral terms are terms involving the derivative of flapwise deflection (radial displacement and its derivative). The composite Simpson's rule method is used for the numerical integrations in the code.

Input Data

The input data for the program consists of the physical characteristics of the wind turbine itself. They consist of physical airfoil data and operation variables. The physical airfoil data and operation variables are

BCRR	chord to radius ratio at blade root (Bc/R)
B	number of blades
EM	slope of linear portion of lift curve/2π
DRR	dr/R
XMIN	tip speed ratio to start program
XMAX	last tip speed ratio - used to end the program
DBX	the increment of tip speed ratio
CD ZERO	minimum lift coefficient
CL FLAT	lift coefficient on the horizontal portion of the lift curve
CL MAX	maximum lift coefficient
ALPHA BREAK	angle of attack where the lift curve changes values, from the maximum value to CL FLAT, degrees

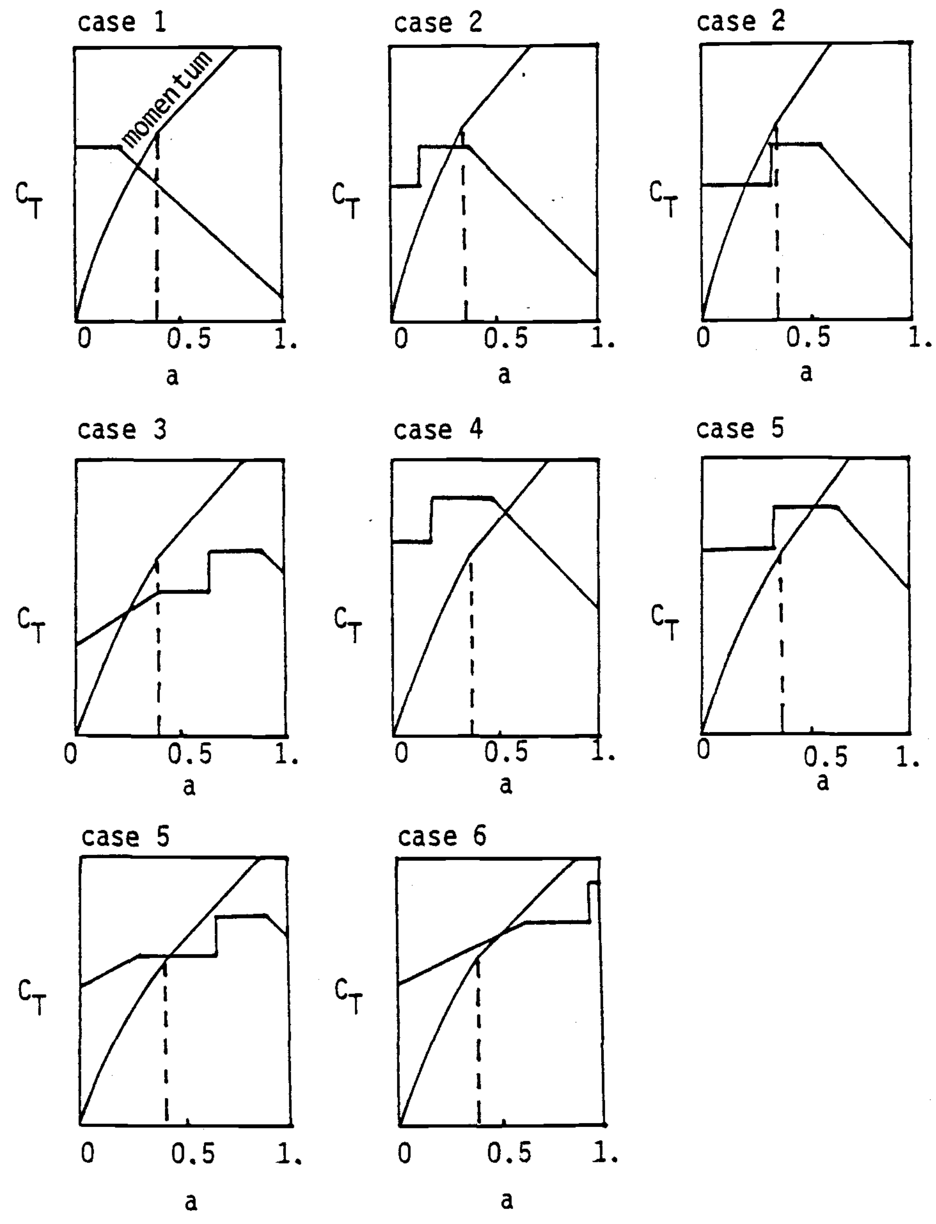

Figure V.1 Regions of operation for momentum calculations.

ALO	angle of attack at zero lift, degrees
AST	stall angle of attack, degrees
SI	coning angle, degrees
PITCH	prepitch angle, degrees
BETA ROOT	pretwist angle at blade root, degrees
DBETA	(βroot - βtip); twist angle change, degrees
RT	local radius at twist angle change from linear to constant twist
DCND	(c/R at chord change - c/R at tip), chord change ratio
RC	local radius at chord change from linear taper to constant chord
RH	hub radius
ESC	blade shear center position given as the ratio of the distance from the blade leading edge to the shear center and blade chord (e_s/c)
XCG	position of blade cross-section's center of mass given as the ratio of distance from blade leading edge to center of mass and blade chord (x_{cg}/c)
E	modulus of elasticity, psi
G	modulus of shear, psi
OMEGA	rotor speed, rad/sec
RHO	air density, slug/ft^3
YL	distance from the nacelle yaw axis to the center of the rotor, ft
R	blade tip radius, ft
M	number of integration steps in subroutine

Output

The output for the program is on a tape file entitled TAPE 1. On this file are written both the program operating conditions and program output. The following are the output quantities:

QS	nondimensional static tip deflection
CP	power coefficient
CT	thrust coefficient
M$\eta\eta$	rotor mass coefficient where $\eta\eta$ is the indication of which variables it represents
C$\eta\eta$	rotor damping coefficient
K$\eta\eta$	rotor stiffness coefficient
HP	rotor forcing function of pitch equation
HF	rotor forcing function of flap equation
SKDEL	coefficient accounting for the variation of the axial induction factor with yaw, k_γ
SJDEL	coefficient accounting for the variation of the axial induction factor with yaw, j_γ
SKRDEL	coefficient accounting for the variation of the axial induction factor with yaw rate, $k_{\dot{\gamma}}$
SJRDEL	coefficient accounting for the variation of the axial induction factor with yaw rate, $j_{\dot{\gamma}}$

For $\eta\eta$ parameters

P	generalized coordinate in pitch
F	generalized coordinate in flap
O	generalized coordinate in speed
D	generalized coordinate in yaw

If the code is not suppressed, additional output quantities are printed on the output list. They are as follows:

PCR	local distance on the blade, r/R
A	axial induction factor
PHI	summation of angle of attack and pretwist angle
BETA	pretwist angle
ALPHA	angle of attack
CL	lift coefficient
CD	drag coefficient
BCR	local chord to radius ratio, Bc/R
CPB	power coefficient
CTB	thrust coefficient

For the tower shadow part in yaw equations, the additional quantities on the output list are:

SMnn	mass coefficient in shadow region per unit shadow width/($B/2\pi$)
GCnn	damping coefficient in shadow region per unit shadow width/($B/2\pi$)
SKnn	stiffness coefficient in shadow region per unit shadow width/($B/2\pi$)
CQO	forcing function per unit shadow width generated from the shadow/($B/2\pi$)

The quantities from the tower shadow effect will be calculated when the magnitude of the velocity deficit is given. For example, if the velocity deficit value is 50%, the forcing function at tip speed ratio of 2 due to tower shadow is given as

$$\frac{B}{2\pi}\left[CQO|_{x=2} - (SF)^2\ CQO|_{x=4}\right] 2 \sin \frac{j}{2}$$

where j = width of the shadow segment (degree)

B = number of blades

x = tip speed ratio

SF = correction factor due to nondimensionalized value at different tip speed value [= 1 - (% velocity deficit)/100]

For the gravity effect, the gravity forces on the pitch equation for a single blade are listed as the components of sine and cosine of the azimuth angle.

GNCOS	Cosine component of the forcing function due to gravity
GNSIN	Sine component of the forcing function due to gravity
GPCOS	Cosine component of the k_{11} of a single blade due to gravity
GPSIN	Sine componet of the k_{11} of the single blade due to gravity
GFCOS	Cosine component of the k_{12} of a single blade due to gravity
GFSIN	Sine component of the k_{12} of a single blade due to gravity
GOCOS	Cosine component of the k_{13} of single blade due to gravity
GOSIN	Sine component of the k_{13} of a single blade due to gravity

The properties of the blade and shear center position are also listed in the output

ER	$\frac{e}{R}$
E1	$\frac{e_1}{R}$
E2	$\frac{e_2}{R}$
E3	$\frac{e_3}{R}$
AE	Modulus of elasticity, psi
AG	Shear modulus of rigidity, psi

The integration step sizes are shown as

N	Number of integration step sizes used in the main program
M	Number of integration step sizes used in subroutine (double integral)

Note

The code does not calculate some of the terms in the expression of the coefficient of rotor equations of motion. These terms have to be calculated by hand then added to the results of the computer code.

These terms are

C_G in C_{33} $\quad$ $n_G T_{G_o}$ in G_{03}

$\frac{1}{q_\infty}(I_H + n_G^2 I_G)\, f_3^2$ in m_{33}

VI.3 Sample Cases

The Grumman WS33 and the Enertech 1500 are used as test cases. The physical characteristics of both rotors are needed as inputs. Some simplifications of these data must be made to use in the computer codes. Some parameters for the simplification schemes are presented in this chapter.

AERO Code

With the lift curve defined in Appendix VI.2, the lift curve's parameters of the Grumman WS33 and the Enertech 1500 are given as

for the Grumman WS33

$$m = 1.0$$
$$C_{L_{max}} = 1.08$$
$$C_{L_{flat}} = 1.08$$
$$\alpha_{L_o} = 1.1^\circ$$
$$\alpha_{BR} = 20^\circ$$
$$\alpha_{stall} = 50^\circ$$

for the Enertech 1500

$$m = 0.89$$
$$C_{L_{max}} = 1.35$$
$$C_{L_{flat}} = 1.0$$
$$\alpha_{L_o} = 4.2^\circ$$
$$\alpha_{BR} = 15^\circ$$
$$\alpha_{stall} = 45^\circ$$

The drag curves of the Grumman WS33 and the Enertech 1500 can be approximated in a series of curve fits. These curve fits are shown as follows:

for the Grumman WS33

$$C_D = C_{D_o}(1 + 30(\alpha - \alpha_d)^2) \qquad \alpha < \alpha_1$$

$$C_D = 1.585\, C_{D_o} + 0.6(\alpha - \alpha_1) \qquad \alpha_1<\alpha<\alpha_2$$

$$C_D = 0.06715 + 2.3(\alpha - \alpha_2) \qquad \alpha_2<\alpha<\alpha_3$$

$$C_D = \frac{5\sin^2\alpha}{4/\pi + \sin\alpha} \qquad \alpha_3<\alpha<\alpha_4$$

$$C_D = \frac{4.5\sin^2\alpha}{4/\pi + \sin\alpha} \qquad \alpha_4<\alpha$$

where $C_{D_o} = 0.0132$

α_i's are given in radians; By converting radians into degrees, the values of α_i's are given as follows: $\alpha_d = 2^\circ$, $\alpha_1 = 10^\circ$, $\alpha_2 = 14^\circ$, $\alpha_3 = 20^\circ$, and $\alpha_4 = 28^\circ$.

for the Enertech 1500

$$C_D = C_{D_o}(1 + 53.81\alpha^2) \qquad \alpha<12^\circ$$

$$C_D = 3.36\, C_{D_o} + (\tan\alpha - \tan 12^\circ) \qquad 12^\circ<\alpha<15^\circ$$

$$C_D = 2.439\, C_{L_{flat}} (\tan\alpha)^{2.15} \qquad 15^\circ<\alpha<\alpha_2$$

$$C_D = C_{L_{flat}} \tan\alpha \qquad \alpha_2<\alpha<\pi/4$$

$$C_D = C_{D_2} \frac{\sin^2\alpha}{1 + \sin\alpha}$$

where $C_{D_o} = 0.014$

$C_{D_2} = 3.4142$

$\alpha_2 = \arctan\{(\frac{.41}{C_{L_{flat}}})^{.87}\}$

For the AERO code, the combination of the effective radius and Prandtl method is used for the calculation of tip loss factor.

The effective radius is given by

$$\frac{R_{eff}}{R} = \left(\frac{B^{2/3}x}{B^{2/3}x + 1.32}\right)^{1/2}$$

and

$$\frac{R_{eff}}{R} = \left(\frac{B^{2/3}x}{B^{2/3}x + 0.44}\right)^{1/2} \qquad \text{for } x < 3$$

which was obtained from an empirical relation which expressed the maximum power coefficient of wind turbines.

The tip loss factor is expressed as

$$F = \frac{2}{\pi} \text{ arc cos (ef)}$$

where

$$ef = \{\cos(\frac{0.7\pi}{2})\}^{(1 - r/R)/(1 - R_{eff}/R)}$$

PROP Code

PROP code uses the actual lift and drag curves of the blade section to calculate the aerodynamic loads. The airfoil sectional data of the NACA 64_4-421 in a reverse position are needed for analyzing the Grumman WS33 in a reverse position. Unfortunately, these data are not available. But by studying the behavior and trend of the aerodynamic characteristics of airfoil sections through 360 - degree angle of attack from references 9, 17, and 18, the lift and drag curves of the reverse NACA 64_4-421 can be expressed as

$$C_L = 6.6463(\alpha - \alpha_o) \qquad \alpha < \alpha_1$$

$$C_L = .020255 + 11.9705\alpha - 54.761\alpha^2 + 136.055\alpha^3$$
$$-144.5923\,\alpha^4 - 13.2926\alpha_o \qquad \alpha_1 < \alpha < \alpha_2$$

$$C_L = 187.3277 - 2335.2577\alpha + 10915.946\alpha^2$$
$$- 22521.2787\alpha^3 + 17287.811\alpha^4 - 13.2926\alpha_o \qquad \alpha_2 < \alpha < \alpha_3$$

$$C_L = 1.89\,\frac{\sin 2\alpha}{4/\pi + \sin\alpha} + 0.0252 \qquad \alpha > \alpha_3$$

for drag curve

$$C_D = C_{D_o}(1 + 20\alpha^2) \qquad \alpha < \alpha_4$$

$$C_D = 0.0225 + 0.6517(\alpha - \alpha_4) \qquad \alpha_4 < \alpha < \alpha_5$$

$$C_D = 0.068 + 2.2164(\alpha - \alpha_5) \qquad \alpha_5 < \alpha < \alpha_6$$

$$C_D = 3.78\,\frac{\sin^2\alpha}{4/\pi + \sin\alpha} + 0.0252 \qquad \alpha > \alpha_6$$

Here α_i's are angles of attack in radians measured from the reverse side of the airfoil (i.e., negative angle of attack of the conventional airfoil). By converting radians into degrees, the values of $_i$'s are as follows: $\alpha_1 = 4^\circ$, $\alpha_2 = 17.7^\circ$, $\alpha_3 = 20^\circ$, $\alpha_4 = 10^\circ$, $\alpha_5 = 14^\circ$, and $\alpha_6 = 20^\circ$.

VI.4 Computer Listings

The listings of the PROP code, the PROP code's output, the AERO code, and the AERO code's output are given as follows:

```
      PROGRAM PROP(INPUT,OUTPUT,TAPE60,TAPE61)
C
C     ....... VERSION - MARCH 1983   .......
C
C     ....... MAIN PROGRAM .......
C     PROP CALCULATES THE THEORETICAL PERFORMANCE PARAMETERS OF A
C     PROPELLER TYPE WIND TURBINE.  IT UTILIZES A SIMPSON#S-RULE
C     METHOD / THREE PASS TECHNIQUE OF NUMERICAL INTEGRATION.
C
      DIMENSION RR(25), CI(25), THETI(25), AAT(25), CLT(25), COT(25)
      DIMENSION STA(100),AXI(100),ALPH(100),FBIG(100)
      COMMON R,DR,HB,B,V,X,THETP,AMOD,H,SI,GO,OMEGA,RHO,VIS,HL,PI,RX,W,
     $NPROF,APP,T1,T2,T3,T4,T5,T6,T7,T8,TEST,XETA,HH,ALO,AC
      COMMON XCG,ESC,AE,AG
      COMMON RR,CI,THETI,NF
C
C     INPUT PARAMETERS:
C
C     ....R--RADIUS OF BLADE - FT
C
C     ....HB--HUB RADIUS - FT
C
C     ....DR--INCREMENTAL PERCENTAGE
C
C     ....THETP--PITCH ANGLE - DEGREES
C
C     ....B--NUMBER OF BLADES
C
C     ....V--WIND VELOCITY - MPH
C
C     ....XETA--VELOCITY POWER LAW EXPONENT
C
C     ....OMEGA--ANGULAR VELOCITY OF PROP - RPM
C
C     ....AMOD--AXIAL INTERFERENCE MODEL CODE
C     .......... 0 -- STANDARD
C     .......... 1 -- WILSON
C
C     ....H--ALTITUDE OF HUB ABOVE SEA LEVEL - FT
C
C     ....HH--ALTITUDE OF HUB ABOVE GROUND LEVEL - FT
C
C     ....SI--CONING ANGLE - DEGREES
C
C     ....NF--NUMBER OF INPUTED STATIONS FOR BLADE GEOMETRY
C
C     ....NPROF--NACA PROFILE OR PROFILE SUBROUTINE
C     ..........4415 -- NACA 4415
C     ..........0012 -- NACA 0012
C     ..........8888 -- DATA INSERTED IN TABULAR FORM
C     ..........9999 -- PROFILE CURVEFIT TO BE USED IN NACAXX
C
C     ....GO--TIP LOSS MODEL CONTROLLER
C     ..........0 - PRANDTL
C     ..........1 - GOLDSTEIN
C     ..........2 - NO TIP LOSS MODEL
C     ..........3 - MOSTAB TIP MODEL
C
C     ....HL--HUB LOSS MODEL CONTROLLER
C     ..........0 - NONE
C     ..........1 - PRANDTL
C
C     ....BO--MOSTAB TIP LOSS MODEL PARAMETER
C
C     ....APP--ANGULAR INTERFERENCE LOCKOUT
C     ..........0 - ANGULAR INTERFERENCE FACTOR CALCULATED
C     ..........1 - ANGULAR INTERFERENCE FACTOR SET EQUAL TO 0
C
C     ....RR(I)--PERCENT RADIUS FOR STATIONS
C
C     ....CI(I)--CHORD FOR STATIONS - FT
C
C     ....THETI(I)--TWIST ANGLE FOR STATIONS - DEGREES
C
C     ....TH--MAX THICKNESS/CHORD RATIO
C
C     ....ALO--ANGLE OF ATTACK FOR ZERO LIFT - DEGREES
C
C     ....CLT(I)--COEF. OF LIFT DATA
C
C     ....COT(I)--COEF. OF DRAG DATA
C
C     ....AAT(I)--ANGLE OF ATTACK - DEGREES
C
C
C     .........READ INPUT DATA.........
C
      READ(60,39)R,DR,HB,B,H,HH
      READ(60,39)GO,HL,APP,XETA,TH,ALO,AMOD
      READ(60,41)NF,NFS,NPROF
      READ(60,10)(RR(I),CI(I),THETI(I),I=1,NF)
      IF (NPROF.NE.8888) GO TO 1
      READ(60,40) (AAT(I),CLT(I),COT(I),I=1,NFS)
 1    CONTINUE
      PI = 3.1415926536
      PRINT 53
      READ*,THETP
      PRINT 54
      READ*,XMIN,XMAX,DX
      PRINT 55
      READ*,OMEGA
      PRINT 56
      READ*,SI
      PRINT 58
      READ*,ESC,XCG,YL
      PRINT 59
      READ*,AE,AG

       YL=YL/R
       X=XMIN
       V=R*OMEGA/X
C
C     ....... PRINT INPUT AND TITLES FOR OUTPUT ......
C
      CALL TITLES (RR,CI,THETI,NF,SOLD)
      RHO=.002376919*EXP(-.297*H/10000.)
C
C     ....... INITIALIZATION AND CONSTANT PARAMETER CALCULATIONS ......
C
100   W = 200.
      I=1
      TUQS=TBQS=0.
      DRI=DR
      ITOT = -1
      T7 = 0.0
      T8 = 0.0
```

```
      XMXX = 0.0
      XMYX = 0.0
      UQS=BQS=0.
      QX = 0.0
      AC=.38
      TX = 0.0
      FXXP1 = 0.0
      FYXP1 = 0.0
      QY = 0.0
      TY = 0.0
      PY = 0.0
      XMXY = 0.0
      XMYY = 0.0
      ASTOP = 0.0
      A = 1.0
      AP = 0.0
      CONTROL = 3.0
      FX6 = 0.
      F=0.
      SI = SI*PI/180.
      REF=R*COS(SI)
      THETF = THETP*PI/180.
      ALO=ALO*PI/180.
      ALPHA=-ALO
      RHO = 0.0023769199*EXP(-0.297*H/10000.)
      VIS = 0.0000003719-0.00000000204*H/1000.
      NN=(R-HB)/(R*DR)+1.
      RX = R
      RLB = (1.-DR)*RX
      DR = (RX-RLB)*COS(SI)
      DRO = DR
      R = R*COS(SI)
      HB = HB*COS(SI)
      RL = R
C
C     ....... THREE PASS - NUMERICAL INTEGRATION FROM TIP TO HUB .......
C
      CAT = 1.
      IF (GO.EQ.2.) CAT = 2.
      CLFA = 1.
      IF (GO.EQ.3.) CLFA = 0.0
      IF (GO.LT.2.) GO TO 2
      CALL SEARCH(RL,RR,CI,THETI,NF,C,THET,SHODE)
      CALL CALC (RL,C,THET,FXXP1,FYXP1,XMXX,XMYX,QX,TX,RE,PHIR,CL,CD,CX,
     $CY,A,AP,XL,AK,ALPHA,F,CLFA,CAT,AAT,CLT,CDT,NFS,SOLD,TH,SHODE,UQS,
     $BQS)
    2 STA(I)=RL/R
      AXI(I)=A
      ALPH(I)=ALPHA
      FBIG(I)=F
      A = 0.0
      CAT = 0.0
      DO 8 L=1,NN
      TIP=0.
         IF ((RL-HB).GE.DR) GO TO 3
         ASTOP = ASTOP+1.
         IF (ASTOP.GE.2.) GO TO 9
         DR = (RL-HB)
    3    IF (GO.LT.3.) GO TO 5
         IF (CONTROL.EQ.0.0) GO TO 5
         TIP = RL-DR
         IF (TIP.GT.REF) GO TO 4
         IF (CONTROL.EQ.2.) GO TO 5
         DR = (RL-REF)
         CLFO = (REF-TIP)/(RL-TIP)
         CLF = .5*CLFO
         CONTROL = 1.
         GO TO 5
    4    CLF = 0.0
    5    DR2 = DR/2.
         DT6 = DR/(6.*COS(SI))
         DRR6=DT6/RX
         RL = RL-DR2
         IF (CONTROL.EQ.0.0) CLF = 1.
         IF (CONTROL.EQ.2.0) CLF = (CLFO+1.)/2.
         AK = 1.
      CALL SEARCH(RL,RR,CI,THETI,NF,C,THET,SHODE)
         CALL CALC (RL,C,THET,FXXP2,FYXP1,XMXXP1,XMYXP1,QXP1,TXP1,RE,
     $   PHIR,CL,CD,CX,CY,A,AP,XL,AK,ALPHA,F,CLF,CAT,AAT,CLT,CDT,NFS,
     $   SOLD,TH,SHODE,UQS1,BQS1)
         K=I+1
         STA(K)=RL/R
         AXI(K)=A
         ALPH(K)=ALPHA
         FBIG(K)=F
         RL = RL-DR2
         IF (CONTROL.EQ.0.0) CLF = 1.
         IF (CONTROL.EQ.2.0) CLF = 1.0
         AK = 0.0
      CALL SEARCH(RL,RR,CI,THETI,NF,C,THET,SHODE)
         CALL CALC (RL,C,THET,FXY,FYY,XMXXP,XMYXP,QXP,TXP,RE,PHIR,CL,CD,
     $   CX,CY,A,AP,XL,AK,ALPHA,F,CLF,CAT,AAT,CLT,CDT,NFS,SOLD,TH,SHODE,
     $   UQS2,BQS2)
         KK=K+1
         STA(KK)=RL/R
         AXI(KK)=A
         ALPH(KK)=ALPHA
         FBIG(KK)=F
         I=KK
         FX6 = FX6+DT6*(FXXP1+4.*FXXP2+FXY)
         QYX = DT6*(QX+4.*QXP1+QXP)
         QY = QY+QYX
         TY = TY+DT6*(TX+4.*TXP1+TXP)
         PY = PY+OMEGA*QYX
         TUQS=TUQS+DRR6*(UQS+4.*UQS1+UQS2)
         TBQS=TBQS+DRR6*(BQS+4.*BQS1+BQS2)
         XMXY = XMXY+DT6*(XMXX+4.*XMXXP1+XMXXP)
         XMYY = XMYY+DT6*(XMYX+4.*XMYXP1+XMYXP)
         IF (CONTROL.EQ.2.) CONTROL = 0.0
         IF (CONTROL.EQ.0.0) GO TO 6
         IF ((RL-TIP).EQ.0.0) GO TO 6
         IF (CONTROL.EQ.1.) DR = REF-TIP
         IF (CONTROL.EQ.1.) CONTROL = 2.
         GO TO 7
    6    DR = DRO
    7    CONTINUE
         QX = QXP
         TX = TXP
         XMXX = XMXXP
         XMYX = XMYXP
         FXXP1=FXY
         UQS=UQS2
         BQS=BQS2
         CTY = TY/(.5*RHO*V**2*PI*RX**2)
         CPY = PY/(.5*RHO*V**3*PI*RX**2)
         TP = PY/737.6
```

```
      PHIO = PHIR*180./PI
      ALPHA = ALPHA*180./PI
      PR = RL/(RX*COS(SI))
C
C     ....... PRINT OUTPUT ......
C
      PCCR=RL/(RX*COS(SI))
      WRITE(61,14)PCCR,A,AP,CL,CD,PHIO,ALPHA,F,RE,CTY,CPY
 8    CONTINUE
 9    HP = TP*1.3410
      WRITE (61,33) X
      WRITE (61,36) CPY
      QS=TUQS/T8QS
      WRITE(61,73) QS
C
      PISTEL = T7/(PI*RX**5)
      PI2STEL = T8*X/(PI*RX**6)
      DCP = (XETA*X*RX**2/(HH*HH))*(XETA*PISTEL+(XETA-1.)*PI2STEL)*B/4.
      CPAV = CPY+DCP
      WRITE (61,37) CPAV
      WRITE (61,38) CTY
      WRITE (61,51) PISTEL
      WRITE (61,52) PI2STEL
      WRITE(61,81) FX6
      CALL ITERAT(QS,ALFH,AXI,STA,PQS,KK,KL)
      WRITE(61,74) QS,PQS,KL
      CALL YAW(QS,ALPH,AXI,STA,FBIG,KK,YL,SKDEL,SJDEL,SKRDEL,SJRDEL,
     $ZMDD,ZCDD,ZKDD,CQ0,ZKDL,ZKDR,ZKDW,WT00,CPAA,CQL1,CQR1)
      WRITE(61,77) ZMDD,ZCDD,ZKDD,CQ0
      WRITE(61,79) SKDEL,SJDEL,SKRDEL,SJRDEL
      WRITE(61,80) CPAA
      X=X+DX
      V=RX*OMEGA/X
      DR=DRI
      HB=HB/COS(SI)
      SI=SI*180./PI
      THETP=THETP*180./PI
      ALD=ALD*180./PI
      R=RX
      IF(X.GT.XMAX) GO TO 101
      WRITE(61,57)
      GO TO 100
101   CONTINUE
C
C     ....... FORMATS FOR INPUT AND OUTPUT STATEMENTS ......
C
C
      STOP
C
C
 10   FORMAT(3F10.4)
 14   FORMAT(1X,F4.3,2X,F6.4,3X,F5.4,2X,F4.2,3X,F5.3,2X,F6.3,2X,F6.3,2X,
     $F6.4,2X,E10.3,2X,F6.4,2X,G13.6)
 33   FORMAT (///,21H PERFORMANCE SUMMARY*,30X,*TIP SPEED RATIO =*,F8.3)
 36   FORMAT (/,15X,27H TOTAL POWER COEFFICIENT = ,F7.5)
 37   FORMAT (/,15X,43H AVERAGE POWER COEFFICIENT WITH GRADIENT = ,F10.5
     $)
 38   FORMAT (/,15X,28H TOTAL THRUST COEFFICIENT = ,F7.4)
 39   FORMAT(7F10.4)
 40   FORMAT(3F10.4)
 41   FORMAT(2I2,I4)
 51   FORMAT (/58H TORQUE VARIATION DUE TO AERODYNAMIC SECOND DERIVATIVE
     $ =  ,F15.4)
```

```
 52   FORMAT (/51H TORQUE VARIATION DUE TO SHEAR SECOND DERIVATIVE = ,
     $F15.4)
 53   FORMAT(*TELETYPE INPUT SECTION*/*INPUT PITCH ANGLE*)
 54   FORMAT(* TIP SPEED RATIO: (MIN),(MAX),(INCREMENT)*)
 55   FORMAT(*ROTOR RAD PER SEC*)
 56   FORMAT(*CONING ANGLE*)
 57   FORMAT(///1X,*PCCR*,6X,*A*,5X,*AP*,5X,*CL*,6X,*CD*,5X,*PHI*,
     $4X,*ALPHA*,5X,*F*,6X,*RE NO*,8X,*CT*,8X,*CP*)
 58   FORMAT(* INPUT ESC,XCG,YL *)
 59   FORMAT(* INPUT AE,AG *)
 73   FORMAT(/,* INITIAL NORMALIZED STATIC TIP DEFLECTION IS *,G13.6)
 74   FORMAT(/,* QS = *,G13.6,3X,*PREVIOUS QS = *,G13.6,3X,* NO OF
     $ ITERATION IS *,I3)
 77   FORMAT(/,7X,*ZMDD*,11X,*ZCDD*,11X,*ZKDD*,11X,*CQ0*/,2X,4(G13.6,2X)
     1)
 79   FORMAT(/,7X,*SKDEL*,11X,*SJDEL*,11X,*SKRDEL*,11X,*SJRDEL*/,2X,
     $4(G13.6,2X))
 80   FORMAT(/,11X,* CPAA  =  *,G13.6)
 81   FORMAT(/,7X,* TANGENTIAL FORCE PER BLADE IN ROTOR PLANE  *,G13.5)

      END

      SUBROUTINE TITLES (RR,CI,THETI,NF,SOLD)
C
C     ....... TITLES - PRINTS OUT INPUT DATA IN A DESCRIPTIVE
C     FORM, AND PRINTS DESCRIPTIONS OF SYMBOLS/TITLES FOR OUTPUT.
C
      DIMENSION RR(25), CI(25), THETI(25)
      COMMON R,DR,HB,B,V,X,THETP,AMOJ,H,SI,GO,OMEGA,RHO,VIS,HL,PI,RX,N,
     $NPROF,APP,T1,T2,T3,T4,T5,T6,T7,T8,TEST,XETA,HH,ALD
      WRITE (61,12)
      WRITE (61,13)
      WRITE (61,14)
      WRITE (61,15) V
      WRITE (61,16) XETA
      WRITE (61,17) HH
      WRITE (61,18) H
      WRITE (61,19) OMEGA
      WRITE (61,20) X
      WRITE (61,21) THETP
      RX = R
      CSI = SI
      SI = SI*PI/180.
      CRL = .75*R
      CALL SEARCH(CRL,RR,CI,THETI,NF,C,THET,SHODE)
      SI = CSI
      BANG = THET*180./PI+THETP
      WRITE (61,22) BANG
      WRITE (61,23) SI
      WRITE (61,24)
      WRITE (61,25) B
      WRITE (61,26) R
      WRITE (61,27) HB
      CALL SOLIDT (RR,CI,NF,B,R,PI,SOLD)
      WRITE (61,28) SOLD
      CALL ACTIVI (RR,CI,NF,B,R,PI,ACF)
      WRITE (61,29) ACF
      WRITE (61,30) NPROF
      WRITE (61,31) NF
      WRITE (61,32)
      WRITE (61,33)
      WRITE (61,34) (RR(I),CI(I),THETI(I),I=1,NF)
      WRITE (61,35)
```

```
      WRITE (61,36) DR                                                  B  42
      IF (APP.EQ.0.0) GO TO 1                                           B  43
      WRITE (61,37)                                                     B  44
 1    IF (AMOD.EQ.0.0) GO TO 2                                          B  45
      WRITE (61,38)                                                     B  46
      GO TO 3                                                           B  47
 2    WRITE (61,39)                                                     B  48
 3    IF (B.GT.2.0) GO TO 4                                             B  49
      IF (GO.EQ.0.0) GO TO 8                                            B  50
      IF (GO.EQ.1.0) GO TO 5                                            B  51
      IF (GO.EQ.2.0) GO TO 6                                            B  52
      IF (GO.EQ.3.0) GO TO 7                                            B  53
      GO TO 9                                                           B  54
 4    IF (GO.EQ.2.0) GO TO 6                                            B  55
      IF (GO.EQ.3.0) GO TO 7                                            B  56
      GO TO 8                                                           B  57
 5    WRITE (61,41)                                                     B  58
      GO TO 9                                                           B  59
 6    WRITE (61,42)                                                     B  60
      GO TO 9                                                           B  61
 7    WRITE (61,43)                                                     B  62
      GO TO 9                                                           B  63
 8    WRITE (61,40)                                                     B  64
 9    IF (HL.EQ.0.0) GO TO 10                                           B  65
      WRITE (61,45)                                                     B  66
      GO TO 11                                                          B  67
 10   WRITE (61,44)                                                     B  68
 11   CONTINUE                                                          B  69
      WRITE (61,46)                                                     B  70
      WRITE (61,47)                                                     B  71
      WRITE(61,48)                                                      B  72
      RETURN                                                            B  73
C                                                                       B  74
C                                                                       B  75
 12   FORMAT (1H1)                                                      B  76
 13   FORMAT (57H THEORETICAL PERFORMANCE OF A PROPELLER TYPE WIND TURBI B  77
     $NE)                                                               B  78
 14   FORMAT (///,5X,22H OPERATING CONDITIONS//)                        B  79
 15   FORMAT (//,15X,23H WIND VELOCITY - FPS = ,F7.4)                   B  80
 16   FORMAT (/,15X,35H WIND VELOCITY GRADIENT EXPONENT = ,F7.4)        B  81
 17   FORMAT (/,15X,39H HUB HEIGHT ABOVE GROUND LEVEL - FT- = ,F12.4)   B  82
 18   FORMAT (/,15X,40H ALTITUDE OF HUB ABOVE SEA LEVEL - FT = ,F15.4)  B  83
 19   FORMAT (/,15X,30H ANGULAR VELOCITY - RAD/SEC = ,F10.4)            B  84
 20   FORMAT (/,15X,19H TIP SPEED RATIO = ,F7.4)                        B  85
 21   FORMAT (/,15X,44H PITCH ANGLE FROM NOMINAL TWIST - DEGREES = ,F10. B  86
     $4)                                                                B  87
 22   FORMAT (/,15X,40H PITCH ANGLE AT 0.75 RADIUS - DEGREES = ,F10.4)  B  88
 23   FORMAT (/,15X,26H CONING ANGLE - DEGREES = ,F10.4)                B  89
 24   FORMAT (///,5X,14H BLADE DESIGN//)                                B  90
 25   FORMAT (//,15X,20H NUMBER OF BLADES = ,F3.0)                      B  91
 26   FORMAT (/,15X,19H TIP RADIUS - FT = ,F7.4)                        B  92
 27   FORMAT (/,15X,19H HUB RADIUS - FT = ,F7.4)                        B  93
 28   FORMAT (/,15X,11H SOLIDTY = ,F12.5)                               B  94
 29   FORMAT (/,15X,19H ACTIVITY FACTOR = ,F12.5)                       B  95
 30   FORMAT (/,15X,16H NACA PROFILE = ,I4)                             B  96
 31   FORMAT (/,15X,33H NUMBER OF STATIONS ALONG SPAN = ,I4)            B  97
 32   FORMAT (//,10X,29H CHORD AND TWIST DISTRIBUTION)                  B  98
 33   FORMAT (//,16X,15H PERCENT RADIUS,3X,8HCHORD-FT,10X,9HTWIST-DEG)  B  99
 34   FORMAT (/,20X,F5.1,8X,F10.5,10X,F10.5)                            B 100
 35   FORMAT (///,5X,30H PROGRAM OPERATING CONDITIONS//)                B 101
 36   FORMAT (//,15X,25H INCREMENTAL PERCENTAGE =,F7.4)                 B 102
 37   FORMAT (//,15X,38H ANGULAR INTERFERENCE FACTOR, AP = 0.0)         B 103
 38   FORMAT (//,15X,38H WILSON AXIAL INTERFERENCE METHOD USED)         B 104
 39   FORMAT (//,15X,40H STANDARD AXIAL INTERFERENCE METHOD USED)       B 104
 40   FORMAT (//,15X,39H TIP LOSSES MODELED BY PRANDTLS FORMULA)        B 105
 41   FORMAT (//,15X,41H TIP LOSSES MODELED BY GOLDSTEINS FORMULA)      B 106
 42   FORMAT (//,15X,18H NO TIP LOSS MODEL)                             B 107
 43   FORMAT (//,15X,31H TIP LOSS MODEL -- NASA VERSION)                B 108
 44   FORMAT (//,15X,22H NO HUBLOSS MODEL USED)                         B 109
 45   FORMAT (//,15X,29H HUBLOSSES MODELED BY PRANDTL)                  B 110
 46   FORMAT (1H1)                                                      B 111
 47   FORMAT (///,22H PERFORMANCE ANALYSIS//)                           B 112
 48   FORMAT(///1X,*PCCR*,6X,*A*,5X,*AP*,5X,*CL*,6X,*CD*,5X,*PHI*,4X,
     $*ALPHA*,5X,*F*,EX,*RE NO*,8X,*CT*,8X,*CP*)
      END                                                               B 113-

      SUBROUTINE SEARCH(RL,RR,CI,THETI,NF,C,THET,SMODE)
C                                                                       C   2
C     ....... SEARCH - DETERMINES THE CHORD AND THE TWIST ANGLE AT      C   3
C     A GIVEN RADIUS ALONG THE SPAN.  IT UTILIZES A LINEAR              C   4
C     INTERPOLATION TECHNIQUE.                                          C   5
C                                                                       C   6
      DIMENSION RR(25), CI(25), THETI(25)                               C   7
      COMMON R,DR,HB,B,V,X,THETP,AMOD,H,SI,GO,OMEGA,RHO,VIS,HL,PI,RX    C   8
      DO 1 I=1,NF                                                       C   9
         RRV = RL/(RX*COS(SI))*100.                                     C  10
         IF (RRV.EQ.RR(1)) GO TO 4                                      C  11
         IF (RRV.GE.RR(I)) GO TO 2                                      C  12
         IF (I.EQ.NF) GO TO 3                                           C  13
 1    CONTINUE                                                          C  14
 2    J = I+1                                                           C  15
      PER = (RRV-RR(J-1))/(RR(J-2)-RR(J-1))                             C  16
      C = PER*(CI(J-2)-CI(J-1))+CI(J-1)                                 C  17
      THET = PER*(THETI(J-2)-THETI(J-1))+THETI(J-1)                     C  18
      GO TO 5                                                           C  19
 3    C = CI(NF)                                                        C  20
      THET = THETI(NF)                                                  C  21
      GO TO 5                                                           C  22
 4    C = CI(1)                                                         C  23
      THET = THETI(1)                                                   C  24
 5    THET = THET*PI/180.                                               C  25
      XOL=(RL-HB)/(P-HB)
      SMODE=XMOD(XOL)
      RETURN                                                            C  26
      END                                                               C  27-

      SUBROUTINE CALC (RL,C,THET,FXF,FYF,XMFXF,XMFYF,QF,TF,RE,PHIR,CL,CD D   1
     $,CX,CY,A,AP,XL,AK,ALPHA,F,CLF,CAT,AAT,CLT,CDT,NFS,SOLD,TH,SMODE,
     $UQS,BQS)
C                                                                       D   3
C     ....... CALC - DETERMINES THE AXIAL AND ANGULAR INTERFERENCE      D   4
C     FACTORS AT A GIVEN RADIUS AND DETERMINES FUNCTIONS DEPENDENT      D   5
C     UPON THESE PARAMETERS.                                            D   6
C                                                                       D   7
      DIMENSION AAT(25), CLT(25), CDT(25)                               D   8
      COMMON R,DR,HB,B,V,X,THETP,AMOD,H,SI,GO,OMEGA,RHO,VIS,HL,PI,RX,W,
     $NPROF,APP,T1,T2,T3,T4,T5,T6,T7,T8,TEST,XET4,HH,AL0,AC
      COMMON XCG,ESC,AE,AG
      XL = RL*OMEGA/V                                                   D  11
      RH = HB                                                           D  14
      MM=40
      DO 15 J=1,40                                                      D  15
         BETA = A                                                       D  16
         DELTA = AP                                                     D  17
         PHI = ATAN((1.-A)*COS(SI)/((1.+AP)*XL))                        D  18
         PHIAA = ABS(PHI)                                               D  19
```

```
      BAD=F*SIN(PHI)**2.
      B1=((1.-2.*AC)*BAD/VBR+2.)
      C1=(1.-BAD*AC*AC/VBR)
      CANN=B1*B1-4.*C1
      IF(CANN.LT.0.0) CANN=0.0
      A=.5*(B1-SQRT(CANN))
 32   CONTINUE
      IF(VAR.EQ.0.) THEN
      AP=0.
      ELSE
      AP = VAR/(F*SIN(PHI)*COS(PHI)-VAR)
      ENDIF
      IF (APP.EQ.1.) AP = 0.0
  9   PCCR=RL/(RX*COS(SI))
C     ....... DAMPENING OF AXIAL AND ANGULAR INTERFERENCE FACTOR
C     ITERATIONS.
C
      IF (J-4) 13,12,10
 10   IF (J-10) 13,12,11
 11   IF (J-15) 13,12,13
 12   A = (A+BETA)*.5
      AP = (AP+DELTA)*.5
 13   CONTINUE
C
C     ....... TEST FOR CONVERGENCE ......
C
      IF (APP.EQ.1.) GO TO 14
      IF (ABS((AP-DELTA)/AP).LE..0001) GO TO 16
      GO TO 15
 14   IF (ABS((A-BETA)/A).LE..0001) GO TO 16
C
 15   CONTINUE
C     IF (AK.GE.1.) GO TO 18
 16   CONTINUE
C     FOR OPERATION OF VORTEX RING STATE REPLACE THE FOLLOWING C CARDS
      PCCR = RL/(RX*COS(SI))
C
C
      IF (J.LT.40) GO TO 17
      WRITE (61,27)
 17   CONTINUE
C
C     ....... CALCULATION OF FUNCTIONS DEPENDENT UPON AXIAL AND
C     ANGULAR INTERFERENCE FACTORS.
C
 18   CONTINUE
      W = SQRT(((1.-A)*V*COS(SI))**2+((1.+AP)*RL*OMEGA)**2)
      RE = RHO*W*C/VIS
      CONST = (0.5*RHO*(W**2)*C)
      FXF = CONST*CX
      FYF = CONST*CY
      XMFXF = FXF*(RL-HB)/COS(SI)
      XMFYF = FYF*(RL-HB)/COS(SI)
      CT1 = (0.5*RHO*B*C)*(W*W)
      QF = CT1*RL*CX
      TF = CT1*CY*COS(SI)
      DPCR = DR/(2.*RX)
      CR = C/RX
      CLA = (CLD-CL)/0.001
      CDA = (CDD-CD)/0.001
      CXP = CLA*SIN(PHI)-CDA*COS(PHI)+CY
      CYP = CLA*COS(PHI)+CDA*SIN(PHI)-CX
      CN=CL*COS(ALPHA)+CD*SIN(ALPHA)
```

```
      SINPHI=SIN(PHIAA)
      IF(SINPHI.EQ.0.00) SINPHI=0.0001
      XXL = COS(PHIAA)/SINPHI
      XXLO = XXL*R/RL
      PHIR = PHI
      ALPHA = PHI-THET-THETP
      DDTC = ATAN((1.-A)/(XL*(1.+2.*AP)))-ATAN((1.-A)/XL)
      DA1 = DDTC/4.
      DA2 = ((4./15.)*(SOLO*TH)/X)/((1./X)**2+(RL/RX)**2)
      DALPHA = DA1+DA2
      ALPHA = ALPHA-DALPHA
      ALPHAD = ALPHA+0.001
C
C     ...... CALCULATION OF SECTIONAL LIFT AND DRAG COEFFICIENTS
C
      IF (NPROF.EQ.4415) GO TO 1
      IF (NPROF.EQ.0012) GO TO 2
      IF (NPROF.EQ.8888) GO TO 3
      IF (NPROF.EQ.9999) GO TO 4
      WRITE (61,20)
  1   CALL NACA44 (RL,RX,SI,ALPHA,CL,CD,AL0,W)
      CALL NACA44 (RL,RX,SI,ALPHAD,CLD,CDD,AL0,W)
      GO TO 5
  2   CALL NACA00 (ALPHA,CL,CD,AL0)
      CALL NACA00 (ALPHAD,CLD,CDD,AL0)
      GO TO 5
  3   CALL NACATT (RL,RX,SI,ALPHA,CL,CD,AL0,W,AAT,CLT,CDT,NFS,SOLO)
      CALL NACATT (RL,RX,SI,ALPHAD,CLD,CDD,AL0,W,AAT,CLT,CDT,NFS,SOLO
     $)
      GO TO 5
  4   CALL NACAXX (RL,RX,SI,ALPHA,CL,CD,AL0,W)
      CALL NACAXX (RL,RX,SI,ALPHAD,CLD,CDD,AL0,W)
  5   CONTINUE
      IF (GO.LT.3.) GO TO 6
      CL = CLF*CL
      CLD = CLF*CLD
      F = 1.
      GO TO 7
C
C     ..... CALCULATION OF TIP AND HUB LOSSES ......
C
  6   IF (CAT.EQ.1.) F = 0.0
      IF (CAT.EQ.1.) GO TO 7
      CALL TIPLOS (XXL,XXLO,F,B,GO,HL,PI,R,RL,PHI,RH)
C
  7   CX = CL*SIN(PHI)-CD*COS(PHI)
      CY = CL*COS(PHI)+CD*SIN(PHI)
      CXX = CL*SIN(PHI)
      CYY = CL*COS(PHI)
      SIG = (B*C)/(PI*RL)
      IF (AMOD.EQ.0.) GO TO 8
      VBR = ((.125*SIG*CYY)*(COS(SI)**2))/(SIN(PHI)**2)
      VAR = (0.125*SIG*CXX)/(F*SIN(PHI)*COS(PHI))
      CAN = F*F+4.*VBR*F*(1.-F)
      IF (CAN.LT.0.0) CAN = 0.0
      A = (2.*VBR+F-SQRT(CAN))/(2.*(VBR+F*F))
      AP = VAR/((1.-A*F)/(1.-A)-VAR)
      IF (APP.EQ.1.) AP = 0.0
      GO TO 9
  8   VBR = 0.125*SIG*CYY*(COS(SI)**2)
      VAR = 0.125*SIG*CXX
      A=VBR/(F*SIN(PHI)**2+VBR)
      IF(A.LE.AC) GO TO 32
```

```
 19   CONTINUE
      IF (NPROF.EQ.9999) THEN
      CALL PROPER(XCG,ESC,RX,R,HB,C,AE,AG,AMASS,AI1,AI2,AI3,ER,E1,E2,
     $E3,FF,FFP,FFPP,FP,FPP,RL,EI,GJ)
      ELSE
      CALL PROPER1(XCG,ESC,RX,R,HB,C,AE,AG,AMASS,AI1,AI2,AI3,ER,E1,E2,
     $E3,FF,FFP,FFPP,FP,FPP,RL,EI,GJ)
      ENDIF
      RHR=HB/R
      RS=1.-RHR
      DYNA=6./(RHO*V*V)
C*****
C*******SOLVE FOR QS (STATIC TIP DEFLECTION)
C
      BEETA=THET+THETP
      CB=COS(BEETA)
      SB=SIN(BEETA)
      CSI=COS(SI)
      SSI=SIN(SI)
      CR=C/RX
      RLR=RL/R
      OM=OMEGA
      IF (NPROF.EQ.9999) THEN
      CALL SUMROW(RLR,RHR,RS,ER,E1,E3,BBUC,MN,EI,GJ,RX)
      ELSE
      CALL SUMROW1(RLR,RHR,RS,ER,E1,E3,BBUC,MN,EI,GJ,RX)
      ENDIF
      BNORMA=-CSI*CB*(1.-A)+X*RLR*CSI*SB-X*E3*SSI
      BTANG=CSI*SB*(1.-A)+X*RLR*CSI*CB
      WNORM=(BNORMA*BNORMA+BTANG*BTANG)

      DS1=DYNA*AMASS*OM*OM*(ER*SB*CB*(1.-SSI*SSI)-RLR*SSI*CB)*FF
      DS2=DYNA*(AI1-AI3)*OM*OM*SSI*CSI*CB*FFP
      DS3=3.*WNORM*FF*CN*CR
C******* SINCE BUC=BBUC*QS
      PAUL=-BBUC
      DSS1=DYNA*AMASS*OM*OM*(RLR*CSI*CSI+ER*SSI*CSI*SB)*PAUL
      DSS2=-DYNA*AMASS*OM*OM*(SB*SB+(SSI*CB)**2.)*FF*FF
      DSS3=DYNA*EI*FFPP*FFPP
      UQS=DS1+DS2+DS3
      BQS=DSS1+DSS2+DSS3
      T7 = T7+(((2.+COS(PHI)**2)*CL*SIN(PHI)-COS(PHI)**3*CD+2.*COS(PHI)*
     $CLA)*(1.-A)**2*RL**3*C)*DR/2.
      T8 = T8+(((1.+SIN(PHI)**2)/COS(PHI)*CL-CD*SIN(PHI)+CLA*SIN(PHI))*
     $(1.+AP)*(1.-A)*RL**4*C)*DR/2.
C
       RETURN
C
C
 28    FORMAT (93H YOU HAVE SPECIFIED A NACA PROFILE NOT STORED IN THE PR
     $OGRAM, THE PROGRAM WILL USE NACA 4415.)
 27    FORMAT (/,5X,49H ***** ATTENTION - NO CONVERGENCE AT THIS STATION)
       END

       SUBROUTINE TIPLOS (U,UO,F,Q,GO,HL,PI,R,RL,PHI,RH)
C
C      ...... TIPLOS - DETERMINES THE TIP AND HUB LOSSES
C      BASED UPON GOLDSTEIN#S THEORY, OR PRANDTL#S THEORY,
C      OR FOR THE CASE OF NO LOSSES.
C
       SUM2 = 0.0
       SUM = 0.0
       AK = 1.
      AMM = 1.
      AM = 0.0
      IF (Q.GT.2.0) GO TO 1
      IF (GO.EQ.0.0) GO TO 2
      IF (GO.EQ.1.0) GO TO 4
      IF (GO.EQ.2.0) GO TO 3
 1    IF (GO.EQ.2.0) GO TO 3
 2    CONTINUE
      YY=-(Q*(R-RL))/(2.*RL*SQRT(SIN(PHI)**2.+0.0001))
      IF(YY.LT.-675.) THEN
      F=1.
      ELSE
      F=(2./PI)*ACOS(EXP(YY))
      ENDIF
      GO TO 5
 3    F = 1.0
      GO TO 5
 4    IF ((ABS(SIN(PHI))).LT..0001) GO TO 2
      CALL GOLDST (U,UO,F,Q,GO,PI,R,RL,PHI,SUM2,SUM,AK,AMM,AM)
C     HUBLOSS CALCULATIONS
C
 5    IF (HL.EQ.1.0) GO TO 6
      FI = 1.0
      GO TO 7
 6    FI = (2./PI)* ACOS(EXP(-(Q*(RL-RH))/(2.*RH*SQRT(SIN(PHI)**2+.0001)
     $)))
 7    F = F*FI
      RETURN
      END

      SUBROUTINE BESSEL (Z,V,AI)
C
C     ....... BESSEL CALCULATES BESSEL FUNCTIONS FOR THE GOLDSTEIN
C     TIP LOSS MODEL......
C
      S = 0.0
      AK = 0.0
      C = 1.
      DO 3 K=1,10
         B = (.25*Z*Z)**AK
         D = V+AK
         P = 1.
 1       TK = D-1.
         IF (TK.LE.0.0) GO TO 2
         P = D*TK*P
         D = D-2.
         GO TO 1
 2       E = P
         S = B/(C*E)+S
         AK = AK+1.
         C = AK*C
 3    CONTINUE
      AI = ((.5*Z)**V)*S
      RETURN
      END

      SUBROUTINE NACA00 (ALPHA,CL,CD,AL0)
C
C     ........ NACA - DETERMINES THE COEFFICIENTS OF LIFT AND DRAG
C     AT A GIVEN ANGLE OF ATTACK, ALPHA; FOR A NACA 0012 AIRFOIL.
C     THE EQUATIONS WERE OBTAINED BY A ORTHOGNAL POLYNOMIAL
C     CURVEFIT OF NACA DATA PUBLISHED IN NACA REPORT NO. 669,PAGE 529.
C
```

```
      A0 = 5.73
      A2 = 7.*A0
      SD0 = 0.0058
      SD1 = 0.0006
      SD2 = .130
      SD3 = 0.0160
      SD4 = 0.0006
      SD5 = 12570.
      AMAX = 0.218
      A = ALPHA-AL0*3.141493/180.
      IF (A.GT.AMAX) GO TO 1
      CL = A0*A
      CD = SD0+(SD1*A)+(SD2*A*A)
      GO TO 3
1     CL = (A0*A)-(A2*(A-AMAX)**2)
      IF (CL.GE.0.0) GO TO 2
      CL = 0.0
2     CD = SD3+SD4*(A-AMAX)**2+SD5*(A-AMAX)**4
      IF (CD.LE.1.0) GO TO 3
      CD = 1.0
3     RETURN
      END

      SUBROUTINE NACA44 (RL,RX,SI,ALPHA,CL,CD,AL0,W)
      PI=3.1415926536
      CLFL=1.
      AMAX=PI/2.
      AST=45.*PI/180.
      EM1=1./(SIN(AMAX-AST))
      CONV=PI/180.
      CD0=.016
      ABSA=ABS(ALPHA)
      AL1=ALPHA
      AL2=AL1*AL1
      AL3=AL2*AL1
      A=ALPHA*180./PI
      IF(A.LE.4.) THEN
      CL=.4031+5.569*AL1
      CD=CD0*(1.+25.65*AL2)
      ELSE IF (A.LE.14..AND.A.GT.4.) THEN
      CL=.33643+7.4249*AL1-13.6295*AL2
        IF(A.LE.10.) THEN
        CD=.018+.1146*(AL1-4.*CONV)
        ELSE
        CD=.03+1.00267*(AL1-10.*CONV)
        ENDIF
      ELSE IF (A.LE.26.) THEN
      CL=.4395+10.5458*AL1-36.5327*AL2+34.6733*AL3
        IF(A.LE.16.) THEN
        CD=.1+2.8648*(AL1-14.*CONV)
        ELSE
        CD=.2+1.637*(AL1-16.*CONV)
        ENDIF
      ELSE
      CL=1.2*SIN(2.*AL1)
      CD=.2+1.637*(AL1-16.*CONV)
      ENDIF
      RETURN
      END

      SUBROUTINE NACAXX (RL,RX,SI,ALPHA,CL,CD,AL0,W)
C
C     ..... NACAXX IS AN EMPTY SUBROUTINE FOR USE FOR A PROFILE
C     NOT PREVIOUSLY STORED.  ONE MUST INSERT CURVE FIT EQUATIONS
C     FOR SECTIONAL LIFT AND DRAG COEFFICIENTS AS A FUNCTION OF
C     ANGLE OF ATTACK IN DEGREES.
C
C     EQUATIONS FOR LIFT AND DRAG COEFFICIENTS FOR
C     NACA 644-421 AIRFOIL HAVE BEEN INSERTED.
C
      A = ALPHA*180./3.141593
C
C     ADD CURVE FIT PROGRAM FOR CL AND CD
      PI=3.1415926536
      CONVT=PI/180.
      CD0=0.014
      AL0=1.1*CONVT
      B0=-0.020255
      B1=11.9705
      B2=-54.761
      B3=136.055
      B4=-144.5923
      C0=187.3277
      C1=-2335.2577
      C2=10915.946
      C3=-22521.2787
      C4=17287.811
      AL1=ALPHA
      AL2=AL1*AL1
      AL3=AL2*AL1
      AL4=AL3*AL1
      CL=6.6463*(AL1+AL0)
      IF(A.GE.4.) CL=B0+B1*AL1+B2*AL2+B3*AL3+B4*AL4
      IF(A.GE.17.7) CL=C0+C1*AL1+C2*AL2+C3*AL3+C4*AL4
      IF(A.GE.21.) CL=2.25*SIN(2.*AL1)/(4./PI+SIN(AL1))+0.04
      CD=CD0*(1.+20.*AL2)
      IF(A.GE.10.) CD=0.0225+0.6517*(AL1-10.*CONVT)
      IF(A.GE.14.) CD=0.060+1.0*2.4627*(AL1-14.*CONVT)
      IF(A.GE.20.) CD=4.5*(SIN(AL1))**2./(4./PI+SIN(AL1))+0.34
      RETURN
      END

      SUBROUTINE NACATT (RL,RX,SI,ALPHA,CL,CD,AL0,W,AAT,CLT,CDT,NFS,SOLD
     1)
C
C     ...... NACATT - IS AN INTERPOLATING SUBROUTINE TO INTERPOLATE
C     AIRFOIL DATA INPUTED IN TABLE FORM.
C
      DIMENSION AAT(25), CLT(25), CDT(25)
      A = ALPHA*180./3.141593-AL0
      DO 1 I=1,NFS
         IF (A.LE.AAT(1)) GO TO 4
         IF (A.LE.AAT(I)) GO TO 2
         IF (I.EQ.NFS) GO TO 3
1     CONTINUE
2     J = I+1
      PER = (A-AAT(J-1))/(AAT(J-2)-AAT(J-1))
      CL = PER*(CLT(J-2)-CLT(J-1))+CLT(J-1)
      CD = PER*(CDT(J-2)-CDT(J-1))+CDT(J-1)
      GO TO 5
3     CL = CLT(NFS)
      CD = CDT(NFS)
      GO TO 5
4     CL = CLT(1)
      CD = CDT(1)
5     CD = (CD*3.475+1.2*.124)/3.475
```

```
      RETURN
      END

      SUBROUTINE SOLIDT (RR,CI,NF,B,R,PI,SOLD)
C
C     ..... SOLIDT - DETERMINES THE TOTAL SOLIDITY OF THE
C     WIND TURBINE DESIGN.
C
      DIMENSION RR(25), CI(25)
      NFX = NF-1
      S1 = 0.
      IF(NF.EQ.1) THEN
      S1=CI(1)*R
      ELSE
      DO 1 I=1,NFX
         SOL = ((CI(I+1)+CI(I))/2.)*(RR(I)-RR(I+1))*R/100.
         S1 = S1+SOL
 1    CONTINUE
      ENDIF
      SOLD = B*S1/(PI*R**2)
      RETURN
      END

      SUBROUTINE ACTIVI (RR,CI,NF,B,R,PI,ACF)
C
C     ..... ACTIVI   - DETERMINES THE ACTIVITY FACTOR OF THE
C     WIND TURBINE DESIGN.
C
      DIMENSION RR(25), CI(25)
      NFX = NF-1
      S1 = 0.
      DO 1 I=1,NFX
         C1 = (CI(I+1)+CI(I))/2.
         ROR = ((RR(I)-RR(I+1))/2.+RR(I+1))/100.
         DROR = (RR(I)-RR(I+1))/100.
         FAC = (C1/(2.*R))*ROR**3*DROR
         S1 = S1+FAC
 1    CONTINUE
      ACF = S1*100000./16.
      RETURN
      END


      SUBROUTINE GOLDST (U,UO,F,Q,GO,PI,R,RL,PHI,SUM2,SUM,AK,ANM,AM)
     1
C
C     ..... GOLDST   - DETERMINES THE GOLDSTEN TIP LOSS
C     FACTORS FOR THE 2 BLADED DESIGN CASE.  FOR DESIGN CASES
C     WITH BLADE NUMBERS OTHER THAN TWO THE PRANDTL
C     MODEL IS USED.  THIS CAN BE CHANGED IF NECESSARY, AND
C     THE  GOLDSTEN MODEL FOR ANY NUMBER OF BLADES MAY BE
C     SUBSTITUTED FOR THIS ROUTINE.
C
      DO 5 M=1,3
         V = (2.*AM+1.)
         Z0 = UO*V
         V2 = V*V
         Z = U*V
         Z2 = Z*Z
         CALL BESSEL (Z,V,AI)
         CALL BESSEL (Z0,V,AI0)
         IF (Z.GE.3.5) GO TO 1
         A = 2.*2.
         B = 4.*4.
         C = 6.*6.
         D = 8.*8.
         T1VZ = Z2/(A-V2)+(Z2*Z2)/((A-V2)*(B-V2))+(Z2**3)/((A-V2)*(B-V2)
     $   *(C-V2))+(Z2**4)/((A-V2)*(B-V2)*(C-V2)*(D-V2))
         CT1VZ = (V*PI*AI)/(2.*SIN(.5*V*PI))-T1VZ
         GO TO 2
 1       T0 = (U*U)/(1.+U*U)
         T2 = 4.*U*U*(1.-U*U)/((1.+U*U)**4)
         T4 = 16.*U*U*(1.-14.*U*U+21.*U**4-4.*U**6)/((1.+U*U)**7)
         T6 = 64.*U*U*(1.-75.*U*U+603.*U**4-1065.*U**6+460.*U**8-36.*U**
     $   10)/((1.+U*U)**10)
         CT1VZ = T0+T2/V2+T4/(V2**2)+T6/(V2**3)
 2       FVU = (U*U)/(1.+U*U)-CT1VZ
         SUM = SUM+FVU/V2
         IF (AM.NE.0.0) GO TO 3
         E = -0.098/(UO**.668)
 3       IF (AM.NE.1.0) GO TO 4
         E = 0.031/(UO**1.285)
 4       IF (AM.GT.1.0) E = 0.0
         SUM2 = SUM2+((UO*UO*ANM)/(1.+UO*UO)-E)*(AI/AI0)
         AM = AM+1.
         AK = ((2.*AM-1.)*AK)/(2.*AM)
 5    ANM = AK/(2.*AM+1.)
      G = (U*U)/(1.+U*U)-(8./(PI*PI))*SUM
      CIRC = G-(2./PI)*SUM2
      F = ((1.+U*U)/(U*U))*CIRC
      RETURN
      END
      FUNCTION XMOD(RP)
      DIMENSION B(10)
      DATA(B(I),I=1,10)/0.,6.,1.8094,-4.8094,1.7420,0.,0.,0.,0.,0./
      SUM=XMOD=0.
      DO 1 I=1,10
      SUM=SUM+B(I)
      XMOD=XMOD+B(I)*RP**I
 1    CONTINUE
      XMOD=XMOD/SUM
      RETURN
      END


      SUBROUTINE PROPER1 (XCG,ESC,RX,R,HB,C,AE,AS,AMASS,AI1,AI2,AI3,
     $ER,E1,E2,E3,FF,FFP,FFPP,FP,FPP,RL,EI,GJ)
      CR=C/RX
      RLR=RL/R
      RHR=HB/R
      ER=(ESC-XCG)*CR
      E1=(ESC-.25)*CR
      E2=(0.75-ESC)*CR
      E3=(0.5-ESC)*CR
C
C*******PROPERTIES OF THE BLADE
C
 20   AFACTO=0.84752/144.
      IF(RLR.LE.1..AND.RLR.GT.0.6545) THEN
      BI2=5.673*EXP(-3.313*RLR)
      BI3=67.3636*EXP(-2.0236*RLR)
      AMASS=15.*AFACTO*EXP(-1.3266*RLR)
      ELSE IF(RLR.LE.0.6545.AND.RLR.GT.0.3640) THEN
      BI2=2.111*EXP(-1.802*RLR)
      BI3=29.44*EXP(-0.76*RLR)
      AMASS=9.65*AFACTO*EXP(-0.6447*RLR)
      ELSE IF(RLR.LE.0.3640.AND.RLR.GT.0.1393) THEN
```

```
      BI2=4.5679*EXP(-4.8604*RLR)
      IF(RLR.GT.0.244) BI2=2.111*EXP(-1.802*RLR)
      BI3=11.3726*RLR**(-0.6585)
      AMASS=5.243*AFACTO*RLR**(-0.3695)
      ELSE
      BI2=2.3210
      BI3=41.924
      AMASS=10.88*AFACTO
      ENDIF
      BI1=BI2+BI3
      EI=BI2*AE
      GJ=BI1*AG
C*********CHANGE UNIT TO FEET
C
      AI1=AFACTO*BI1/(144.*RX*RX)
      AI2=AFACTO*BI2/(144.*RX*RX)
      AI3=AFACTO*BI3/(144.*RX*RX)
      EI=EI/(144.*RX**4.)
      GJ=GJ/(144.*RX**4.)

C
C**************
C
      FO=1.
      FD=1.
      RS=(1.-RHR)
      ZP=(RLR-RHR)/RS
      ZP2=ZP*ZP
      ZP3=ZP2*ZP
      ZP4=ZP3*ZP
      FF=6.*ZP2-4.*ZP3+ZP4
      FFP=12.*ZP-12.*ZP2+4.*ZP3
      FFPP=12.-24.*ZP+12.*ZP2
      FP=2.*ZP-ZP*ZP
      FPP=2.*(1.-ZP)
C*********CORRECTION OF MODE SHAPE THAT BASED ON LENGTH OF THE BLADE
C*********(R-RH) NOT ON THE RADIUS OF THE ROTOR ( CORRECTION FOR
C*********MASS,DAMPING,STIFFNESS MATRICES )
C
      FF=FF*RS
      FFPP=FFPP/RS
      FPP=FPP/RS
      RETURN
      END

      SUBROUTINE PROPER (XCG,ESC,RX,R,HB,C,AE,AG,AMASS,AI1,AI2,AI3,
     $ER,E1,E2,E3,FF,FFP,FFPP,FP,FPP,RL,EI,GJ)
      CF=C/RX
      RLR=RL/R
      RHR=HB/R
      ER=(ESC-XCG)*CR
      E1=(ESC-.25)*CR
      E2=(0.75-ESC)*CR
      E3=(0.5-ESC)*CR
C
C*******PROPERTIES OF THE BLADE
C
      BI2=0.0069734
      BI3=0.011479
      BI1=BI2+BI3
      DENSI=5.2502
      AMASS=0.386546
      AI1=DENSI*BI1
      AI2=DENSI*BI2
      AI3=DENSI*BI3
      EI=AE*BI2*144.
      GJ=AG*BI1*144.
      AI1=AI1/(RX*RX)
      AI2=AI2/(RX*RX)
      AI3=AI3/(RX*RX)
      EI=EI/(RX**4.)
      GJ=GJ/(RX**4.)
      GJ0=7.2047E05
      EI0=1.7833E06
      EI0=EI0/(RX**4)
      GJ0=GJ0/(RX**4.)
C
C**************
C
      FO=1.
      FD=1.
      RS=(1.-RHR)
      ZPA=RHR/RS
      ZP=(RLR-RHR)/RS
      ZP2=ZP*ZP
      ZP3=ZP2*ZP
      ZP4=ZP3*ZP
      AKJ0=2.*ZPA*GJ/GJ0
      AKK0=2.*EI/EI0*ZPA*ZPA*(3.+4.*ZPA)
      AKK1=12.*EI/EI0*ZPA*(1.+ZPA)
      FF=AKK0+AKK1*ZP+6.*ZP2-4.*ZP3+ZP4
      FFP=AKK1+12.*ZP-12.*ZP2+4.*ZP3
      FFPP=12.-24.*ZP+12.*ZP2
      FP=AKJ0+2.*ZP-ZP*ZP
      FPP=2.*(1.-ZP)
C*********CORRECTION OF MODE SHAPE THAT BASED ON LENGTH OF THE BLADE
C*********(R-RH) NOT ON THE RADIUS OF THE ROTOR ( CORRECTION FOR
C*********MASS,DAMPING,STIFFNESS MATRICES )
C
      FF=FF*RS
      FFPP=FFPP/RS
      FPP=FPP/RS
      RETURN
      END

      SUBROUTINE ITERAT(QS,ALPH,AXI,STA,PQS,KK,KL)
      DIMENSION RR(25), CI(25), THETI(25), AAT(25), CLT(25), COT(25)       A  11
      DIMENSION STA(100),AXI(100),ALPH(100)
      COMMON R,CR,HB,B,V,X,THETP,AMOU,N,SI,GO,OMEGA,RHO,VIS,HL,PI,RX,W,     A  12
     $NPROF,APP,T1,T2,T3,T4,T5,T6,T7,T8,TEST,XETA,HH,AL0,AC                A  13
      COMMON XCG,ESC,AE,AG
      COMMON RR,CI,THETI,NF
      EXTERNAL TOM,TIH
      KL=1
      MH=40
 22   ALEFT=RIGHT=0.
      DO 10 I=1,KK
      NHALF=I/2
      L=I+1
      NTEST=I-2*NHALF
      RLR=STA(I)
      A=AXI(I)
      ALPHA=ALPH(I)
      ALPHAD=ALPHA+0.001
      RL=RLR*R
      CALL SEARCH(RL,RR,CI,THETI,NF,C,THET,SMODE)
```

```
      IF(NPROF.EQ.9999) THEN
      CALL PROPER(XCG,ESC,RX,R,HB,C,AE,AG,AMASS,AI1,AI2,AI3,ER,E1,E2,
     $E3,FF,FFP,FFPP,FP,FPP,RL,EI,GJ)
      CALL NACAXX(RL,RX,SI,ALPHA,CL,CD,AL0,W)
      CALL NACAXX(RL,RX,SI,ALPHAD,CLD,COD,AL0,W)
      ELSE
      CALL PROPER1(XCG,ESC,RX,R,HB,C,AE,AG,AMASS,AI1,AI2,AI3,EP,E1,E2,
     $E3,FF,FFP,FFPP,FP,FPP,RL,EI,GJ)
      CALL NACA44(RL,RX,SI,ALPHA,CL,CD,AL0,W)
      CALL NACA44(RL,RX,SI,ALPHAD,CLD,COD,AL0,W)
      ENDIF
      RHR=HB/R
      RS=1.-RHR
      WR=RS*FF*QS
      WP=FFP*QS
      CW=COS(WP)
      SW=SIN(WP)
      C2W=CW*CW-SW*SW
      BEETA=THET+THETP
      CB=COS(BEETA)
      SB=SIN(BEETA)
      CSI=COS(SI)
      SSI=SIN(SI)
      CR=C/RX
      OM=OMEGA
      IF(L.LE.KK) THEN
      DRR=STA(I)-STA(L)
      ELSE
      LL=I-1
      DRR=STA(LL)-STA(I)
      ENDIF
      CN=CL*COS(ALPHA)+CD*SIN(ALPHA)
      CQ=CL*SIN(ALPHA)-CD*COS(ALPHA)
      X=OM*RX/V
C*****
C
      IF(NPROF.EQ.9999)THEN
      CALL SUMSUM(TOM,TIM,RLR,ER,E1,E3,UC,AUC,BUC,AAUC,ABUC,BBUC,AUM,AAU
     1M,ABUM,AUD,MM,QS,RHR,EI,GJ,RX)
      ELSE
      CALL SUMSUM1(TOM,TIM,RLR,ER,E1,E3,UC,AUC,BUC,AAUC,ABUC,BBUC,AUM,AA
     1UM,ABUM,AUD,MM,QS,RHR,EI,GJ,RX)
      ENDIF
      UD=UM=UC
      UCPD=AUC
      UCFD=BUC
      UDFD=UMFD=BUC
      UMPD=AUM
      BUD=BUM=BUC
      AUCPD=AAUC
      AUMPD=AAUM
      BUCPD=AUCFD=ABUC
      BUMPD=AUMFD=ABUM
      BUCFD=BUMFD=BBUC
      BBUM=BBUC
      DIS=(RLR+UC)*CSI-WR*SSI
C*****SOME COFACTORS
      PART1=SSI*SW-CSI*CW*CB
      PART12=SSI*CW+CSI*SW*CB
C
      TAIL1=(RLR+UM)*CW*CSI*SB+WR*SW*CSI*SB+E1*PART12
      TAIL2=(RLR+UM)*CSI*SB-WR*SSI
C
      WT=CSI*SB*(1.-A)+X*((RLR+UD)*CSI*CB-WR*SSI)
      WN=-PART1*(1.-A)-X*((RLR+UD)*CW*CSI*SB+WR*SW*CSI*SB-E3*PART12)
      WE2=WN*WN+WT*WT
      WTB=WE2*CQ*CR
      WNB=WE2*CN*CR
C*****MASS MATRIX
      QVEL=0.5*RHO*V*V
      DYNA=(3./QVEL)
C
      HF3=(AI1-AI3)*OM*OM*(SSI*CSI*CB*C2W+SW*CW*((CSI*CB)**2.-SSI*SSI))
      HF5=3.*WNB*(FF*CW-UMFD*SW)
      TF1=ER*SB*CB*(1.-SSI*SSI)-(RLR+UC)*SSI*CB
      TF2=BUC*((RLR+UC)*CSI*CSI+ER*SSI*CSI*SB)
      TF4=AMASS*OM*OM*(-(SB*SB+(SSI*CB)**2)*FF*FF+SSI*CSI*CB*BUC)
      TF5=EI*FFPP*FFPP
      DALEFT=DYNA*(TF4+TF5)*DRR
      DRIGHT=DYNA*(AMASS*OM*OM*(TF1*FF+TF2)+HF3*FFP)+HF5
      DRIGHT=DRIGHT*DRR
      FEB=2./3.
      IF(NTEST.EQ.0) FEB=4./3.
      IF(I.EQ.1.OR.I.EQ.KK) FEB=1./3.
C*****START THE SIMPSON INTEGRATION
      ALEFT=ALEFT+FEB*DALEFT
      RIGHT=RIGHT+FEB*DRIGHT
10    CONTINUE
      PQS=QS
      QS=RIGHT/ALEFT
      IF(QS.EQ.0.) GO TO 18
      CHECK=ABS((QS-PQS)/QS)
      IF(CHECK.LT.0.01)GO TO 555
      KL=KL+1
      IF(KL.GT.10) GO TO 555
      GO TO 22
18    WRITE(61,13)
13    FORMAT(/,'  QS = 0.')
555   CONTINUE
      RETURN
      END

      SUBROUTINE SUMROW1(RLR,RHR,RS,ER,E1,E3,BBUC,MM,EI,GJ,RX)
      BBUC=0.
      ALOW=0.
      AHIGH=(RLR-RHR)/RS
      N=MM
      DRS=(AHIGH-ALOW)/N
      DRS3=DRS/3.
      RLS=ALOW
      K=N+1
      DO 10 I=1,K
      IHALF=I/2
      ITEST=I-2*IHALF
      ZP=RLS
      ZP2=ZP*ZP
      ZP3=ZP2*ZP
      ZP4=ZP3*ZP
      FF=6.*ZP2-4.*ZP3+ZP4
      FFP=12.*ZP-12.*ZP2+4.*ZP3
      FFPP=12.-24.*ZP+12.*ZP2
      FP=2.*ZP-ZP2
      FPP=2.*(1.-ZP)
      DBBUC=-FFP*FFP*RS
      FEB=2.
      IF(ITEST.EQ.0) FEB=4.
```

```
      IF(I.EQ.1.OR.I.EQ.K) FEB=1.
      BBUC=BBUC+FEB*DDBUC*DRS3
      RLS=RLS+DRS
10    CONTINUE
      RETURN
      END

      SUBROUTINE SUMROW(RLR,RHR,RS,ER,E1,E3,BBUC,MM,EI,GJ,RX)
      BBUC=0.
      GJ0=7.2847E05
      EI0=1.7833E06
      GJ0=GJ0/(RX**4.)
      EI0=EI0/(RX**4.)
      ALOW=0.
      AHIGH=RLR/RS
      ZPA=RHR/RS
      N=MM
      DRS=(AHIGH-ALOW)/N
      DRS3=DRS/3.
      RLS=-ZPA
      K=N+1
      DO 10 I=1,K
      IHALF=I/2
      ITEST=I-2*IHALF
      ZP=RLS
      ZP2=ZP*ZP
      ZP3=ZP2*ZP
      ZP4=ZP3*ZP
       IF(RLS.GE.0.) THEN
      AKJ0=2.*ZPA*GJ/GJ0
      AKK0=2.*EI/EI0*ZPA*ZPA*(3.+4.*ZPA)
      AKK1=12.*EI/EI0*ZPA*(1.+ZPA)
      FF=AKK0+AKK1*ZP+6.*ZP2-4.*ZP3+ZP4
      FFP=AKK1+12.*ZP-12.*ZP2+4.*ZP3
      FFPP=12.-24.*ZP+12.*ZP2
      FP=AKJ0+2.*ZP-ZP*ZP
      FPP=2.*(1.-ZP)
      ELSE
      FF=2.*(ZPA+ZP)**2.*(3.+4.*ZPA-2.*ZP)
      FFP=12.*(ZPA+ZP)*(1.+ZPA-ZP)
      FFPP=12.*(1.-2.*ZP)
      FP=2.*ZPA*(1.+ZP/ZPA)
      FPP=2.
      ENDIF
      DBBUC=-FFP*FFP*RS
      FEB=2.
      IF(ITEST.EQ.0) FEB=4.
      IF(I.EQ.1.OR.I.EQ.K) FEB=1.
      BBUC=BBUC+FEB*DBBUC*DRS3
      RLS=RLS+DRS
10    CONTINUE
      RETURN
      END
      SUBROUTINE SUMSUM1(TOM,TIM,RLR,ER,E1,E3,UC,AUC,BUC,AAUC,ABUC,BBUC,
     1AUM,AAUM,ABUM,AUD,MM,QS,RHR,EI,GJ,RX)
C
      UC=AUC=AAUC=ABUC=BBUC=AUM=AAUM=ABUM=AUD=0.
      ALOW=0.
      RS=1.-RHR
      AHIGH=(RLR-RHR)/RS
      N=MM
      DRS=(AHIGH-ALOW)/N
      DRS3=DRS/3.
      RLS=ALOW
      K=N+1
      DO 10 I=1,K
      IHALF=I/2
      ITEST=I-2*IHALF


      ZP=RLS
      ZP2=ZP*ZP
      ZP3=ZP2*ZP
      ZP4=ZP3*ZP
      FF=6.*ZP2-4.*ZP3+ZP4
      FFP=12.*ZP-12.*ZP2+4.*ZP3
      FFPP=12.-24.*ZP+12.*ZP2
      FP=2.*ZP-ZP2
      FPP=2.*(1.-ZP)
      WR=FF*QS*RS
      WP=FFP*QS
      WPP=FFPP*QS
      CW=COS(WP)
      SW=SIN(WP)
      DUC=-0.5*RS*WP*WP
      TOM0=TOM(ER,CW,SW,FP,FPP,WPP)
      TOM1=TOM(E1,CW,SW,FP,FPP,WPP)
      EE3=-E3
      TOM3=TOM(EE3,CW,SW,FP,FPP,WPP)
      DAUC=-WP*TOM0
      DAUM=-WP*TOM1
      DAUD=-WP*TOM3
      DAAUC=-TOM0*TOM0/RS
      DAAUM=-TOM1*TOM1/RS
      TIM0=TIM(ER,CW,SW,FP,FPP,WPP,FFP,FFPP)
      TIM1=TIM(E1,CW,SW,FP,FPP,WPP,FFP,FFPP)
      DABUC=WP*TIM0-FFP*TOM0
      DABUM=WP*TIM1-FFP*TOM1
      DBBUC=-FFP*FFP*RS
      FEB=2.
      IF(ITEST.EQ.0) FEB=4.
      IF(I.EQ.1.OR.I.EQ.K) FEB=1.
      UC=UC+FEB*DUC*DRS3
      AUC=AUC+FEB*DAUC*DRS3
      AUM=AUM+FEB*DAUM*DRS3
      AUD=AUD+FEB*DAUD*DRS3
      AAUC=AAUC+FEB*DAAUC*DRS3
      AAUM=AAUM+FEB*DAAUM*DRS3
      ABUC=ABUC+FEB*DABUC*DRS3
      ABUM=ABUM+FEB*DABUM*DRS3
      BBUC=BBUC+FEB*DBBUC*DRS3
      BUC=BBUC*QS
      RLS=RLS+DRS
10    CONTINUE
      RETURN
      END

      SUBROUTINE SUMSUM(TOM,TIM,RLR,ER,E1,E3,UC,AUC,BUC,AAUC,ABUC,BBUC,A
     1UM,AAUM,ABUM,AUD,MM,QS,RHR,EI,GJ,RX)
C
      UC=AUC=AAUC=ABUC=BBUC=AUM=AAUM=ABUM=AUD=0.
      GJ0=7.2847E05
      EI0=1.7833E06
      EI0=EI0/(RX**4.)
      GJ0=GJ0/(RX**4.)
      ALOW=0.
```

```
      RS=1.-RHR
      AHIGH=RLR/RS
      ZPA=RHR/RS
      N=MM
      DRS=(AHIGH-ALOW)/N
      DRS3=DRS/3.
      RLS=-ZPA
      K=N+1
      DO 10 I=1,K
      IHALF=I/2
      ITEST=I-2*IHALF


      ZP=RLS
      ZP2=ZP*ZP
      ZP3=ZP2*ZP
      ZP4=ZP3*ZP
      IF(RLS.GE.0.) THEN
      AKJ0=2.*ZPA*GJ/GJ0
      AKK0=2.*EI/EI0*ZPA*ZPA*(3.+4.*ZPA)
      AKK1=12.*EI/EI0*ZPA*(1.+ZPA)
      FF=AKK0+AKK1*ZP+6.*ZP2-4.*ZP3+ZP4
      FFP=AKK1+12.*ZP-12.*ZP2+4.*ZP3
      FFPP=12.-24.*ZP+12.*ZP2
      FP=AKJ0+2.*ZP-ZP*ZP
      FPP=2.*(1.-ZP)
      ELSE
      FF=2.*(ZPA+ZP)**2.*(3.+4.*ZPA-2.*ZP)
      FFP=12.*(ZPA+ZP)*(1.+ZPA-ZP)
      FFPP=12.*(1.-2.*ZP)
      FF=2.*ZPA*(1.+ZP/ZPA)
      FPP=2.
      ENDIF
      WR=FF*QS*RS
      WP=FFP*QS
      WPP=FFPP*QS
      CW=COS(WP)
      SW=SIN(WP)
      DUC=-0.5*RS*WP*WP
      TOM0=TOM(ER,CW,SW,FP,FPP,WPP)
      TOM1=TOM(E1,CW,SW,FP,FPP,WPP)
      EE3=-E3
      TOM3=TOM(EE3,CW,SW,FP,FPP,WPP)
      DAUC=-WP*TOM0
      DAUN=-WP*TOM1
      DAUD=-WP*TOM3
      DAAUC=-TOM0*TOM0/RS
      DAAUM=-TOM1*TOM1/RS
      TIM0=TIM(ER,CW,SW,FP,FPP,WPP,FFP,FFPP)
      TIM1=TIM(E1,CW,SW,FP,FPP,WPP,FFP,FFPP)
      DABUC=WP*TIM0-FFP*TOM0
      DABUM=WP*TIM1-FFP*TOM1
      DBBUC=-FFP*FFP*RS
      FEB=2.
      IF(ITEST.EQ.0) FEB=4.
      IF(I.EQ.1.OR.I.EQ.K) FE9=1.
      UC=UC+FEB*DUC*DRS3
      AUC=AUC+FE9*DAUC*DRS3
      AUM=AUM+FE8*DAUN*DRS3
      AUD=AUD+FE9*DAUD*DRS3
      AAUC=AAUC+FE8*DAAUC*DRS3
      AAUM=AAUM+FE8*DAAUM*DRS3
      ABUC=ABUC+FE8*DABUC*DRS3
      ABUM=ABUM+FE8*DABUM*DRS3
      BBUC=BBUC+FEB*DBBUC*DRS3
      BUC=BBUC*QS
      RLS=RLS+DRS
10    CONTINUE
      RETURN
      END
      FUNCTION TOM(A,B,C,D,E,F)
      TOM=A*B*E-A*C*F*D
      RETURN
      END
      FUNCTION TIM(A,B,C,D,E,F,G,H)
      TIM=A*C*E*G+A*F*B*D*G+A*C*D*H
      RETURN
      END
      SUBROUTINE YAW(QS,ALPH,AXI,STA,FBIG,KK,YL,SKDEL,SJDEL,SKRDEL,
     $SJRDEL,ZMDD,ZCDD,ZKDD,CQ0,ZKDL,ZKDR,ZKDW,WT00,CPAA,CQL1,CQR1)
      DIMENSION RR(25), CI(25), THETI(25), AAT(25), CLT(25), CDT(25)      A  11
      DIMENSION STA(100),AXI(100),ALPH(100),FBIG(100)
      COMMON R,DR,HB,B,V,X,THETP,AMOD,H,SI,G0,OMEGA,RHO,VIS,HL,PI,RX,W,   A  12
     $NPROF,APP,T1,T2,T3,T4,T5,T6,T7,T8,TEST,XETA,MM,AL0,AC              A  13
      COMMON XCG,ESC,AE,AG
      COMMON RR,CI,THETI,NF
      EXTERNAL TOM,TIM
      IM=1
      ABR=.26179939
      MM=40
      KHALF=KK/2
      IF((KK-2*KHALF).EQ.0) IM=0
      GLUART=4.*(1.-2.*AC)
      IL=3
      F0=1.
      F0=1.
      ZI1=ZI2=ZI3=ZI4=ZI5=ZI6=ZI7=ZI8=ZI9=ZI10=ZI11=ZI12=0.
      ZI13=ZI14=ZI15=ZI16=ZI17=ZI18=ZI19=0.
      ZMDD=ZCDZ=ZCD1=ZCD2=ZKDZ=ZKD1=ZKD2=WT00=CPAA=CQ0=0.
      ZDL1=ZDL2=ZDL3=ZDR1=ZDR2=ZDR3=ZDW1=ZDW2=ZDW3=CQL1=CQR1=0.
      ZZD11=ZZD12=ZZD21=ZZD22=ZZD23=0.
      DO 10 I=1,KK
      L=I+1
      NHALF=I/2
      NTEST=I-2*NHALF
      RLR=STA(I)
      A=AXI(I)
      ALPHA=ALPH(I)
      FLOSS=FBIG(I)
      ALPHAD=ALPHA+0.001
      RL=RLR*RX*COS(SI)
      CALL SEARCH(RL,RR,CI,THETI,NF,C,THET,SMODE)
      IF(NPROF.EQ.9999) THEN
      CALL PROPER(XCG,ESC,RX,R,HB,C,AE,AG,AMASS,AI1,AI2,AI3,ER,E1,E2,
     $E3,FF,FFP,FFPP,FP,FPP,RL,EI,GJ)
      CALL NACAXX(RL,RX,SI,ALPHA,CL,CD,AL0,W)
      CALL NACAXX(RL,RX,SI,ALPHAD,CLD,CDD,AL0,W)
      ELSE
      CALL PROPER1(XCG,ESC,RX,R,HB,C,AE,AG,AMASS,AI1,AI2,AI3,ER,E1,E2,
     $E3,FF,FFP,FFPP,FP,FPP,RL,EI,GJ)
      CALL NACA44(RL,RX,SI,ALPHA,CL,CD,AL0,W)
      CALL NACA44(RL,RX,SI,ALPHAD,CLD,CDD,AL0,W)
      ENDIF
      CLA=(CLD-CL)/0.001
      CDA=(CDD-CD)/0.001
      RHR=HB/(RX*COS(SI))
```

```
      RS=1.-RHR
      WR=RS*FF*QS
      WP=FFP*QS
      CW=COS(WP)
      SW=SIN(WP)
      C2W=CW*CW-SW*SW
      BEETA=THET+THETP
      CB=COS(BEETA)
      SB=SIN(BEETA)
      CSI=COS(SI)
      SSI=SIN(SI)
      CR=C/RX
      OM=OMEGA
      IF(L.LE.KK) THEN
      DRR=STA(I)-STA(L)
      ELSE
      LL=I-1
      DRR=STA(LL)-STA(I)
      ENDIF
      CN=CL*COS(ALPHA)+CD*SIN(ALPHA)
      CQ=CL*SIN(ALPHA)-CD*COS(ALPHA)
      X=OM*RX/V
C*****
C
      IF (NPROF.EQ.9999) THEN
      CALL SUMSUM(TOM,TIM,RLR,ER,E1,E3,UC,AUC,BUC,AAUC,ABUC,BBUC,AUM,AAU
     1M,ABUM,AUD,MM,QS,RHR,EI,GJ,RX)
      ELSE
      CALL SUMSUM1(TOM,TIM,RLR,ER,E1,E3,UC,AUC,BUC,AAUC,ABUC,BBUC,AUM,AA
     1UM,ABUM,AUD,MM,QS,RHR,EI,GJ,RX)
      ENDIF
      UD=UM=UC
      UCPD=AUC
      UCFD=BUC
      UOFD=UMFD=BUC
      UMPD=AUM
      BUD=BUM=BUC
      AUCPD=AAUC
      AUMPD=AAUM
      BUCPD=AUCFD=ABUC
      BUMPD=AUMFD=ABUM
      BUCFD=BUMFD=BBUC
      BBUM=BBUC
      DIS=(RLR+UC)*CSI-WR*SSI
C*****SOME COFACTORS
      R=RX
      PART1=SSI*SW-CSI*CW*CB
      PART2=CSI*SB
      PART3=CSI*CW-SSI*SW*CB
      PART4=(RLR+UM)*CW+WR*SW
      PART5=(RLR+UM)*SW-WR*CW
      PART6=CSI*SW+SSI*CW*CB
      PART7=R/V*(YL*SB*CW+(RLR+UD)*SSI*SB*CW+WR*SW*SSI*SB+E3*PART3)
      PART8=R/V*(YL*CB+(RLR+UD)*SSI*CB+WR*CSI)
      PART9=R/V*(YL*PART6+(RLR+UD)*CB*CW+WR*SW*CB+E3*SW*SB)
      PART10=R/V*(YL*SSI*SB+(RLR+UD)*SB)
      PART11=WR*SB*CSI+ER*CSI*CB
      PART12=SSI*CW+CSI*SW*CB
      PART13=WR*SSI*SB+ER*CB*SSI
      TLF1=(YL*SB*SW+(RLR+UM)*SSI*SB*SW-WR*CW*SSI*SB-E1*PART6)*FFP
      TLF1=TLF1-SW*SSI*SB*FF-BUM*SSI*SB*SW
      PAL1=(RLR+UC)*CSI-WR*SSI*CB+ER*SSI*SB
      PAL2=YL+(RLR+UC)*SSI+WR*CSI*CB-ER*SB*CSI
C
      TAIL1=(RLR+UM)*CW*CSI*SB+WR*SW*CSI*SB+E1*PART12
      TAIL2=(RLR+UM)*CSI*SB-WR*SSI
      TAIL3=YL*SB*CW+(RLR+UM)*SSI*SB*CW+WR*SW*SSI*SB-E1*PART3
      TAIL33=(RLR+UM)*SSI*SB*CW+WR*SW*SSI*SB-E1*PART3
      TAIL4=YL*PART6+(RLR+UM)*CB*CW+WR*SW*CB-E1*SW*SB
      TAIL5=YL*CB+(RLR+UM)*SSI*CB+WR*CSI
      TAIL55=(RLR+UM)*SSI*CB+WR*CSI
      TAIL6=YL*SSI*SB+(RLR+UM)*SB
C
      WT=CSI*SB*(1.-A)+X*((RLR+UD)*CSI*CB-WR*SSI)
      WN=-PART1*(1.-A)-X*((RLR+UD)*CW*CSI*SB+WR*SW*CSI*SB-E3*PART12)
      WE2=WN*WN+WT*WT
      WTO=WE2*CQ*CR
      WNO=WE2*CN*CR
      APPI=(WNO*(E1*SSI+RLR*CSI*SB)+WTO*RLR*CSI*CB)*X*3./PI
      CNA=CLA*COS(ALPHA)+CDA*SIN(ALPHA)
      CTA=CLA*SIN(ALPHA)-CDA*COS(ALPHA)
      CNP=CNA-CQ
      CQP=CTA+CN
      F1=CR*(2.*CN*WN+CNP*WT)
      F2=CR*(2.*CN*WT-CNP*WN)
      G1=CR*(2.*CQ*WN+CQP*WT)
      G2=CR*(2.*CQ*WT-CQP*WN)
      F4=CR*WE2*CNA*FP
      G4=CR*WE2*CTA*FP
      HELP2=AUD*(-CW*CSI*SB*G1+CSI*CB*G2)
      WP2=X*E3*PART12*FP
      WF11=-PART12*(1.-A)*FFP
      WF12=X*(RLR+UD)*SW*CSI*SB*FFP-X*SW*CSI*SB*FF-X*WR*CW*CSI*SB*FFP
      WF13=-X*E3*PART1*FFP-X*BUD*CW*CSI*SB
      WF1=WF11+WF12+WF13
      WF2=-X*(SSI*FF-BUC*CSI*CB)
      WO1=((RLR+UD)*CW*CSI*SB+WR*SW*CSI*SB-E3*(SSI*SW+CSI*SW*CB))*R*FO/V
      WO2=(WR*SSI-(RLR+UD)*CSI*CB)*R*FO/V
      WD1=(YL*SB*CW+(RLR+UD)*SSI*SB*CW+WR*SW*SSI*SB+E3*PART3)*R/V
      WD2=R/V*(YL*CB+(RLR+UD)*SSI*CB+WR*CSI)
      WD3=R/V*(YL*(SSI*CB*CW+SW*CSI)+(RLR+UD)*CB*CW+WR*SW*CB+E3*SW*SB)
      WD4=R/V*(YL*SSI*SB+(RLR+UD)*SB)
      WND1=PART1*F1-PART2*F2
      WTD1=PART1*G1-PART2*G2
      WND2=PART6*F1+SSI*SB*F2
      WND3=CW*SB*F1-CB*F2
      WTD2=PART6*G1+SSI*SB*G2
      WTD3=CW*SB*G1-CB*G2
      WNDD2=WD3*F1+WD4*F2
      WNDD3=WD1*F1-WD2*F2
      WTDD2=WD3*G1+WD4*G2
      WTDD3=WD1*G1-WD2*G2
C*****FIND THE INTEGRAL COEFFICIENTS OF YAW AND YAW RATE
C
      SAM=(1.5/PI)
      DCTOA=4.*(1.-2.*A)
      DZI1=DCTOA*DIS*DIS*DIS*DRR*FLOSS*CSI
      IF(A.LT.AC) GO TO 901
      DZI1=(GLUART/DCTOA)*DZI1
901   ADZI2=(PART1*F1-PART2*F2)*(E1*PART3-PART4*SSI*SB)
      BDZI2=+(PART1*G1-PART2*G2)*(PART5*PART3-PART4*PART6)
      DZI2=SAM*(ADZI2+BDZI2)*DIS*DRR
      ADZI3=(PART1*F1-PART2*F2)*(-E1*SW*SB+PART4*CB)
      BDZI3=-(PART1*G1-PART2*G2)*(PART5*SW*SB+PART4*CW*SB)
      DZI3=SAM*(ADZI3+BDZI3)*DIS*DRR
```

```
      DZI4=SAM*(CH*SB*F1-CB*F2)*(E1*PART3-PART4*SSI*SB)*FD*DRR
      DZI5=SAM*(PART6*F1+SSI*SB*F2)*(E1*SH*SB-PART4*CB)*FD*DRR
      DZI6=+SAM*(CH*SB*G1-CB*G2)*(PART5*PART3-PART4*PART6)*FD*DRR
      DZI7=+SAM*(PART6*G1+SSI*SB*G2)*(PART4*CH*SB+PART5*SH*SB)*FD*DRR
      DZI8=SAM*(PART7*F1-PART8*F2)*(E1*PART3-PART4*SSI*SB)*FD*DRR
      DZI9=-SAM*(PART9*F1+PART10*F2)*(PART4*CB-E1*SH*SB)*FD*DRR
      DZI10=+SAM*(PART7*G1-PART8*G2)*(PART5*PART3-PART4*PART6)*FD*DRR
      DZI11=+SAM*(PART9*G1+PART10*G2)*(PART4*CH*SB+PART5*SH*SB)*FD*DRR
      DZI12=SAM*(CH*SB*F1-CB*F2)*(E1*SH*SB-PART4*CB)*FD*DRR
      DZI13=SAM*(PART6*F1+SSI*SB*F2)*(-E1*PART3+PART4*SSI*SB)*FD*DRR
      DZI14=+SAM*(CH*SB*G1-CB*G2)*(PART5*SH*SB+PART4*CH*SB)*FD*DRR
      DZI15=-SAM*(PART6*G1+SSI*SB*G2)*(PART5*PART3-PART4*PART6)*FD*DRR
      DZI16=SAM*(PART7*F1-PART8*F2)*(E1*SH*SB-PART4*CB)*FD*DRR
      DZI17=-SAM*(PART9*F1+PART10*F2)*(E1*PART3-PART4*SSI*SB)*FD*DRR
      DZI18=+SAM*(PART7*G1-PART8*G2)*(PART5*SH*SB+PART4*CH*SB)*FD*DRR
      DZI19=-SAM*(PART9*G1+PART10*G2)*(PART5*PART3-PART6*PART4)*FD*DRR
C*****MASS MATRIX
      QVEL=0.5*RHO*V*V
      DYNA=(3./QVEL)
      DD1=2.*YL*YL+4.*YL*WR*CSI*CB+4.*YL*(RLR+UC)*SSI-4.*YL*ER*CSI*SB
      DD2=WR*WR*(1.+(CSI*CB)**2.)+ER*ER*(1.+(SB*CSI)**2.)
      DD3=(RLR+UC)**2.*(1.+SSI*SSI)-2.*ER*WR*SB*CB*(1.-SSI*SSI)
      DD4=2.*(RLR+UC)*WR*SSI*CSI*CB-2.*(RLR+UC)*ER*SSI*CSI*SB
      DD5=(CSI*CH)**2.+(SSI*SH*CB)**2.+(SH*SB)**2.-2.*SSI*CSI*SH*CH*CB
      DD6=((SSI*SB)**2.+CB*CB)*AI2
      DD7=(CSI*SH)**2.+(SSI*CH*CB)**2.+(CH*SB)**2.+2.*SH*CH*SSI*CSI*CB
      DZMDD=DYNA*(AMASS*(DD1+DD2+DD3+DD4)+AI1*DD5+DD6+AI3*DD7)*FD*FD*DRR
C
C*****DAMPING COEFFICIENTS MATRIX
C
      COD1=((WD1*F1-WD2*F2)*TAIL3+(WD3*F1+WD4*F2)*TAIL4)*FD*FD
      COD2=(+(WD1*G1-WD2*G2)*TAIL5-(WD3*G1+WD4*G2)*TAIL6)*FD*FD
      DZCDZ=1.5*(COD1+COD2)*DRR
      DZCD1=(PART1*F1-PART2*F2)*TAIL3+(PART1*G1-PART2*G2)*TAIL5
      DZCD1=1.5*DZCD1*DIS*FD*DRR
      DZCD2=(PART1*F1-PART2*F2)*TAIL4-(PART1*G1-PART2*G2)*TAIL6
      DZCD2=1.5*DZCD2*DIS*FD*DRR
C
C*****STIFFNESS COEFFICIENTS MATRIX
C
      ZDD1=((CH*SB*F1-CB*F2)*TAIL3+(PART6*F1+SSI*SB*F2)*TAIL4)*FD*FD
      ZDD2=(+(CH*SB*G1-CB*G2)*TAIL5-(PART6*G1+SSI*SB*G2)*TAIL6)*FD*FD
      DZKDZ=1.5*(ZDD1+ZDD2)*DRR
      DZKD1=(PART1*F1-PART2*F2)*TAIL3+(PART1*G1-PART2*G2)*TAIL5
      DZKD1=1.5*DZKD1*DIS*FD*DRR
      DZKD2=(PART1*F1-PART2*F2)*TAIL4-(PART1*G1-PART2*G2)*TAIL6
      DZKD2=1.5*DZKD2*DIS*FD*DRR
      ZDD11=1.5*(CH*SB*F1-CB*F2)*TAIL3*FD*FD*DRR
      ZDD12=1.5*(PART6*F1+SSI*SB*F2)*TAIL4*FD*FD*DRR
      ZDD21=1.5*CH*SB*G1*TAIL5*FD*FD*DRR
      ZDD22=-1.5*CB*G2*TAIL5*FD*FD*DRR
      ZDD23=-1.5*(PART6*G1+SSI*SB*G2)*TAIL6*FD*FD*DRR
C******* STIFFNESS IN YAW
      DZDDL1=((CH*SB*F1-CB*F2)*SB*CH+(CH*SB*G1-CB*G2)*CB)*FD*FD
      DZDDL2=(PART6*F1+SSI*SB*F2)*(SSI*CB*CH+SH*CSI)*FD*FD
      DZDDL3=-(PART6*G1+SSI*SB*G2)*SSI*SB*FD*FD
      DZDDL4=((PART1*F1-PART2*F2)*SB*CH+(PART1*G1-PART2*G2)*CB)*DIS*FD
      DZDDL5=-(PART1*F1-PART2*F2)*(SSI*CB*CH+SH*CSI)*DIS*FD
      DZDDL6=(PART1*G1-PART2*G2)*SSI*SB*DIS*FD
      DZDL1=1.5*(DZDDL1+DZDDL2+DZDDL3)*DRR
      DZDL2=1.5*DZDDL4*DRR
      DZDL3=1.5*(DZDDL5+DZDDL6)*DRR
      DZDDW1=((CH*SB*F1-CB*F2)*WR*SH*SSI*SB+(CH*SB*G1-CB*G2)*WR*CSI)
      DZDDW1=DZDDW1*FD*FD
      DZDDW2=(PART6*F1+SSI*SB*F2)*WR*SH*CB*FD*FD
      DZDDW3=(PART1*F1-PART2*F2)*WR*SH*SSI*SB*DIS*FD
      DZDDW4=(PART1*G1-PART2*G2)*WR*CSI*DIS*FD
      DZDDW5=-(PART1*F1-PART2*F2)*WR*SH*CB*DIS*FD
      DZDW1=1.5*(DZDDW1+DZDDW2)*DRR
      DZDW2=1.5*(DZDDW3+DZDDW4)*DRR
      DZDW3=1.5*(DZDDW5)*DRR
      DZDDR1=(CH*SB*F1-CB*F2)*((RLR+UM)*SSI*SB*CH+E1*(SSI*SH*CB-CSI*CH))
      DZDDR1=DZDDR1*FD*FD
      DZDDR2=(PART6*F1+SSI*SB*F2)*((RLR+UM)*CB*CH-E1*SH*SB)*FD*FD
      DZDDR3=(CH*SB*G1-CB*G2)*((RLR+UM)*SSI*CB)*FD*FD
      DZDDR4=-(PART6*G1+SSI*SB*G2)*((RLR+UM)*SB)*FD*FD
      DZDDR5=(RLR+UM)*SSI*SB*CH+E1*(SSI*SH*CB-CSI*CH)
      DZDDR5=DZDDR5*(PART1*F1-PART2*F2)*FD*DIS
      DZDDR6=(PART1*G1-PART2*G2)*((RLR+UM)*SSI*CB*DIS)*FD
      DZDDR7=-(PART1*F1-PART2*F2)*((RLR+UM)*CB*CH-E1*SH*SB)*DIS*FD
      DZDDR8=(PART1*G1-PART2*G2)*(RLR+UM)*SB*DIS*FD
      DZDR1=1.5*(DZDDR1+DZDDR2+DZDDR3+DZDDR4)*DRR
      DZDR2=1.5*(DZDDR5+DZDDR6)*DRR
      DZDR3=1.5*(DZDDR7+DZDDR8)*DRR
**********
********  EFFECT OF TOWER SHADOW
**********
      DCQ0=-(WN0*TAIL3+WT0*TAIL5)*FD*DRR
      DCQL1=-(WN0*SB*CH+WT0*CB)*FD*DRR
      DCQR1=-(WN0*TAIL33+WT0*TAIL55)*FD*DRR
      IF(IM.EQ.1) THEN
      FEB=9./8.
      IF(I.EQ.1.OR.I.EQ.4) FEB=3./8.
      IF(I.GE.4) IM=0
      ELSE

      FEB=2./3.
      IF(NTEST.EQ.0) FEB=4./3.
      IF(I.EQ.1.OR.I.EQ.KK) FEB=1./3.
      ENDIF
C*****START THE SIMPSON INTEGRATION
      ZI1=ZI1+FEB*DZI1
      ZI2=ZI2+FEB*(DZI2)
      ZI3=ZI3+FEB*(DZI3)
      ZI4=ZI4+FEB*(DZI4)
      ZI5=ZI5+FEB*(DZI5)
      ZI6=ZI6+FEB*(DZI6)
      ZI7=ZI7+FEB*(DZI7)
      ZI8=ZI8+FEB*(DZI8)
      ZI9=ZI9+FEB*(DZI9)
      ZI10=ZI10+FEB*(DZI10)
      ZI11=ZI11+FEB*(DZI11)
      ZI12=ZI12+FEB*(DZI12)
      ZI13=ZI13+FEB*(DZI13)
      ZI14=ZI14+FEB*(DZI14)
      ZI15=ZI15+FEB*(DZI15)
      ZI16=ZI16+FEB*(DZI16)
      ZI17=ZI17+FEB*(DZI17)
      ZI18=ZI18+FEB*(DZI18)
      ZI19=ZI19+FEB*(DZI19)
      ZMDD=ZMDD+FEB*(DZMDD)
      ZCDZ=ZCDZ+FEB*(DZCDZ)
      ZCD1=ZCD1+FEB*(DZCD1)
      ZCD2=ZCD2+FEB*(DZCD2)
      ZKD1=ZKD1+FEB*(DZKD1)
      ZKD2=ZKD2+FEB*(DZKD2)
```

```
      ZKDZ=ZKDZ+FEB*DZKDZ
      CQ0=CQ0+FEB*DCQ0
      ZDL1=ZDL1+FEB*DZDL1
      ZDL2=ZDL2+FEB*DZDL2
      ZDL3=ZDL3+FEB*DZDL3
      ZDW1=ZDW1+FEB*DZDW1
      ZDW2=ZDW2+FEB*DZDW2
      ZDW3=ZDW3+FEB*DZDW3
      ZDR1=ZDR1+FEB*DZDR1
      ZDR2=ZDR2+FEB*DZDR2
      ZDR3=ZDR3+FEB*DZDR3
      CPAA=CPAA+FEB*APPI*DRR
      WT00=WT00+FEB*WTO*DRR
      ZZD11=ZZD11+FEB*ZD011
      ZZD12=ZZD12+FEB*ZD012
      ZZD21=ZZD21+FEB*ZD021
      ZZD22=ZZD22+FEB*ZD022
      ZZD23=ZZD23+FEB*ZD023
      CQL1=CQL1+FEB*DCQL1
      CQR1=CQR1+FEB*DCQR1
      R=RX*COS(SI)
      IF(I.EQ.IL) THEN
      IL=I+2
      ELSE
      ENDIF
10    CONTINUE
C
C******CALCULATE THE YAW AND YAW RATE VARIATION
C
      IF(RLR.EQ.1.) THEN
      SKDEL=SJDEL=SKRDEL=SJRDEL=0.
      ELSE
73    DENO=(ZI1-ZI3)**2+ZI2*ZI2
      SKDEL=((ZI4+ZI5+ZI6+ZI7)*(ZI1-ZI3)-ZI2*(ZI12+ZI13+ZI14+ZI15))/DENO
      SJDEL=((ZI4+ZI5+ZI6+ZI7)*ZI2+(ZI1-ZI3)*(ZI12+ZI13+ZI14+ZI15))/DENO
      SJDEL=-SJDEL
      SKRDEL=(ZI8+ZI9+ZI10+ZI11)*(ZI1-ZI3)
      SKRDEL=(SKRDEL-ZI2*(ZI16+ZI17+ZI18+ZI19))/DENO
      SJRDEL=(ZI8+ZI9+ZI10+ZI11)*ZI2
      SJRDEL=-(SJRDEL+(ZI1-ZI3)*(ZI16+ZI17+ZI18+ZI19))/DENO
      ENDIF
      ZCDD=ZCDZ+SJRDEL*ZCD1-SKRDEL*ZCD2
      ZKDD=ZKDZ+SJDEL*ZKD1-SKDEL*ZKD2
      ZKDL=ZDL1+SJDEL*ZDL2+SKDEL*ZDL3
      ZKDR=ZDR1+SJDEL*ZDR2+SKDEL*ZDR3
      ZKDW=ZDW1+SJDEL*ZDW2+SKDEL*ZDW3
      R=RX*COS(SI)
      RETURN
      END
```

PROP's Output

1
THEORETICAL PERFORMANCE OF A PROPELLER TYPE WIND TURBINE

OPERATING CONDITIONS:

WIND VELOCITY - FPS = 32.3114

WIND VELOCITY GRADIENT EXPONENT = .0000

HUB HEIGHT ABOVE GROUND LEVEL - FT- = 50.0000

ALTITUDE OF HUB ABOVE SEA LEVEL - FT = 100.0000

ANGULAR VELOCITY - RAD/SEC = 7.7597

TIP SPEED RATIO = 4.0000

PITCH ANGLE FROM NOMINAL TWIST - DEGREES = 6.0000

PITCH ANGLE AT 0.75 RADIUS - DEGREES = 6.0000

CONING ANGLE - DEGREES = 3.5000

BLADE DESIGN:

NUMBER OF BLADES = 3.

TIP RADIUS - FT = 16.6560

HUB RADIUS - FT = 1.6250

SOLIDTY = .08600

ACTIVITY FACTOR = .00000

NACA PROFILE = 9999

NUMBER OF STATIONS ALONG SPAN = 1

CHORD AND TWIST DISTRIBUTION

PERCENT RADIUS	CHORD-FT	TWIST-DEG
100.0	1.50000	.00000

PROGRAM OPERATING CONDITIONS:

INCREMENTAL PERCENTAGE = .0200

ANGULAR INTERFERENCE FACTOR, AP = 0.0

STANDARD AXIAL INTERFERENCE METHOD USED

TIP LOSSES MODELED BY PRANDTLS FORMULA

NO HUBLOSS MODEL USED

ANGULAR INTERFERENCE FACTOR, AP = 0.0

STANDARD AXIAL INTERFERENCE METHOD USED

TIP LOSSES MODELED BY PRANDTLS FORMULA

NO HUBLOSS MODEL USED

1

PERFORMANCE ANALYSIS:

PCCR	A	AP	CL	CD	PHI	ALPHA	F	RE NO	CT	CP
.980	.3548	.0000	.51	.015	9.347	3.279	.3784	.123E+07	.0096	.443165E-02
.960	.2970	.0000	.62	.016	10.375	4.304	.5000	.120E+07	.0246	.130155E-01
.940	.2638	.0000	.69	.016	11.077	5.004	.5840	.118E+07	.0412	.234352E-01
.920	.2419	.0000	.74	.017	11.641	5.565	.6486	.116E+07	.0585	.348648E-01
.900	.2260	.0000	.78	.017	12.133	6.054	.7008	.114E+07	.0762	.468801E-01
.880	.2139	.0000	.81	.018	12.588	6.506	.7439	.111E+07	.0938	.592242E-01
.860	.2043	.0000	.84	.018	13.024	6.937	.7800	.109E+07	.1114	.717261E-01
.840	.1964	.0000	.86	.019	13.450	7.360	.8106	.107E+07	.1287	.842640E-01
.820	.1897	.0000	.89	.019	13.876	7.782	.8367	.104E+07	.1458	.967476E-01
.800	.1840	.0000	.91	.020	14.306	8.208	.8591	.102E+07	.1625	.109107
.780	.1799	.0000	.93	.020	14.745	8.642	.8783	.995E+06	.1789	.121287
.760	.1742	.0000	.95	.021	15.197	9.099	.8949	.972E+06	.1948	.133243
.740	.1700	.0000	.97	.022	15.664	9.551	.9092	.948E+06	.2102	.144938
.720	.1660	.0000	.99	.023	16.150	10.031	.9215	.925E+06	.2252	.156340
.700	.1622	.0000	1.01	.029	16.658	10.533	.9322	.901E+06	.2397	.167319
.680	.1585	.0000	1.03	.035	17.190	11.058	.9414	.878E+06	.2537	.177795
.660	.1550	.0000	1.05	.041	17.749	11.610	.9494	.855E+06	.2672	.187742
.640	.1515	.0000	1.06	.047	18.338	12.191	.9563	.832E+06	.2802	.197197
.620	.1480	.0000	1.08	.054	18.961	12.806	.9623	.809E+06	.2927	.206157
.600	.1444	.0000	1.09	.062	19.621	13.457	.9675	.786E+06	.3046	.214628
.580	.1408	.0000	1.11	.074	20.321	14.148	.9721	.763E+06	.3160	.222603
.560	.1371	.0000	1.12	.106	21.068	14.884	.9760	.740E+06	.3269	.229775
.540	.1332	.0000	1.13	.140	21.865	15.670	.9794	.718E+06	.3374	.236044
.520	.1290	.0000	1.14	.176	22.721	16.513	.9823	.696E+06	.3473	.241475
.500	.1245	.0000	1.15	.215	23.641	17.420	.9849	.673E+06	.3568	.246126
.480	.1181	.0000	1.13	.259	24.670	18.434	.9870	.652E+06	.3658	.250027
.460	.1041	.0000	1.05	.313	25.960	19.708	.9886	.631E+06	.3741	.252987
.440	.0911	.0000	.96	.395	27.314	21.044	.9901	.611E+06	.3814	.254391
.420	.0902	.0000	.99	.428	28.438	22.149	.9918	.589E+06	.3882	.255434
.400	.0891	.0000	1.02	.463	29.652	23.341	.9933	.568E+06	.3948	.256416
.380	.0880	.0000	1.05	.502	30.964	24.630	.9945	.547E+06	.4011	.257335
.360	.0866	.0000	1.08	.546	32.386	26.026	.9956	.526E+06	.4072	.258192
.340	.0851	.0000	1.10	.594	33.929	27.541	.9965	.506E+06	.4131	.258988
.320	.0834	.0000	1.13	.648	35.607	29.188	.9973	.486E+06	.4187	.259724
.300	.0814	.0000	1.15	.707	37.434	30.980	.9980	.466E+06	.4241	.260400
.280	.0792	.0000	1.17	.772	39.425	32.935	.9985	.447E+06	.4292	.261019
.260	.0767	.0000	1.19	.844	41.598	35.067	.9990	.429E+06	.4341	.261583
.240	.0739	.0000	1.19	.923	43.970	37.395	.9993	.411E+06	.4388	.262092
.220	.0708	.0000	1.20	1.008	46.559	39.936	.9996	.395E+06	.4432	.262550
.200	.0673	.0000	1.19	1.101	49.381	42.707	.9998	.379E+06	.4475	.262958
.180	.0634	.0000	1.17	1.200	52.450	45.722	.9999	.364E+06	.4515	.263320
.160	.0591	.0000	1.14	1.304	55.776	48.992	1.0000	.351E+06	.4554	.263636
.140	.0544	.0000	1.09	1.411	59.364	52.523	1.0000	.339E+06	.4592	.263911
.120	.0494	.0000	1.03	1.520	63.210	56.312	1.0000	.328E+06	.4628	.264146
.100	.0439	.0000	.94	1.626	67.298	60.346	1.0000	.320E+06	.4662	.264342
.098	.0432	.0000	.93	1.639	67.811	60.853	1.0000	.319E+06	.4666	.264364

PERFORMANCE SUMMARY: TIP SPEED RATIO = 4.000

TOTAL POWER COEFFICIENT = .26436

INITIAL NORMALIZED STATIC TIP DEFLECTION IS -.290825E-03

AVERAGE POWER COEFFICIENT WITH GRADIENT = .26436

TOTAL THRUST COEFFICIENT = .4666

TORQUE VARIATION DUE TO AERODYNAMIC SECOND DERIVATIVE = .0290

TORQUE VARIATION DUE TO SHEAR SECOND DERIVATIVE = .0287

TANGENTIAL FORCE PER BLADE IN ROTOR PLANE 34.5114

QS = -.327011E-03 PREVIOUS QS = -.325095E-03 NO OF ITERATION IS 3

ZMDD	ZCDD	ZKDD	CQO
.378797	.194085	.245376E-01	-.102976E-01

SKDEL	SJDEL	SKRDEL	SJRDEL
-.219537E-01	-.995018E-01	-.135379	-.101738E-01

CPAA = .260650

```
      PROGRAM AERO (INPUT,OUTPUT,TAPE1)
      COMMON L,,,NS
      COMMON /STIFF/ AII,EI0,AGJ,GJ0,RHR,OS
      EXTERNAL TOM,TIM
C     ****************************************************************
C
C     THIS PROGRAM CALCULATES THE POWER COEFFICIENT AND WINDWISE
C     FORCE COEFFICIENT FOR A HORIZONTAL AXIS WIND TURBINE
C     AND GENERATES THE COEFFICIENTS OF EQUATION OF MOTION
C     OF THE TURBINE SYSTEM
C
C
C
C
C
C
C     OREGON STATE UNIVERSITY
C     MARCH 1983
C
C
C     FILE ASSIGNMENTS
C
C        INPUT          FOR INPUT OF INDEPENDENT VARIABLES
C        OUTPUT         FOR PROGRAM MESSAGES TO THE USER
C        TAPE 1         FOR A LISTING OF THE PROGRAM OUTPUT
C
C
C     VARIABLES INPUT FROM TELETYPE
C
C     B       NUMBER OF BLADES
C     BCRR    DIMENSIONLESS CHORD TO RADIUS RATIO AT BLADE ROOT
C     EM      SLOPE OF LIFT COEFFICIENT CURVE
C     DRR       INCREMENTAL INTEGRATION STEP ALONG THE BLADE
C     CD0     MINIMUM DRAG COEFFICIENT
C     CLM     MAXIMUM LIFT COEFFICIENT
C     PTCH    PITCH ANGLE-IN DEGREES
C     BRT      TWIST ANGLE AT BLADE ROOT-IN DEGREES
C     DBTA     INCREMENAL TWIST ANGLE CHANGE -IN DEGREES
C     AL0      ANGLE OF ATTACK FOR ZERO LIFT
C     AST      STALL ANGLE OF ATTACK
C     SI       CONING ANGLE
C     RT       RADIAL POSITION AT WHICH TWIST ANGLE CHANGES
C     DCND     INCREMENTAL CHORD CHANGE RATIO
C     RC       RADIAL POSITION AT WHICH BLADE CHORD CHANGES
C     RH       HUB RADIAL POSITION
C     ABR      LIFT BREAK ANGLE OF ATTACK
C
C
C      OTHER VARIABLE ASSIGNMENTS
C
C      A        AXIAL INDUCTION FACTOR
C      CP       POWER COEFFICIENT
C      CT       WINDWISE FORCE COEFFICIENT
C      XL       LOCAL TIP SPEED RATIO
C      BETA     LOCAL TWIST ANGLE.
C      CL       LOCAL LIFT COEFFICIENT
C      CD       LOCAL DRAG COEFFICIENT
C      BCR      LOCAL DIMENSIONLESS CHORD TO RADIUS RATIO
C      PHI      LOCAL ANGLE OF RELATIVE VELOCITY WITH ROTOR PLANE
C      ALPHA    LOCAL ANGLE OF ATTACK
C
C
C      ****************************************************************
       PI=3.1415926356
```

```
C     ****************************************************************
C
C     INDEPENDENT VARIABLE INPUT SECTION
C
C     ****************************************************************
      TIMIN=SECOND()
      PRINT1
      PRINT2
      READ*,B,BCRR,EM,DRR,XMIN,XMAX,DDX
      PRINT 3
      READ*,CD0,CLM,CLFL,ABR
      PRINT 65
      READ*,AL0,AST,SI,PTCH,BRT,DBTA
      PRINT 66
      READ*,RT,DCND,RC,RH
      PRINT 67
67    FORMAT(' INPUT SHEAR CENTER POSITION ES/C, XCG: CENTER OF MASS')
      READ*,ESC,XCG
      PRINT 50
50    FORMAT('  INPUT E AND G ')
      READ*,AE,AG
      PRINT 51
51    FORMAT (' INPUT OMEGA,RHO,YL,R,M' )
      READ*,OM,RHO,YL,R,MM
      PRINT 68
      READ5,SUPP
  68  FORMAT('SUPPRESS INTERMED. OUTPUT? (Y)')
C     ****************************************************************
C
C     HEADINGS AND CALCULATION OF CONSTANTS
C
C     ****************************************************************
      WRITE(1,60)
      WRITE(1,19) B,BCRR,DCND,RT,RC,RH,BRT,DBTA
      WRITE(1,8)CLM,CLFL,EM,AST,ABR,AL0,CD0
      WRITE(1,9) XMIN,XMAX,DRR,SI
      CONVT=PI/180.
      AC=.38
      FAT=1.
      YL=YL/R
      SI=SI*CONVT
      CSI=COS(SI)
      SSI=SIN(SI)
      DBTA=DBTA*CONVT
      ABR=ABR*CONVT
      AL0=AL0*CONVT
      AST=AST*CONVT
      AMAX=PI/2.
      ZLDT=1.
      CD1=CLFL/ZLDT
      CD2=(CLFL/ZLDT)*(1.+SIN(AST))/(.5*SIN(2.*AST))
      ROSE=ATAN((.41/CLFL)**.57)
      EM1=CLFL/(SIN(AMAX-AST))
 200  WRITE(1,21)PTCH
      X=XMIN
      ANG=BRT*CONVT
      RTR=RT/R
      RCR=RC/R
      RHR=RH/R

  27  CONTINUE
      KK=0
      V=OM*R/X
```

```
      KL=1
      IM=1
      OS=.023
      DX=DFR*X
      DP=DFF*F
      TNUM=(R-RH)/DR
      NUM=TNUM
      N=NUM
      IF(NUM.NE.TNUM) N=NUM+1
      XL=X
C
C*******INITIALIZED
C
      ZI1=ZI2=ZI3=ZI4=ZI5=ZI6=ZI7=ZI8=ZI9=ZI10=ZI11=ZI12=ZI13=ZI14=0.
      ZI15=ZI16=ZI17=ZI18=ZI19=0.
      ZMPP=ZMPF=ZMPO=ZMFF=ZMFO=ZMOO=ZMDO=ZCPP=ZCPF=ZCPO=ZCFP=ZCFF=0.
      ZCFO=ZCOP=ZCOF=ZCOO=ZCDZ=ZCD1=ZCD2=ZKPP=ZKPF=ZKPO=ZKFP=ZKFF=0.
      ZKFO=ZKOP=ZKOF=ZKOO=ZKDZ=ZKD1=ZKD2=ZHP=ZHF=ZHO=0.
      COO=SMDP=SMDF=SMDO=SMOD=SCDP=SCDF=SCDO=SCD1=SCDJ=SCDK=0.
      SKDP=SKDF=SKDO=SKD1=SKDJ=SKDK=0.
      SCPD1=SCPD2=SCFD1=SCFD2=SCOD1=SCOD2=0.
      SKPD1=SKPD2=SKFD1=SKFD2=SKOD1=SKOD2=0.
      S1=S2=S3=SS1=SS2=SS3=0.
      GHCOS=GHSIN=GPCOS=GPSIN=GFCOS=GFSIN=GOCOS=GOSIN=0.
      G=32.2
      GR=G/C
      ZDL1=ZDL2=ZDL3=ZDR1=ZDR2=ZDR3=ZDM1=ZDM2=ZDM3=0.
      CT=0.
      CP=0.
      AT=AP=ATB=0.
      APQ=-X**3.*COC*(BCRR-B*DCND)
      ZF=0.7
      Z9=COS(PI/2.*ZF)
      RE=SQRT((X*B**.6666)/(X*B**.6666+1.32))
      IF(X.LT.3.) RE=SQRT(B**.6666/(B**.6666+.44))
      GLUART=4.*(1.-2.*AC)
      KL=1
      NN=N+1
      JU=1
      I=1
C
C******* CHECK TO SEE IF NUMBER OF INTERVAL IS EVEN
C******* EVEN---1/3 RULE   ODD---3/8 RULE ON THE FIRST
C******* THREE INTERVALS
C
      KHALF=N/2
      IF((N-2*KHALF).EQ.0) IM=0
      IF(KL.EQ.1) GO TO 555
553   IF(SUPP.EQ.1HY) GO TO 555
      WRITE(1,15)
555   IF(KL.EQ.1) THEN
      NHALF=JU/2
      NTEST=JU-2*NHALF
      ELSE
      NHALF=I/2
      NTEST=I-2*NHALF
      ENDIF
      RLR=XL/X
      RLR2=RLR*RLR
      RLR3=RLR2*RLR
      RLR4=RLR3*RLR
C     ***************************************************************
C
C     CALCULATION OF LOCAL TWIST ANGLE AND
C     LOCAL CHORD TO RADIUS RATIO
C
C     ***************************************************************
      PCR=XL/X
      EA=(1.-PCR)/(1.-RA)
      EFSML=Z9**EA
      FBIG=2./PI*ACOS(EFSML)
      Z1=(1.-PCR)*10.
      Z1=(2.**Z1)-1.
      BCR=BCRF
      IF(RLR.GE.RCR) BCR=BCRR-B*DCND*(RLR-RCR)/(1.-RCR)
      IF(FBIG.NE.0.) BCRF=BCR/FBIG
      CR=BCR/B
      EP=(ESC-XCG)*CR
      E1=(ESC-.25)*CR
      E2=(0.75-ESC)*CR
      E3=(0.5-ESC)*CR
      CV=CR*R/V
      BETA=ANG
      IF(RLR.GE.RTR) BETA=ANG-DATA*(RLR-RTR)/(1.-RTR)
      BETA=BETA+PTCH*CONVT
      IF(FBIG.NE.0.) EM2=EM1*BCRF*X*CSI/(2.*PI)
      STEL=BCR/B*(XL/X)
      AM=ASIN(CLM/(2.*PI*EM))-AL0
C     ***************************************************************
C
C     CALCULATION OF AXIAL INDUCTION FACTOR
C
C     ***************************************************************
      IF(RLR.EQ.1.) THEN
      CL=ALPHA=0.
      PHI=BETA
      A=1.
      ELSE
      G=4.*(1.-2.*AC)
      H=4.*AC*(1.-AC)-G*AC
      AB=BCRF*X*EM*CSI*(COS(BETA-AL0)-XL*SIN(BETA-AL0))-H
      A=AB/(BCRF*X*EM*CSI*COS(BETA-AL0)+G)
      PHI=ATAN((1.-A)/XL)
      ALPHA=PHI-BETA
      IF(A.GT.AC) GO TO 30
      B1=4.+BCRF*EM*X*CSI*COS(BETA-AL0)
      C1=BCRF*EM*X*CSI*(COS(BETA-AL0)-XL*SIN(BETA-AL0))
      A=(B1-SQRT(B1**2-16.*C1))/8.
      PHI=ATAN((1.-A)/XL)
      ALPHA=PHI-BETA
30    CL=2.*PI*EM*SIN(ALPHA+AL0)
      IF(ABS(CL).LT.CLM) GO TO 509
      CL=(ABS(ALPHA)/ALPHA)*CLM
      IF(ABS(ALPHA).GT.ABR) CL=(ALPHA/ABS(ALPHA))*CLFL
      EN=BCRF*X*CL*CSI/(2.*PI)
      B2=(G*H+EN**2)/(G**2-EN**2)
      C2=(EN**2*(1.+XL**2)-H**2)/(G**2-EN**2)
      BOOM=B2**2+C2
       IF(BOOM.LT..0) A=0.
       IF(BOOM.LT..0) GO TO 32
      A=-B2+SQRT(B2**2+C2)
32    CONTINUE
      PHI=ATAN((1.-A)/XL)
      ALPHA=PHI-BETA
      IF(ABS(ALPHA).LE.ABR) CL=(ABS(ALPHA)/ALPHA)*CLM
      IF(ABS(ALPHA).GT.ABR) CL=(ALPHA/ABS(ALPHA))*CLFL
```

```
      IF(A.GT.AC) GO TO 35
      DO 31 K=1,5
      B3=BCPF*XL*X*CL*CSI*SQRT(1.+((1.-A)/XL)**2)/(2.*PI)
      A=(1.-SQRT(1.-B3))/2.
      PHI=ATAN((1.-A)/XL)
      ALPHA=PHI-BETA
      IF(ABS(ALPHA).GT.ABR) CL=(ALPHA/ABS(ALPHA))*CLFL
      IF(ABS(ALPHA).LE.ABR) CL=(ALPHA/ABS(ALPHA))*CLM
 31   CONTINUE
 35   CONTINUE
      IF(ALPHA.LT.AST) GO TO 500
      ETA=BETA+AMAX
      CETA=COS(ETA)
      SETA=SIN(ETA)
      EMA=BCRF*X/(2.*PI*SIN(AMAX-AST))
      A=(EMA*(XL*SETA-CETA)-H)/(G-EMA*CETA)
      PHI=ATAN((1.-A)/XL)
      ALPHA=PHI-BETA
      CL=EM1*SIN(AMAX-ALPHA)
      IF(A.GT.AC.AND.CL.LT.CLFL) GO TO 500
      B4=4.-EM2*COS(ETA)
      C4=EM2*(XL*SIN(ETA)-COS(ETA))
      A=(B4-SQRT(B4**2-16.*C4))/8.
      PHI=ATAN((1.-A)/XL)
      ALPHA=PHI-BETA
      CL=EM1*SIN(AMAX-ALPHA)
 500  ALPHA=PHI-BETA
      ENDIF
C     ****************************************************************
C
C     CALCULATION OF DRAG COEFFICIENT
C
C     ****************************************************************
      ABSAL=ABS(ALPHA)
      SA=SIN(ABSAL)
      COA=COS(ABSAL)
      SA2=SA*SA
      BOB=.20944
      BOB2=ABR
      IF(ABSAL.LT.BOB) CD=CD0*(1.+53.91*(ABSAL**2.))
      IF(ABSAL.LT.BOB) CDA=107.62*CD0*ABSAL
      IF(ABSAL.GE.BOB) CD=3.36*CD0-TAN(BOB)+TAN(ABSAL)
      IF(ABSAL.GE.BOB) COA=1.+(TAN(ABSAL))**2.
      IF(ABSAL.GT.BOB2) CD=2.439*CLFL*(TAN(ABSAL)**2.15)
      IF(ABSAL.GT.BOB2) THEN
      CDA=5.24385*CLFL*(TAN(ABSAL))**1.15*(1.+(TAN(ABSAL))**2)
      ELSE
      ENDIF
      IF(ABSAL.GE.ROSE)COA=CD1*(1.+(TAN(ABSAL))**2)
      IF(ABSAL.GE.ROSE) CD=CD1*TAN(ABSAL)
      IF(ABSAL.GE.AST) CD=CD2*SA2/(1.+SA)
      IF(ABSAL.GE.AST) CDA=CD2*(2*SA*COA+SA*SA*COA)/(1.+SA)**2
      CSP=COS(PHI)
      SNP=SIN(PHI)
      CAS=COS(ALPHA)
      SAS=SIN(ALPHA)
      CN=CL*CAS+CD*SAS
      CO=CL*SAS-CD*CAS
      CLA=2.*PI*EM
      IF(ABSAL.GT.AM) CLA=0.
      IF(ABSAL.GT.AST) CLA=-EM1*COS(AMAX-ABSAL)
      COP=CLA*SAS-CDA*CAS+CN
      CNP=CLA*CAS+CDA*SAS-CO
```

```
      CNA=CLA*CAS+CDA*SAS
      CTA=CLA*SAS-CDA*CAS
      DPHI=PHI/CONVT
      DAL=ALPHA/CONVT
      DBET=BETA/CONVT
      IF(KL.EQ.1) GO TO 20

      IF(RLR.EQ.1.) THEN
      AP=0.
      AT=0.
      ELSE
      AP=((1.-A)*CL-XL*CD)*XL**2.*SQRT(1.+((1.-A)/XL)**2.)*BCR
      AT=((1.-A)*CD+XL*CL)*XL*SQRT(1.+((1.-A)/XL)**2.)*BCR
      ENDIF
      CPB=CSI**3.*(AP+APB)*DX/(2.*PI*X)
      CTB=CSI**3.*(AT+ATB)*DX/(2.*PI*X)
      CT=CT+CTB
      CP=CP+CPB
      ATB=AT
      APB=AP
C
C*******PROPERTIES OF THE BLADE
C
20    AFACTO=0.04752/144.
      IF(RLR.LE.1..AND.RLR.GT.0.6545) THEN
      BI2=5.673*EXP(-3.313*RLR)
      BI3=67.3636*EXP(-2.0236*RLR)
      AMASS=15.*AFACTO*EXP(-1.3266*RLR)
      ELSE IF(RLR.LE.0.6545.AND.RLR.GT.0.3649) THEN
      BI2=2.111*EXP(-1.802*RLR)
      BI3=29.44*EXP(-0.76*RLR)
      AMASS=9.65*AFACTO*EXP(-0.6447*RLR)
      ELSE IF(RLR.LE.0.3540.AND.RLR.GT.0.1393) THEN
      BI2=4.5679*EXP(-4.6604*RLR)
      IF(RLR.GT.0.244) BI2=2.111*EXP(-1.802*RLR)
      BI3=11.3726*RLR**(-0.6585)
      AMASS=5.243*AFACTO*RLR**(-0.3695)
      ELSE
      BI2=2.3210
      BI3=41.924
      AMASS=10.89*AFACTO
      ENDIF
      BI1=BI2+BI3
      EI=BI2*AE
      EI0=2.321*AE
      GJ=BI1*AG
      GJ0=44.245*AG
C********CHANGE UNIT TO FEET
C
      AI1=AFACTO*BI1/(144.*R*R)
      AI2=AFACTO*BI2/(144.*R*R)
      AI3=AFACTO*BI3/(144.*R*R)
      EI=EI/(144.*R**4.)
      EI0=EI0/(144.*R**4.)
      GJ=GJ/(144.*R**4.)
      GJ0=GJ0/(144.*R**4.)
      AEI=AE*1./(144*R**4.)
      AGJ=AG*(21.)/(144.*R**4.)

C
C*************
C
```

```
      QVEL=0.5*RHO*V*V
      FU=1.
      FO=1.
      RS=(1.-RHR)
      ZP=(RLR-RHR)/RS
      ZP2=ZP*ZP
      ZP3=ZP2*ZP
      ZP4=ZP3*ZP
      FF=6.*ZP2-4.*ZP3+ZP4
      FFP=12.*ZP-12.*ZP2+4.*ZP3
      FFPP=12.-24.*ZP+12.*ZP2
      FP=2.*ZP-ZP*ZP
      FPP=2.*(1.-ZP)
      FPH=0.
      FPHP=0.
C******ASSUME STATIC MODE SHAPE EQUAL DYNAMIC MODE SHAPE
C
      FFS=FF
      FFSP=FFP
      FFSPP=FFPP
      FFHS=FFH
      FFHSP=FFHP
      FFHSPP=FFHPP
      WR=FFS*QS*RS
      WP=FFSP*QS
      WPP=FFSPP*QS
      CW=COS(WP)
      SW=SIN(WP)
      C2W=CW*CW-SW*SW
      CB=COS(BETA)
      SB=SIN(BETA)
C
C*********CORRECTION OF MODE SHAPE THAT BASED ON LENGTH OF THE BLADE
C*********(R-RH) NOT ON THE RADIUS OF THE ROTOR ( CORRECTION FOR
C*********MASS,DAMPING,STIFFNESS MATRICES )
C
      FF=FF*RS
      FFPP=FFPP/RS
      FPP=FPP/RS
C
      CALL SUPFCN(TCM,TIM,RLR,ER,E1,E3,UC,AUC,BUC,AAUC,ABUC,BBUC,AUM,AAU
     1M,ABUM,AUC,MM)
      UO=UM=UC
      UCPO=AUC
      UCFO=BUC
      UCFO=UMFO=BUC
      UMPO=AUM
      BUD=BUM=BUC
      AUCPD=AAUC
      AUMPD=AAUM
      BUCPD=AUCFO=ABUC
      BUMPD=AUMFO=ABUM
      BUCFD=BUMFD=BBUC
      BBUM=BBUC
      SB=SIN(BETA)
      CB=COS(BETA)
      OIS=(RLR+UC)*CSI-WR*SSI
      DYNA=6./(RHO*V*V)
C*****
C*******SOLVE FOR QS (STATIC TIP DEFLECTION)
C
      IF(KL.EQ.1) THEN
      BNORMA=-CSI*CB*(1.-A)+X*RLR*CSI*SB-X*E3*SSI
      BTANG=CSI*SB*(1.-A)+X*RLR*CSI*CB
      WNORM=(BNORMA*BNORMA+BTANG*BTANG)

      DS1=DYNA*AMASS*OM*OM*(ER*SB*CB*(1.-SSI*SSI)-RLR*SSI*CB)*FF*DRR
      DS2=DYNA*(AI1-AI3)*OM*OM*SSI*CSI*CB*FFP*DRR
      DS3=3.*WNORM*FF*CN*CR*DRR
C******** SINCE BUC=BBUC*QS
      PAUL=-BBUC
      DSS1=DYNA*AMASS*OM*OM*(RLR*CSI*CSI+ER*SSI*CSI*SB)*PAUL*DRR
      DSS2=-DYNA*AMASS*OM*OM*(SB*SB+(SSI*CB)**2.)*FF*FF*DRR
      DSS3=DYNA*EI*FFPP*FFPP*DRR
      IF(IM.EQ.1) THEN
      FEB=9./8.
      IF(JU.EQ.1.OR.JU.EQ.4) FEB=3./8.
      IF(JU.GE.4) IM=0
      ELSE

      FEB=2./3.
      IF(NTEST.EQ.0) FEB=4./3.
      IF(JU.EQ.1.OR.JU.EQ.NN) FEB=1./3.
      ENDIF
C**** START THE INTEGRATION
      S1=S1+FEB*DS1
      S2=S2+FEB*DS2
      S3=S3+FEB*DS3
      SS1=SS1+FEB*DSS1
      SS2=SS2+FEB*DSS2
      SS3=SS3+FEB*DSS3
      XL=XL-DX
      RLR=XL/X
      IF(RLR.LT.RHR) THEN
      RLR=RHR
      XL=RHR*X
      DRR=(TNUM-NUM)*DRR
      ELSE
      ENDIF
      JU=JU+1
      IF(JU.LE.NN) GO TO 555
      ELSE
      ENDIF
      IF(KL.EQ.1) THEN

      QS=(S1+S2+S3)/(SS1+SS2+SS3)
      WRITE(1,510) QS
      KL=KL+1
      XL=X
      DRR=DX/X
      IF((N-2*KHALF).EQ.0) THEN
      IM=0
      ELSE
      IM=1
      ENDIF
      GO TO 553
      ELSE
      ENDIF
C*****SOME COFACTORS
      PART1=SSI*SW-CSI*CW*CB
      PART2=CSI*SB
      PART3=CSI*CW-SSI*SW*CB
      PART4=(RLR+UM)*CW+WR*SW
      PART5=(RLR+UM)*SW-WR*CW
      PART6=CSI*SW+SSI*CW*CB
      PART7=R/V*(YL*SB*CW+(RLR+UD)*SSI*SB*CW+WR*SW*SSI*SB+E3*PART3)
```

```
      CPO6=3.*(HO1*F1+HO2*F2)*(E1*FP-UMPD*SH)
      DZCPO=(2.*DYNA*(AMASS*OM*(CPO1+CPO2+CPO3+CPO4)+CPO5)*FO+CPO6)*DRR
      CFP1=BUCPD*PART11+UCPD*SB*CSI*FF+ER*(RLR+UC)*SB*SH*FFP*FP
      CFP2=ER*ER*SSI*SH*FFP*FP+ER*SB*CB*SSI*CH*FF*FP-ER*BUC*CH*SB*CSI*FP
      CFP3=ER*CH*PART11*FFP*FP-ER*SH*SB*CSI*FP*FF
      CFP4=AI1*OM*PART1*FFP*FP
      CFP5=3.*WT*CR*CHA*E2*(FF*CH-UMFD*SH)*FP*R/V
      DZCFP=(DYNA*(AMASS*OM*(CFP1+CFP2+CFP3)+CFP4)+CFP5)*DRR
      DZCFF=DYNA*(AMASS*OM*(BUCFD*PART11+UCFD*SB*CSI*FF))
      DZCFF=(DZCFF+3.*F1/V*(-R*UDFD*SH+CH*FF*R)*(FF*CH-UMFD*SH))*DRR
      CFO1=WR*(SB*SB+(SSI*CB)**2.)+ER*SB*CB*(1.-SSI*SSI)-(RLR+UC)*SSI*CB
      CFO2=((RLR+UC)*CSI*CSI-WR*SSI*CSI*CB+ER*SSI*CSI*SB)*AUC
      CFO3=(AI2-AI3)*OM*(SSI*CSI*CB*C2H+SH*CH*((CSI*CB)**2.-SSI*SSI))
      CFO4=3.*(HO1*F1+HO2*F2)*(FF*CH-UMFD*SH)
      DZCFO=(-2.*DYNA*(AMASS*OM*(CFO1*FF+CFO2)*FO+CFO3*FFP*FO)+CFO4)*DRR
      DZCOP=3.*WT*CR*(E2*R*(CHA*TAIL1+CTA*TAIL2)+PI/8.*CR*CR*R*PART12)/V
      DZCOP=DZCOP*FP*FO*DRR
      DZCOF=3./V*(-R*UDFD*SH+CH*FF*R)*(F1*TAIL1+G1*TAIL2)*FO*DRR
      DZCCO=3.*((HO1*F1+HO2*F2)*TAIL1+(HO1*G1+HO2*G2)*TAIL2)*FO*DRR
      COD1=((HO1*F1-HO2*F2)*TAIL3+(HO3*F1+HO4*F2)*TAIL4)*FD*FD
      COD2=((HO1*G1-HO2*G2)*TAIL5-(HO3*G1+HO4*G2)*TAIL6)*FD*FD
      DZCOZ=1.5*(COD1+COD2)*DRR
      DZCD1=(PART1*F1-PART2*F2)*TAIL3+(PART1*G1-PART2*G2)*TAIL5
      DZCD1=1.5*DZCD1*DIS*FO*DRR
      DZCD2=(PART1*F1-PART2*F2)*TAIL4-(PART1*G1-PART2*G2)*TAIL6
      DZCD2=1.5*DZCD2*DIS*FO*DRR
C
C*****STIFFNESS COEFFICIENTS MATRIX
C
      HELP=AUC*(-CH*CSI*SB*F1+CSI*CB*F2)
      PP1=-ER*ER*(CH*CH*(SB*SB+(SSI*CB)**2.)-(CB*CB+(SSI*SB)**2.))
      PP2=-ER*ER*CSI*CSI*(2.*SSI*CB*SH*CH+SH*SH)
      PP3=ER*WR*SB*CB*(1.-SSI*SSI)+ER*(RLR+UC)*SSI*CSI*SB
      PP4=-AUC*AUC*CSI*CSI-AAUC*((RLR+UC)*CSI*CSI-SSI*CSI*(WR*CB-ER*SB))
      PP5=GJ*FPP*FPP
      PP6=3.*(-X*HELP-WP2*F2-WE2*CP*CNA*FP)*(E1*FP-UMPD*SH)
      PP7=3.*(WNO*SH*AUMPD+WTO*F1*FP*FP)
      DZKPP=(DYNA*(AMASS*OM*OM*((PP1+PP2+PP3)*FP*FP+PP4)+PP5))
      PP8=(AI2-AI3)*OM*OM*(SSI*SH-CSI*CH*CB)**2*FP*FP
      PP9=(AI2-AI3)*OM*OM*CSI*CSI*SB*SB*FP*FP
      DZKPP=DZKPP+DYNA*(PP8+PP9)
      DZKPP=(DZKPP+PP6+PP7)*DRR
      PF1=ER*ER*SB*(CB*SH*(1.-SSI*SSI)-SSI*CSI*CH)*FFP*FP
      PF2=-ER*(CH*(SB*SB+(SSI*CB)**2.)+SSI*CSI*CB*SH)*FF*FP
      PF3=ER*WR*(SH*(SB*SB+(SSI*CB)**2.)-CH*SSI*CSI*CB)*FFP*FP
      PF4=-ER*(RLR+UC)*(SSI*CSI*CB*SH-CSI*CSI*CH)*FFP*FP
      PF5=-AUC*BUC*CSI*CSI-ABUC*((RLR+UC)*CSI*CSI-SSI*CSI*(WR*CB-ER*SB))
      PF6=-(AI2-AI3)*OM*OM*CSI*SB*PART12*FFP*FP
      PF7=-3.*(HF1*F1+HF2*F2)*(E1*FP-UMPD*SH)
      PF8=3.*WNO*(BUMPD*SH+UMPD*CH*FFP)
      DZKFF=(DYNA*(AMASS*OM*OM*(PF1+PF2+PF3+PF4+PF5)+PF6)+PF7+PF8)*DRR
      ZFP1=3.*(-X*HELP-WP2*F2)*(FF*CH-UMFD*SH)+3.*AUMFD*WNO*SH
      ZFP1=ZFP1-3.*WE2*CR*CHA*FP*(FF*CH-UMFD*SH)
      DZKFP=(DYNA*(AMASS*OM*OM*(PF1+PF2+PF3+PF4+PF5)+PF6)+ZFP1)*DRR
      ZFF1=-(SB*SB+(CB*SSI)**2.)*FF*FF-CSI*CSI*BUC*BUC
      ZFF2=-((RLR+UC)*CSI*CSI-SSI*CSI*(WR*CB-ER*SB))*BBUC
      ZFF3=(AI1-AI3)*OM*OM*C2H*(SSI*SSI-(CSI*CB)**2.)*FFP*FFP
      ZFF4=4.*(AI1-AI3)*OM*OM*SSI*CSI*SH*CH*CB*FFP*FFP
      ZFF5=EI*FFPP*FFPP
      ZFF6=-3.*((HF1*F1+HF2*F2)*(FF*CH-UMFD*SH))
      ZFF7=3.*WNO*(SH*FF*FFP+SH*BUMFD+UMFD*CH*FFP)
      DZKFF=DYNA*(AMASS*OM*OM*(ZFF1+ZFF2)+ZFF3+ZFF4+ZFF5)
      DZKFF=(DZKFF+ZFF6+ZFF7)*DRR
      OP1=-WP2*FO*(F2*TAIL1+G2*TAIL2)-WNO*AUM*CH*CSI*SB*FO
      OP1=OP1-(F4*TAIL1+G4*TAIL2)*FO
      OP2=-WTO*(AUM*CSI*CB*FO-PART12*FP*FO*E1)
      OP3=(-X*HELP*TAIL1-X*AUD*(-CH*CSI*SB*G1+CSI*CB*G2)*TAIL2)*FO
      DZKOP=3.*(OP1+OP2+OP3)*DRR
      OF1=-(HF1*F1+HF2*F2)*TAIL1*FO-(HF1*G1+HF2*G2)*TAIL2*FO
      OF2=WNO*CSI*SB*(SH*(RLR+UM)*FFP-BUM*CH-WR*CH*FFP-FF*SH)*FO
      OF3=WNO*E1*PART1*FFP*FO-WTO*(BUM*CSI*CB-SSI*FF)*FO
      DZKOF=3.*(OF1+OF2+OF3)*DRR
      ZOD1=((CH*SB*F1-CB*F2)*TAIL3+(PART6*F1+SSI*SB*F2)*TAIL4)*FD*FD
      ZOD2=((CH*SB*G1-CB*G2)*TAIL5-(PART6*G1+SSI*SB*G2)*TAIL6)*FD*FD
      DZKDZ=1.5*(ZOD1+ZOD2)*DRR
      DZKD1=(PART1*F1-PART2*F2)*TAIL3+(PART1*G1-PART2*G2)*TAIL5
      DZKD1=1.5*DZKD1*DIS*FD*DRR
      DZKD2=(PART1*F1-PART2*F2)*TAIL4-(PART1*G1-PART2*G2)*TAIL6
      DZKD2=1.5*DZKD2*DIS*FO*DRR
C
C***** FORCING FUNCTIONS
C
      HP1=ER*ER*(SB*CB*CH*(1.-SSI*SSI)-SSI*CSI*SB*SH)*FP
      HP2=ER*WR*(CH*(SB*SB+(SSI*CB)**2.)+SSI*CSI*CB*SH)*FP
      HP3=-ER*(RLR+UC)*(CSI*CSI*SH+SSI*CSI*CB*CH)*FP
      HP4=AUC*((RLR+UC)*CSI*CSI-WR*SSI*CSI*CB+ER*SSI*CSI*SB)
      HP5=(AI2-AI3)*OM*OM*CSI*SB*PART1*FP
      HP6=3.*WNO*(E1*FP-UMPD*SH)
      DZHP=(DYNA*(AMASS*OM*OM*(HP1+HP2+HP3+HP4)+HP5)+HP6)*DRR
      HF1=WR*(SB*SB+(SSI*CB)**2.)+ER*SB*CB*(1.-SSI*SSI)-(RLR+UC)*SSI*CB
      HF2=BUC*((RLR+UC)*CSI*CSI-WR*SSI*CSI*CB+ER*SSI*CSI*SB)
      HF3=(AI1-AI3)*OM*OM*(SSI*CSI*CB*C2H+SH*CH*((CSI*CB)**2.-SSI*SSI))
      HF4=-EI*FFPP*FFPP*OS
      HF5=3.*WNO*(FF*CH-UMFD*SH)
      DZHF=(DYNA*(AMASS*OM*OM*(HF1*FF+HF2)+HF3*FFP+HF4)+HF5)*DRR
      DZHO=3.*(WNO*TAIL1-WTO*TAIL2)*FO*DRR
********  EFFECT OF TOWER SHADOW
**********
      DCO0=-(WNO*TAIL3+WTO*TAIL5)*FD*DRR
      DZSMP1=-UCPD*PART13+ER*CH*SB*(YL+(RLR+UC)*SSI)*FP-ER*ER*CH*CSI*FP
      DZSMDP=(AMASS*DZSMP1-AI1*PART3*FP)*FO*DRR/OVLL
      DZSMF1=-UCFD*PART13+SB*(YL+(RLR+UC)*SSI)*FF-ER*CSI*FF
      DZSMDF=(AMASS*DZSMF1+AI2*SSI*SB*FFP)*FD*DRR/OVEL
      DZSMO1=(AMASS*PAL1*PAL2-AI1*PART12*PART3-AI2*CSI*SSI*SB*SB)
      DZSMDO=(DZSMO1+AI3*PART1*PART6)*FO*FO*DRR/OVEL
      ZSMO1=(YL*CSI-WR*CB+ER*SB)**2+(YL*SSI+(RLR+UC))**2
      ZSMO2=-(PART13**2+PAL2**2+PART11**2)
      ZSMO3=AI1*(SH*SB)**2+AI2*CB*CB+AI3*(CH*SB)**2
      ZSMO4=-(AI1*PART3**2+AI2*(SSI*SB)**2+AI3*PART6**2)
      DZSMDO=(AMASS*(ZSMO1+ZSMO2)+ZSMO3+ZSMO4)*FD*FD*DRR/OVLL
C
      ZSCP1=-CR*E2*R*WT*FP*(CHA*TAIL3+CTA*TAIL5)*FO/V
      ZSCP2=-PI/8.*WT*CR*CR*CV*FP*PART3*FD
      DSCDP=(ZSCP1+ZSCP2)*DRR
      ZSCP3=((AUC*CSI-ER*PART6*FP)*PAL2+PAL1*(AUC*SSI-ER*PART1*FP))
      ZSCP4=(AI3-AI2)*(SB*SH*(CSI*CSI-SSI*SSI)+2.*SSI*CSI*CH*SB*CB)*FP
      ZSCP5=-WNDO3*(E1*FP-UMPD*SH)*FD
      DSCPD2=-WNO1*DIS*(E1*FP-UMPD*SH)*DRR
      DSCPD1=(ZSCP5+OM*(AMASS*ZSCP3+ZSCP4)*FD/OVEL)*DRR
      DSCDF=(R*UDFD*SH-CH*FF*R)/V*(F1*TAIL3+G1*TAIL5)*FD*DRR
      ZSDF2=AMASS*OM*((BUC*CSI-SSI*CB*FF)*PAL2+PAL1*(BUC*SSI+CSI*CB*FF))
      ZSDF3=-(AI1-AI3)*OM*CB*FFP
      ZSDF4=-WNDO3*(FF*CH-UMFD*SH)*FD*DRR
      DSCFD2=-WNO1*DIS*(FF*CH-UMFD*SH)*DRR
      DSCFD1=ZSDF4+(-ZSDF2+ZSDF3)*FD*DRR/OVEL
```

```
      PART8=R/V*(YL*C3+(RLF+UD)*SSI*CB+WR*CSI)
      PART9=R/V*(YL*PART6+(RLR+UD)*C9*CH+WR*SH*CB+E3*SH*SA)
      PAPT10=R/V*(YL*SSI*SA+(RLR+UD)*SA)
      PART11=WF*S9*CSI+ER*CSI*CA
      PART12=SSI*CH+CSI*SH*CA
      PART13=WF*SSI*SB+ER*CB*SSI
      TLF1=(YL*SB*SH+(RLR+UM)*SSI*S9*SH-WR*CH*SSI*SA-E1*PART6)*FFP
      TLF1=TLF1-SH*SSI*SA*FF-JUH*SSI*SA*CH
      PAL1=(RLF+UC)*CSI-WR*SSI*CB+ER*SSI*SB
      PAL2=YL+(RLF+UC)*SSI+WR*CSI*CB-ER*S9*CSI
C
      TAIL1=(RLF+UM)*CH*CSI*SB+WR*SH*CSI*SB+E1*PART12
      TAIL2=(RLF+UM)*CSI*SB-WR*SSI
      TAIL3=YL*SB*CH+(RLR+UM)*SSI*SA*CH+WR*SH*SSI*SB-E1*PART3
      TAIL4=YL*PART6+(RLR+UM)*CA*CH+WR*SH*CB-E1*SH*SB
      TAIL5=YL*CA+(RLR+UM)*SSI*CA+WR*CSI
      TAIL6=YL*SSI*SB+(RLR+UM)*SB
C
      WT=CSI*SA*(1.-A)+X*((RLR+UD)*CSI*CA-WR*SSI)
      WN=-PART1*(1.-A)-X*((RLR+UD)*CH*CSI*SA+WR*SH*CSI*SB-E3*PART12)
      WE2=WN*WN+WT*WT
      WTO=WE2*CC*CR
      WNO=WE2*CN*CR
      F1=CR*(2.*CN*WN+CNP*WT)
      F2=CR*(2.*CN*WT-CNP*WN)
      G1=CR*(2.*CO*WN+COP*WT)
      G2=CR*(2.*CO*WT-COP*WN)
      F4=CR*WE2*CNA*FP
      G4=CR*WE2*CTA*FP
      HELP2=AUD*(-CH*CSI*SB*G1+CSI*C9*G2)
      WP2=X*E3*PART12*FP
      WF11=-PART12*(1.-A)*FFP
      WF12=X*(RLR+UD)*SW*CSI*SB*FFP-X*SH*CSI*SB*FF-X*WR*CH*CSI*SB*FFP
      WF13=-X*E3*PART1*FFP-X*AUD*CH*CSI*SB
      WF1=WF11+WF12+WF13
      WF2=-X*(SSI*FF-AUD*CSI*CB)
      WO1=((RLF+UD)*CH*CSI*S9+WR*SH*CSI*SB-E3*(SSI*SH+CSI*SH*CB))*R*FO/V
      WO2=(WR*SSI-(RLR+UD)*CSI*C9)*R*FO/V
      WD1=(YL*S9*CH+(RLR+UD)*SSI*SB*CH+WR*SH*SSI*SB+E3*PART3)*R/V
      WD2=R/V*(YL*CA+(RLR+UD)*SSI*CA+WR*CSI)
      WD3=R/V*(YL*(SSI*C9*CH+SH*CSI)+(RLR+UD)*CB*CH+WR*SH*CB+E3*SH*SB)
      WD4=R/V*(YL*SSI*SA+(RLR+UD)*SB)
      WNO1=PART1*F1-PART2*F2
      WTO1=PART1*G1-PART2*G2
      WNO2=PART6*F1+SSI*S9*F2
      WNO3=CH*SA*F1-C9*F2
      WTO2=PART6*G1+SSI*SA*G2
      WTO3=CH*SB*G1-CB*G2
      WNDD2=WD3*F1+WD4*F2
      WNDD3=WD1*F1-WD2*F2
      WTDD2=WD3*G1+WD4*G2
      WTDD3=WD1*G1-WD2*G2
C*****FIND THE INTEGRAL COEFFICIENTS OF YAW AND YAW RATE
C
      SAM=(1.5/PI)
      DCTDA=4.*(1.-2.*A)
      DZI1=DCTDA*DIS*DIS*DIS*DRR*FRIG*CSI
      IF(A.LT.AC) GO TO 901
      DZI1=(GLUART/DCTDA)*DZI1
 901  ADZI2=(PART1*F1-PART2*F2)*(E1*PART3-PART4*SSI*SB)
      BDZI2=+(PART1*G1-PART2*G2)*(PART5*PART3-PART4*PART6)
      DZI2=SAM*(ADZI2+BDZI2)*DIS*DRR
      ADZI3=(PART1*F1-PART2*F2)*(-E1*SH*SB+PART4*CB)
      BDZI3=-(PART1*G1-PART2*G2)*(PART5*SH*S9+PART4*CH*SB)
      DZI3=SAM*(ADZI3+BDZI3)*DIS*DRR
      DZI4=SAM*(CH*SB*F1-CB*F2)*(E1*PART3-PART4*SSI*SB)*FD*DRR
      DZI5=SAM*(PART6*F1+SSI*SB*F2)*(E1*SH*SB-PART4*CB)*FD*DRR
      DZI6=+SAM*(CH*SB*G1-CB*G2)*(PART5*PART3-PART4*PART6)*FD*DRR
      DZI7=+SAM*(PART6*G1+SSI*SB*G2)*(PART4*CH*SB+PART5*SH*S9)*FD*DRR
      DZI8=SAM*(PART7*F1-PART8*F2)*(E1*PART3-PART4*SSI*SB)*FD*DRR
      DZI9=-SAM*(PART9*F1+PART10*F2)*(PART4*CB-E1*SH*SB)*FD*DRR
      DZI10=+SAM*(PART7*G1-PART8*G2)*(PART5*PART3-PART4*PART6)*FD*DRR
      DZI11=+SAM*(PART9*G1+PART10*G2)*(PART4*CH*SB+PART5*SH*SB)*FD*DRR
      DZI12=SAM*(CH*SB*F1-CB*F2)*(E1*SH*SA-PART4*CB)*FD*DRR
      DZI13=SAM*(PART6*F1+SSI*SB*F2)*(-E1*PART3+PART4*SSI*SB)*FD*DRR
      DZI14=+SAM*(CH*SB*G1-C9*G2)*(PART5*SH*SB+PART4*CH*SB)*FD*DRR
      DZI15=-SAM*(PART6*G1+SSI*SD*G2)*(PART5*PART3-PART4*PART6)*FD*DRR
      DZI16=SAM*(PART7*F1-PART8*F2)*(E1*SH*SB-PART4*C9)*FD*DRR
      DZI17=-SAM*(PART9*F1+PART10*F2)*(E1*PART3-PART4*SSI*SB)*FD*DRR
      DZI18=+SAM*(PART7*G1-PART8*G2)*(PART5*SH*S9+PART4*CH*SB)*FD*DRR
      DZI19=-SAM*(PART9*G1+PART10*G2)*(PART5*PART3-PART6*PART4)*FD*DRR
C*****MASS MATRIX
      QVEL=0.5*RHO*V*V
      DYNA=(3./QVEL)
      DZMPP1=(UCPD*UCPD-2.*UCPD*ER*SH*FP+ER*ER*FP*FP)*AMASS+AI1*FP*FP
      DZMPP=DYNA*DZMPP1*DRR
      DZMFF=DYNA*(AMASS*(UCFD*UCFD+FF*FF)+AI2*FFP*FFP)*DRR
      O1=(WR*WR*(SB*SB+(SSI*CB)**2.)+ER*ER*(CB*CB+(SSI*SB)**2.))
      O2=(RLR+UC)**2.*CSI*CSI+2.*(RLR+UC)*SSI*CSI*(ER*SA-WR*C9)
      O3=2.*WR*ER*SB*CB*CSI*CSI
      O4=AI1*(SSI*CH+CSI*CB*SH)**2.+AI2*CSI*CSI*SB*SB+AI3*PART1**2.
      DZMOO=DYNA*(AMASS*(O1+O2+O3)+O4)*FO*FO*DRR
      DD1=2.*YL*YL+4.*YL*WR*CSI*C9+4.*YL*(RLR+UC)*SSI-4.*YL*ER*CSI*SB
      DD2=WR*WR*(1.+(CSI*CB)**2.)+ER*ER*(1.+(SB*CSI)**2.)
      DD3=(RLR+UC)**2.*(1.+SSI*SSI)-2.*ER*WR*SB*CB*(1.-SSI*SSI)
      DD4=2.*(RLR+UC)*WR*SSI*CSI*CB-2.*(RLR+UC)*ER*SSI*CSI*SB
      DD5=(CSI*CH)**2.+(SSI*SH*CB)**2.+(SH*SB)**2.-2.*SSI*CSI*SH*CH*CB
      DD6=((SSI*S9)**2.+C9*C9)*AI2
      DD7=(CSI*SH)**2.+(SSI*CH*CB)**2.+(CH*SB)**2.+2.*SH*CH*SSI*CSI*CB
      DZMDD=DYNA*(AMASS*(DD1+DD2+DD3+DD4)+AI1*DD5+DD6+AI3*DD7)*FD*FD*DRR
      DZMPF=DYNA*AMASS*(UCPD*UCFD-UCFD*ER*SH*FP+ER*CH*FF*FP)*DRR
      PO1=PART11*(-UCPD+ER*SH*FP)+ER*CH*((RLR+UC)*CSI*SB+ER*SSI)*FP
      PO2=AI1*(SSI*CH+CSI*CB*SH)*FP
      DZMPO=DYNA*(AMASS*PO1+PO2)*FO*DRR
      ZFO1=-UCFD*PART11+((RLR+UC)*SB*CSI+ER*SSI)*FF
      ZFO2=AI2*CSI*C9*FFP
      DZMFO=DYNA*(AMASS*ZFO1+ZFO2)*FO*DRR
C
C*****DAMPING COEFFICIENTS MATRIX
C
      CPP1=AUCPD*PART11+UCPD*ER*CSI*CH*S9*FP-AUC*ER*CH*SB*CSI*FP
      CPP2=-ER*WR*SSI*FP*FP+ER*(RLR+UC)*CA*CSI*FP*FP
      CPP3=3.*WT*CR*FP*(CNA*E2*(E1*FP-UMPD*SH)+PI/8.*CR*CR*F)/V
      DZCPP=(DYNA*(AMASS*OM*(CPP1+CPP2))+CPP3)*DRR
      CFF1=AUCFD*PART11+UCFD*ER*CSI*S9*CH*FP+ER*SB*SH*CSI*FF*FP
      CPF2=ER*(RLR+UC)*SH*S9*CSI*FFP*FP+ER*ER*SSI*SH*FFP*FP
      CPF3=-ER*CH*PART11*FFP*FP
      CPF4=(AI2-AI3)*OM*PART1*FFP*FP
      CPF5=3.*F1/V*(-R*UDFD*SH+CH*FF*P)*(E1*FP-UMPD*SH)
      DZCPF=(DYNA*(AMASS*OM*(CPF1+CPF2+CPF3)-CPF4)+CPF5)*DRR
      CPO1=ER*FP*(SSI*CSI*SA*SH-S9*C9*CH*(1.-SSI*SSI))*FP
      CPO2=-ER*WR*(CH*(S9*SA+(SSI*CA)**2.)+SSI*CSI*C9*SH)*FP
      CPO3=ER*(RLR+UC)*(CSI*CSI*SH+SSI*CSI*CB*CH)*FP
      CPO4=AUC*((RLF+UC)*CSI*CSI-WR*SSI*CSI*C9+ER*SSI*CSI*SB)
      CPO5=-(AI2-AI3)*OM*CSI*SB*PART1*FP
```

```
      DSCDO=-((WO1*F1+WO2*F2)*TAIL3+(WO1*G1+WO2*G2)*TAIL5)*FD*DRR
      DSCO2=-((HR*S9+(R+C9)*YL+(HR*C9-CR*S9)*PART11+(RLR+UC)*PART13)*FO
      DSCO3=((AI1-AI3)*(SH*CH*SB*SSI-CH*CH*CSI*SB*CB)-AI2*CSI*SB*CB)*FO
      DSCO4=-(WNDD3*TAIL1+WTDD3*TAIL2)*FO*FO*DRR
      DSCOD2=-(WND1*TAIL1+WTD1*TAIL2)*DIS*FO*DRR
      DSCOD1=DSCO4+(AMASS*DSCO2+DSCO3)*UM*FO*DRR/QVEL
      DSOD1=(-WNDD2*TAIL4+WNDD3*TAIL3+WTDD2*TAIL5+WTDD3*TAIL5)*FD*FO*DRR
      DSODJ=(WND1*TAIL3+WTD1*TAIL5)*FO*DIS*DRR
      DSODK=(WND1*TAIL4-WTD1*TAIL6)*DIS*FO*DRR
C
      DSKP1=(WT0*(E1*PART3*FP+AUM*SSI*CB)+WN0*AUM*SSI*SB*CH)*FD*DRR
      DSKP2=((WP2*F2+X*HELP+F4)*TAIL3+(WP2*G2+X*HELP2+G4)*TAIL5)*FD*DRR
      DSKP2=DSKP2+WE2*CH*FP*(CHA*TAIL3+CTA*TAIL5)*FD*DRR
      DSKDP=DSKP1+DSKP2
      DSKF1=(-WN0*TLF1+WT0*BUM*SSI*CB)*FO*DRR
      DSKF2=((WF1*F1+WF2*F2)*TAIL3+(WF1*G1+WF2*G2)*TAIL5)*FD*DRR
      DSKDF=DSKF1+DSKF2
      DSKOO=(-WN0*TAIL4+WT0*TAIL6)*FO*DRR
      DSKO1=(-WND2*TAIL4+WND3*TAIL3+WTD2*TAIL6+WTD3*TAIL5)*FD*FO*DRR
      DSKDJ=(WND1*TAIL3+WTD1*TAIL5)*DIS*FO*DRR
      DSKDK=(WND1*TAIL4-WTD1*TAIL6)*DIS*FO*DRR
      DSKPD1=-WND3*(E1*FP-UMPO*SH)*FO*DRR
      DSKPD2=-WND1*DIS*(E1*FP-UMPD*SH)*DRR
      DSKFD1=-WND3*(FF*CH-UMFO*SH)*FD*DRR
      DSKFD2=-WND1*DIS*(FF*CH-UMFD*SH)*DRR
      DSKOD1=-(WND1*TAIL1+WTD1*TAIL2)*FD*FO*DRR
      DSKOD2=-(WND1*TAIL1+WTD1*TAIL2)*DIS*FO*DRR

C*****
C******* GRAVITY TERMS
C*****
      DGNCOS=AMASS*GR*((UCPO-ER*SH*FP)*CSI-ER*SSI*CB*CH*FP)*DRR/QVEL
      DGNSIN=-AMASS*GR*ER*CH*SB*DRR/QVEL
      DGPCOS=AMASS*GR*(AUCPO*CSI-ER*SSI*SB*FP*FP)*DRR/QVEL
      DGPSIN=AMASS*GR*ER*CB*FP*FP*DRR/QVEL
      DGFCOS=AMASS*GR*((BUCPO-ER*CH*FP*FFP)*CSI+ER*SSI*CB*SH*FP*FFP)*DRR
      DGFCOS=DGFCOS/QVEL
      DGFSIN=AMASS*GR*ER*SH*SB*FP*FFP*DRR/QVEL
      DGOCOS=-AMASS*GR*ER*CH*SB*FP*FO*DRR/QVEL
      DGOSIN=AMASS*GR*(ER*SSI*CB*CH*FP-UCPO*CSI)*FO*DRR/QVEL
      IF(IM.EQ.1) THEN
      FEB=9./8.
      IF(I.EQ.1.OR.I.EQ.4) FEB=3./8.
      IF(I.GE.4) IM=0
      ELSE

      FEB=2./3.
      IF(NTEST.EQ.0) FEB=4./3.
      IF(I.EQ.1.OR.I.EQ.NN) FEB=1./3.
      ENDIF
C*****START THE SIMPSON INTEGRATION
      ZI1=ZI1+FEB*DZI1
      ZI2=ZI2+FEB*(DZI2)
      ZI3=ZI3+FEB*(DZI3)
      ZI4=ZI4+FEB*(DZI4)
      ZI5=ZI5+FEB*(DZI5)
      ZI6=ZI6+FEB*(DZI6)
      ZI7=ZI7+FEB*(DZI7)
      ZI8=ZI8+FEB*(DZI8)
      ZI9=ZI9+FEB*(DZI9)
      ZI10=ZI10+FEB*(DZI10)
      ZI11=ZI11+FEB*(DZI11)
      ZI12=ZI12+FEB*(DZI12)
      ZI13=ZI13+FEB*(DZI13)
      ZI14=ZI14+FEB*(DZI14)
      ZI15=ZI15+FEB*(DZI15)
      ZI16=ZI16+FEB*(DZI16)
      ZI17=ZI17+FEB*(DZI17)
      ZI18=ZI18+FEB*(DZI18)
      ZI19=ZI19+FEB*(DZI19)
      ZMPP=ZMPP+FEB*(DZMPP)
      ZMPF=ZMPF+FEB*(DZMPF)
      ZMPO=ZMPO+FEB*(DZMPO)
      ZMFF=ZMFF+FEB*(DZMFF)
      ZMOO=ZMOO+FEB*(DZMOO)
      ZMDD=ZMDD+FEB*(DZMDD)
      ZMFO=ZMFO+FEB*(DZMFO)
      ZCPP=ZCPP+FEB*(DZCPP)
      ZCPF=ZCPF+FEB*(DZCPF)
      ZCPO=ZCPO+FEB*(DZCPO)
      ZCFP=ZCFP+FEB*(DZCFP)
      ZCFF=ZCFF+FEB*(DZCFF)
      ZCFO=ZCFO+FEB*(DZCFO)
      ZCOP=ZCOP+FEB*(DZCOP)
      ZCOF=ZCOF+FEB*(DZCOF)
      ZCOO=ZCOO+FEB*(DZCOO)
      ZCOZ=ZCOZ+FEB*(DZCOZ)
      ZCO1=ZCO1+FEB*(DZCO1)
      ZCO2=ZCO2+FEB*(DZCO2)
      ZKPP=ZKPP+FEB*(DZKPP)
      ZKPF=ZKPF+FEB*(DZKPF)
      ZKFP=ZKFP+FEB*(DZKFP)
      ZKFF=ZKFF+FEB*(DZKFF)
      ZKDZ=ZKDZ+FEB*(DZKDZ)
      ZKOP=ZKOP+FEB*DZKOP
      ZKOF=ZKOF+FEB*DZKOF
      ZKD1=ZKD1+FEB*(DZKD1)
      ZKD2=ZKD2+FEB*(DZKD2)
      ZHP=ZHP+FEB*(DZHP)
      ZHF=ZHF+FEB*(DZHF)
      COO=COO+FEB*DCOO
      SMOP=SMOP+FEB*DZSMOP
      SMOF=SMOF+FEB*DZSMOF
      SMOO=SMOO+FEB*DZSMOO
      SMOD=SMOD+FEB*DZSMOD
      SCDP=SCDP+FEB*DSCDP
      SCDF=SCDF+FEB*DSCDF
      SCDO=SCDO+FEB*DSCDO
      SCD1=SCD1+FEB*DSDD1
      SCDJ=SCDJ+FEB*DSDDJ
      SCDK=SCDK+FEB*DSDDK
      SKDP=SKDP+FEB*DSKDP
      SKDF=SKDF+FEB*DSKDF
      SKDO=SKDO+FEB*DSKDO
      SKD1=SKD1+FEB*DSKD1
      SKDJ=SKDJ+FEB*DSKDJ
      SKDK=SKDK+FEB*DSKDK
      SCPD1=SCPD1+FEB*DSCPD1
      SCPD2=SCPD2+FEB*DSCPD2
      SCFD1=SCFD1+FEB*DSCFD1
      SCFD2=SCFD2+FEB*DSCFD2
      SCOD1=SCOD1+FEB*DSCOD1
      SCOD2=SCOD2+FEB*DSCOD2
      SKPD1=SKPD1+FEB*DSKPD1
      SKPD2=SKPD2+FEB*DSKPD2
      SKFD1=SKFD1+FEB*DSKFD1
```

```
      SKFD2=SKFD2+FEB*DSKFD2
      SKOD1=SKOD1+FEB*DSKOD1
      SKOD2=SKOD2+FEB*DSKOD2
      GNCOS=GNCOS+FEB*DGNCOS
      GNSIN=GNSIN+FEB*DGNSIN
      GPCOS=GPCOS+FEB*DGPCOS
      GPSIN=GPSIN+FEB*DGPSIN
      GFCOS=GFCOS+FEB*DGFCOS
      GFSIN=GFSIN+FEB*DGFSIN
      GOCOS=GOCOS+FEB*DGOCOS
      GOSIN=GOSIN+FEB*DGOSIN
      ZHO=ZHO+FEB*(DZHO)
C
      IF(CUPP.EQ.1HY) GO TO 43
      IF(RLR.EQ.RHR) GO TO 554
      IF(KK.LT.5) GO TO 43
554   WRITE(1,16)RLR,A,DPHI,DDET,DAL,CL,CD,RCR,CPB,CTB
      KK=0
43    CONTINUE
      KK=KK+1
      XL=XL-DX
      RLR=XL/X
      I=I+1
      IF(RLR.LT.RHR) THEN
      RLR=RHR
      XL=RHR*X
      DRR=(TNUM-NUM)*DRR
      ELSE
      ENDIF
      IF(I.LE.NN) GO TO 555
C
C******CALCULATE THE YAW AND YAW RATE VARIATION
C
      IF(RLR.EQ.1.) THEN
      SKDEL=SJDEL=SKRDEL=SJRDEL=0.
      ELSE
73    DENO=(ZI1-ZI3)**2+ZI2*ZI2
      SKDEL=((ZI4+ZI5+ZI6+ZI7)*(ZI1-ZI3)-ZI2*(ZI12+ZI13+ZI14+ZI15))/DENO
      SJDEL=((ZI4+ZI5+ZI6+ZI7)*ZI2+(ZI1-ZI3)*(ZI12+ZI13+ZI14+ZI15))/DENO
      SJDEL=-SJDEL
      SKRDEL=(ZI8+ZI9+ZI10+ZI11)*(ZI1-ZI3)
      SKRDEL=(SKRDEL-ZI2*(ZI16+ZI17+ZI18+ZI19))/DENO
      SJRDEL=(ZI8+ZI9+ZI10+ZI11)*ZI2
      SJRDEL=-(SJRDEL+(ZI1-ZI3)*(ZI16+ZI17+ZI18+ZI19))/DENO
      ENDIF
      ZCOD=ZCD2+SJRDEL*ZC01-SKRDEL*ZC02
      ZKDD=ZKD2+SJDEL*ZK01-SKDEL*ZKD2
      SCDD=SCO1+SJRDEL*SCDJ+SKRDEL*SCDK
      SKDD=SKD1+SJDEL*SKDJ+SKDEL*SKDK
      SCPD=SCPD1+SJRDEL*SCPD2
      SCFD=SCFD1+SJRDEL*SCFD2
      SCOD=SCOD1+SJRDEL*SCOD2
      SKPD=SKPD1+SJDEL*SKPD2
      SKFD=SKFD1+SJDEL*SKFD2
      SKOD=SKOD1+SJDEL*SKOD2
C
C*******CORRECTION FOR MASS COEF. DUE TO TOWER SHADOW SO IT IS IN
C*******FORM OF (MIJ-MIJS)
       SMDP=-SMDP
       SMDF=-SMDF
       SMDO=-SMDO
       SMDD=-SMDD
       WRITE(1,700)LR,E1,E2,E3,AE,AG
```

```
      WRITE(1,402)N,MM
      WRITE(1,509) CP,CT
      WRITE(1,505)
      WRITE(1,405) ZMPF,ZMPF,ZMPO,ZMFF,ZMFO,ZMOO,ZMOD
      WRITE(1,506)
      WRITE(1,406) ZCPP,ZCPF,ZCPO,ZCFP,ZCFF,ZCFO,ZCOP,ZCOF,ZCOO,ZCOD
      WRITE(1,507)
      WRITE(1,405) ZKPP,ZKPF,ZKFP,ZKFF,ZKOP,ZKOF,ZKOD
      WRITE(1,508)
      WRITE(1,408) ZHP,ZHF
      WRITE(1,407) SKDEL,SJDEL,SKRDEL,SJRDEL
      WRITE(1,513)
      WRITE(1,514) GNCOS,GNSIN,GPCOS,GPSIN,GFCOS,GFSIN,GOCOS,GOSIN
      WRITE(1,515) SMDP,SMDF,SMDO,SMDD
      WRITE(1,516) SCDP,SCDF,SCDO,SCDD
      WRITE(1,517) SKDP,SKDF,SKDO,SKDD
      WRITE(1,311) SCPD,SCFD,SCOD
      WRITE(1,312) SKPD,SKFD,SKOD
      WRITE(1,518) COD

      DPR=DX/X
      X=X+DBX
      IF(X.GT.XMAX) GO TO 40
      GO TO 27
40    CONTINUE
      PRINT 4
      READ5,CANSR
      IF(CANSR.NE.1HY) GO TO 300
      PRINT 6
      READ*,PTCH
      GO TO 200
C     ****************************************************************
C
C     FORMAT STATEMENTS
C
C     ****************************************************************
    1 FORMAT('  FORCES INPUT SEQUENCE')
    2 FORMAT(' WRITE B,BCRR,EM,DRR,XMIN,XMAX,DBX')
   65 FORMAT(' WRITE ALC,AST,SI,PITCH,BETA FOOT,DBETA')
   66 FORMAT(' WRITE RT,DCND,RC,RH')
    3 FORMAT(' WRITE CD ZERO, CL MAX, CL FLAT, ALPHA BREAK')
    4 FORMAT('DO YOU WANT ANOTHER PITCH ANGLE? (Y)')
    5 FORMAT(A1)
    6 FORMAT('INPUT PITCH ANGLE')
    8 FORMAT(15X,'AERODYNAMIC DATA'//,6X,'CLM',6X,'CLFL',8X,'M',8X,'AST'
     1,7X,'ABR',7X,'ALC',7X,'CD0'/7F10.3/)
    9 FORMAT(15X,'OPERATIONAL VARIABLES'//5X,'XMIN',6X,'XMAX',7X,'DRR',
     18X,'SI'/4F10.3/)
   19 FORMAT(15X,'PHYSICAL AIRFOIL DATA'//,7X,'B',7X,'BCRR',6X,'DCND'
     1,7X,'RT',8X,'RC',5X,'RH',8X,'BRT',6X,'DBTA'/8F10.3/)
   60 FORMAT(////25X,'PROGRAM OPERATING CONDITIONS'/)
   21 FORMAT(///25X,'PROGRAM FORCES OUTPUT AT PITCH =',F7.3,' DEGREES')
   15 FORMAT(////,6X,'RCR',8X,'A',8X,'PHI',6X,'DLTA',
     15X,'ALPHA',7X,'CL',7X,'CD',7X,'BCR',7X,'CPB',7X,'CTB')
   16 FORMAT(2F10.4,6F10.3,4X,2F9.5)
  100 FORMAT(//,5X,'THIS RUN USED',F9.3,3X,'SECONDS')
407   FORMAT(/,3X,'SKDEL',12X,'SJDEL',12X,'SKRDEL',12X,'SJRDEL'/,
     14(3X,G12.6))
405   FORMAT (7(3X,G12.6))
406   FORMAT(10(1X,G12.6))
408   FORMAT(3(4X,G12.6))
402   FORMAT(4X,'  N = ',I3,'    MM = ',I3)
505   FORMAT(//,6X,'MPP',12X,'MPF',12X,'MPO',12X,'MFF',12X,'MFO',12X
```

```
      1,'MOO',12X,'MOD')
506   FORMAT(//,6X,'CPF',11X,'CPF',11X,'CPO',11X,'CFP',11X,'CFF',11X,
     1'CFO',11X,'COP',11X,'COF',11X,'COC',11X,'CDO')
507   FORMAT(//,6X,'KPP',12X,'KPF',12X,'KFP',12X,'KFF',12X,'KOP',12X,
     1'KOF',12X,'KOD')
508   FORMAT(//,6X,'HP',12X,'HF',12X,'HO')
509   FORMAT(/,3X,'CP=   ',F10.5,8X,' CT=   ',F10.5)
510   FORMAT(/,1X,'  QS   =   ',G12.6)
513   FORMAT(//,2X,'GNCOS',9X,'GNSIN',9X,'GPCOS',9X,'GPSIN',9X,'GFCOS',
     19X,'GFSIN',9X,'GOCOS',9X,'GOSIN')
514   FORMAT(8(1X,G12.6))
515   FORMAT(/,4X,'SMOP = ',G12.6,' SMOF = ',G12.5,' SMOO = ',G12.6,'
     1SMOD = ',G12.6)
516   FORMAT(/,4X,'SCOP = ',G12.6,' SCOF = ',G12.6,' SCDO = ',G12.6,'
     1SCOD = ',G12.6)
517   FORMAT(/,4X,'SKOP = ',G12.6,' SKDF = ',G12.6,' SKDO = ',G12.6,'
     1SKDO = ',G12.6)
518   FORMAT(/,4X,'COD = ',G12.6)
311   FORMAT(/,4X,'SCPO = ',G12.6,' SCFD = ',G12.6,' SCOD = ',G12.6)
312   FORMAT(/,4X,'SKPO = ',G12.6,' SKFD = ',G12.6,' SKCD = ',G12.6)
700   FORMAT(/,8X,' ER',9X,'E1',9X,'E2',9X,'E3',9X,'AE',9X,'AG'
     1/,2X,6(G12.6,2X))
  300 TIMOUT=SECOND()-TIMIN
      WRITE(1,100) TIMOUT
      STOP
      END
      SUBROUTINE SUMROM(TOM,TIM,RLR,ER,E1,E3,UC,AUC,BUC,AAUC,ABUC,BBUC,A
     1UM,AAUM,ABUM,AUD,MM)
      COMMON L,F,RS
      COMMON /STIFF/ EI,EIO,GJ,GJO,RHR,OS
C
      UC=AUC=AAUC=ABUC=BBUC=AUM=AAUM=ABUM=AUD=0.
      ALOW=RHR
      AHIGH=(RLR-RHR)/RS
      N=MM
      DRS=(AHIGH-ALOW)/N
      DRS3=DRS/3.
      RLS=ALOW
      K=N+1
      DO 10 I=1,K
      IHALF=I/2
      ITEST=I-2*IHALF


      ZP=RLS
      ZP2=ZP*ZP
      ZP3=ZP2*ZP
      ZP4=ZP3*ZP
      FF=6.*ZP2-4.*ZP3+ZP4
      FFP=12.*ZP-12.*ZP2+4.*ZP3
      FFPP=12.-24.*ZP+12.*ZP2
      FP=2.*ZP-ZP2
      FPP=2.*(1.-ZP)
      WR=FF*OS*RS
      WP=FFP*OS
      WPP=FFPP*OS
      CW=COS(WP)
      SW=SIN(WP)
      DUC=-0.5*WP*WP*RS
      TOM0=TOM(ER,CW,SW,FP,FPP,WPP)
      TOM1=TOM(E1,CW,SW,FP,FPP,WPP)
      EE3=-E3
      TOM3=TOM(EE3,CW,SW,FP,FPP,WPP)
      DAUC=-WP*TOM0
      DAUM=-WP*TOM1
      DAUD=-WP*TOM3
      DAAUC=-TOM0*TOM0/RS
      DAAUM=-TOM1*TOM1/RS
      TIM0=TIM(ER,CW,SW,FP,FPP,WPP,FFP,FFPP)
      TIM1=TIM(E1,CW,SW,FP,FPP,WPP,FFP,FFPP)
      DABUC=WP*TIM0-FFP*TOM0
      DABUM=WP*TIM1-FFP*TOM1
      DBBUC=-FFP*FFP*RS
      FEB=2.
      IF(ITEST.EQ.0) FEB=4.
      IF(I.EQ.1.OR.I.EQ.K) FEB=1.
      UC=UC+FEB*DUC*DRS3
      AUC=AUC+FEB*DAUC*DRS3
      AUM=AUM+FEB*DAUM*DRS3
      AUD=AUD+FEB*DAUD*DRS3
      AAUC=AAUC+FEB*DAAUC*DRS3
      AAUM=AAUM+FEB*DAAUM*DRS3
      ABUC=ABUC+FEB*DABUC*DRS3
      ABUM=ABUM+FEB*DABUM*DRS3
      BBUC=BBUC+FEB*DBBUC*DRS3
      BUC=BBUC*OS
      RLS=RLS+DRS
10    CONTINUE
      RETURN
      END
      FUNCTION TOM(A,B,C,D,E,F)
      COMMON L,F,RS
      TOM=A*B*E-A*C*F*D
      RETURN
      END
      FUNCTION TIM(A,B,C,D,E,F,G,H)
      COMMON L,F,RS
      TIM=A*C*E*G+A*F*B*D*G+A*C*D*H
      RETURN
      END
```

AERO's Output

PROGRAM OPERATING CONDITIONS

PHYSICAL AIRFOIL DATA

B	BCRR	DCNO	RT	RC	RH	BRT	DBTA
3.000	.259	.009	.840	4.293	.840	5.000	4.000

AERODYNAMIC DATA

CLM	CLFL	M	AST	ABR	ALO	CDO
1.350	1.000	.890	45.000	15.000	4.200	.014

OPERATIONAL VARIABLES

XMIN	XMAX	DRR	SI
5.000	8.000	.010	0.000

PROGRAM FORCES OUTPUT AT PITCH = 0.000 DEGREES

QS = .184856E-02 CPA = .340291

PCR	A	PHI	BETA	ALPHA	CL	CD	BCR	CPB	CTB
.9500	.5496	5.416	1.229	4.187	.816	.018	.236	.00442	.01364
.9000	.4361	7.142	1.459	5.684	.960	.021	.240	.00681	.01498
.8500	.3853	8.230	1.688	6.542	1.042	.024	.244	.00761	.01487
.8000	.3591	9.103	1.917	7.185	1.104	.026	.248	.00773	.01424
.7500	.3446	9.914	2.147	7.767	1.160	.028	.252	.00753	.01341
.7000	.3354	10.751	2.376	8.375	1.217	.030	.256	.00718	.01250
.6500	.3288	11.670	2.606	9.064	1.283	.033	.259	.00676	.01157
.6000	.3123	12.911	2.835	10.076	1.350	.037	.259	.00628	.01051
.5500	.2725	14.819	3.064	11.754	1.350	.046	.259	.00560	.00894
.5000	.1624	18.524	3.294	15.230	1.000	.149	.259	.00362	.00669
.4500	.1452	20.803	3.523	17.279	1.000	.198	.259	.00190	.00489
.4000	.1291	23.530	3.752	19.777	1.000	.270	.259	.00125	.00409
.3500	.1141	26.849	3.982	22.867	1.000	.381	.259	.00067	.00344
.3000	.1002	30.958	4.211	26.747	1.000	.504	.259	.00032	.00288
.2500	.0874	36.132	4.441	31.691	1.000	.617	.259	.00023	.00236
.2000	.0760	42.739	4.670	38.069	1.000	.783	.259	.00016	.00197
.1500	.0645	51.282	4.899	46.383	.976	1.038	.259	.00011	.00171
.1200	.0556	55.866	5.000	50.866	.893	1.157	.259	.00006	.00157

ER E1 E2 E3 AE AG
.561383E-02 .215917E-01 .215917E-010. .184000E+07 108900.
N = 88 MM = 40

CP= .33989 CT= .72787

MPP	MPF	MPO	MFF	MFO	MOO	MOD
.357624E-04	.651147E-03	.144155E-04	.219368	.368113E-02	.522231E-01	.100066

CPP	CPF	CPO	CFP	CFF	CFO	COP	COF	COO	COD
.536570E-02	.783335E-03	-.295227E-02	.199193E-01	2.32045	-.247565	.314543E-03	.377816E-01	-.454314E-02	.114960

KPP	KPF	KFP	KFF	KOP	KOF	KOD
86.3678	.603835	-16.2901	1846.81	.490216E-04	-.166985	.803421E-02

MP	MF	MO
.391777E-01	-.133782E-04	.535171E-01

```
 SKDEL          SJDEL           SKRDEL          SJRDEL
 -.828084E-02   -.184270        -.135561        -.178343E-01

  ZKDL  =    .002750  ZKDR =    .006862  ZKDW =    .000141

 GNCOS          GNSIN          GPCOS          GPSIN          GFCOS          GFSIN          GOCOS          GOSIN
-.860416E-05 -.889352E-04 -.862575E-05  .665593E-03 -.465337E-02  .811153E-06 -.424971E-04  .310925E-05
  SHDP =  .130047E-04 SHDF = -.447942E-03 SHDO = -.105516E-01   SHOD = -.172469E-01

  SCDP = -.113900E-03 SCDF = -.537733E-02 SCDO =  .295852E-03   SCOD = -.757413E-01

  SKDP =  .202176E-01 SKDF = -.106168E-02 SKDO = -.536618        SKOD =  .487995E-02

  SCPD =  .230411E-02 SCFD = -.585418       SCOD = -.376797

  SKPD =  .280282E-02 SKFD =  .166275       SKOD =  .234246E-01

  CQ8 = -.235453E-01
```